

**UCSF**

**UC San Francisco Electronic Theses and Dissertations**

**Title**

Studies on the metabolism and bioactivation of (S)-nicotine and beta-nicotyrine

**Permalink**

<https://escholarship.org/uc/item/8pc3c8qj>

**Author**

Shigenaga, Mark Kazuo

**Publication Date**

1989

Peer reviewed|Thesis/dissertation

STUDIES ON THE METABOLISM AND BIOACTIVATION  
OF (S)-NICOTINE AND BETA-NICOTYRINE  
by

MARK KAZUO SHIGENAGA

DISSERTATION

Submitted in partial satisfaction of the requirements for the degree of

DOCTOR OF PHILOSOPHY

in

COMPARATIVE PHARMACOLOGY AND TOXICOLOGY

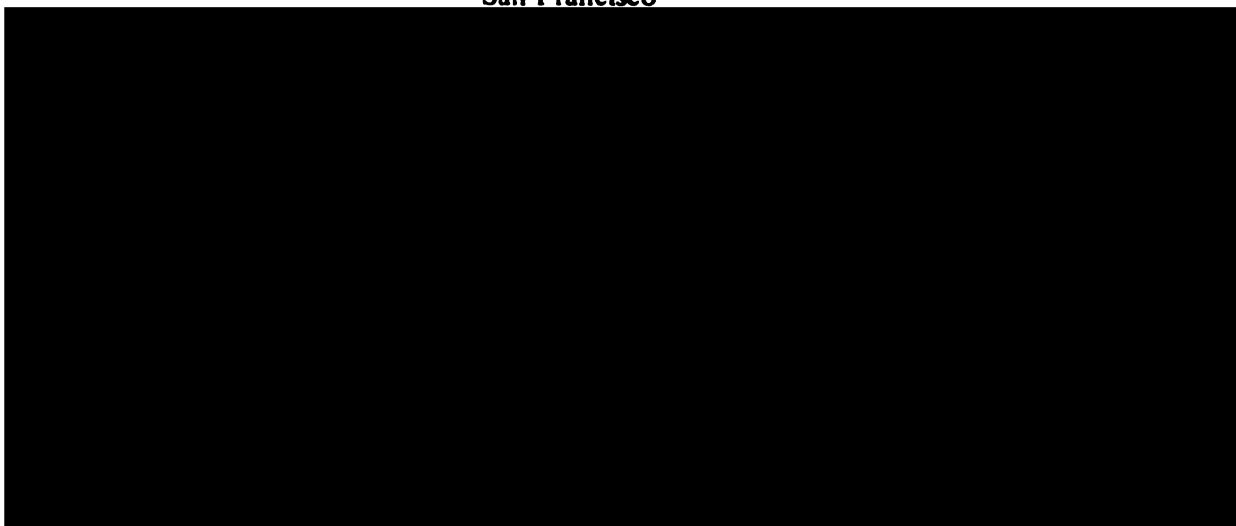
in the

GRADUATE DIVISION

of the

UNIVERSITY OF CALIFORNIA

San Francisco



Date

University Librarian

Degree Conferred: . . . . .

*To my parents, my wife Judy and my son Christopher  
for their love, understanding and support.*

## **Acknowledgments**

**Many thanks to the following:**

**Dr. Anthony J. Trevor, for his kindness, encouragement and support.**

**Dr. Neal Castagnoli Jr., for all of his spirited encouragement and for teaching me the joys of science.**

**The members of the Castagnoli/Trevor group, for providing me with a rich and stimulating environment for learning.**

**Dr. Almira Correia, for her always helpful advice and useful critique of this work.**

**Dr. Peyton Jacob III, for teaching me the enthusiastic and highly energetic approach to science.**

**This work was supported by Public Health Service Training Grant 5-T32 GM07175 and the University of California Toxic Substances Program**



# **Studies on the Metabolism and Bioactivation of (S)-Nicotine and $\beta$ -Nicotyrine**

**Mark Kazuo Shigenaga**

## **Abstract**

(S)-Nicotine has long been suspected of contributing to the chronic toxicities associated with the use of cigarettes and other tobacco products. The possibility that (S)-nicotine could contribute to these chronic toxicities by causing irreversible damage to cellular macromolecules has prompted studies aimed at characterizing the metabolic pathways of (S)-nicotine that form reactive metabolites which bind covalently. In order to study these processes, (S)-5-<sup>3</sup>H-nicotine was synthesized by catalytic tritiation of (S)-5-bromonicotine with carrier free tritium gas, purified by HPLC and characterized by tritium NMR, diode array UV and HPLC chromatographic analysis.

The metabolism of (S)-5-<sup>3</sup>H-nicotine by rabbit liver and lung microsomal enzymes produced reactive intermediates which bound covalently to microsomal macromolecules in a time, NADPH and cytochrome P-450 dependent manner. The results of studies employing rabbit lung microsomes and agents which inhibit or alter the expression of the cytochrome P-450 isozyme composition in this tissue indicated that the covalent binding of (S)-nicotine requires (S)-nicotine  $\Delta^{1',5'}$ -iminium ion as an obligate intermediate and the catalytic activity of lung cytochrome P-450 isozyme-2.

Investigations of the effects of (S)-nicotine and related tobacco alkaloids on the oxidation of the Parkinson's disease inducing agent MPTP by the mitochondrial enzyme MAO-B were prompted by the inverse correlation between cigarette smoking and Parkinson's disease. In our studies (S)-nicotine  $\Delta^{1',5'}$ -iminium *bis*perchlorate inhibited the MAO-B catalyzed oxidation of MPTP by a linear-mixed type mechanism. Subsequent studies identified  $\beta$ -nicotyrine as a MAO-B catalyzed oxidation product of (S)-nicotine  $\Delta^{1',5'}$ -iminium ion.

The structural similarities of  $\beta$ -nicotyrine to other 5-membered heterocyclic aromatic compounds which are metabolically activated to toxic intermediates encouraged us to characterize the metabolic fate of this pyrrole derivative. Metabolic studies of  $\beta$ -nicotyrine with rabbit lung and liver microsomal preparations led to the detection of a  $\beta$ -nicotyrine metabolite that was too unstable to isolate. HPLC-mass spectrometry led to the identification of this metabolite as  $\Delta^{4',5'}$ -dehydrocotinine, a possible rearrangement product of the chemically unstable arene oxide species  $\beta$ -nicotyrine  $\Delta^{2',3'}$ -epoxide. Studies on the chemical decomposition of the  $\Delta^{4',5'}$ -dehydrocotinine intermediate led to the identification of 5'-hydroxy  $\Delta^{3',4'}$ -dehydrocotinine.

## Table of Contents

<b>List of Tables</b>	x
<b>List of Figures</b>	xii
<b>List of Schemes</b>	xvi
<b>Index of Chemical Structures</b>	xvii
<b>Chapter I</b>	
<b>Introduction and Background</b>	1
la. Introduction	2
lb. Pharmacology and Toxicology of (S)-nicotine	4
lc. Autoradiographic Studies with Radiolabeled (S)-Nicotine	15
ld. Bioactivation	20
le. (S)-Nicotine Metabolism	28
References	39
<b>Chapter II</b>	
<b>Synthesis of Specifically Labeled (S)-5-<sup>3</sup>H-Nicotine by Carrier Free Tritiolysis of the Corresponding 5-Bromo Derivative</b>	47
Introduction	48
Results and Discussion	49
Deuterolysis Experiments	51
Tritiolysis	54
Notes Concerning Radiochemical Decomposition	58
Materials and Methods	61
References	67
<b>Chapter III</b>	
<b>Metabolism Dependent Covalent Binding of (S)-5-<sup>3</sup>H-Nicotine</b>	69
Introduction	70

<b>Results</b>	<b>72</b>
<i>In vitro</i> Metabolism of (S)-Nicotine	72
Metabolism Dependent Covalent Binding of (S)-5- <sup>3</sup> H-Nicotine	75
Attempted Trapping of (S)-Nicotine $\Delta^{1',5'}$ -Iminium Ion and Inhibition of Covalent Binding by Cyanide	77
Cyanide Binding to Microsomal Cytochrome P-450	79
<b>Discussion</b>	<b>80</b>
<b>Materials and Methods</b>	<b>84</b>
<b>Addendum</b>	<b>89</b>
NADPH Dependent Oxidation of (S)-Nicotine $\Delta^{1',5'}$ -Iminium Ion	89
Measurement of (S)-Nicotine Covalent Binding by SDS-Equilibrium Dialysis: Assessing the Bioalkylation Properties of (S)-Nicotine $\Delta^{1',5'}$ -Iminium Ion	92
<b>Methods-Addendum</b>	<b>97</b>
<b>References</b>	<b>99</b>
<b>Chapter IV</b>	
<b>Lung Microsomal Metabolism and Bioactivation of (S)-Nicotine</b>	<b>101</b>
Introduction	102
<b>Results</b>	<b>109</b>
Lung Microsomal Metabolism of (S)-Nicotine: Comparison of Lung and Liver Microsomal Oxidation of (S)-Nicotine	109
Effects of Cytochrome P-450 Inhibitors on the Lung Microsomal Metabolism of (S)-Nicotine	111
Detection of an Unknown Metabolite Produced by Lung Microsomal Oxidation of (S)-Nicotine	113
Characterization of Lung Cytochrome P-450 Isozymes Participating in the Oxidation of (S)-Nicotine	117
Effect of Various Pretreatments on the Lung Microsomal Metabolism of (S)-Nicotine	118

Effects of Various Inhibitors and Pretreatments on the (S)-Nicotine Metabolite Profile	123
Effects of Lung P-450 Isozyme-2 Inhibition of the Covalent Binding of (S)-5- <sup>3</sup> H-Nicotine to Lung Microsomal Proteins	128
Metabolic Oxidation of (S)-Nicotine $\Delta^{1',5'}$ -Iminium Ion: Investigation of the Relationship Between its Further Oxidation and the Bioactivation of (S)-Nicotine	130
Comparison of the (S)-Nicotine $\Delta^{1',5'}$ -Iminium Oxidase Activity of Lung and Liver 100,000 x g Soluble Fraction	131
Discussion	138
Materials and Methods	144
References	153
<b>Chapter V</b>	
<b>Monoamine Oxidase B and (S)-Nicotine <math>\Delta^{1',5'}</math>-Iminium Ion: Identification of <math>\beta</math>-Nicotyrine as a <math>\Delta^{1',5'}</math>-Iminium Ion Derived Metabolite</b>	157
Introduction	158
Results	160
Effects of (S)-Nicotine and Related Compounds on the MAO-B Catalyzed Oxidation of MPTP	160
Time and Concentration Dependent Inhibition of the MAO-B Catalyzed Oxidation of MPTP by (S)-Nicotine $\Delta^{1',5'}$ -Iminium Ion	162
Enzyme Kinetics of the (S)-Nicotine $\Delta^{1',5'}$ -Iminium Ion Dependent Inhibition of the MAO-B Catalyzed Oxidation of MPTP	162
Inhibition of MAO-B Activity by Phencyclidine Iminium Ion	166
Identification of $\beta$ -Nicotyrine as a MAO-B Catalyzed Oxidation Product of (S)-Nicotine $\Delta^{1',5'}$ -Iminium Ion	168
MAO-B Catalyzed Oxidation of (S)-Nicotine $\Delta^{1',5'}$ -Iminium <i>bis</i> perchlorate to $\beta$ -Nicotyrine	171
Discussion	174
Materials and Methods	180
References	185

<b>Chapter VI</b>	
<b>Metabolic Fate of <math>\beta</math>-Nicotyrine</b>	<b>187</b>
Introduction	188
Results	202
Binding of $\beta$ -Nicotyrine to Unreduced Liver Cytochrome P-450: Characterization of Substrate Binding	202
NADPH Dependent Formation of a $\beta$ -Nicotyrine Derived Metabolite	202
$\beta$ -Nicotyrine Metabolism by Lung Microsomes	204
Inhibition of $\beta$ -Nicotyrine Oxidase: Role of Cytochrome P-450 in the Oxidation of $\beta$ -Nicotyrine	206
$\beta$ -Nicotyrine Metabolite: Stability Studies	208
HPLC-Mass Spectral Characterization of the $\beta$ -Nicotyrine Metabolite	211
Synthesis of $\Delta^{3',4'}$ - and $\Delta^{4',5'}$ -Dehydrocotinine	218
Deuterium Exchange Experiment	220
Characterization of the Decomposition Product "Y"	224
Discussion	231
Materials and Methods	234
Addendum	241
Displacement of the Type I Binding Species Ketamine by $\beta$ -Nicotyrine	241
Effects of Phenobarbital and 3-Methylcholanthrene Pretreatment of Rabbits on the Liver Microsomal Metabolism of $\beta$ -Nicotyrine	243
Effects of TCDD, Aroclor 1260 and Phenobarbital on the Lung Microsomal Metabolism of $\beta$ -Nicotyrine	243
Effects of Inhibitors of Lung P-450 Isozymes on the Metabolism of $\beta$ -Nicotyrine	245
Discussion-Addendum	247
Materials and Methods-Addendum	247
References	250
<b>Chapter VII</b>	
<b>Summary and Conclusions</b>	<b>254</b>
References	263

<b>List of Tables</b>		<b>Page</b>
<b>II.1</b>	<b>Summary of the Model Deuterolysis Studies</b>	<b>51</b>
<b>II.2</b>	<b>Estimation by Probe Chemical Ionization Mass Spectrometry of the Palladium on Charcoal (Pd/C) Catalyzed Incorporation of Deuterium into (S)-5-Br-Nicotine</b>	<b>53</b>
<b>II.3</b>	<b>Summary of Conditions and Results from the Catalytic Tritiolysis of (S)-5-Br-Nicotine to (S)-5-<sup>3</sup>H-Nicotine</b>	<b>56</b>
<b>III.1</b>	<b>NADPH Dependent Metabolism and Covalent Binding of (S)-5-<sup>3</sup>H-Nicotine in Various Tissue Preparations</b>	<b>75</b>
<b>III.2</b>	<b>Effects of Enzyme Inhibitors on Metabolism Dependent Covalent Binding of (S)-5-<sup>3</sup>H-Nicotine to Liver Microsomes</b>	<b>77</b>
<b>III.3</b>	<b>Comparison of Three Covalent Binding Methods</b>	<b>94</b>
<b>III.4</b>	<b>Effect of Sodium Cyanide on the Covalent Binding of (S)-5-<sup>3</sup>H-Nicotine to Rabbit Liver Microsomal Proteins</b>	<b>95</b>
<b>III.5</b>	<b>Recovery of (S)-Nicotine <math>\Delta^{1',5'}</math>-Iminium Ion Equivalents in the Absence and Presence of Excess Sodium Cyanide (100 mM)</b>	<b>97</b>
<b>IV.1</b>	<b>Inhibitory Effects of <math>\alpha</math>-Methylbenzylaminobenzotriazole on (S)-Nicotine Metabolism by Rabbit Lung Microsomes</b>	<b>117</b>
<b>IV.2</b>	<b>Effect of <math>\alpha</math>-Methylbenzylaminobenzotriazole on P-450 Isozyme-2 and -6 Catalyzed Oxidations</b>	<b>118</b>
<b>IV.3</b>	<b>Lung Microsome Catalyzed Benzphetamine N-Demethylation</b>	<b>119</b>
<b>IV.4</b>	<b>Effect of Selective and Nonselective Lung P-450 Inhibitors on the Lung Microsomal Oxidation of (S)-Nicotine to its Major Metabolites (S)-Nicotine <math>\Delta^{1',5'}</math>-Iminium Ion, (S)-Nicotine N'-Oxide, (S)-Cotinine and (S)-Nornicotine</b>	<b>127</b>
<b>IV.5</b>	<b>Effect of Lung P-450 Isozyme-2 Inhibition on the Covalent Binding of (S)-5-<sup>3</sup>H-Nicotine to Rabbit Lung Microsomal Protein</b>	<b>129</b>
<b>IV.6</b>	<b>Bioactivation of (S)-5-<sup>3</sup>H-Nicotine: Effect of Treatments Which Modify the Level of (S)-Nicotine <math>\Delta^{1',5'}</math>-Iminium Ion in Lung Microsomal Incubations</b>	<b>135</b>
<b>IV.7</b>	<b>Effect of Glutathione on the Rabbit Lung Microsomal Oxidation and Covalent Binding of (S)-5-<sup>3</sup>H-Nicotine</b>	<b>137</b>

<b>V.1</b>	<b>Inhibition of the MAO-B Catalyzed Oxidation of MPTP by Various Agents</b>	<b>161</b>
<b>V.2</b>	<b>Inhibition of the MAO-B Catalyzed Oxidation of MPTP and Benzylamine by Phencyclidine Iminium Perchlorate, Structurally Related Analogs and Sodium Cyanide</b>	<b>167</b>
<b>VI.1</b>	<b>Effect of Various Treatments on the Microsomal Metabolism of <math>\beta</math>-Nicotyrine</b>	<b>208</b>
<b>VI.2</b>	<b>Daughter Ions from the m/z 175 Precursor Ion Derived from the <math>\beta</math>-Nicotyrine Metabolite</b>	<b>218</b>
<b>VI.3</b>	<b>Deuterium Exchange and Back-Exchange Experiment</b>	<b>222</b>
<b>VI.4</b>	<b>Major Fragments Obtained from the CI/MS and CAD/MS Analysis of Various Lactam Derivatives of (S)-Nicotine</b>	<b>229</b>



	<b>List of Figures</b>	<b>Page</b>
<b>II.1</b>	Kinetics of Deuteration of (S)-5-Bromonicotine to (S)-5-d <sub>1</sub> -Nicotine Under Various Reaction Conditions	52
<b>II.2</b>	Partial Pressure of Tritium Gas in the Tritiolysis Reaction Vessel vs. Time	55
<b>II.3</b>	Radiochemical Purity of Synthetic (S)-5- <sup>3</sup> H-Nicotine (1a) Prepared by the Catalytic Tritiolysis of (S)-5-Bromonicotine (46)	57
<b>II.4</b>	<sup>3</sup> H-NMR of (S)-5- <sup>3</sup> H-Nicotine (1a)	58
<b>III.1</b>	HPLC Analysis of (S)-5- <sup>3</sup> H-Nicotine Metabolism by Rabbit Liver Microsomes	73
<b>III.2</b>	Liver Microsomal Metabolism of (S)-Nicotine	74
<b>III.3</b>	Metabolism Dependent Covalent Binding of (S)-5- <sup>3</sup> H-Nicotine to Liver Microsomes	76
<b>III.4</b>	Effect of Sodium Cyanide on the Metabolism Dependent Covalent Binding of (S)-5- <sup>3</sup> H-Nicotine to Liver Microsomes	78
<b>III.5</b>	Effect of Sodium Cyanide on Liver Microsomal Metabolism of (S)-Nicotine	79
<b>III.6</b>	Concentration Dependent Inhibition of (S)-Nicotine Metabolism by Sodium Cyanide	80
<b>III.7</b>	Concentration Dependent Inhibition of (S)-Nicotine Metabolism by (S)-Nicotine $\Delta^{1',5'}$ -Iminium Ion	89
<b>III.8</b>	Estimation of Spectrally Detectable (S)-Nicotine $\Delta^{1',5'}$ -Iminium Ion Binding to Liver Microsomal Cytochrome P-450	90
<b>III.9</b>	NADPH Dependent Oxidation of (S)-Nicotine $\Delta^{1',5'}$ -Iminium <i>bis</i> perchlorate	91
<b>IV.1</b>	A Comparison Between the Lung and Liver Microsomal Metabolism of (S)-Nicotine	110
<b>IV.2 A-E</b>	HPLC Chromatograms of (S)-Nicotine and its Metabolites Following Incubation with Lung Microsomes Under Various Conditions	112
<b>IV.3 A and B</b>	Analysis of the Lung Microsomal Metabolism of (S)-5- <sup>3</sup> H-Nicotine by HPLC with (A) UV and (B) Radiochemical Detection	114

<b>IV.4</b>	<b>UV Spectra of the Unknown Metabolite Derived from the Lung Microsomal Metabolism of (S)-Nicotine and Synthetic <math>\beta</math>-Nicotyrine Tartrate</b>	<b>115</b>
<b>IV.5</b>	<b>Lung Microsomal Oxidation of (S)-Nicotine: Effects of Phenobarbital, TCDD and Aroclor 1260 Pretreatments</b>	<b>120</b>
<b>IV.6</b>	<b>Reversed Phase HPLC Analysis of the Lung Microsomal Metabolism of (S)-Nicotine</b>	<b>122</b>
<b>IV.7</b>	<b>Comparison of the Metabolite Profiles of the Control and Aroclor 1260 Pretreated Rabbit Lung Microsomal Oxidation of (S)-Nicotine</b>	<b>124</b>
<b>IV.8</b>	<b>Effect of Selective and Nonselective Lung P-450 Inhibitors on the Lung Microsomal Oxidation of (S)-Nicotine to its Major Metabolites (S)-Nicotine <math>\Delta^{1',5'}</math>-Iminium Ion, Nicotine N'-Oxide and Nornicotine</b>	<b>126</b>
<b>IV.9</b>	<b>A Comparison of the Lung and Liver Aldehyde Oxidase (AO) Activities Present in the Rabbit 100,000 x g Soluble Fraction</b>	<b>132</b>
<b>IV.10</b>	<b>Lung and Liver 100,000 x g Soluble Fraction Catalyzed Oxidation of (S)-Nicotine <math>\Delta^{1',5'}</math>-Iminium Ion</b>	<b>134</b>
<b>V.1 A and B</b>	<b>Preincubation Time Dependent and Concentration Dependent Inhibition of the MAO-B Catalyzed Oxidation of MPTP by (S)-Nicotine <math>\Delta^{1',5'}</math>-Iminium <i>bis</i>perchlorate</b>	<b>164</b>
<b>V.2 A and B</b>	<b>Enzyme Kinetic Analyses of the (S)-Nicotine <math>\Delta^{1',5'}</math>-Iminium <i>bis</i>perchlorate Dependent Inhibition of the MAO-B Catalyzed Oxidation of MPTP</b>	<b>165</b>
<b>V.3</b>	<b>Enzyme Kinetic Analysis of the (S)-Nicotine <math>\Delta^{1',5'}</math>-Iminium <i>bis</i>perchlorate Dependent Inhibition of the MAO-B Catalyzed Oxidation of Benzylamine</b>	<b>166</b>
<b>V.4</b>	<b>Enzyme Kinetic Analysis of the Phencyclidine Iminium Perchlorate Inhibition of the MAO-B Catalyzed Oxidation of Benzylamine</b>	<b>168</b>
<b>V.5</b>	<b>HPLC Diode Array UV Analysis of the MAO-B Catalyzed Oxidation of (S)-Nicotine <math>\Delta^{1',5'}</math>-Iminium <i>bis</i>perchlorate in the Presence or Absence of Pargyline (10 <math>\mu</math>M)</b>	<b>169</b>
<b>V.6</b>	<b>Capillary GC-El Mass Spectra Obtained from (A) the HPLC Purified Product Derived from the MAO-B Catalyzed Oxidation of (S)-Nicotine <math>\Delta^{1',5'}</math>-Iminium <i>bis</i>perchlorate and Comparison to (B) Synthetic <math>\beta</math>-Nicotyrine Tartrate</b>	<b>170</b>

<b>V.7</b>	<b>Kinetics of the MAO-B Catalyzed Oxidation of (S)-Nicotine <math>\Delta</math> 1',5'-Iminium <i>bis</i>perchlorate to <math>\beta</math>-Nicotyrine in the Presence or Absence of Pargyline</b>	<b>171</b>
<b>V.8</b>	<b>MAO-B Concentration Dependent Oxidation of (S)-Nicotine <math>\Delta</math>1',5'-Iminium ion to <math>\beta</math>-Nicotyrine</b>	<b>172</b>
<b>V.9</b>	<b>MAO-B Catalyzed Oxidation of (S)-Nicotine <math>\Delta</math>1',5'-Iminium ion to <math>\beta</math>-Nicotyrine as a Function of pH</b>	<b>174</b>
<b>VI.1</b>	<b><math>\beta</math>-Nicotyrine Binding to Unreduced Rabbit Liver Microsomes (1 mg/ml) Isolated from Phenobarbital Pretreated Rabbits</b>	<b>203</b>
<b>VI.2</b>	<b>Liver Microsomal Metabolism of <math>\beta</math>-Nicotyrine</b>	<b>204</b>
<b>VI.3</b>	<b>HPLC Chromatographic Characteristics of <math>\beta</math>-Nicotyrine (6) and its Metabolite (Met). Inset: UV-Diode Array Analysis of the <math>\beta</math>-Nicotyrine Metabolite (Met)</b>	<b>205</b>
<b>VI.4</b>	<b>Comparison Between the Liver and Lung Microsomal Metabolism of <math>\beta</math>-Nicotyrine per (A) mg of Microsomal Protein or (B) nmole Cytochrome P-450</b>	<b>207</b>
<b>VI.5</b>	<b>Stability of the <math>\beta</math>-Nicotyrine Derived Metabolite at pH 1, 7.6 and 11</b>	<b>209</b>
<b>VI.6</b>	<b>HPLC Analysis of the <math>\beta</math>-Nicotyrine Metabolite and its Two Base-Catalyzed Decomposition Products "X" and "Y"</b>	<b>210</b>
<b>VI.7</b>	<b>Stability of the <math>\beta</math>-Nicotyrine Metabolite in the Presence of (A) 0.5% n-Propylamine/Acetonitrile (B) 3.0% n-Propylamine/Acetonitrile: Formation of Two Base-Catalyzed Decomposition Products vs. Time</b>	<b>212</b>
<b>VI.8</b>	<b>UV Diode Array Spectra of (A) the <math>\beta</math>-Nicotyrine Metabolite and (B) the Base-Catalyzed Decomposition Product "X" and (C) Decomposition Product "Y"</b>	<b>213</b>
<b>VI.9</b>	<b>HPLC-CAD/MS of the m/z 159 Precursor Ion Derived from <math>\beta</math>-Nicotyrine</b>	<b>214</b>
<b>VI.10</b>	<b>Total Ion Chromatogram Obtained from the HPLC-CI/MS of <math>\beta</math>-Nicotyrine and its Metabolite</b>	<b>215</b>
<b>VI.11</b>	<b>HPLC-CI/MS of the <math>\beta</math>-Nicotyrine Metabolite</b>	<b>216</b>
<b>VI.12</b>	<b>Candidate Structures for the <math>\beta</math>-Nicotyrine Metabolite</b>	<b>216</b>

<b>VI.13</b>	CAD/MS of the m/z Precursor Ion Derived from the $\beta$ -Nicotyrine Metabolite	217
<b>VI.14</b>	Diode-Array UV Spectra of Synthetic <b>8</b> and the $\beta$ -Nicotyrine Metabolite	219
<b>VI.15</b>	Total Ion Chromatogram Obtained from the Capillary GC-EIMS Analysis of Synthetic <b>7</b> and <b>8</b> Incubated in Deuterated Phosphate Buffer	220
<b>VI.16</b>	Electron Impact Mass Spectra of <b>7</b> and <b>8</b> Following Incubation in Deuterated Phosphate Buffer	221
<b>VI.17</b>	Total Ion Chromatogram Obtained from the CI/MS of the $\beta$ -Nicotyrine Metabolite and its Base-Catalyzed Decomposition Products	224
<b>VI.18</b>	CI/MS of Base-Catalyzed Decomposition Products "X" and "Y"	225
<b>VI.19</b>	Daughter Ion Spectrum Obtained from the CAD/MS Analysis of the m/z 191 Precursor Ion Derived from "Y"	226
<b>VI.20 and B</b>	<b>A</b> CI/MS of Synthetic 5'-hydroxy $\Delta^{3',4'}$ -Dehydrocotinine ( <b>51</b> ) and CAD/MS of the Precursor Ion Derived from <b>51</b>	228
<b>VI.21</b>	Displacement of the Type I Substrate Ketamine (100 $\mu$ M) by the Type II Substrate $\beta$ -Nicotyrine (5 and 10 $\mu$ M) from Unreduced Liver Microsomal Cytochrome P-450	242
<b>VI.22</b>	$\beta$ -Nicotyrine Metabolism by Liver Microsomes Isolated from Phenobarbital Pretreated, 3-Methylcholanthrene Pretreated and Control (Untreated) Rabbits	244
<b>VI.23</b>	Effect of Phenobarbital, TCDD and Aroclor 1260 Pretreatment on the Rabbit Lung Microsomal Metabolism of $\beta$ -Nicotyrine	246

	<b>List of Schemes</b>	<b>Page</b>
<b>I. 1</b>	Proposed Activation of Molecular Oxygen by the Cytochrome P-450 Monooxygenase System	33
<b>I. 2</b>	Proposed Cytochrome P-450 Catalyzed Oxidation of (S)-Nicotine to (S)-Nicotine $\Delta^{1',5'}$ -Iminium Ion	34
<b>II. 1</b>	Radiochemical Syntheses of (S)-5- <sup>3</sup> H-Nicotine ( <b>1a</b> ) and (S)-5- <sup>3</sup> H-Cotinine ( <b>3a</b> )	50
<b>III. 1</b>	Major Pathways for the Metabolic Oxidation of (S)-Nicotine	71
<b>IV. 1</b>	Equilibrium Among the Isoelectronic Species <b>2</b> , <b>15</b> and <b>20</b> and Proposed Trapping of <b>20</b> by a Soluble Nucleophile	130
<b>IV. 2</b>	Lung Cytochrome P-450 Isozyme-2 Catalyzed Metabolic Activation of (S)-Nicotine and Trapping of the Proposed Reactive Intermediate(s) by Glutathione and Tissue Protein	137
<b>V. 1</b>	Bioactivation of MPTP by MAO-B	160
<b>V. 2</b>	Equilibrium Among the Isoelectronic Species <b>19</b> , <b>2</b> and <b>15</b>	173
<b>V. 3</b>	Proposed Mechanism for the MAO-B Catalyzed Oxidation of (S)-Nicotine $\Delta^{1',5'}$ -Iminium Ion to $\beta$ -Nicotyrine	178
<b>VI. 1</b>	Proposed Sequence of Events Leading to the Toxicity of Cyclopentadienoid Heterocyclic Compounds	192
<b>VI. 2</b>	Synthesis of Pyrrolinones <b>7</b> and <b>8</b>	219
<b>VI. 3</b>	Proposed Cytochrome P-450 Catalyzed Oxidation Pathway of $\beta$ -Nicotyrine	223
<b>VI. 4</b>	Autoxidative Degradation of Pyrrolinones <b>7</b> and <b>8</b> via anion <b>70</b>	230
<b>VII. 1</b>	Summary of Proposed Bioactivation Pathways for (S)-Nicotine	261

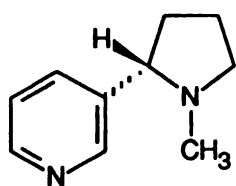
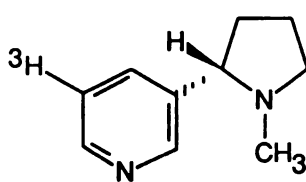
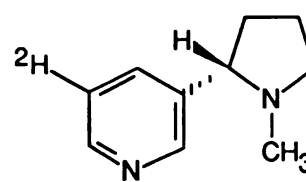
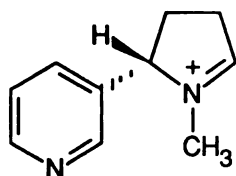
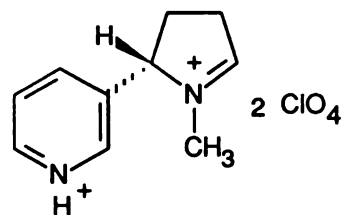
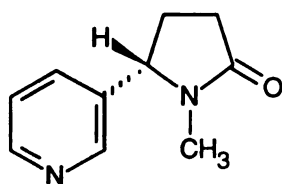
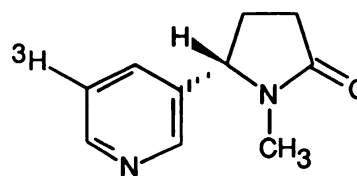
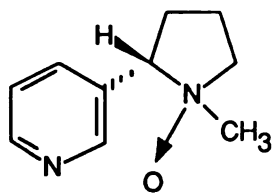
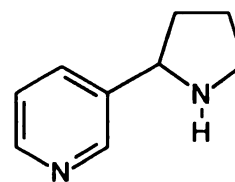
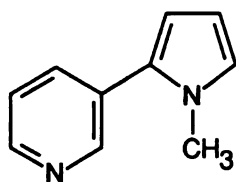
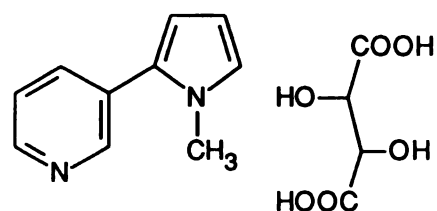
## Index of Chemical Structures

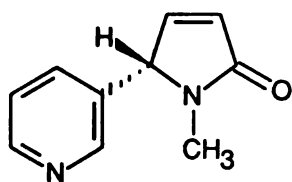
Compound	Number
(S)- <b>Nicotine</b> _____	1
(S)- <b>5-3</b> H-Nicotine_____	1 a
(S)- <b>5-2</b> H-Nicotine_____	1 b
(S)- <b>Nicotine</b> $\Delta^{1',5'}$ -iminium ion_____	2
(S)- <b>Nicotine</b> $\Delta^{1',5'}$ -iminium <i>bis</i> perchlorate_____	2 a
(S)- <b>Cotinine</b> _____	3
(S)- <b>5-3</b> H-Cotinine_____	3 a
(S)- <b>Nicotine</b> N'-oxide_____	4
<b>Nornicotine</b> _____	5
$\beta$ - <b>Nicotyrine</b> _____	6
$\beta$ - <b>Nicotyrine</b> tartrate_____	6 a
$\Delta^{3',4'}$ - <b>Dehydrocotinine</b> _____	7
$\Delta^{4',5'}$ - <b>Dehydrocotinine</b> _____	8
<b>Phencyclidine</b> _____	9
<b>Phencyclidine</b> iminium ion_____	10
<b>1-Methyl-4-phenyl-1,2,3,6-tetrahydropyridine</b> (MPTP) _____	11
<b>1-Methyl-4-phenyl-2,3-dihydropyridinium</b> (MPDP <sup>+</sup> )_____	12
<b>Methapyrilene</b> _____	13
(S)- <b>Nicotine</b> methyleneiminium ion_____	14
(S)- <b>5*</b> - <b>Hydroxynicotine</b> _____	15
(S)- <b>N</b> - <b>Hydroxymethylnornicotine</b> _____	16
(S)- <b>5*</b> - <b>Cyanonicotine</b> _____	17
(S)- <b>N</b> - <b>Cyanomethylnornicotine</b> _____	18
$\Delta^{2',3'}$ - <b>Dehydro-(S)-nicotine</b> [(S)-Nicotine $\Delta^{2',3'}$ enamine]_____	19
<b>4-Methylamino-4-(3-pyridyl)butanal</b> _____	20
<b>Cyanophencyclidine</b> (CN-PCP)_____	21
(S)- <b>3*</b> - <b>Hydroxycotinine</b> _____	22
(S)- <b>Nicotine</b> $\Delta^{2',3'}$ -epoxide_____	23
<b>2'-Cyanonicotine</b> _____	24
<b>4-Isopomeanol</b> _____	25
<b>5'-Methyl-<math>\beta</math>-nicotyrine</b> (1,5-dimethyl-2-(3-pyridyl)pyrrole)_____	26
<b>Methylanabasine</b> _____	27
$\beta$ - <b>Nornicotyrine</b> _____	28

<b>Compound</b>	<b>Number</b>
<b>Myosmine</b> _____	<b>29</b>
<b>Mepyramine</b> _____	<b>30</b>
<b>Pyribenzamine</b> _____	<b>31</b>
<b>1,3,4 -Trimethylpyrrole</b> _____	<b>32</b>
<b>Pyrrolnitrin</b> _____	<b>33</b>
<b>Ketamine</b> _____	<b>34</b>
<b>Dichlorfurime</b> _____	<b>35</b>
<b>Ring opened dichlorfurime</b> _____	<b>36</b>
<b>Lactone derivative of dichlorfurime</b> _____	<b>37</b>
<b>Furosemide</b> _____	<b>38</b>
<b>1-Methyl-3,4-bis(hydroxymethyl)pyrrole</b> _____	<b>39</b>
<b>Cephaloridine</b> _____	<b>40</b>
<b>Ticrynafen</b> _____	<b>41</b>
<b>Pyrrole</b> _____	<b>42</b>
<b>Thiophene</b> _____	<b>43</b>
<b>Furan</b> _____	<b>44</b>
<b>N,N-Dimethyl-4-aminobenzene</b> _____	<b>45</b>
<b>(S)-5-Bromonicotine</b> _____	<b>46</b>
<b><math>\beta</math>-Nicotyrine N-oxide</b> _____	<b>47</b>
<b><math>\beta</math>-Nicotyrine 2',3'-epoxide</b> _____	<b>48</b>
<b>2'-Hydroxy-<math>\beta</math>-nicotyrine</b> _____	<b>49</b>
<b>Phenylselenyl adduct of (S)-cotinine</b> _____	<b>50</b>
<b>5'-Hydroxy <math>\Delta^{3',4'}</math>-dehydrocotinine</b> _____	<b>51</b>
<b>Diol derived from <math>\beta</math>-nicotyrine <math>\Delta^{2',3'}</math>-epoxide</b> _____	<b>52</b>
<b>(S)-5-Bromocotinine</b> _____	<b>53</b>
<b>(S)-5-Bromonornicotine</b> _____	<b>54</b>
<b>(S)-3',3',5'-Tribromocotinine</b> _____	<b>55</b>
<b>Phenylselenyloxo derivative of (S)-cotinine</b> _____	<b>56</b>
<b>5-Phenyl N-methylpyrrolidine-2,3-dione</b> _____	<b>57</b>
<b>Cotinine N-oxide</b> _____	<b>58</b>
<b>Tetrahydrofuranyl derivative of furosemide</b> _____	<b>59</b>
<b>1-Methyl-4-phenylpyridinium (MPP<sup>+</sup>)</b> _____	<b>60</b>
<b>N-Methylnicotinamide (NMN)</b> _____	<b>61</b>
<b>2-Pyridone derivative of NMN</b> _____	<b>62</b>
<b>Norbenzphetamine</b> _____	<b>63</b>

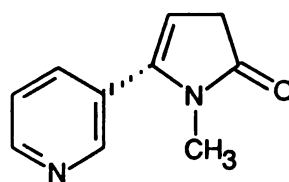
<b>Compound</b>	<b>Number</b>
N-Hydroxyamphetamine_____	64
$\alpha$ -Methylbenzylaminobenzotriazole_____	65
N-Methyl-N-(3-pyridyl)methylpropionamide_____	66
3-Chloro-4-(2-nitro-3-chlorophenyl)maleimide_____	67
3-Thio-(2-hydroxyethane)-4-[2-nitro-3-chlorophenyl]pyrrole_____	68
Ring-opened metabolite of $\beta$ -nicotyrine epoxide_____	69
Anionic species of 2'-hydroxy- $\beta$ -nicotyrine_____	70
Resonance stabilized radical species of 2'-hydroxy- $\beta$ -nicotyrine_____	71 a-c
3'-hydroxy $\Delta^{4',5'}$ -dehydrocotinine_____	72
Nicotine $\Delta^{2',3'}$ -dehydroaminium cation radical_____	73
Nicotine $\Delta^{2',3'}$ -dehydro 5'-yl radical_____	74
Nicotine $\Delta^{4',5'}$ -dehydro $\Delta^{1',2'}$ -iminium ion_____	75
Nicotine $\Delta^{1',2'}$ -iminium ion_____	76



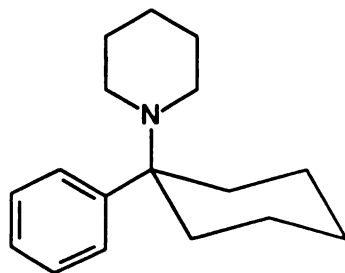
**1****1 a****1 b****2****2 a** $2 \text{ ClO}_4^-$ **3****3 a****4****5****6****6 a**



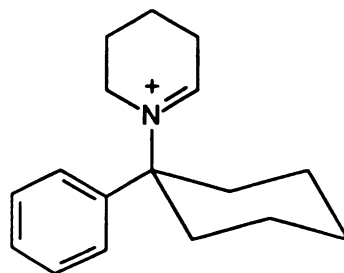
7



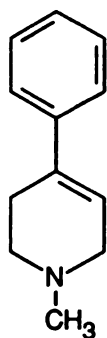
8



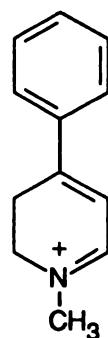
9



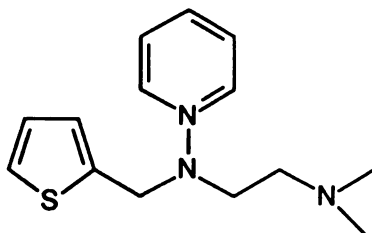
10



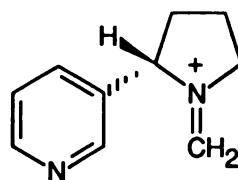
11



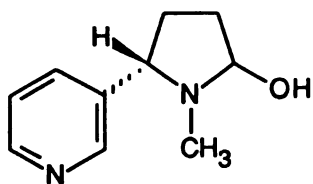
12



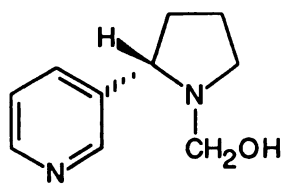
13



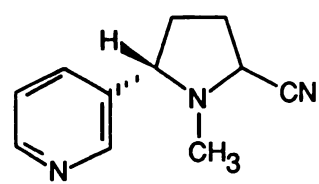
14



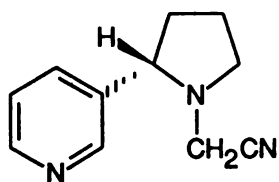
15



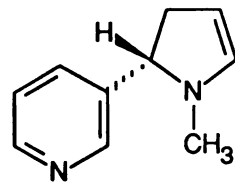
16



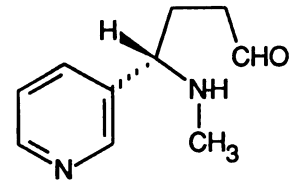
17



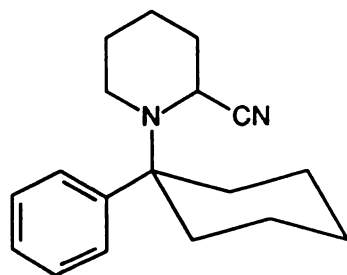
18



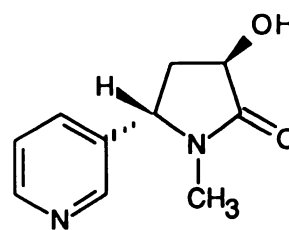
19



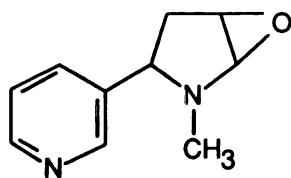
20



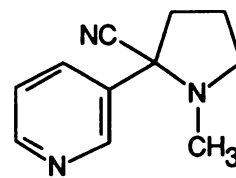
21



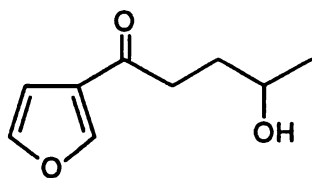
22



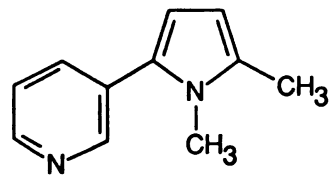
23



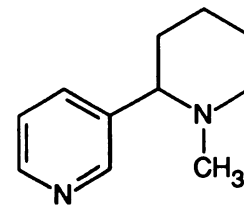
24



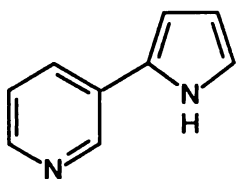
25



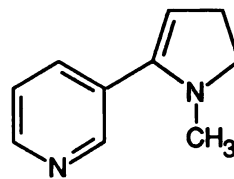
26



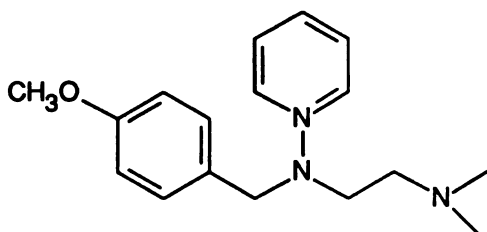
27



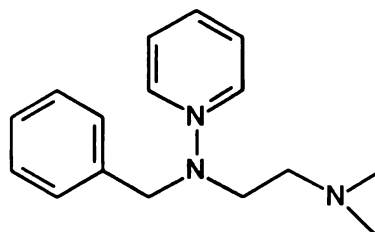
28



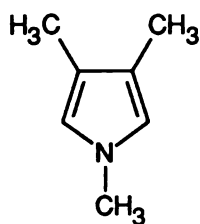
29



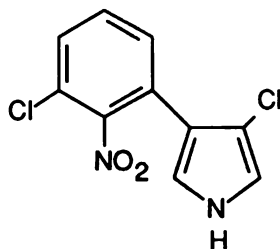
30



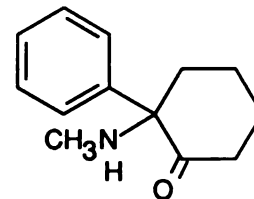
31



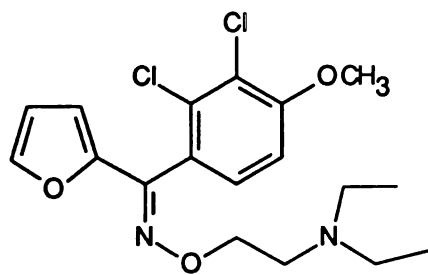
32



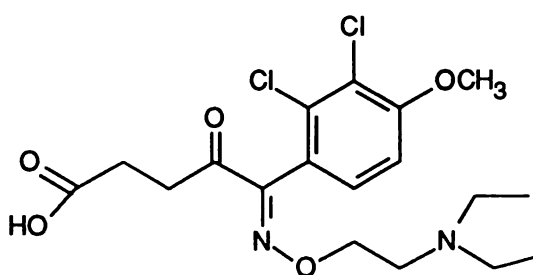
33



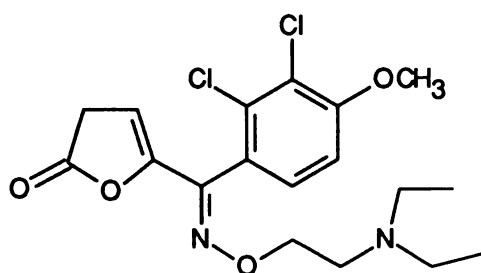
34



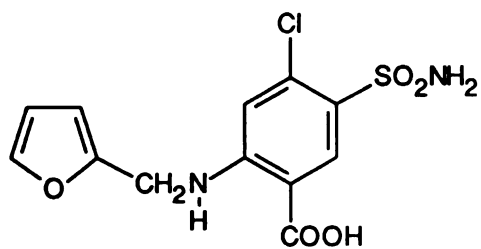
35



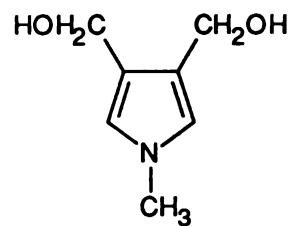
36



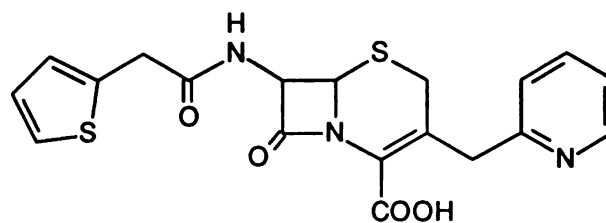
37



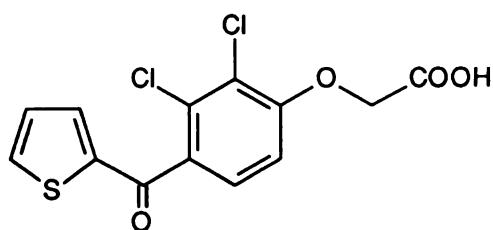
38



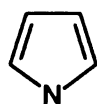
39



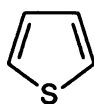
40



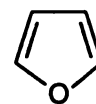
41



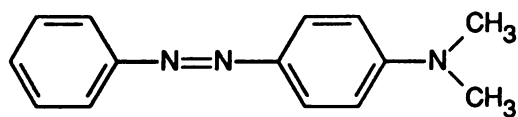
42



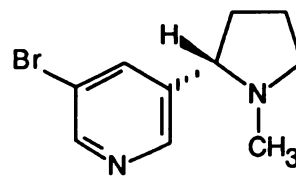
43



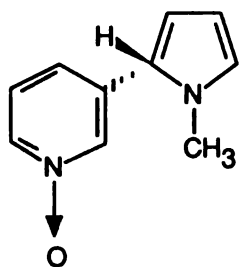
44



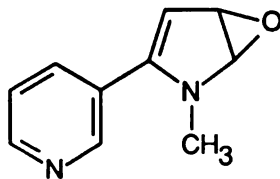
45



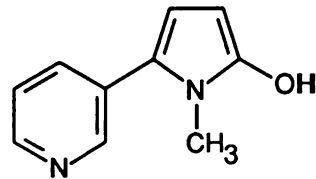
46



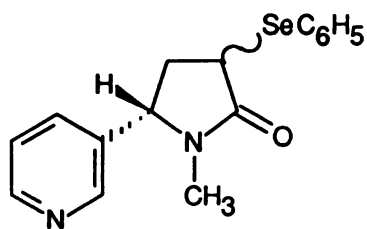
47



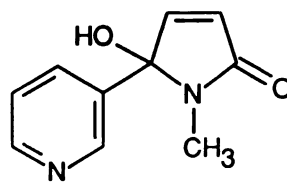
48



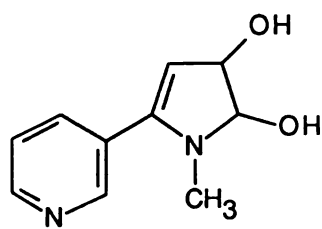
49



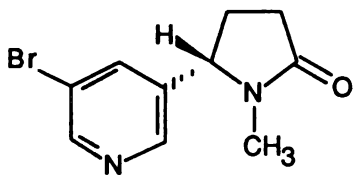
50



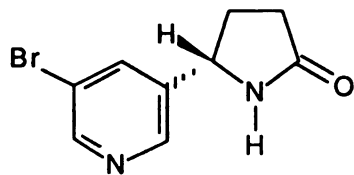
51



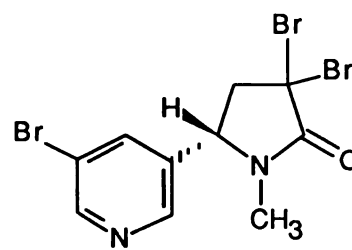
52



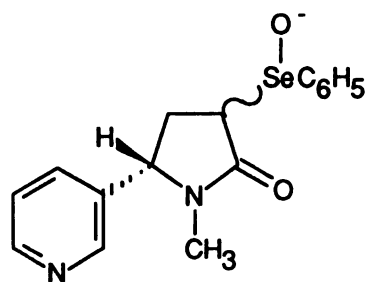
53



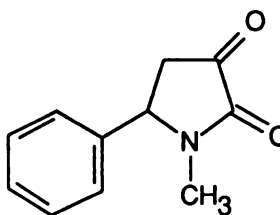
54



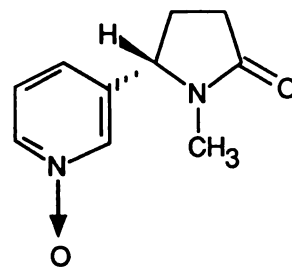
55



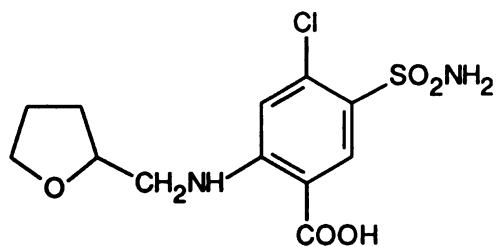
56



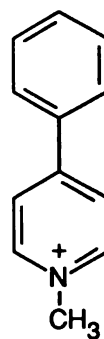
57



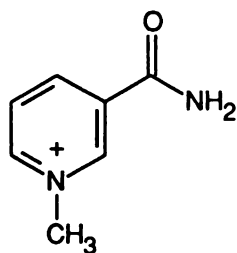
58



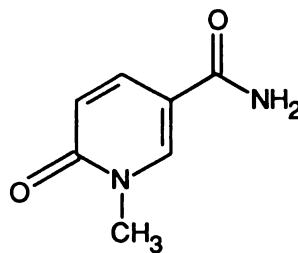
59



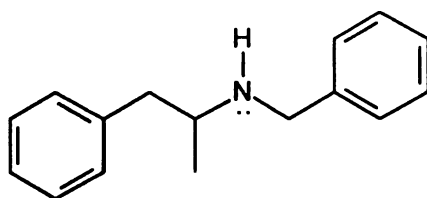
60



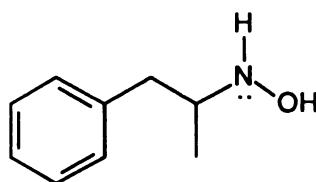
61



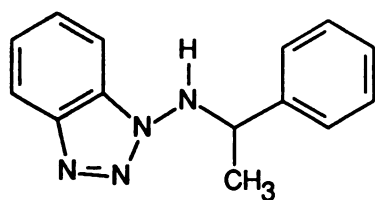
62



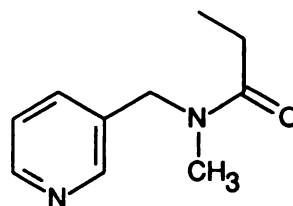
63



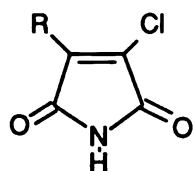
64



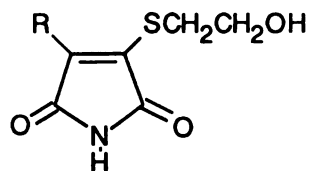
65



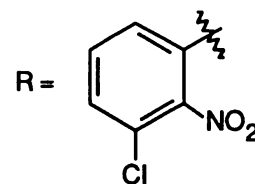
66

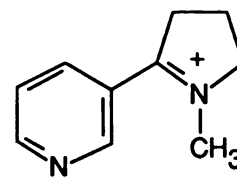
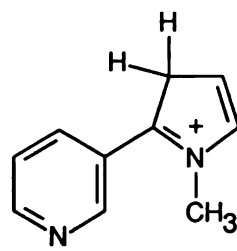
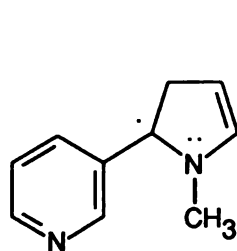
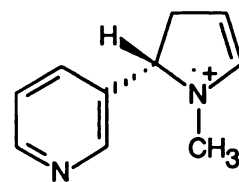
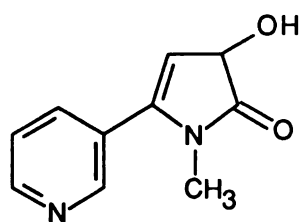
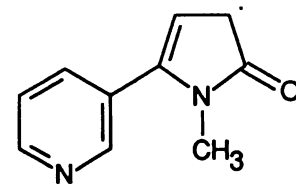
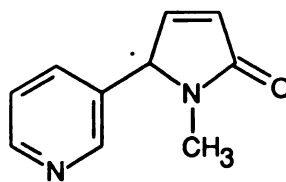
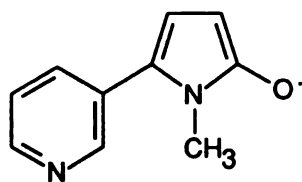
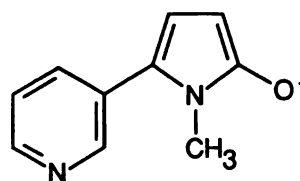
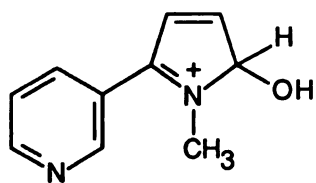


67



68







**Chapter I**  
**Introduction and Background**

(S)-Nicotine is quantitatively the most important of the tobacco alkaloids and is present in concentrations of approximately 1-2 mg/cigarette. Consequently, heavy smokers and tobacco chewers consume large quantities of (S)-nicotine over the course of their lifetime (5-10 g/year). (S)-Nicotine stimulates the central and peripheral nervous systems, is highly addictive and at higher doses can produce acute toxicities by virtue of its cholinergic stimulating properties.<sup>1</sup> (S)-Nicotine is also suspected of contributing to some of the irreversible tissue lesions and other toxic effects observed in humans and animals who are exposed chronically to tobacco products. Because of the complex chemical makeup of tobacco and cigarette smoke, however, its contribution towards the chronic toxicities associated with tobacco usage is difficult to assess. The chronic dosing of animals with (S)-nicotine and the measurement of its long term toxic effects represents a possible approach to understanding more fully the contribution which this compound makes to tobacco related human diseases. Performing such studies, however, is limited by the potent cholinergic stimulating properties of this compound. Therefore, in contrast to the relatively large doses used to assess the toxicity (i.e. carcinogenic properties) of many compounds, doses of (S)-nicotine are necessarily limited to typically less than 5 mg/kg of animal body weight.

Previous studies have shown an association between the exposure of an animal to certain chemical substances and pathological conditions such as cancer.<sup>2</sup> In many cases, the chemically induced toxicity is dependent upon the metabolic activation of the parent compound to reactive metabolite(s) which may bind covalently to critical target macromolecules such as DNA, protein and lipid. Thus, metabolism dependent covalent binding of a substance to target macromolecules is an endpoint which may be used to monitor the formation of chemically reactive metabolites. Covalent binding of such metabolites to DNA can produce mutations which may lead to tumor formation or other pathological conditions associated with genetic damage. Certain proteins also appear to be critical targets for the covalent binding of toxic substances. For example,

metabolically activated compounds which bind covalently to plasma membrane calcium ATPase may result in loss of this enzymatic function followed by cell death. It has been proposed that chemically reactive substances which cause cellular necrosis may do so by lesioning this enzyme.<sup>3</sup>

Previous investigations which have led up to the current studies have shown that (S)-nicotine is oxidized enzymatically *in vitro* and *in vivo*. Two of the products formed from this metabolic oxidation are the (S)-nicotine  $\Delta^{1',5'}$ -iminium ion and (S)-nicotine methyleneiminium ion, both of which are reactive electrophiles. *In vitro* studies have documented their reactivity through the trapping of the respective iminium ion metabolites with the soluble nucleophile cyanide ion.<sup>4,5</sup> The existence of such chemically reactive species has led to the current proposal that oxidative metabolism of this important tobacco alkaloid may result in chemically induced toxicities associated with cigarette smoking. These observations have encouraged the present studies which were designed to investigate further the reactivity of (S)-nicotine metabolites with biomacromolecules by employing the covalent binding approach described above. The studies to be described emphasize various approaches used to determine the metabolic routes involved in the bioactivation of (S)-nicotine by liver and lung microsomal preparations and the identity of the reactive species. Since the lung is a principal target organ for pathologies related to tobacco usage, a major emphasis of this dissertation was dedicated towards understanding the metabolic fate of (S)-nicotine and its metabolites in the presence of microsomal and soluble enzymes isolated from rabbit lung tissues. Also described in this dissertation is the monoamine oxidase-B catalyzed oxidation of (S)-nicotine  $\Delta^{1',5'}$ -iminium ion to the pyrrolic compound  $\beta$ -nicotyrine. The identification of  $\beta$ -nicotyrine as a product of the enzymatic oxidation of (S)-nicotine  $\Delta^{1',5'}$ -iminium ion, the principal two electron oxidized intermediate of (S)-nicotine, represents a novel metabolic pathway for the iminium species. The enzymatic oxidation of  $\beta$ -nicotyrine and its principal metabolite were also characterized.

## Pharmacology and Toxicology of (S)-Nicotine

### Pharmacokinetics and Absorption of (S)-Nicotine

(S)-Nicotine is a weak base with a  $pK_a$  of 7.9 (pyrrolidine nitrogen).<sup>6</sup> Smoke from flue cured tobacco, the type used in most domestic cigarettes, is acidic with a pH of approximately 5.5. At this pH (S)-nicotine is essentially completely ionized and therefore absorption through the oral cavity is low even when the smoke is held intentionally in the mouth.<sup>7</sup> (S)-Nicotine derived from air cured tobaccos, which are used for pipes, cigars and a few European cigarettes, however, is absorbed efficiently in the oral cavity since the pH of the smoke generated from this type of tobacco is alkaline (pH = 8.5).<sup>8</sup> (S)-Nicotine derived from chewing tobacco, snuff and Nicoret™ gum is also well absorbed through the oral cavity since these preparations are buffered to alkaline pH.

Absorption of (S)-nicotine in the lung occurs primarily in the terminal airways and alveoli. This process, which is rapid and independent of the pH of tobacco smoke, is most likely a consequence of the enormous surface area provided by the alveoli and the terminal airways and the rapid dissolution of (S)-nicotine into biological fluids.<sup>9</sup> Once absorbed, (S)-nicotine reaches the brain in approximately 8 seconds. Over the course of a day, concentrations of (S)-nicotine approach values of approximately 25-50 ng/ml in the blood of moderate to heavy smokers. (S)-Nicotine is removed from the circulation mostly through oxidative metabolism in the liver and excretion via the kidneys. The elimination half time of (S)-nicotine has been estimated to be approximately 2 hr in humans.<sup>10</sup>

### (S)-Nicotine Pharmacology

(S)-Nicotine is the major component responsible for the stimulatory effects of tobacco on the sympathetic nervous system. These effects are supported by clinical

studies which demonstrate a correlation between the content of (S)-nicotine in cigarettes and stimulation of the nervous system.<sup>11</sup> In addition to its direct effects on the central nervous system, (S)-nicotine stimulates the cardiovascular system. (S)-Nicotine promotes the release of epinephrine and norepinephrine through interactions with nicotinic acetylcholine receptors present at sympathetic nerve endings, peripheral ganglia, and the adrenal medulla.<sup>12</sup> The physiological consequence of these interactions include increases in heart rate, blood pressure, bloodflow, cardiac output as well as changes in dilation of peripheral vessels, such as the coronary arteries. Increases in heart rate and systolic blood pressure have also been correlated with plasma (S)-nicotine concentrations.<sup>13</sup> Many of the stimulatory effects of (S)-nicotine on the cardiovascular system may be blocked effectively by  $\alpha$ - and  $\beta$ -adrenergic antagonists, an action consistent with the adrenergic receptor mediated stimulant properties of (S)-nicotine.<sup>14</sup>

The stimulatory effects of (S)-nicotine on the cardiovascular system are complex and involve a number of integrated physiological processes. Through its adrenergic stimulating properties, (S)-nicotine activates peripheral chemoreceptors in the central nervous system as well as the medullary center of the brain. These actions in the brain lead to the direct release of epinephrine which, in the periphery, results in the release of catecholamines.

The direct action of (S)-nicotine on the peripheral ganglia results in the stimulation of sympathetic and/or parasympathetic nerves.<sup>12</sup> At larger doses stimulation of the sympathetic ganglia can result in ganglionic transmission blockade.<sup>12</sup> (S)-Nicotine also stimulates the parasympathetic ganglia and thus exerts muscarinic like activities, especially in the gastrointestinal tract and eye. (S)-Nicotine stimulates the chemoreceptor trigger zone of the medulla oblongata and the vagus nerve to produce nausea and vomiting. Neural adrenergic stimulation is responsible for the release of norepinephrine from the hypothalamus. (S)-Nicotine also induces cutaneous

**vasoconstriction** and systemic venoconstriction with a consequent decrease in skin **temperature**. (S)-Nicotine produces an alerting pattern in electroencephalograms, **decreases** skeletal muscle tone and deep tendon reflexes. (S)-Nicotine also stimulates **the release** of antidiuretic hormone, cortisol and growth hormone from the pituitary **gland**.<sup>15</sup> The stimulation of the adrenal glands by (S)-nicotine results in the release of **epinephrine** into the general circulation. (S)-Nicotine also affects carbohydrate and fat **metabolism**. Through its catecholamine releasing activity, (S)-nicotine has been shown **to increase** the levels of plasma free fatty acids and to elevate the secretion of very low **density lipoprotein (VLDL) triglycerides**.<sup>16</sup>

## **Toxicology of (S)-Nicotine**

### **Cigarette Smoking and (S)-Nicotine**

Cigarette smoking is the major preventable cause of mortality and health **disability** in the United States.<sup>17</sup> Despite increasing efforts to educate the public about **the health** hazards of smoking, cigarette consumption in the United States still remains **high**. The mortality rate for lung cancer continues to increase, particularly among **women**.<sup>18</sup> Cigarette smoking contributes to coronary heart disease, chronic bronchitis and **emphysema**, and various cancers. Maternal smoking is associated with low infant **birth weight**, increased perinatal mortality and complications of pregnancy.<sup>19</sup>

Within the past several years, concern over the contribution of (S)-nicotine to **the health** hazards of cigarette smoking has prompted a number of studies aimed at **assessing** its toxicological properties. In addition to cigarettes, other sources of (S)-**nicotine** such as chewing tobacco and snuff have recently gained increased **popularity**.<sup>20,21</sup> Studies have indicated that smokeless tobaccos are a major risk factor for **oral cancer**.<sup>22</sup> The unusually high rate of oral cancers associated with the high **prevalance** of smokeless tobacco usage in the Asian Indian population supports this **conclusion**.<sup>23,24</sup>

The highly addictive nature of cigarettes and smokeless tobaccos has been attributed to (S)-nicotine. In fact, studies have indicated that individuals regulate cigarette smoke inhalation in order to maintain plasma levels of (S)-nicotine satisfactory to their needs.<sup>25</sup> Therefore, in subjects given low (S)-nicotine cigarettes, inhalation patterns are changed to accommodate an increased intake of this substance. It is because of this strong physiological dependence that (S)-nicotine chewing gum is used to assist people to stop smoking.<sup>26</sup> Recent evidence indicates that the release of endorphins by (S)-nicotine may contribute, in part, to this addiction.<sup>27</sup>

### **Smokeless Tobacco**

In the United States, the predominant forms of smokeless tobacco are chewing tobacco and snuff. In 1985, it was estimated that in this country there were approximately 12 million users of smokeless tobacco, age 12 or older. Epidemiologic, experimental and clinical data which have been related to oral use of smokeless tobacco indicate that this practice is a significant health risk. Use of smokeless tobacco has been proposed as a risk factor for cancer especially those of the oral cavity.<sup>28</sup>

### **Cytogenetic Effect of (S)-Nicotine**

Bishun *et al.*<sup>29</sup> studied the cytogenetic effects of (S)-nicotine *in vitro* on human leucocytes in culture and *in vivo* in mice. *In vitro*, (S)-nicotine did not exhibit any chromosomal damaging activity, although it was found to contribute to the cytotoxicity of the cultured leucocytes. However, in the *in vivo* mouse studies, gross chromosomal aberrations were noted, including fuzzy chromosomes, aneuploidy and translocations. The relatively high frequency of aneuploid cells and translocations into the acrocentric chromosomes supports the possibility that (S)-nicotine could be acting as a genotoxic agent.

**The Effects of (S)-Nicotine on Lung Tissue**

The effects of (S)-nicotine on lung tissue have been examined. In a recent study, **the effect** of pre- and/or postnatal exposure to (S)-nicotine on neonatal mouse lungs **was examined** using cumulative scanning electron microscopic analyses. When the **offspring** from (S)-nicotine exposed and control mice were cross-fostered at birth and **analyzed** by scanning electron microscopy, it was found that newborn mice which were **born to** and/or fostered by (S)-nicotine exposed mothers developed large and irregular **nodular** mucosal bulges (neuroepithelial bodies) and possessed bronchioles which were **tortuous**.<sup>30</sup> Newborn mice who were exposed to intermediate levels of (S)-nicotine, **that is**, born to exposed mothers but cross fostered by control mothers or born to control **mothers** but fostered by (S)-nicotine exposed mothers, exhibited fewer of these **pulmonary** abnormalities. Mice who were not exposed to (S)-nicotine did not display **these** morphological changes. These structural deviations, which were originally **observed** 5 days postpartum, disappeared by day 30 if the exposure to (S)-nicotine was **discontinued** at birth. Although these authors did not offer an explanation for these **effects**, the alterations observed may be due to the cholinergic stimulating properties of **(S)-nicotine**. Further studies will be required to determine the causes of these **pathological** alterations.

The effect of (S)-nicotine on the pathogenesis of experimental emphysema was **examined** in rats. In this study, a relatively high dose (3 or 7.5 mg/kg) of (S)-**nicotine**, administered to rats by endotracheal instillation, did not lead to any structural **changes** indicative of emphysema. Furthermore, (S)-nicotine did not enhance or **accelerate** the development of pancreatic elastase induced emphysema. Therefore, the **acute**, one-time, administration of (S)-nicotine does not appear to promote the **development** of emphysema nor does it influence experimentally induced emphysema.



**However**, the effects of long term chronic administration of (S)-nicotine on this toxic **endpoint** still remain to be examined.

### **Carcinogenic Effects of (S)-Nicotine**

Toth *et al.*<sup>31</sup> investigated the long term administration of (S)-nicotine on the **development** of tumors in mice. Solutions of 0.94 and 0.63 mg/ml (S)-nicotine **hydrochloride** were administered to 5-7 week old mice in drinking water for the **remainder** of their lifespan. The authors focused specifically on the identification of **lung**, lymph gland and blood vessel tumors. Treatment of these animals with (S)-**nicotine**, at the concentrations indicated above, did not result in any acute toxicities nor **did this** compound affect their lifespan. When compared to untreated controls, **significant** differences in the occurrence of these various tumors were not observed. **Therefore** it was concluded that (S)-nicotine, at least under the conditions used in this **study**, did not enhance tumor formation.

### **Effects of (S)-Nicotine on Tumorigenesis when Co-Administered with Known Carcinogens**

Bock,<sup>32</sup> reported that (S)-nicotine enhanced the tumorigenic activity of **benzo[a]pyrene** when assayed in a mouse skin carcinogenicity test. In these studies, 0.2 ml of a test solution containing 10 µg of benzo[a]pyrene and 0.6 µg of the tumor **promoting** agent 12-O-tetradecanoylphorbol-13-acetate (TPA) per ml was applied ten **times** a week to the skin of ICR Swiss female mice for a period of 39 weeks. In order to **test** the effects of (S)-nicotine on the carcinogenicity of benzo[a]pyrene, this **experimental** test solution was supplemented with 2.5 and 5.0 mg (S)-nicotine/ml. **Comparisons** between the group of mice receiving the (S)-nicotine supplemented **solution** showed a significant increase in the number of skin tumors formed (49% for the **control** group receiving a benzo[a]pyrene/TPA solution versus 78 and 82% tumor

incidence for the mice treated with 2.5 and 5.0 mg of (S)-nicotine/ml benzo[a]pyrene/TPA solution, respectively;  $p < 0.001$  in both cases). In contrast, when benzo[a]pyrene/TPA solutions containing 2.5 and 5.0 mg cotinine/ml were prepared, the tumor incidence was 58% ( $p$  value was not statistically significant compared to control) and 64% ( $p < 0.03$ ), respectively. Treatment of mice with the benzo[a]pyrene/TPA solutions containing 2.5 and 5.0 mg (S)-nicotine N'-oxide led to a lower tumor incidence of 22% ( $p < 0.001$ ) and 27% ( $p < 0.01$ ) compared to control. Additional studies suggested that the enhanced tumor formation observed when (S)-nicotine was co-applied with benzo[a]pyrene and TPA was not due to initiation or promotion activity on the part of this tobacco alkaloid. The conclusions drawn from this study indicate that (S)-nicotine is a co-carcinogen when applied to mouse skin in conjunction with the tumor initiator benzo[a]pyrene and the tumor promoter TPA. The effects of cotinine indicates that its contribution to (S)-nicotine co-carcinogenesis is minor. (S)-Nicotine N'-oxide when applied to mouse skin in conjunction with benzo[a]pyrene/TPA solution inhibited skin tumor formation and thus is not likely to contribute to the co-carcinogenic effects of (S)-nicotine described above.

(S)-Nicotine has been shown to influence the development of experimental stomach tumors. (S)-Nicotine was shown to enhance N-methyl-N'-nitro-N-nitrosoguanidine (MNNG) induced stomach tumors in rats.<sup>33</sup> Compared to MNNG treatment alone, the long-term administration of MNNG and (S)-nicotine together led to an earlier development of stomach cancer, a two-fold increase in the frequency of tumor development, a progressive decrease in acetylcholinesterase activity and pretumor changes in the whole mucous membrane of the stomach. The mechanism of the action of (S)-nicotine on the enhancement of MNNG induced tumorigenesis was not determined. The authors of this study discuss the possible role of the autonomic nervous system in this effect. Based on its documented co-carcinogenic activity, it is reasonable that (S)-nicotine could be serving a similar role in MNNG induced cancers.

### **Mutagenic Activity**

Florin *et al.*<sup>34</sup> reported on the mutagenicity of a number of tobacco smoke constituents using the Ames test. The tester strains utilized in these studies included TA 98, 100, 1535 and 1537. Of the 239 compounds tested only 9 were found to be mutagenic. (S)-Nicotine and  $\beta$ -nicotyrine were among those compounds which did not exhibit any mutagenic activity in the presence or absence of the bioactivating system containing S9 fraction.

In a separate report, Riebe *et al.*<sup>35</sup> tested the mutagenic activity of various tobacco alkaloids including (S)-nicotine and  $\beta$ -nicotyrine by the Ames assay and the *E. coli* pol A<sup>+</sup>/pol A<sup>-</sup> system. Neither (S)-nicotine nor  $\beta$ -nicotyrine was found to be mutagenic in the Ames assay using the tester strains TA98, 100 and 1537. However, both compounds gave positive results in the *E. coli* pol A<sup>+</sup>/pol A<sup>-</sup> system which is used as a rapid test for the detection of repairable DNA modifications. The contrasting conclusions drawn from these two tests make it difficult to assign either compound as a mutagen. Nevertheless, the positive results obtained from the *E. coli* polA<sup>+</sup>/polA<sup>-</sup> system should encourage further investigations on the mutagenic potentials of these two tobacco alkaloids.

### **Effects on Pregnancy**

The effects of (S)-nicotine on pregnancy and fetal development has been examined in rats.<sup>36</sup> In this study, (S)-nicotine was administered twice daily throughout the gestation period at doses of 1, 3 and 5 mg/kg. At doses of 3 and 5 mg/kg, birth weights of the offspring were lower, fewer offspring survived and maternal weight gain during the course of the 21 day pregnancy was less than that of untreated pregnant control rats. In a second set of experiments, (S)-nicotine was administered during the first 8 days of gestation and was found to produce effects on the mother and fetuses

**similar** to the 21 day treatment. Therefore, (S)-nicotine appears to diminish **substantially** the capacity of the pregnant rat to reproduce normally.

In a separate study, male mice were fed (S)-nicotine for 20 weeks and mated **with** untreated female mice.<sup>37</sup> According to this report, (S)-nicotine consumption **resulted** in gross anatomical deformities in fetuses of mice which had been inseminated **with** the sperm from the (S)-nicotine treated male mice. As the time between the **termination** of (S)-nicotine treatment and insemination of the female mice increased the **incidence** of teratogenicity decreased. When female mice were inseminated with sperm **from** male mice treated for only 7 weeks, no teratogenic effects were observed in the **offspring**. The author proposed that prolonged exposure to (S)-nicotine may result in a **cumulative** teratogenic action on spermatids and spermatozoa.

### **Hypersensitivity**

(S)-Nicotine may be responsible for some of the allergies associated with **exposure** to tobacco and cigarette smoke. In one report, the *in vitro* human basophil **degranulation** test gave positive results when either tobacco or nicotine coupled to human **serum** albumin was used. It was concluded by these authors that nicotine may be a **contributing** factor for some cases of tobacco induced dermatitis.<sup>38,39</sup>

### **Atherosclerosis**

(S)-Nicotine has been shown to be associated with the development of **atherosclerotic** lesions. The mechanism by which (S)-nicotine accelerates this disease **process** is not completely clear. It has been postulated that atherosclerosis may be **mechanically** induced through intimal damage and possibly hypoxia. The involvement of (S)-nicotine in atherogenesis could be related to several of its pharmacological and **biochemical** effects on the cardiovascular system. For example, it is known that (S)-**nicotine** increases catecholamine release, which in turn, has been related to an increase

**in the** release of free fatty acids and very low density lipoprotein triglycerides (VLDL), **components** which contribute to atherosclerotic plaque formation.<sup>16</sup> (S)-Nicotine also **increases** platelet aggregation,<sup>40</sup> an effect probably related to its inhibition of **prostacyclin** (PGI<sub>2</sub>) formation, the prostaglandin responsible for inhibiting platelet **aggregation**.<sup>41,42</sup> The ability of (S)-nicotine to inhibit selectively PGI<sub>2</sub> synthesis **severely** alters the balance between this substance and thromboxane (TxA<sub>2</sub>), a **prostaglandin** which stimulates platelet aggregation. As a consequence of this imbalance **platelet** aggregation is stimulated, thus increasing the likelihood of atherosclerotic **plaque** formation.

The studies described above indicate that (S)-nicotine may contribute to some of the **diseases** associated with the usage of tobacco products. In some reports, however, (S)-nicotine appears to have little if any effect on the toxic endpoint measured. For **example**, it does not appear to be a mutagen in the Ames assay, nor does it appear to be a **direct** initiator of skin tumors as measured in a mouse skin carcinogenicity assay. It **also** does not appear to play a causal role in emphysema. Because of the nature of these **studies** and the potent acute toxicities associated with (S)-nicotine, it is difficult to **address** certain questions related to the chronic toxicological properties of this alkaloid. **Certain** experiments which may be useful in answering critical questions about its **chronic** toxicological potential remain to be performed. For example, the effect of (S)-**nicotine** administered over the course of a lifetime on the lung tissues of experimental **animals** has not been examined. Although the cocarcinogenic effect of (S)-nicotine has **been** examined using skin and stomach as target tissues, no attempt has been made to **assess** this activity in the lung, one of the major target organs affected by cigarette **smoking**. However, the acutely toxic nature of (S)-nicotine makes it difficult, if not **impossible**, to test the chronic toxicity or carcinogenicity of this compound at **concentrations** which may be required to observe over a reasonable study period the **proposed** toxic endpoint, such as tumor formation. The apparent lack of pharmacological

activity of a number of carcinogens or other types of toxic agents for example, permits one to dose experimental animals with enormous amounts of these substances relative to those of (S)-nicotine. It is possibly because of these latter considerations, that the long term *in vivo* chronic toxicity studies of (S)-nicotine have not yet been performed. It is in part due to these limitations that the approaches taken in this dissertation were pursued.

### **Autoradiographic Studies with Radiolabeled (S)-Nicotine**

Lindquist *et al.*<sup>43</sup> used autoradiographic techniques to demonstrate that intravenous infusion of <sup>14</sup>C-(S)-nicotine, labeled in the N-methyl group, led initially to the localization of radioactivity in highly perfused organs such as the lungs, brain and adrenal glands. However, 1 hr following the administration of this compound the predominate site of <sup>14</sup>C-(S)-nicotine accumulation was in the respiratory tract which included the nasal mucosa, larynx, trachea and bronchi. Radioactivity present in the respiratory tract was reduced but still significant after 30 days. The skeletal muscle, myocardium, urinary bladder and melanin containing tissues also displayed a persistent localization of radioactivity after this period.

In a follow up study, Waddell *et al.*<sup>44</sup> confirmed the preferential localization of (S)-<sup>14</sup>C-nicotine (labeled in either the N-methyl or 2'-carbon atom) in the tissues described earlier by Lindquist. In contrast to the observations of Lindquist *et al.*,<sup>43</sup> (S)-<sup>14</sup>C-cotinine did not localize in any specific tissue. (S)-<sup>14</sup>C-nicotine N'-oxide did not localize in the bronchial or nasal epithelium during the first 6 minutes following the administration of this radiolabeled compound. However, after 1 hr radioactivity associated with (S)-nicotine N'-oxide was found to accumulate in these tissues. The authors suggested that the N'-oxide may have been reduced to (S)-nicotine, the compound which they proposed was being accumulated. Interestingly, in a separate study, the accumulation of radioactivity 4 days following the intravenous administration of these compounds was found to be approximately 15 times greater for (S)-nicotine labeled in the N-methyl position than for the (S)-2'-nicotine derivative.<sup>45</sup> Although an explanation for this finding was not provided, this result is consistent with the irreversible association of radiolabeled formaldehyde derived from the N-demethylation of (S)-nicotine. The observation that the derivative labeled at the 2'-carbon atom also accumulates, although to a lesser degree, indicates that (S)-nicotine or one of its

metabolites may irreversibly associate with biomacromolecules present in the mouse lungs.

Evidence for the metabolism dependent accumulation of radiolabeled (S)-nicotine in the bronchial epithelium was equivocal. Pretreatment of mice with metyrapone, a cytochrome P-450 inhibitor and ligand,<sup>46</sup> prevented accumulation of radiolabeled (S)-nicotine in the lung tissue, a result which supports the proposal that cytochrome P-450 mediates the oxidation of (S)-nicotine to bioalkylating species.<sup>47</sup> Progesterone, a cytochrome P-450 substrate, also inhibited the accumulation of (S)-nicotine, although to a lesser degree than metyrapone. Pretreatment with piperonyl butoxide or SKF 525-A, classical inhibitors of cytochrome P-450, was found to be ineffective in preventing this accumulation. However, the time between the administration of piperonyl butoxide and radiolabeled (S)-nicotine (30 min) may not have been sufficient for the inhibition of cytochrome P-450 activity to be observed. The ineffectiveness of SKF 525-A as an inhibitor of this accumulation may have been due to its poor access to the lung cytochrome P-450 enzymes. Alternatively, SKF 525-A may not have been a good inhibitor of the isozyme which catalyzes the metabolism of (S)-nicotine or a proximate bioalkylating metabolite of (S)-nicotine. Because of the ambiguous nature of these results further studies will need to be performed in order to address the question of whether the persistent localization of (S)-nicotine in lung tissue is dependent on cytochrome P-450. In addition, tissue slices isolated from the lungs of mouse and rabbit exhibited the selective uptake of (S)-<sup>14</sup>C-nicotine into the bronchi observed in the *in vivo* studies. Freezing the tissue slices abolished the selective accumulation of (S)-<sup>14</sup>C-nicotine. However, the accumulation of (S)-<sup>14</sup>C-nicotine remained unchanged when the inactivation of lung enzymes by microwave heating for 10-20 seconds was attempted.

In contrast to the lung, the brain, which contains very low concentrations of this enzyme,<sup>48</sup> did not accumulate radioactivity. Unlike the adult mice, (S)-nicotine did not



appear to localize in the bronchi of fetuses and 1 day old newborn mice. The difference in the localization of (S)-nicotine in these tissues at different ages is not known but may reflect an underdeveloped xenobiotic metabolizing system in the younger animals.<sup>44</sup> Evidence for the age dependent onset of lung cytochrome P-450 monooxygenase activity has been observed in rabbits<sup>49</sup> and hamsters<sup>50</sup> and thus supports further the notion that (S)-nicotine localization in this tissue may be cytochrome P-450 dependent.

Szűts *et al.*,<sup>45</sup> using whole-body autoradiographic techniques similar to those employed by Waddell *et al.*,<sup>44</sup> showed that N-<sup>14</sup>C-methyl and 2'-carbon atom labeled (S)-<sup>14</sup>C-nicotine were retained in the bronchial walls as well as the urinary bladder wall and melanin containing tissues of C57BL and NMRI mice for a period of up to 1 month after the administration of these radiolabeled compounds. Thin-layer chromatographic studies of the lung tissue showed that (S)-nicotine was not present after 24 hr indicating that the persistent localization of the radiolabel was most likely due to a metabolite of this substance. In contrast, (S)-nicotine was recovered intact from melanin. The most persistent localization of radiolabel in both the lung and urinary bladder occurred with (S)-N-<sup>14</sup>C-methylnicotine. Quantitation of radioactivity associated with lung tissue showed that (S)-nicotine labeled at the 2'-carbon atom position decreased more rapidly than that of the N-methyl derivative. Taken together, the studies by Waddell and Szűts support the possible involvement of formaldehyde derived from (S)-nicotine N-demethylation in the bioaccumulation process. In addition, lung metabolism of (S)-nicotine to other electrophilic intermediates, including the two iminium ions mentioned previously, may lead to covalent interactions with biomacromolecules. The persistent, although quantitatively lower, binding of (S)-<sup>14</sup>C-nicotine labeled at the 2'-carbon atom may be explained by covalent interactions with such reactive intermediates.

The localization of (S)-<sup>14</sup>C-nicotine in the bronchi of mice treated with this radiolabeled substance has been documented in a number of reports.<sup>43,45</sup> The

observation that this accumulation occurs in the small bronchi is consistent with its possible distribution in the cytochrome P-450 rich Clara cells. Furthermore, the accumulation of radioactivity observed in perfused rabbit lungs appeared to be selectively localized in the smaller bronchi (bronchioles). Indeed, radiolabeled (S)-nicotine was not detectable in the larger bronchi. Interestingly, the covalent binding of reactive metabolites of 4-ipomeanol, a well studied lung toxin which will be described in Chapter VI, exhibited a similar distribution in mouse lungs. In this study, the bronchiolar covalent binding and cellular necrosis caused by reactive metabolites of 4-ipomeanol became more pronounced as the airway size decreased. Therefore, at low doses which caused cellular necrosis, covalent binding of 4-ipomeanol was restricted to the smallest airways whereas the larger airways were affected only at larger doses. The apparent difference in the localization of radioactivity was suggested to reflect a greater proportion of Clara cells in the smaller airways than in the larger, less sensitive bronchi. Collectively these observations suggest that (S)-nicotine is likely to localize in the mouse and rabbit bronchiolar Clara cell population. In addition, the observation that the selective accumulation of (S)-nicotine can be inhibited by the cytochrome P-450 inhibitor metyrapone and the observed lack of its accumulation in the lungs of immature animals which apparently contain low cytochrome P-450 activity, suggest that the persistent localization of (S)-nicotine described in the studies above may be dependent on xenobiotic metabolizing enzymes, such as the cytochrome P-450 monooxygenases, present in this cell population.

Despite the large contribution of the liver to the metabolism of (S)-nicotine, long term retention of (S)-nicotine metabolites was not observed in this tissue.<sup>43</sup> An explanation for the apparent lack of bioaccumulation in the liver was not given by the investigators mentioned above. In view of the high monooxygenase activity in this tissue and our proposal that oxidative metabolism may contribute to the bioactivation of (S)-nicotine to intermediates which interact irreversibly with tissue macromolecules, it

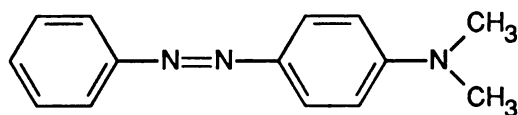
seems surprising that radiolabeled derivatives of (S)-nicotine do not also accumulate in the liver. However, as described in greater detail in Chapter IV, the enzyme which may play a detoxification role appears to be in much higher concentrations in the liver than in the lung and perhaps other extrahepatic tissues as well.

## **Bioactivation**

Enzymes capable of oxidatively metabolizing foreign compounds play an important role in the body. Enzymes which participate in these reactions include, but are not limited to, the cytochrome(s) P-450 and the flavin containing monooxygenases (FCM). In general, the reactions catalyzed by these enzyme systems produce metabolites which are more polar and more readily eliminated from the body than the parent compound. Thus these enzymes are, in large part, responsible for eliminating foreign compounds which could otherwise accumulate in the body and possibly interfere with normal cellular functions. Often, however, they may also catalyze the oxidation of foreign compounds to metabolites which are highly reactive and which bind covalently to tissue macromolecules, a process referred to as metabolic activation or bioactivation. The extent of covalent binding in many instances has been shown to be directly correlated with the severity of the xenobiotic induced toxicity. It has therefore been proposed that the irreversible interactions between the bioactivated compound and critical biomacromolecule(s) may be a requirement for the expression of many chemically induced toxicities.

### **Bioactivation, an Historical Perspective**

By the mid-1960's, the Millers had popularized the concept that cancer could be caused by modification of DNA by chemically reactive substances formed through the enzyme catalyzed oxidation of the parent compound.<sup>51</sup> These concepts, which were developed through their pioneering studies in the late 1940's, led to investigations aimed at characterizing the possible mechanisms of N,N-dimethyl-4-aminoazobenzene (DAB) (45) induced liver cancer in rats.



45

Because of the severe limitations in the analytical techniques (radiolabeled carcinogens were not introduced until a few years later) and instrumentation available at the time of these studies, the Miller's chose to investigate the cancer inducing properties of a compound which was readily detectable by visible spectrophotometry. Because of the high extinction coefficients characteristic of the azo dyes, the rat hepatocarcinogen DAB (45) was chosen for study in their early investigations on metabolic activation. During the course of these studies, it became evident that DAB became irreversibly bound to liver protein of rats following its administration. This conclusion was based on the observation that the administered aminoazo dye retained the indicator properties of the parent compound but could not be released from liver protein following trichloroacetic acid precipitation. The irreversible binding of the DAB derived compound was interpreted as an indicator of a reaction possibly involved in tumor formation. Further studies indicated that the level of covalent binding of a series of aminoazo dyes was correlated with their known carcinogenic potency. In addition, the greatest level of covalent binding was in the liver, the principal target organ for cancers induced by this series of compounds. In the years that followed, fluorescent derivatives of benzo[*a*]pyrene were found to bind covalently to protein. In the early 1950's, when radiolabeled compounds became available, [<sup>14</sup>C]dibenz[*a,h*]anthracene and 2-[<sup>14</sup>C]acetylaminofluorene were found to form protein bound adducts.<sup>52,53</sup>

In 1953, at about the time the studies on carcinogen-protein bound adducts were being performed, new insights on the informational role of DNA was advanced by Watson and Crick.<sup>54</sup> The identification of the possible manner in which DNA could pass genetic information on to newer generation of cells prompted a number of researchers to pursue studies aimed at the identification of DNA-carcinogen adducts formed *in vivo*. By the

early 1960's, these studies led to the identification and characterization of a number of DNA adducts which included those formed from derivatives of sulfur mustard, dimethylnitrosamine, ethionine, 2-acetylaminofluorene, DAB and polycyclic aromatic hydrocarbons (PAH's).<sup>55</sup>

In the late 1940's, the availability of techniques which allowed the isolation of enzymatically active cellular subfractions facilitated the study of the metabolism of carcinogenic compounds. In 1948, Mueller and Miller reported that DAB (45) was subject to N-demethylation and aromatic ring hydroxylation reactions during aerobic incubation of this compound in the presence of rat liver homogenate and pyridine nucleotides.<sup>56</sup> These initial studies were followed by the identification of the endoplasmic reticulum derived microsomes as the cellular subfraction responsible for catalyzing the cleavage of the azo linkage.<sup>57</sup> NADPH and O<sub>2</sub> were found to be necessary cofactors for this reaction.<sup>58</sup> Soon after these findings, microsomes were found to catalyze a number of oxidative reactions including N-dealkylation and ring hydroxylation.<sup>59,60</sup> The use of microsomes for studying the *in vitro* metabolism and bioactivation of carcinogenic compounds has since become a very popular technique, one which has been used extensively in work described in this dissertation.

Several reports have now documented a possible link between enzyme dependent oxidation of foreign compounds to cancers and other toxicities, including hepatotoxicity, bone marrow aplasia, methemoglobinemia and hemolysis, and renal and pulmonary toxicity.<sup>61</sup> Many compounds have been demonstrated to undergo such biotransformations. The carcinogenic compounds benzo[a]pyrene, aflatoxin B<sub>1</sub> and N-nitrosamines all appear to require metabolic activation to produce intermediates which react irreversibly with critical biomacromolecules such as DNA and which presumably are necessary for their toxicological properties. The hepatotoxic compounds acetaminophen, furosemide, isoniazid and the pyrrolizidine alkaloids also appear to require bioactivation to produce their respective toxicities in experimental animals.<sup>61</sup>

Derivatives of furan, such as 4-ipomeanol, are bioactivated to intermediates which damage lung tissue in animals containing pulmonary cytochrome P-450 monooxygenase activity. Bone marrow aplasia, methemoglobinemia and hemolysis, diseases suspected of being caused by the bioactivation of benzene and aromatic amines, respectively, have also been reported.<sup>62</sup>

Many of the concepts on the bioactivation of foreign compounds originally developed by the Millers in the 1940's and 1950's have become widespread. Several of the compounds which are suspected of producing chronic toxicities such as cancer and cellular lesions have been shown to be readily metabolized to intermediates which are electrophilic in nature. These electrophilic metabolites appear in many instances to react with cellular nucleophiles. The most commonly used index for detecting the reactivity of these compounds therefore is covalent binding of the metabolically activated species to biological macromolecules. This assay, which utilizes radiolabeled compounds, involves measuring radioactivity which has become irreversibly associated with protein or DNA following administration of the compound to experimental animals or addition to incubations with metabolically active enzymes. This assay is convenient and is extremely sensitive, permitting the quantitation of irreversibly bound substances at the level of pmole/mg of protein or DNA. Some of the criteria which are used to characterize metabolism dependent covalent binding include demonstrating a parallel increase or decrease in the level of this binding with pretreatments which are known to modulate the concentration of the enzymes involved, demonstrating a decrease in the level of this binding with inhibitors of these enzymes, the requirement for molecular oxygen and time dependency of the reaction.

### **Bioactivation of Tertiary Amines**

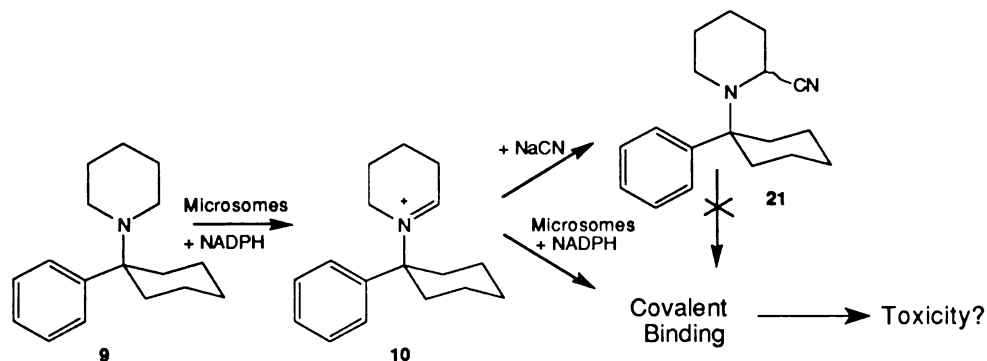
The toxicities associated with a number of tertiary amines has been proposed to be related to the metabolism of these compounds to their respective iminium ion

species.<sup>63</sup> The reactive nature of these electrophilic intermediates has encouraged a number of studies aimed at assessing their bioalkylation properties.<sup>64,65,66</sup> This group of compounds include the psychoactive street drug phencyclidine (PCP), the Parkinson's disease inducing neurotoxicant 1-methyl-4-phenyl-1,2,3,6-tetrahydropyridine (MPTP) and the hepatocarcinogen methapyrilene.

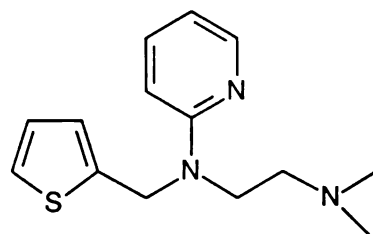
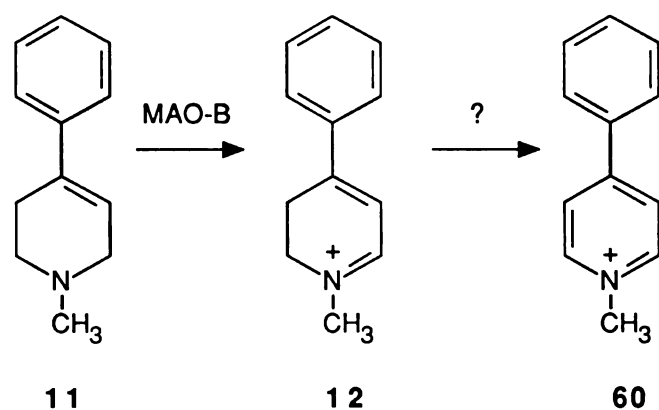
Of the three tertiary amine substances mentioned above, phencyclidine has been the most well studied with regard to its bioactivation. These studies were performed in an attempt to provide a possible mechanism for the known long term psychotic effects elicited in individuals exposed to this drug. The possibility that these effects could be manifested through covalent interaction of reactive metabolites of PCP with critical biomacromolecules has led to detailed studies aimed at identifying the metabolic routes involved in the bioactivation of this tertiary amine.<sup>64,66</sup> PCP (**9**) is metabolized extensively at the  $\alpha$ -carbon position of the piperidine ring to yield a reactive and electrophilic iminium ion **10** (See Inset). Addition of the nucleophile cyanide, which effectively traps the iminium ion species **10** as the corresponding cyanoadduct **21** without inhibiting its metabolism, inhibits the covalent binding of radiolabeled PCP to microsomal macromolecules. This evidence supports the proposal that metabolic activation of PCP via the iminium ion pathway is necessary to produce the covalent binding observed. With the availability of synthetic tritium labeled PCP iminium ion, direct demonstration of its reactivity towards liver microsomal macromolecules was documented. However, when NADPH was added to the incubation mixture a 3-4 fold increase in covalent binding was observed, indicating that further metabolism of the iminium species was required to produce maximal binding. In addition, inactivation of cytochrome P-450 and irreversible inhibition of ketamine N-demethylase activity by PCP iminium ion required its further metabolism to produce these effects. These studies indicate that the ultimate reactive species of phencyclidine is formed via further oxidation of the phencyclidine iminium ion.



## Bioactivation of Phencyclidine



Recently, 1-methyl-4-phenyl-1,2,3,6-tetrahydropyridine (MPTP) (11), a contaminant of an illicit heroin substitute<sup>67</sup> and a common intermediate used in the synthesis of a number of compounds, has been shown to be a potent neurotoxicant.<sup>68</sup> Metabolic oxidation of this compound by MAO-B<sup>69</sup> results in the formation of species which are capable of irreversibly lesioning the dopaminergic cells of the substantia nigra and producing symptoms identical to those of idiopathic Parkinson's disease.<sup>68</sup> Metabolism studies which utilized rat brain mitochondrial fraction indicated that MPTP was transformed metabolically to the pyridinium species 1-methyl-4-phenylpyridinium (MPP<sup>+</sup>) (60) via the intermediacy of the corresponding iminium ion 1-methyl-4-phenyl-2,3-dihydropyridinium (MPDP<sup>+</sup>) (12). The inhibition of this 2 electron oxidation reaction by the MAO-B inhibitors pargyline and deprenyl was shown to prevent the expression of neurotoxicity, thus illustrating the requirement of MAO-B in the bioactivation of this tertiary allylamine.<sup>70</sup>



13

The H<sub>1</sub> antagonist methapyrilene (N,N-dimethyl-N'-2-pyridyl-N'-[2-thienylmethyl]-1,2 ethanediamine) (13), was available for many years until its hepatocarcinogenic activity in rats was reported.<sup>71</sup> Studies aimed at determining the mechanism of methapyrilene induced liver cancers revealed that this drug was bioactivated to reactive intermediates which covalently bound to protein. For many years this hepatocarcinogen was regarded as a nongenotoxic carcinogen since it was inactive in short term mutagenesis tests and did not appear to bind covalently to DNA. Recent *in vitro* studies by Lampe *et al.*,<sup>72</sup> however, show that methapyrilene binds to DNA in a reaction catalyzed by cytochrome P-450. The reactive intermediate responsible for the covalent binding of methapyrilene has not yet been identified. Studies on the metabolism of this compound, however, have identified several metabolites which have been postulated to be formed via the intermediacy of reactive iminium ions. The identity of one of the proposed iminium species was confirmed

through the characterization of an isolable and stable cyanoadduct formed in metabolic incubation mixtures containing the parent compound, sodium cyanide and liver microsomes.<sup>73</sup> In addition to the oxidations which occur at the corresponding  $\alpha$ -carbons of methapyrilene, the oxidative metabolism of the electron rich thienyl moiety of methapyrilene may result in the formation of reactive species which might contribute to the toxicity of this compound. Further discussion concerning this latter possibility are presented in Chapter VI.

The metabolism of tertiary amines to reactive intermediates is a reaction which has been documented with several compounds. Metabolically generated iminium ion intermediates may contribute to the variety of toxicities attributed to the corresponding parent compounds. The metabolism of (S)-nicotine, as described in more detail later in this chapter, proceeds via a metabolic pathway involving oxidation of the  $\alpha$ -carbon atom to form the iminium ion species which can be trapped with cyanide to produce the corresponding  $\alpha$ -cyanoamines.<sup>5</sup> The possibility that such metabolic transformations could lead also to potentially toxic bioalkylation events forms the major theme of this dissertation. The characterization of such metabolic pathways will be described in greater detail in Chapters III and V of this dissertation.

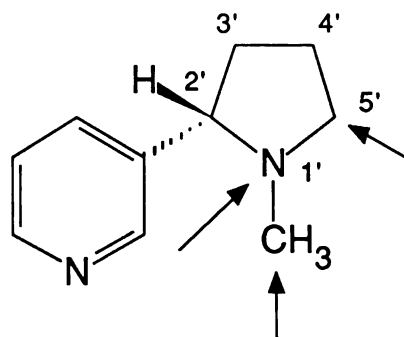
## (S)-Nicotine Metabolism

(S)-Nicotine is oxidatively metabolized in humans<sup>74</sup> as well as in a number of experimental animals including rabbits, mice, guinea pigs, cats and dogs.<sup>75</sup> Many of the *in vitro* studies on the biotransformation of (S)-nicotine have focused on the enzymes present in the liver. The importance of this organ in the overall metabolism of (S)-nicotine is perhaps best illustrated by a study which demonstrated tolerance toward the acute toxic effects of (S)-nicotine in animals dosed with nicotine which had previously been allowed to pass through the liver.<sup>76</sup> This desensitization apparently reflects the lower plasma concentrations of the toxic parent compound since hepatic enzymes metabolize (S)-nicotine to its more polar and pharmacologically less potent metabolites.<sup>77</sup> In addition to the liver, the enzymatic oxidation of this alkaloid has also been shown to be catalyzed by enzymes present in lung and kidney tissue.<sup>78,79</sup> Pulmonary metabolism of (S)-nicotine has been demonstrated in rabbits and guinea pigs although the enzyme systems responsible have not been identified.<sup>80</sup> The contribution of the pulmonary system to the overall metabolism of (S)-nicotine has been estimated to account for less than 5% of the metabolism catalyzed by liver enzymes.<sup>78</sup> Although other extrahepatic tissues are likely to contribute to the metabolism of (S)-nicotine, these activities have not yet been documented.

The *in vitro* metabolism of (S)-nicotine has been studied in liver tissue isolated from various experimental animals.<sup>81,82,83</sup> The metabolic biotransformation of (S)-nicotine has been shown to be NADPH and O<sub>2</sub> dependent and is catalyzed by two enzyme systems. The enzymes which participate in these biotransformations include the cytochrome(s) P-450,<sup>84</sup> a family of hemoproteins which form a characteristic ferrocyanide complex displaying an absorbance with a  $\lambda_{max}$  at 450 nm,<sup>85</sup> and the flavin containing monooxygenases (FCM), a group of enzymes which catalyzes the oxidation of many nitrogen and sulfur containing compounds.<sup>86</sup> Studies on the *in vitro*

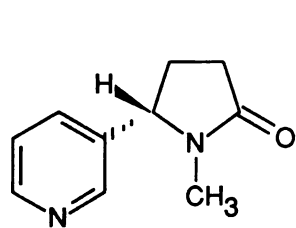
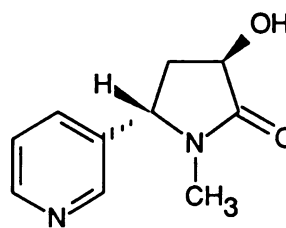
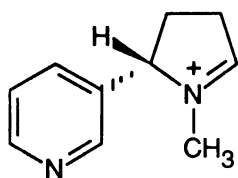
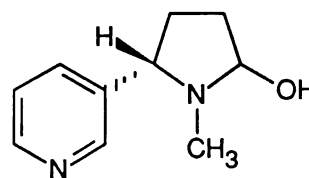
biotransformation of foreign compounds such as (S)-nicotine are usually performed with cellular fractions containing high concentrations of the respective enzymes. Cytochrome(s) P-450 and FCM are membrane bound enzymes found in the endoplasmic reticulum (ER) of various cell types. The highest concentrations of cytochrome P-450 appear to reside in the ER of hepatocytes.<sup>87</sup> The ER of lung derived Clara cells also appears to contain an appreciable amount of this enzyme.<sup>88</sup> The most easily isolable source of P-450 and FCM is the microsomal fraction of hepatocytes. Since both enzymes are found in the same tissue subfraction and are both dependent on NADPH and O<sub>2</sub> for maximal activity, it is not possible to distinguish between their activities in the overall metabolism of nitrogen containing substrates such as (S)-nicotine unless selective inhibitors of the respective enzymes are included in the metabolic incubations. For example, cytochrome P-450 can be specifically inhibited by introducing carbon monoxide into microsomal suspensions without affecting the catalytic activity of the FCM. A number of other cytochrome P-450 inhibitors have also been documented in the literature. The activity of hepatic FCM, but not cytochrome P-450 has been shown to be extremely sensitive to heat denaturation (2 min at 45°C inactivates >90% activity).<sup>89</sup> In contrast to the diversity of selective inhibitors available for the cytochrome P-450 enzymes, agents which specifically inhibit liver FCM have yet to be developed.

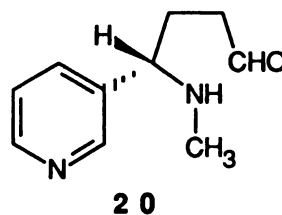
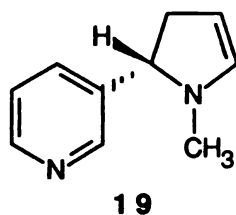
(S)-Nicotine is oxidized by liver enzymes at the pyrrolidine nitrogen atom as well as the endocyclic 5' carbon atom (see below) and the exocyclic N-methyl carbon atom. Oxidation at the 5' carbon atom represents the principal site of metabolism for (S)-nicotine in humans as well as experimental animals.<sup>4</sup> This is reflected by the recovery of (S)-cotinine (**3**) and (S)-3'-*trans*hydroxycotinine (**22**) as major urinary metabolites<sup>74</sup> which are endproducts of the initial oxidation of (S)-nicotine at the 5' position. The two electron oxidized products of (S)-nicotine, (S)-nicotine  $\Delta^{1',5'}$ -iminium ion (**2**) and (S)-5'-hydroxynicotine (**15**), have been proposed to



### Principal Sites of (S)-Nicotine Metabolism

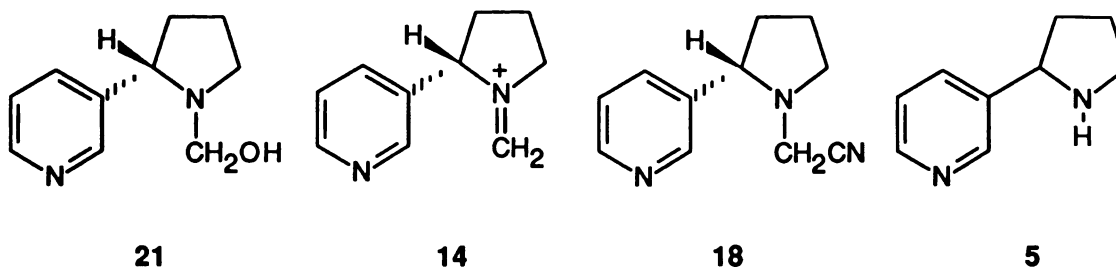
be the initial product of metabolic oxidation at the 5' position. The initial intermediate formed from this oxidation, however, has not been unambiguously characterized since both forms exist in equilibrium at physiological pH.<sup>90</sup> Furthermore, the molecular mechanism of the cytochrome P-450 catalyzed oxidation of heteroatomic compounds, which would assist in revealing the identity of an initial product, has not been satisfactorily determined. In addition to the equilibrium between (S)-nicotine  $\Delta^{1',5'}$ -iminium ion (**2**) and (S)-5'-hydroxynicotine (**15**) two other isoelectronic forms

**3****22****2****15**



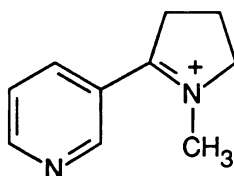
have been proposed to exist, the enamine  $\Delta^{2',3'}$ -dehydro-(S)-nicotine (19)<sup>91</sup> and the ring opened aldehyde 4-methylamino-4-(3-pyridyl)butanal (20).<sup>92</sup>

Metabolism of (S)-nicotine at the N-methyl carbon atom is thought to proceed through the intermediacy of the carbinolamine species (S)-N-hydroxymethylnornicotine (21). This metabolic intermediate, which has been proposed to exist in equilibrium with the corresponding methyleneiminium ion (14), spontaneously decomposes to form formaldehyde and the N-demethylated product nornicotine (5), a relatively minor metabolite of (S)-nicotine.<sup>93</sup> The existence of the methyleneiminium species has been confirmed in experiments which have demonstrated the formation of the stable and isolable N-cyanomethylnornicotine species (18) from metabolic incubations which have been supplemented with sodium cyanide.

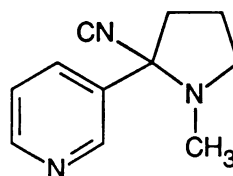


Oxidative metabolism of (S)-nicotine at the 2'-carbon atom has not been observed, perhaps because steric constraints limit the accessibility of cytochrome P-450 to this position. However, it is of interest to note that non P-450 model heme containing enzyme systems such as horseradish peroxidase, methemoglobin and

chloroperoxidase catalyze the oxidation of (S)-nicotine at the 2'-carbon atom<sup>91</sup> in addition to the two carbon atoms at the 5' and N-methyl positions. Evidence for the oxidation of (S)-nicotine at this position comes from studies where the putative nicotine  $\Delta^{1',2'}$ -iminium ion (76) is trapped with cyanide to form the isolable 2'-cyanonicotine species 24.<sup>94</sup>



76



24

The participation of cytochrome P-450 in the overall oxidation of (S)-nicotine has been demonstrated in studies utilizing inhibitors of this enzyme. For example, carbon monoxide, a specific inhibitor of cytochrome P-450, was shown to markedly inhibit the overall oxidation of (S)-nicotine and  $\alpha$ -carbon oxidation in particular.<sup>83</sup> Under these conditions, however, the recovery of (S)-nicotine N'-oxide is increased,<sup>95</sup> indicating that the carbon monoxide insensitive flavin containing monooxygenase contributes, at least in part, to the N'-oxidation of this tobacco alkaloid.

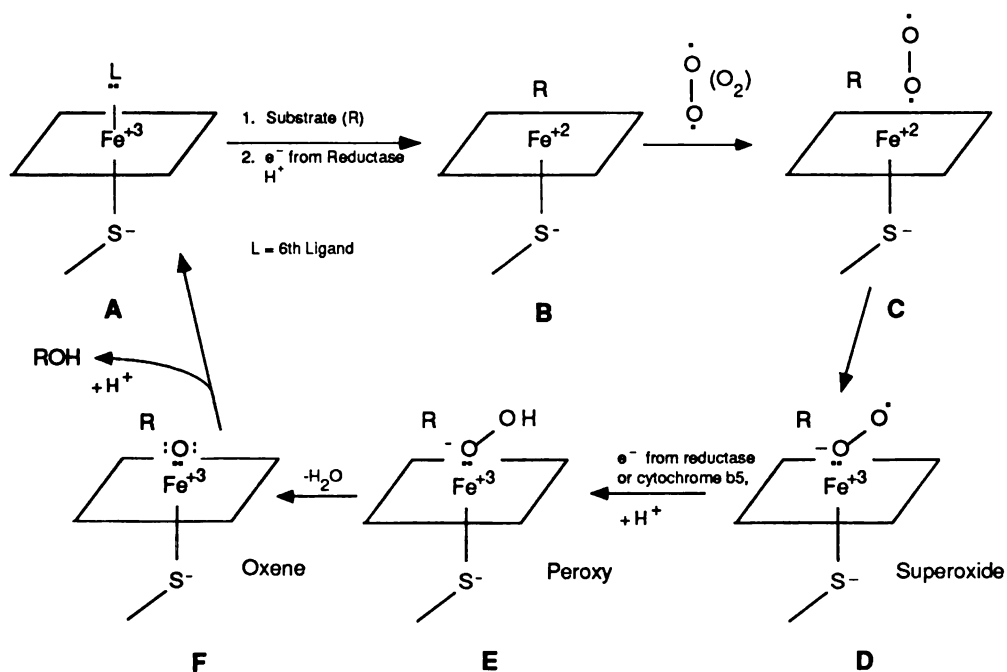
### Cytochrome P-450 Catalyzed Oxidation of (S)-Nicotine

As described above, cytochrome P-450 plays a key role in the oxidative metabolism of (S)-nicotine. The cytochrome P-450 monooxygenase system is a family of heme containing proteins comprised of two main components, the apoprotein, which has a molecular weight of approximately 50,000 daltons, and the prosthetic heme group. These two components interact noncovalently in a 1:1 ratio to form a catalytically active complex. The iron of the prosthetic heme is stabilized by four of the porphyrin nitrogen atoms which serve as ligands. A cysteinyl thiolate anion also interacts with the heme iron and is designated as the fifth ligand. The identity of the sixth ligand has not been



determined conclusively although a hydroxide anion is considered the most likely candidate.

The mechanism involved in substrate oxidation by P-450 has been studied extensively. Oxidation of substrates by this hemoprotein system is briefly summarized below (**Scheme 1.1**) and involves the following steps: Ferric P-450 binds the substrate and is then reduced by one electron via NADPH cytochrome P-450 reductase to yield a ferrous heme-substrate complex (**A** → **B**). Once the heme iron is reduced, molecular oxygen binds to produce a ternary ferrous heme-O<sub>2</sub>-substrate complex (**C**). At this point, molecular oxygen may be reduced by a single electron supplied by the

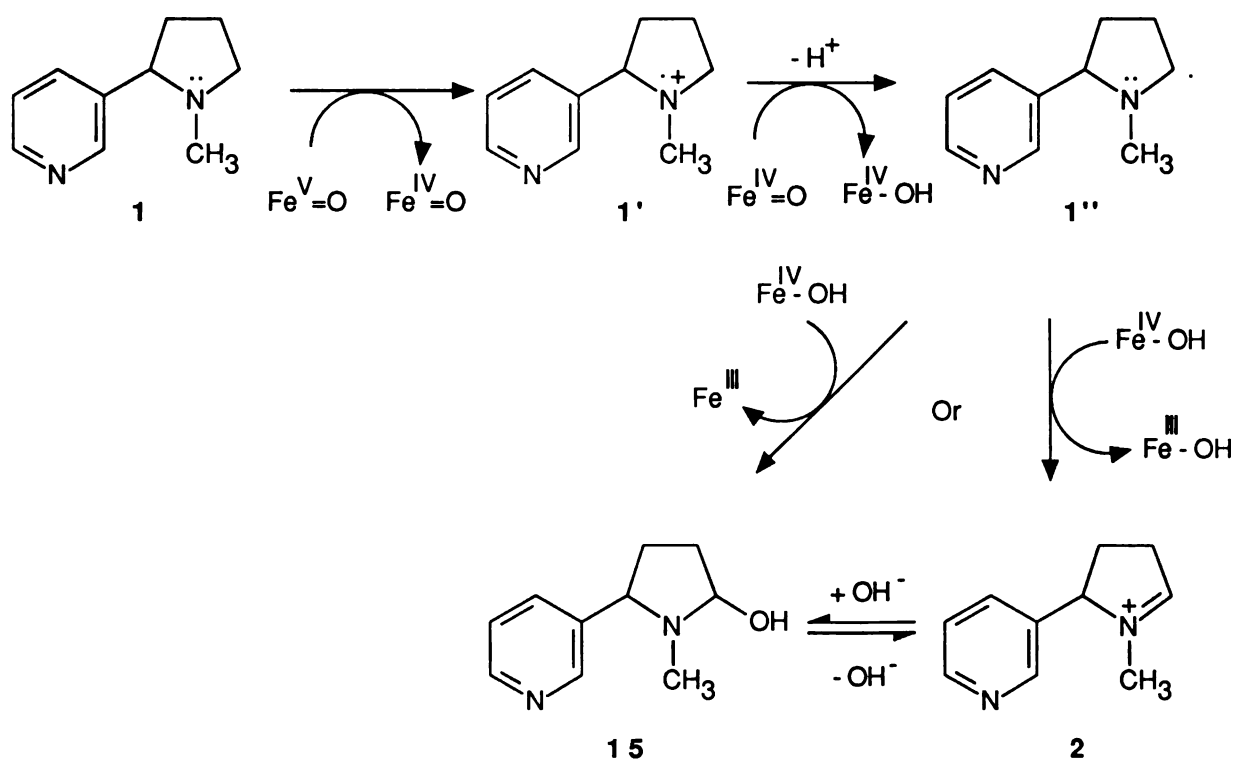


**Scheme 1.1** Proposed Activation of Molecular Oxygen by the Cytochrome P-450 Monooxygenase System

ferrous heme to produce the corresponding ferric heme-superoxide anion-substrate complex (**D**). This second electron, donated from either NADPH cytochrome P-450 reductase or cytochrome b<sub>5</sub> is believed to initiate dioxygen bond cleavage resulting in the

catalytically active form of oxygen ( $E \rightarrow F$ ). Introduction of the activated oxygen atom into the substrate molecule yields the hydroxylated product and the regenerated ferric P-450 (A). The precise details of this mechanism are not well understood since the steps which follow the introduction of the second electron produce short lived intermediates which are difficult to observe.<sup>96</sup>

The initial step in the oxidation of tertiary amine substrates appears to be the transfer of one of the heteroatom lone pair electrons to the catalytic oxygen complex. The resulting nitrogen radical cation may either combine with the activated oxygen



**Scheme 1.2** Proposed Cytochrome P-450 Catalyzed Oxidation of (S)-Nicotine to (S)-Nicotine  $\Delta^{1',5'}$ -Iminium Ion

yielding the corresponding N-oxide, or lose a proton from the  $\alpha$ -carbon to yield a heteroatom-substituted carbon centered radical which is then trapped by the activated oxygen. The resulting  $\alpha$ -hydroxylated product, identical to that expected from a conventional carbon hydroxylation reaction, in turn decomposes to produce the

dealkylation or ring opened products. In the case of (S)-nicotine, loss of hydroxide ion yields the corresponding iminium species as described above.

Cytochrome P-450 catalyzes the oxidation of (S)-nicotine in a multistep process (See **Scheme 1.2**. For brevity, only 5'-carbon oxidation is shown) which involves the following steps: An initial 1 electron transfer from the nitrogen lone pair to an electron deficient perferryl oxygen complex,  $\text{Fe}^{\text{V}}=\text{O}$  or  $(\text{FeO})^{\text{III}}$  (see **F** in **Scheme 1.1**), results in the generation of an aminium radical **1'** and a formal  $\text{Fe}^{\text{IV}}=\text{O}$  complex. Loss of a proton at either the 5'- or N-methyl carbon atom may lead to the formation of a transient carbon centered radical **1''** and a  $\text{Fe}^{\text{IV}}\text{-OH}$  complex. This radical can then recombine with the activated oxygen species, in this case the equivalent of a neutral hydroxyl radical, to yield the corresponding carbinolamines **15** or **21**, respectively. The equivalent of the carbon centered radical species **1''** could, however, conceivably give up another electron (presumably) to the  $\text{Fe}^{\text{IV}}\text{-OH}$  complex to yield the  $\text{Fe}^{\text{III}}\text{-OH}$  complex and the corresponding 2 electron oxidized species (S)-nicotine  $\Delta^{1',5'}$ -iminium ion (**2**) or (S)-nicotine methyleneiminium ion (**14**), respectively. Recombination of the iminium ion with the equivalent of a hydroxide anion would then yield the carbinolamine species **15** or **21**. Alternatively, the respective iminium ion species might escape from the P-450 pocket and later recombine with hydroxide ion present in the cytosol to give **15** or **21**. The current knowledge of cytochrome P-450 oxygen activation does not allow us to distinguish between these two possible mechanisms. Once the initial 2 electron oxidized product is formed, an equilibrium exists between the carbinolamine (S)-5'-hydroxynicotine (**5**) and (S)-nicotine  $\Delta^{1',5'}$ -iminium ion (**2**), with the later favored at pH 7.4 by a molar ratio of approximately 9:1.<sup>92</sup> In contrast, the carbinolamine formed at the N-methyl position, (S)-N-methylhydroxynornicotine, rapidly decomposes to afford the N-demethylated species nornicotine (**5**).<sup>97</sup>

### Aldehyde Oxidase Catalyzed Oxidation of (S)-Nicotine $\Delta^{1',5'}$ -Iminium Ion

The cytosolic enzyme aldehyde oxidase catalyzes the oxidation of (S)-nicotine  $\Delta^{1',5'}$ -iminium ion (2) to the corresponding lactam cotinine (3).<sup>90</sup> This enzyme, which has been extensively characterized from the livers of rabbit and pig, is a large metalloflavoprotein with a molecular weight of approximately 260,000 daltons. It is composed of two apparently identical subunits, each of which contains iron-sulfur clusters, flavin and molybdenum in a ratio of 4:1:1.<sup>98</sup> This enzyme, in contrast to the cytochrome P-450 monooxygenases, derives its oxygen equivalents from H<sub>2</sub>O instead of molecular oxygen. The ability of aldehyde oxidase to utilize H<sub>2</sub>O as the source of oxygen is believed to be due to the presence of molybdenum at the active site. This enzyme is inhibited by electron accepting agents such as menadione.<sup>99</sup> Semipurified preparations of rabbit aldehyde oxidase have been shown to oxidize (S)-nicotine  $\Delta^{1',5'}$ -iminium *bis*perchlorate with a  $K_m$  of 2  $\mu$ M.<sup>90</sup> In addition, at concentrations of 0.83 mM, (S)-nicotine  $\Delta^{1',5'}$ -iminium *bis*perchlorate completely inhibited the oxidation of 1.0 mM 3-aminocarbonyl-1-methylpyridinium chloride (N-methylnicotinamide, [NMN]), a classic substrate for this enzyme.<sup>100</sup> More detailed studies showed that (S)-nicotine  $\Delta^{1',5'}$ -iminium *bis*perchlorate competitively inhibited the aldehyde oxidase catalyzed oxidation of NMN with a  $K_i$  of 1  $\mu$ M.<sup>90</sup> At concentrations of  $\geq 0.3$  mM, (S)-nicotine  $\Delta^{1',5'}$ -iminium *bis*perchlorate has been shown to inhibit its own oxidation. Therefore, the oxidation of (S)-nicotine to one of its primary urinary metabolites, (S)-cotinine, requires the activities of two enzyme systems, the cytochrome P-450 monooxygenase system and a cytosolic aldehyde oxidase.

### N-Oxidation of Tertiary Amines by Flavin Containing Monooxygenase (FCM) and Cytochrome P-450

Flavin containing monooxygenase (FCM), an enzyme which has been isolated and purified from pig liver<sup>86</sup> and rabbit lung<sup>101</sup> catalyzes the oxidation of secondary and

tertiary amines. N-oxidation of various amine containing substrates by pig liver FCM is activated by alkylamines such as n-octylamine.<sup>102</sup> In contrast, the FCM isolated from rabbit lung is not stimulated by n-octylamine<sup>103</sup> nor does this lung enzyme catalyze the oxidation of imipramine or chlorpromazine, two of the better substrates for the pig liver enzyme.<sup>101,104</sup>

The mechanism of the FCM catalyzed oxidation of secondary and tertiary amines includes incorporation of molecular oxygen<sup>105</sup> into the enzyme followed by transfer of a single oxygen atom to the substrate molecule. FCM first binds NADPH followed by O<sub>2</sub> and finally the substrate in a sequence characterized kinetically as Ter-Bi.<sup>106</sup> The hydroperoxyflavin form is believed to be the activated form of the enzyme. The involvement of the 4a-hydroperoxyflavin radical anion intermediate in the N-oxidation reaction has been ruled out since N-oxidation of N,N-dimethylaniline did not occur via this synthetic activated form of oxygen.<sup>107</sup> Furthermore, the radical trapping agent 2,6-di-*tert*-butyl-*p*-cresol (BHT) was not effective in blocking N-oxidation.<sup>108</sup> Oxygenation of secondary and tertiary amines is thought to involve the direct nucleophilic displacement of the terminal oxygen of the hydroperoxyflavin form of the enzyme.<sup>109</sup>

Although N-oxidation of amines is thought to be catalyzed primarily by the flavin containing monooxygenase, there is evidence that cytochrome P-450 catalyzes the N-oxidation of certain substrates. This evidence includes the observation that pregnenolone-16 $\alpha$ -carbonitrile (PCN), an inducer of cytochrome P-450 and its reductase, enhances the oxidation of N,N-dimethylaniline to the corresponding N-oxide.<sup>110</sup> In addition, cobaltous chloride, an inhibitor of cytochrome P-450, was shown to inhibit the formation of N,N-dimethylaniline N-oxide. Therefore, it is apparent that cytochrome P-450 may participate in the N-oxidation of tertiary amines. Mechanistically, the insertion of oxygen by cytochrome P-450 onto the heteroatom can be easily rationalized. As already described above, following the initial transfer of one

of the heteroatom lone pair electrons to the catalytic oxygen complex, the resulting activated oxygen species may collapse to the nitrogen radical cation to yield the corresponding N-oxide.

- 
1. U.S. Department of Health and Human Services, "The Health Consequence of Smoking: Nicotine addiction a report of the Surgeon's General 1988," U.S. Department of Health and Human Services DHHS Publication No. (CDC) 88-8406 637 pp. (1988).
  2. Environmental Cancer (H.F. Kraybill and M.A. Mehlman, Ed. ) Vol. 3 in the series: Advances in Modern Toxicology, John Wiley and Sons, New York (1977).
  3. Tsokos-Kuhn, J.O., H. Hughes, C.V. Smith and J.R. Mitchell, "Alkylation of the liver plasma membrane and inhibition of the Ca<sup>2+</sup> ATPase by acetaminophen," *Biochem. Pharmacol.* **37**, 2125-2131 (1988).
  4. Murphy, P.J., "Enzymatic oxidation of nicotine to nicotine  $\Delta^{1,5}$ iminium ion," *J. Biol. Chem.* **218**, 2796-2800 (1972).
  5. Nguyen, T-L., L.D. Gruenke and N. Castagnoli Jr., "Metabolic oxidation of nicotine to chemically reactive intermediates," *J. Med. Chem.* **22**, 259-263 (1979).
  6. Brunemann, K.D. and D. Hoffmann, "The pH of tobacco smoke," *Fd. Cosmet. Tox.* **12**, 115-124 (1974).
  7. Gori, G.B., N.L. Benowitz and C.J. Lynch, "Mouth and deep airways absorption of nicotine in cigarette smokers," *Pharmacol. Biochem. Behav.* **25**, 1181-1184 (1986).
  8. Armitage, A., C. Dollery, T. Houseman, E. Kohner, P.J. Lewis and D. Turner, "Absorption of nicotine from small cigars," *Clin. Pharmacol. Ther.* **23**, 143-150 (1978).
  9. Armitage, A.K., C.T. Dollery, C.F. George, T.H. Houseman, P.J. Lewis and D.M. Turner, "Absorption and metabolism of nicotine from cigarettes," *Br. Med. J.* **4**, 313-316 (1975).
  10. Benowitz, N.L., F. Kuyt and P. Jacob III, "Circadian blood nicotine concentrations during cigarette smoking," *Clin. Pharmacol. Ther.* **32**, 758-764 (1982).
  11. Aronow, W.S., B.S. Dendinger and S.N. Rokaw, "Heart rate and carbon monoxide level after smoking high, low and non-nicotine cigarettes," *Ann. Intern. Med.* **74**, 697-702 (1971).
  12. Gunzel, K.H., "Introduction to the effects of nicotine on the central nervous system," *Ann. N.Y. Acad. Sci.* **142**, 101-120 (1967).
  13. Cryer, P.E., M.W. Haymond, J.V. Santiago and S.D. Shah, "Norepinephrine and epinephrine release and adrenergic mediation of smoking-associated hemodynamic and metabolic events," *N. Engl. J. Med.* **295**, 573-577 (1976).
  14. Westfall, T.C. and M. Brasted, "The mechanism of action of nicotine on adrenergic neurons in the perfused guinea-pig heart," *J. Pharmacol. Exp. Ther.* **182**, 409-418 (1972).

- 
15. Seyler, L.E., O.F. Pomerleau, J.B. Fertig, D. Hunt and K. Parker, "Pituitary hormone response to cigarette smoking," *Pharmacol. Biochem. Behav.* **24**, 159-162 (1986).
  16. Bizzi, A., M.T. Tacconi, A. Medea and S. Garattini, "Some aspects of the effect of nicotine on plasma FFA and tissue triglycerides," *Pharmacology* **7**, 219-224 (1972).
  17. U.S. Department of Health and Human Services, "The Health Consequence of Smoking: Cardiovascular disease, a report of the Surgeon's General 1984," U.S. Department of Health and Human Services DHHS Publication No. (PHS) 84-50204, 384 pp. (1984).
  18. Vial W.C., "Cigarette smoking and lung disease," *Amer. J. Med. Sci.* **291**, 130-42 (1986).
  19. Nieburg, P., J.S. Marks, N.M. McLaren and P.L. Remington, "The fetal tobacco syndrome," *JAMA* **253**, 2998-2999 (1985).
  20. Russell, M.A.H., M.J. Jarvis, G. Devitt and C. Feyerabend, "Nicotine intake by snuff users," *Br. Med. J.* **283**, 814-818 (1981).
  21. Gritz, E.R., V. Baer-Weiss, N.L. Benowitz, H. Van Vunakis and M.E. Jarvik, "Plasma nicotine and cotinine concentrations in habitual smokeless tobacco users," *Clin. Pharmacol. Ther.* **30**, 201-298 (1981).
  22. Winn, D.M., W.J. Blot, C.M. Shy, L.W. Pickle, A. Toledo and J.F. Fraumeni, Jr., "Snuff dipping and oral cancer among women in the southern United States," *N. Engl. J. Med.* **304**, 745-749 (1981).
  23. Gupta, P.C., F.S. Mehta, D.K. Daftary, J.J. Pindborg, R.B. Bhonsle, P.N. Jainawalla, P.N. Sinor, V.K. Pitkar, P.R. Murti ; R.R. Irani, H.T. Shah, P.M. Kadam, K.S. Iyer, H.M. Iyer, A.K. Hegde, G.K. Chandrashekar, B.C. Shiroff, B.E. Sahiar and M.N. Mehta, "Incidence rates of oral cancer and natural history of oral precancerous lesions in a 10-year follow-up study of Indian villagers," *Community Dent. Oral Epidemiol.* **8**, 287-333 (1980).
  24. Jayant, K., V. Balakrishnan, L.D. Sanghvi and D.J. Jussawalla, "Quantification of the role of smoking and chewing tobacco in oral, pharyngeal, and oesophageal cancers," *Br. J. Cancer* **35**, 232-235 (1977).
  25. Russell, M.A.H., "Tobacco smoking and nicotine dependence," In: Research advances in alcohol and drug problems. (R.J. Gibbins, Y. Israel, H. Kalant, R.E. Popham, W. Schmidt and R.G. Smart, Eds) pp. 1-47. New York, John Wiley and Sons (1976).
  26. Russell, M.A.H., C. Wilson, C. Feyerabend and P.V. Cole, "Effect of nicotine chewing on smoking behaviour and as an aid to cigarette withdrawal," *Br. Med. J.* **2**, 391-393 (1976).
  27. Read, R.C., "Presidential address. Systemic effects of smoking," *Am. J. Surg* **148**, 706-711 (1984).



- 
28. Cullen, J.W., W. Blot, J. Henningfield, G. Boyd, R. Mecklenburg and M.M. Massey, "Health consequences of using smokeless tobacco: Summary of the Advisory Committee's report to the Surgeon General," *Public Health Rep.* **101**, 355-73 (1986).
  29. Bishun, N.P., N. Lloyd, R.W. Raven and D.C. Williams, "The *in vitro* and *in vivo* cytogenetic effects of nicotine," *Acta Biol. Acad. Sci. Hung.* **23**, 175-180 (1972).
  30. Wang, N-S., M-F. Chen and D.E. Schraufnagel, "The cumulative scanning electron microscopic changes in baby mouse lungs following prenatal and postnatal exposures to nicotine," *J. Pathol.* **144**, 89-100 (1984).
  31. Toth, B., "Effects of long term administration of nicotine hydrochloride and nicotinic acid in mice," *Anticancer Research* **2**, 71-74 (1982).
  32. Bock, F.G., "Cocarcinogenic properties of nicotine," In: Banbury Report: A safe cigarette? (G.B. Gori and F.G. Bock, Eds.) pp. 129-138 Cold Spring Harbor Laboratory, New York (1980).
  33. Gurkalo, V.K. and N.I. Volfson, "Nicotine influence upon the development of experimental stomach tumors," *Arch. Geschwulstforsch* **52**, 259-265 (1982).
  34. Florin, I., L. Rutberg, M. Curvall and C.R. Enzell, "Screening of tobacco smoke constituents for mutagenicity using the Ames' test," *Toxicology* **18**, 219-232 (1980).
  35. Riebe, M., K. Westphal and P. Fortnagel, "Mutagenicity testing, in bacterial test systems, of some constituents of tobacco," *Mutat. Res.* **101**, 39-43 (1982).
  36. Hudson, D.B. and P.S. Timiras, "Nicotine injection during gestation: Impairment of reproduction, fetal viability, and development," *Biol. Reprod.* **7**, 247-253 (1972).
  37. Hemsworth, B.N., "Deformation of the mouse fetus after ingestion of nicotine by the male," *IRCS Med. Sci. Libr. Compend.* **9**, 728-729 (1981).
  38. Sudan, B.J.L. and J. Sterboul, "Nicotine: an hapten," *Br. J. Dermatol.* **104**, 349-350 (1981).
  39. Sudan, B.J.L., "Passive smoking: Nicotine, a hapten," *Fd. Chem. Toxic.* **20**, 629 (1982).
  40. Folts, J.D. and F.C. Bonebrake, "The effects of cigarette smoke and nicotine on platelet thrombus formation in stenosed dog coronary arteries: Inhibition with phentolamine." *Circulation* **65**, 465-470 (1982).
  41. Wennmalm, A., "Nicotine inhibits hypoxia- and arachidonate-induced release of prostacyclin-like activity in rabbit hearts." *Br. J. Pharmacol.* **69**, 545-549 (1980).
  42. Wennmalm, A., "Interaction of nicotine and prostaglandins in the cardiovascular system," *Prostaglandins* **23**, 139-144 (1982).

- 
43. Lindquist, N.G. and S. Ullberg, "Autoradiography of intravenously injected  $^{14}\text{C}$ -nicotine indicates long-term retention in the respiratory tract," *Nature (London)* **248**, 600-601 (1974).
  44. Waddell, W. and C. Marlowe, "Localization of nicotine- $^{14}\text{C}$  cotinine- $^{14}\text{C}$  and nicotine- $^{14}\text{C}$ -N-oxide- $^{14}\text{C}$  in tissues of the mouse. *Drug Metab. Dispos.* **4**, 530-539 (1976).
  45. Szűts, T., S. Olsson, N.G. Lindquist, S. Ullbert, A. Pilotti and C. Enzell, "Long-term fate of [ $^{14}\text{C}$ ]nicotine in the mouse: Retention in the bronchi, melanin-containing tissues and urinary bladder wall," *Toxicology* **10**, 207-220 (1978).
  46. Ortiz de Montellano, P.R. and N.O. Reich, "Inhibition of cytochrome P-450 enzymes," In: *Cytochrome P-450: Structure, mechanism and biochemistry*, (P.R. Ortiz de Montellano, Ed.) pp. 273-314 Plenum Press, New York (1986).
  47. Waddell, W.J. and C. Marlowe, "Inhibition by metyrapone of the accumulation of nicotine  $^{14}\text{C}$  in bronchial epithelium of mice," *Arch. int. Pharmacodyn.* **234**, 294-307 (1978).
  48. Marietta, M.P., E.S. Vessel, R.D. Hartman, J. Weisz and B.H. Dvorchik, "Characterization of cytochrome P-450-dependent aminopyrine N-demethylase in rat brain," *J. Pharmacol. Exp. Ther.* **208**, 271-279 (1979).
  49. Fouts, J.R. and T.R. Devereux, "Developmental aspects of hepatic and extrahepatic drug metabolizing enzyme systems: Microsomal enzymes and components in rabbit liver and lung during the first month of life," *J. Pharmacol. Exp. Ther.* **183**, 458-468 (1972).
  50. Nebert, D.W. and H.V. Gelboin, "The *in vivo* and *in vitro* induction of aryl hydrocarbon hydroxylase in mammalian cells of different species, tissues, strains and development and hormonal states," *Archs. Biochem. Biophys.* **134**, 76-89 (1969).
  51. Miller, E.C. and J.A. Miller, "Searches for ultimate chemical carcinogens and their reactions with cellular molecules," *Cancer*, **47** 2327-2345 (1981).
  52. Wiest, W.G. and C. Heidelberger, "The interaction of carcinogenic hydrocarbons with tissue constituents. II. 1,2,5,6-dibenzanthracene-9,10- $\text{C}^{14}$  in skin," *Cancer Res.* **13**, 250-254 (1953).
  53. Weisburger, E.K., J.H. Weisburger and H.P. Morris, "Studies on the metabolism of 2-acetylaminofluorene-9- $\text{C}^{14}$ ," *Arch. Biochem. Biophys.* **43**, 474-484 (1953).
  54. Watson, J.D. and F.H.C. Crick, "Molecular structure of nucleic acids: A structure for deoxyribose nucleic acid," *Nature (London)* **171**, 737-738 (1953).
  55. Miller, E.C. and J.A. Miller, "Mechanisms of chemical carcinogenesis: Nature of proximate carcinogens and interactions with macromolecules," *Pharmacol. Rev.* **18**, 805-838 (1966).
  56. Mueller, G.C. and J.A. Miller, "The metabolism of 4-dimethylaminoazobenzene by rat liver homogenates," *J. Biol. Chem.* **176**, 535-544 (1948).

- 
57. Mueller, G.C. and J.A. Miller, "The reductive cleavage of 4-dimethylaminoazobenzene by rat liver: The intracellular distribution of the enzyme system and its requirement for triphosphopyridine nucleotide," *J. Biol. Chem.* **180**, 1125-1136 (1949).
  58. Mueller, G.C. and J.A. Miller, "The metabolism of methylated aminoazo dyes. II. Oxidative demethylation by rat liver homogenates," *J. Biol. Chem.* **202**, 579-587 (1953).
  59. La Du, B.N., L. Gaudette, N. Trousof and B.B. Brodie, "Enzymatic dealkylation of aminopyrine (Pyramidon) and other alkylamines," *J. Biol. Chem.* **214**, 741-752 (1955).
  60. Mitoma, C., H.S. Posner, H.C. Reitz and S. Udenfried, "Enzymatic hydroxylation of aromatic compounds," *Arch. Biochem. Biophys.* **61**, 431-441 (1956).
  61. Nelson, S., "Metabolic activation and drug toxicity," *J. Med. Chem.* **25**, 753-765 (1982).
  62. Gillette, J.R., J.R. Mitchell and B.B. Brodie, "Biochemical mechanisms of drug toxicity," *Annu. Rev. Pharmacol.* **14**, 271-288 (1974).
  63. Overton, M., J.A. Hickman, M.D. Threadgill, K. Vaughan and A. Gescher, "The generation of potentially toxic, reactive iminium ions from the oxidative metabolism of xenobiotic N-alkyl compounds," *Biochem. Pharmacol.* **34**, 2055-2061 (1985).
  64. Ward, D.P., A.J. Trevor, J.D. Adams, T.A. Baillie and N. Castagnoli Jr., "Metabolism of phencyclidine: The role of iminium ion formation in covalent binding of rabbit microsomal protein," *Drug Metab. Dispos.* **10**, 690-695 (1982).
  65. Ho, B. and N. Castagnoli Jr., "Trapping of metabolically generated electrophilic species with cyanide ion: Metabolism of 1-benzylpyrrolidine," *J. Med. Chem.* **23**, 133-139 (1980).
  66. Hoag, M.K.P., A.J. Trevor, Y. Asscher, J. Weissman and N. Castagnoli Jr., "Metabolism-dependent inactivation of liver microsomal enzymes by phencyclidine", *Drug Metab. Dispos.* **12**, 371-375 (1984).
  67. Langston, J.W., P.A. Ballard, J.W. Tetrad and I. Irwin, "Chronic Parkinsonism in humans due to a product of meperidine-analog synthesis," *Science* **219**, 979-980 (1983).
  68. Langston, J.W., "MPTP: insights into the etiology of Parkinson's disease," *Eur. Neurol.* **26 Suppl 1**, 2-10 (1987).
  69. Chiba, K., A. Trevor, and N. Castagnoli, Jr., "Metabolism of the neurotoxic tertiary amine, MPTP, by brain monoamine oxidase," *Biochem. Biophys. Res. Commun.* **120**, 574-578 (1984).
  70. Langston, J.W., I. Irwin, E.B. Langston and L.S. Forno, "Pargyline prevents MPTP-induced Parkinsonism in primates," *Science* **225**, 1480-1482 (1984).

- 
71. Lijinsky, W., M.D. Reuber and B.N. Blackwell, "Liver tumors induced in rats by oral administration of the antihistaminic methapyrilene hydrochloride," *Science* **209**, 817-819 (1980).
  72. Lampe, M.A. and R.C. Kammerer, "Cytochrome P-450 dependent binding of methapyrilene to DNA *in vitro*," *Carcinogenesis* **8**, 1525-1529 (1987).
  73. Ziegler, R., B. Ho and N. Castagnoli Jr., "Trapping of metabolically generated electrophilic species with cyanide ion: Metabolism of methapyrilene," *J. Med. Chem.* **24**, 1133-1138 (1981).
  74. Jacob, P. III, N.L. Benowitz, A.T. Shulgin, "Recent studies of nicotine metabolism in humans," *Biochem. Behav.* **30**, 249-253 (1988).
  75. Gorrod, J.W. and P. Jenner, "The metabolism of tobacco alkaloids," In: *Essays in Toxicology* (W.J. Hayes, Jr., Ed.), Vol. 6, pp. 35-78 Academic Press, New York (1975).
  76. Lautenbach, B.F., "On a new function of the liver," *Philadelphia Med. Times* **7**, 387-394 (1876).
  77. Clark, M.S.G., M.J. Rand and S. Vanov, "Comparison of pharmacological activity of nicotine and related alkaloids occurring in cigarette smoke," *Arch. Int. Pharmacodyn. Ther.* **156**, 363-379 (1965).
  78. McGovren, J.P., W.C. Lubawy and H.B. Kostenbauder, "Uptake and metabolism of nicotine by the isolated perfused rabbit lung," *J. Pharmacol. Exp. Ther.* **199**, 198-207 (1976).
  79. Booth, J. and E. Boyland, "Enzymatic oxidation of (-)-nicotine by guinea-pig tissues *in vitro*," *Biochem. Pharmacol.* **20**, 407-415 (1971).
  80. Turner, D.M., A.K. Armitage, R.H. Briant and C.T. Dollery, "Metabolism of nicotine by the isolated perfused dog lung," *Xenobiotica* **5**, 539-551 (1975).
  81. Nakayama, H., T. Nakashima and Y. Kurogochi, "Cytochrome P-450-dependent nicotine oxidation by liver microsomes of guinea pigs: Immunochemical evidence with antibody against phenobarbital-inducible cytochrome P-450," *Biochem. Pharmacol.* **34**, 2281-2286 (1985).
  82. Stalhandske, T., "The metabolism of nicotine and cotinine by a mouse liver preparation," *Acta Physiol. Scand.* **78**, 236-248 (1970).
  83. Hucker, H.B., J.R. Gillette and B.B. Brodie, "Enzymatic pathway for the formation of cotinine, a major metabolite of nicotine in rabbit liver," *J. Pharmacol. Exp. Ther.* **129**, 94-100 (1960).
  84. Nakayama, H., T. Nakashima and Y. Kurogochi, "Participation of cytochrome P-450 in nicotine oxidation," *Biochem. Biophys. Res. Comm.* **108**, 200-205 (1982).

- 
85. Omura, T. and R. Sato, "A new cytochrome in liver microsomes," *J. Biol. Chem.* **237**, 1375-1376 (1962).
  86. Ziegler, D.M. and C.H. Mitchell, "Microsomal oxidase IV: Properties of a mixed-function amine oxidase isolated from pig liver microsomes," *Arch. Biochem. Biophys.* **150**, 116-125 (1972).
  87. Sherratt A.J. and L.A. Damani, "Activities of cytosolic and microsomal drug oxidases of rat hepatocytes in primary culture," *Drug Metab. Dispos.* **17**, 20-25 (1989).
  88. Boyd, M.R., "Evidence for the Clara cell as a site of cytochrome P-450 dependent mixed-function oxidase activity in lung," *Nature (London)* **269**, 713-715 (1977).
  89. Ziegler, D.M., "Microsomal flavin-containing monooxygenase: Oxygenation of nucleophilic nitrogen and sulfur compounds," In: *Enzymatic Basis of Detoxification* (W. Jacoby, Ed.), Vol. 1, pp. 201-227 Academic Press, New York (1980).
  90. Brandange, S. and L. Lindbloom, "The enzyme "aldehyde oxidase" is an iminium oxidase. Reaction with nicotine  $\Delta^{1' \cdot (5)}$  iminium ion," *Biochem. Biophys. Res. Comm.* **91**, 991-996 (1979).
  91. Peterson, L.A., "Stereochemical studies of the cytochrome P-450 catalyzed oxidation of (S)-nicotine to nicotine  $\Delta^{1' \cdot 5}$ -iminium ion," Ph.D. Dissertation. University of California, San Francisco (1986).
  92. Brandange, S. and L. Lindblom, "Synthesis, structure and stability of nicotine  $\Delta^{1' \cdot (5)}$  iminium ion, an intermediary metabolite of nicotine," *Acta Chem. Scand. B* **33**, 187-191 (1979).
  93. McKennis, H., L.B. Turnbull, S.L. Schwartz, E. Tamaki and E.R. Bowman, "Demethylation in the metabolism of (-)-nicotine," *J. Biol. Chem.* **237**, 541-545 (1962).
  94. Peterson, L. and N. Castagnoli Jr., "Regio- and stereochemical studies on the  $\alpha$ -carbon oxidation of (S)-nicotine by cytochrome P-450 model systems," *J. Med. Chem.* **31**, 637-640 (1988).
  95. Jenner, P., J.W. Gorrod and A.H. Beckett, "Factors affecting the *in vitro* metabolism of R-(+)- and S-(-)-Nicotine by guinea-pig liver preparations," *Xenobiotica* **3**, 563-572 (1973).
  96. Ortiz de Montellano, P.R., "Oxygen activation and transfer," In: *Cytochrome P-450: Structure, mechanism and biochemistry*, (P.R. Ortiz de Montellano, Ed.) pp. 217-271 Plenum Press, New York (1986).
  97. Nguyen, T-L., L.D. Gruenke and N. Castagnoli Jr., "Metabolic N-demethylation of nicotine. Trapping of a reactive iminium species with cyanide ion," *J. Med. Chem.* **19**, 1168-1169 (1976).

- 
98. Rajagopalan, K.V., "Xanthine oxidase and aldehyde oxidase," In: *Enzymatic Basis of Detoxification* (W. Jacoby, Ed.), Vol. 1, pp. 295-309, Academic Press, New York (1980).
  99. Rajagopalan, K.V. and P. Handler, "Hepatic aldehyde oxidase: II Differential inhibition of electron transfer to various electron acceptors," *J. Biol. Chem.* **239**, 2022-2026 (1964).
  100. Felsted, R.L., A.E.-Y. Chu and S. Chaykin, "Purification and properties of the aldehyde oxidases from hog and rabbit livers," *J. Biol. Chem.* **248** 2580-2587 (1973).
  101. Williams, D.E., S.E. Hale, A.S. Muerhoff and B.S.S. Masters, "Rabbit lung flavin-containing monooxygenase; Purification, characterization, and induction during pregnancy," *Mol. Pharmacol.* **28**, 381-390 (1985).
  102. Ziegler, D.M. and L.L. Poulsen, "Hepatic microsomal mixed-function amine oxidase," In: *Methods in Enzymology*, (S. Fleischer and L. Packer, Eds.) Vol. 52, pp. 142-151 Academic Press, New York (1978).
  103. Williams, D.E., D.M. Ziegler, D.J. Nordin, S.E. Hale and B.S.S. Masters, "Rabbit lung flavin-containing monooxygenase is immunochemically and catalytically distinct from the liver enzyme," *Biochem. Biophys. Res. Comm.* **125**, 116-122 (1984).
  104. Poulsen, L.L., K. Taylor, D.E. Williams, B.S.S. Masters and D.M. Ziegler, "Substrate specificity of the rabbit lung flavin-containing monooxygenase for amines: Oxidation products of primary alkylamines," *Mol. Pharmacol.* **30**, 680-685 (1986).
  105. Baker, J. and S. Chaykin, "The biosynthesis of trimethylamine-N-oxide," *Biochem. Biophys. Acta.* **41**, 548-550 (1960).
  106. Poulsen, L.L. and D.M. Ziegler, "The liver microsomal FAD-containing monooxygenase. Spectral characterization and kinetic studies," *J. Biol. Chem.* **254**, 6449-6455 (1979).
  107. Ball, S. and T.C. Bruice, "4a-Hydroperoxyflavin N-oxidation of tertiary amines," *J. Am. Chem. Soc.* **101**, 4017-4019 (1979).
  108. Ball, S. and T.C. Bruice, "Oxidation of amines by a 4a-hydroperoxyflavin," *J. Am. Chem. Soc.* **102**, 6498-6503 (1980).
  109. Rose, J. and N. Castagnoli, Jr., "The metabolism of tertiary amines," *Med. Res. Rev.* **3**, 73-80 (1983).
  110. Hlavica, P. and M. Kehl, "Studies on the mechanism of hepatic microsomal N-oxide formation: The role of cytochrome P-450 and mixed-function amine oxidase in the N-oxidation of N,N-dimethylaniline," *Biochem. J.* **164**, 487-496 (1977).

**Chapter II**  
**Synthesis of Specifically Labeled (S)-5-<sup>3</sup>H-Nicotine**  
**by Carrier Free Tritiolysis of**  
**the Corresponding 5-Bromo Derivative**

## Introduction

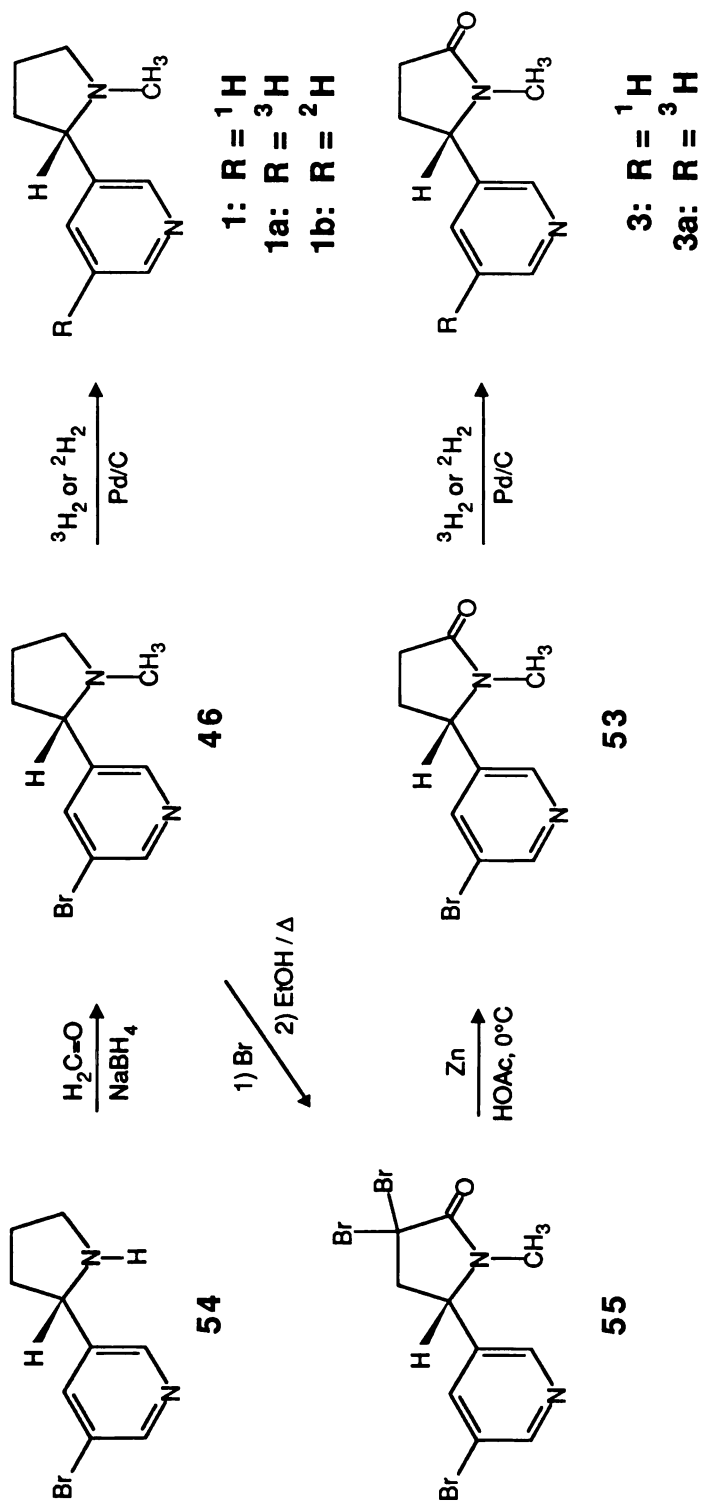
Previous studies directed toward understanding the potentially toxic effects of (S)-nicotine have indicated that this compound may contribute to a number of tobacco related pathologies such as cardiovascular disease and cancer.<sup>1,2</sup> Results of these efforts have prompted us to investigate the mechanisms by which the oxidative metabolism of (S)-nicotine could result in the formation of potentially toxic metabolites. Studies which have attempted to characterize the mechanism of action of compounds known to produce chemically induced toxicities have indicated that, in many cases, chemically reactive species formed through metabolic oxidation of the parent compound bind covalently to biomacromolecules to produce structural alterations which may be deleterious to normal cellular functions.<sup>3</sup> In instances where covalent binding of metabolically activated foreign compounds is quantitatively assessed, radiolabeled analogs are utilized. Previous studies which have led up to the present investigation have indicated that (S)-nicotine is metabolized by cytochrome P-450 to chemically reactive electrophilic intermediates.<sup>4</sup> In the studies to be described in subsequent chapters, experiments will be performed to evaluate whether (S)-nicotine is metabolically activated by this enzyme system to species capable of binding covalently to nucleophilic functionalities present in biomacromolecules. In order to perform this evaluation, a radiolabeled analog of (S)-nicotine is necessary. Since we are following the metabolic fate of this compound, the tritium atom must be incorporated into a position which is stable to metabolic transformations. Currently available tritium labeled (S)-nicotine analogs are labeled at either the N-methyl- or the 4'-carbon atom,<sup>5,6</sup> positions which are not suitable for our studies since the tritium atom may be lost as a result of known metabolic transformations.<sup>7,8,9</sup> For example, oxidation of N-methyl labeled (S)-nicotine may result in the hydroxylation of the N-methyl carbon, a reaction which leads to the spontaneous cleavage of the carbon-nitrogen bond with



subsequent loss of the carbon atom bearing the tritium label. Metabolic oxidation of (S)-nicotine at the 5' carbon atom results in the formation of a 2 electron oxidized metabolic intermediate, (S)-nicotine  $\Delta^{1',5'}$ -iminium ion, which can exist in equilibrium with the corresponding (S)- $\Delta^{2',3'}$ -dehydronicotine species. Due to this equilibrium, label attached at the 4'-position may be lost since protons attached to this carbon atom appear to be susceptible to exchange reactions.<sup>9</sup> To avoid these complications, an alternative synthetic approach was designed which involved the introduction of an atom of tritium into (S)-nicotine at a metabolically stable position. Since the pyridyl moiety of (S)-nicotine does not appear to undergo any bond cleaving metabolic reactions in mammals,<sup>10</sup> we have developed a synthetic route which leads to the formation of high specific activity (S)-5-<sup>3</sup>H-nicotine (**1a**). This approach also has been applied to the synthesis of the corresponding analog of (S)-cotinine (**3**), namely (S)-5-<sup>3</sup>H-cotinine (**3a**). Both products were prepared in enantiomerically pure form.

## Results and Discussion

Our approach to this problem focused on the carrier free tritioysis of (S)-5-bromonicotine (**46**) and (S)-5-bromocotinine (**53**). The key intermediate in these syntheses was (S)-5-bromonornicotine (**54**) which was available in a state of high enantiomeric purity (>98%) by total synthesis and resolution of the corresponding racemate with (+)- $\alpha$ -methoxy- $\alpha$ -trifluoromethylphenylacetic acid.<sup>11</sup> The conversion of **54** to (S)-5-bromonicotine (**46**) was accomplished by reductive amination using formaldehyde and sodium borohydride (**Scheme II.1**). Reaction of **46** with excess bromine in acetic acid for 1 hr produced (S)-3',3',5'-tribromocotinine hydrogen tribromide (**55 HBr<sub>3</sub>**) which subsequently was obtained as the corresponding free base **55**. Conversion of **55** to (S)-5-bromocotinine (**53**) was achieved by careful reduction with zinc dust in acetic acid. It was important to carry out the reaction at 0°C

Scheme II.1 Radiochemical Syntheses of (S)-5-<sup>3</sup>H-Nicotine (1a) and (S)-5-<sup>3</sup>H-Cotinine (3a)

and to monitor the progress of the reaction by TLC in order to prevent reductive cleavage of the bromo group from the pyridine ring.

### Deuterolysis Experiments

Prior to performing the carrier free tritiation reactions, a series of preliminary deuterolysis studies was conducted to optimize reaction conditions. The course of these reactions was monitored by an HPLC assay which provided quantitative estimations of both starting material and product (Fig.II.1). A summary of these results, which are described in detail below, is presented in Table II.1. Deuterolysis of **46** in tetrahydrofuran using a Pd/C catalyst was found to proceed at a rate of 0.67 mmol/min at room temperature. In the presence of triethylamine the same reaction proceeded at a rate of 1.8 mmol/min. This observation as well as that of others<sup>12</sup> point to the importance of neutralizing the reaction generated acid (DBr) which has been shown to poison the Pd/C catalyst.

**Table II.1 Summary of the Model Deuterolysis Study**

Condition	[ <b>46</b> ] mM	kcat <sup>a</sup>	% conversion <sup>b</sup>	%remaining <sup>c</sup>
A. THF -TEA	52	0.67	8.2	44.2
B. THF + TEA	33	1.8	17.0	6.1
C. ETOH + TEA	50	9.2	92.0	< 1.0
D. ETOH + TEA	166	26.0	73.0	< 1.0

<sup>a</sup> mM (S)-5-<sup>2</sup>H-Nicotine formed.min<sup>-1</sup>

<sup>b</sup> determined at 5 min

<sup>c</sup> after 60 min reaction time

A comparison of reaction rates in tetrahydrofuran and ethanol in the presence of triethylamine showed that the deuterolysis proceeded approximately 5 times faster in

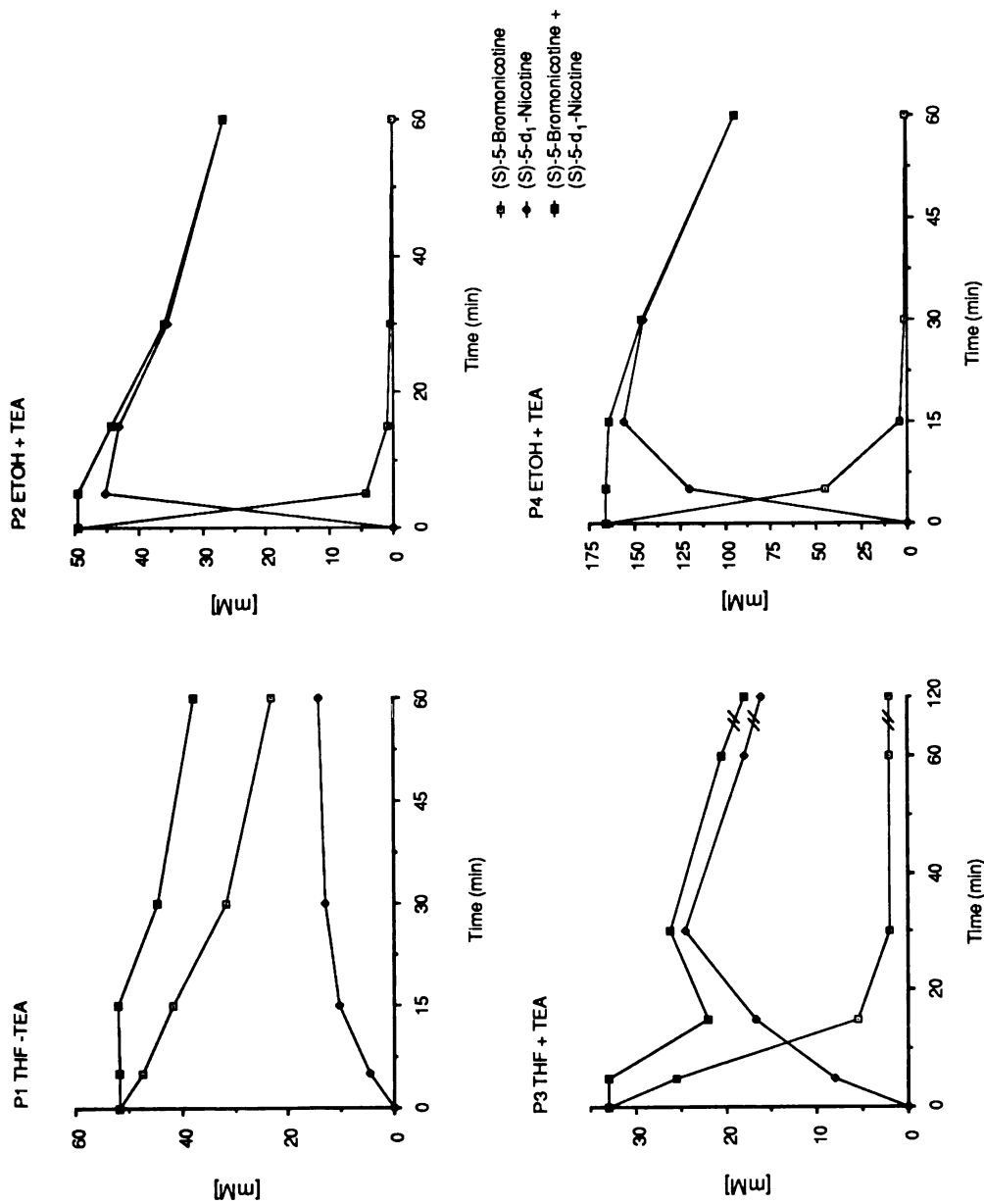
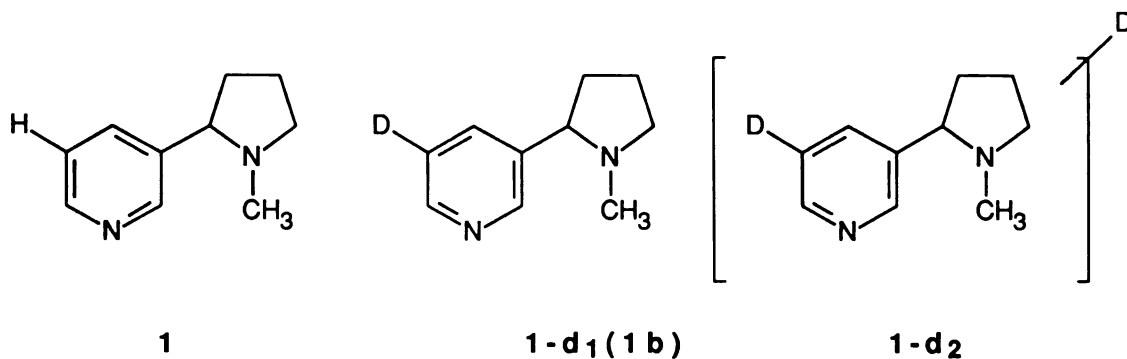


Fig.II.1 Kinetics of Deuteration of (S)-5-Bromonicotine to (S)-5-d<sub>1</sub>-Nicotine Under Various Reaction Conditions. (S)-5-Bromonicotine and (S)-5-d<sub>1</sub>-nicotine were quantitated by the HPLC method described in the text.

ethanol (9.2 vs 1.8 mmol/min) and that the yield of (S)-5-<sup>2</sup>H-nicotine(**1c**) in the ethanol reaction mixture peaked at about 15 min compared to 30 min in the tetrahydrofuran reaction mixture. We also observed that the ratio of deuterium consumed to product formed in these reactions increased with time. These observations are consistent with the possibility that the initially formed deuterolysis product may undergo further reduction. The absence of detectable levels of side products as evi-

**Table II.2** Estimation by Probe Chemical Ionization Mass Spectrometry of the Palladium on Charcoal (Pd/C) Catalyzed Incorporation of Deuterium into (S)-5-Br-Nicotine. Samples obtained from either a tetrahydrofuran (P3, 15 min sample\* ) or an ethanol (P2, 5 min sample\*) reaction mixture were analyzed.

	m/z	Relative Peak Intensity		Distribution of Label	
		<u>THF</u>	<u>EtOH</u>	<u>THF</u>	<u>EtOH</u>
<b>1</b>	163	63.2	36.0	37.2	24.7
<b>1-d<sub>1</sub></b>	164	100.0	100.0	58.8	68.7
<b>1-d<sub>2</sub></b>	165	6.9	9.6	4.0	6.6



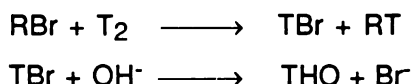
\*refer to Fig.II.3

denced by HPLC, capillary column GC and UV analysis of the reaction mixture suggests that, if formed, such overreduction products may undergo spontaneous oxidation during workup.<sup>13</sup> Support for this suggestion comes from the observation that the peak height ratios of **1b** to starting material analyzed in a reaction mixture that had been stopped

short of completion increases upon storage overnight in the presence of air. In order to provide more direct evidence for this effect, chemical ionization mass spectral analysis of these reaction mixtures (Table II.2) showed that in addition to the monodeuterated derivative, a significant amount of signal corresponding to the dideuteronicotine species was observed accounting for 4% and 7% of the overall deuterolysis products observed in the tetrahydrofuran and ethanol reaction mixtures, respectively. This observation is not trivial since overreduction of the pyridine ring by tritium could lead to undesired radiochemical contaminants.

### Tritiolysis

The tritiolysis procedure utilized tritium gas (T<sub>2</sub>) at a specific activity of 58 Ci/mmol and involved the replacement of the bromine atom at the 5 position of the pyridine ring with an atom of tritium (Also see Scheme I.1).



Where: R = (S)-nicotine  
T = tritium

As shown in the equation above, one half of the tritium molecule (T<sub>2</sub>) becomes associated with the liberated atom of bromine as TBr. Accumulation of TBr in the reaction mixture could present a problem since, at the high specific activities of tritium used in these syntheses, this compound could serve as a secondary source of radioactive energy which may contribute to possible side reactions and/or radiation damage to the principal tritiolysis product **1a**. In addition to TBr, tritiated water (THO and T<sub>2</sub>O) is formed and accumulated during the course of the reaction. The tritiated water generated in this reaction can pose a problem especially in the presence of a metal hydrogen-transfer catalyst such as the palladium charcoal catalyst used in these experiments. Under prolonged reaction conditions the catalyst may promote the exchange of tritium between

T<sub>2</sub>O and either the product or reactant resulting in non-specific incorporation of tritium. In order to minimize these side reactions as well as to achieve the highest degree of specific tritium incorporation, precautions were taken to limit the tritiumolysis reaction to the shortest period of time necessary for quantitative tritium-halogen exchange. We describe these steps in greater detail below.

---

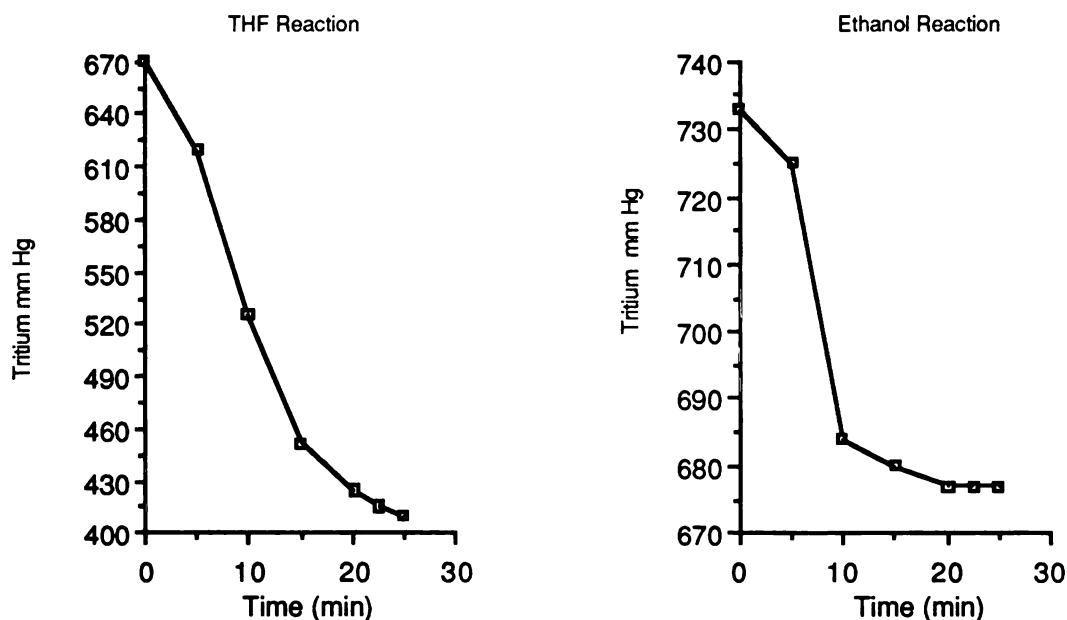


**Fig II.2.** Partial Pressure of Tritium Gas in the Tritiumolysis Reaction Vessel vs. Time. The partial pressure of tritium gas in the THF and ethanol reaction mixtures was used to monitor the progress of the tritiumolysis reaction.

---

The tritiumolysis was carried out in two separate reaction vessels using either ethanol or tetrahydrofuran as the reaction solvent and performed in the presence of slightly less than one atmosphere of tritium gas using a custom built manifold. The progress of the reaction was monitored by measuring the partial pressure of tritium gas in each reaction vessel (Fig.II.2). The reaction was terminated when the partial pressure of tritium gas in each reaction vessel approached a plateau. At this time point (25 min), the reactions were terminated by voiding tritium gas from the reaction

vessel. The isolation of (S)-5-<sup>3</sup>H-nicotine was accomplished by partial lyophilization of the solvents. In the case of the ethanol containing vessel, a further addition of ethanol followed by partial lyophilization was done to facilitate the removal of exchangeable tritium. Purification of both preparations was accomplished by semipreparative normal phase HPLC. The purity of the tritium labeled (S)-5-<sup>3</sup>H-nicotine was confirmed by HPLC analysis employing a UV diode array detector which showed superimposable UV spectra, identical to those of a reference standard, at different positions along the eluting peak (upward inflection, apex, and downward inflection). Concurrent analysis with a radioactivity flow detector established that all of the

**Table II.3** Summary of Conditions and Results from the Catalytic Tritiolysis of (S)-5-Br-Nicotine to (S)-5-<sup>3</sup>H-Nicotine

	Solvent	
	Ethanol	THF
(S) 5'-Bromonicotine	0.18 mM	0.42 mM
Catalyst (10% Pd/C)	20.0 mg	40.0 mg
Volume <sub>solvent</sub>	1.0 ml	2.5 ml
Triethylamine	Equimolar to reactant	
Volume <sub>reaction vessel</sub>	25.0 ml	10.0 ml
Volume <sub>T<sub>2</sub> above rxn vessel</sub>	25.0 cc	16.0 cc
Percent conversion*	> 99.0	91.0
Specific Activity (Ci/mmol)	32	28

\*determined by HPLC with UV detection at 260 nm.

radioactivity coeluted with the (S)-nicotine peak. The specific location of the tritium label at the 5-position of the pyridyl moiety was confirmed by <sup>3</sup>H NMR analysis which displayed a single signal at  $\delta$  7.33 ppm which corresponds to the chemical shift value for the C-5 proton resonance of (S)-nicotine.<sup>14</sup> The radiochemical purity of the product



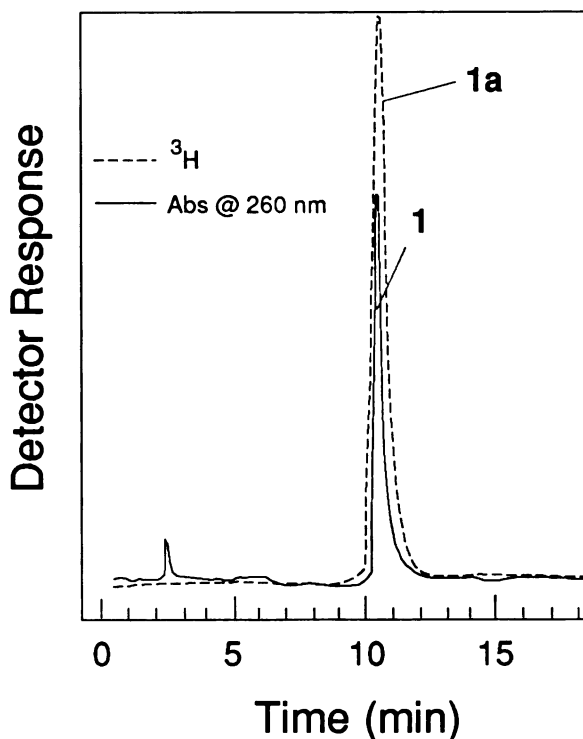


**Fig.II.3** Radiochemical Purity of Synthetic (S)-5-<sup>3</sup>H-Nicotine (**1a**) Prepared by the Catalytic Tritiolysis of (S)-5-Bromonicotine (**46**). HPLC purified (S)-5-<sup>3</sup>H-nicotine was analyzed by radiochemical detection following separation on a 5  $\mu$ m Alltech silica HPLC column at a flow rate of 1 ml/min. The mobile phase was 0.5% n-propylamine in acetonitrile. For comparison, nonradiolabeled (S)-nicotine (**1**) was analyzed and was shown to coelute with (S)-5-<sup>3</sup>H-nicotine (**1a**).

isolated from these reactions was estimated by HPLC to be  $\geq 99\%$ . The specific activities of the **1a** isolated from the ethanol reaction mixtures were 32 Ci/mmol and 28 Ci/mmol, respectively. The higher than theoretical (29 Ci/mmol) incorporation of tritium in the ethanol reaction may be due to overreduction followed by oxidation of the initially formed product. A summary of the conditions and results obtained from these studies is presented in **Table II.3**. This synthetic scheme proved to also be effective for the preparation of (S)-5-<sup>3</sup>H-cotinine (**3a**). In the past, commercially available tritium labeled nicotine was prepared by N-methylation of naturally occurring nornicotine, a tobacco plant product which is a 60:40 mixture of the (S)- and (R)-isomers. Since the synthesis of enantiomerically pure (R)- and (S)-nornicotine has been achieved,<sup>11</sup> radiolabeled (S)-nicotine of high enantiomeric purity may be

prepared by this route. Recently an alternative synthetic approach has provided both enantiomers of 4'-<sup>3</sup>H-nicotine.<sup>6</sup> Unfortunately, the label of both of these analogs of (S)-nicotine is metabolically labile and therefore not suitable to our needs. The synthetic route described in this chapter provides a third approach to tritium labeled (S)-nicotine which also is applicable to the synthesis of tritium labeled (S)-cotinine and which produces high specific activity analogs in which the tritium label is metabolically stable.

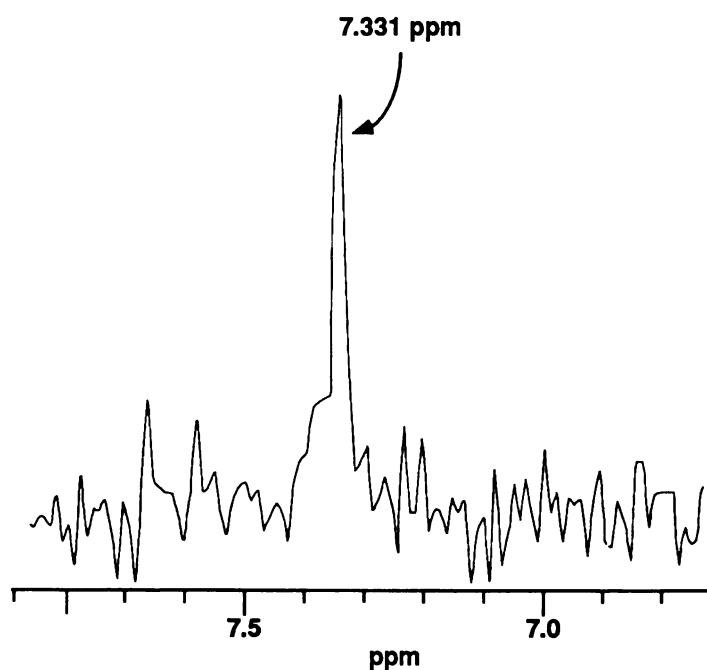


**Fig. II.4** <sup>3</sup>H-NMR of (S)-5-<sup>3</sup>H-Nicotine (1a) Expansion of the <sup>3</sup>H-NMR of approximately 100 mCi of (S)-5-<sup>3</sup>H-Nicotine.

#### Notes Concerning Radiochemical Decomposition

One of the difficulties encountered during the workup of high specific activity preparations of (S)-5-<sup>3</sup>H-nicotine (1a) was its apparent susceptibility to radiochemical decomposition (autoradiolysis). Over relatively short periods of time (weeks to months), 1a was observed to decompose rapidly to several unknown products. Explanations for the observed decomposition of 1a extend beyond considerations of

conventional chemical stability. Our experience, for example, indicates that (S)-nicotine is quite stable when stored in methylene chloride, the organic solvent used initially in the extraction of the radiolabeled compound from the reaction mixture. However, under conditions where the compound is isotopically labeled with tritium, the contribution of radiation energy to the decomposition of the reaction product needs to be considered.

Decomposition of a compound by radioactive energy can occur by three modes.<sup>15</sup> The **primary internal** mode of decomposition refers to the natural isotopic decay of a particular isotope. This rate is constant for a specific isotope. Decomposition by this mode can not be controlled and is unavoidable. **Primary external** mode of decomposition refers to the structural damage caused by the energy emitted from the radiolabeled compound. This damage may occur either inter- or intramolecularly. The most direct solution to this problem is dispersal of the radiolabeled compound in an appropriate solvent, preferably one containing radical scavenging agents such as ethanol or benzene. **Secondary** mode of decomposition refers to the damage caused by highly reactive molecules which are generated from the energy emitted from the radiolabeled compound. For example, this energy has been shown to promote the radiolysis of water, a solvent commonly used for the storage of isotopically labeled compounds. Radiolysis of water produces reactive oxygen species such as the highly reactive hydroxyl radical which in turn may interact with the radiolabeled compound to produce decomposition products. This route of decomposition can be controlled by dilution of the excited molecule with unreactive solvent, addition of radical scavenging agents to the aqueous solution, or cooling of the mixture.

Since the storage conditions utilized in the initial radiochemical synthesis and purification of (S)-5-<sup>3</sup>H-nicotine were inappropriate, extensive radiochemical decomposition of the product was observed. Two key factors influenced this decomposition. First, (S)-5-<sup>3</sup>H-nicotine was stored at high concentrations (>100

mCi/ml), a condition which favors the primary external mode of decomposition. Second, (S)-5-<sup>3</sup>H-nicotine was extracted into an organic solvent which is itself susceptible to decomposition by radiation. Methylene chloride, as well as other halogenated solvents, are subject to radiation induced decomposition which involves the formation of reactive radical species. The interaction of such reactive species with (S)-5-<sup>3</sup>H-nicotine may lead to the decomposition products observed in our initial attempt at radiosynthesis.

The frustrations encountered during the purification of (S)-5-<sup>3</sup>H-nicotine, which ultimately represented less than 1% of the total radiolabel in the methylene chloride extract, prompted us, in our second radiochemical synthesis of (S)-5-<sup>3</sup>H-nicotine, to incorporate into our workup procedure a number of precautions necessary for stabilizing the tritium labeled molecule. In order to prevent the undesirable side reactions described above, (S)-5-<sup>3</sup>H-nicotine was stored as a dilute aqueous solution (1 mCi/ml) containing 0.01 N HCl. Ethanol (~15% by volume) was included in the solution since this organic solvent has been shown to scavenge reactive oxygen species, such as those produced from the radiolysis of water, which may react with (S)-5-<sup>3</sup>H-nicotine to produce undesirable side products.<sup>16,17</sup> It is because of its effective radical scavenging ability that ethanol is used commonly by commercial radioisotope manufacturers to prevent the secondary mode of decomposition of a wide variety of radiolabeled compounds.<sup>12</sup> Another precaution taken was the storage of (S)-5-<sup>3</sup>H-nicotine at a temperature above the freezing point of the solution since the decomposition of radiolabeled products are accelerated at temperatures between 0° to -100°C.<sup>18</sup> Although the exact mechanism for this accelerated decomposition is unknown, it has been suggested that at these lower temperatures, the radiolabeled solution freezes slowly to form heterogeneous microaggregations or molecular clusters of the tritiated compound. The formation of "pockets" of highly concentrated radioactivity is thought to promote radiochemical decomposition of the compound by the primary external mode.

## Materials and Methods

### General

Melting points (Mel-Temp apparatus) are uncorrected. The tritiations were performed at the National Tritiation Facility, University of California, Berkeley using a custom made tritiation apparatus. Analysis of the radiolabeled products was achieved by HPLC with UV diode array and radiochemical detection. Instrumentation included the following: Waters model 680 automated gradient controller, M-45 HPLC pump, Z-module, and a Whatman 10  $\mu\text{m}$  Porasil silica cartridge; Hewlett Packard model 85 computer linked to a 1040A UV diode array detector; Berthold ratemeter model BF2304, LSC-module model BF2240, flowmeter model D7547 and a Tracor Northern model TN7200 oscilloscope. Purification of radiolabeled (S)-5-<sup>3</sup>H-nicotine was accomplished by semi-preparative HPLC utilizing a Rainin 5  $\mu\text{m}$  microsorb silica column (10 mm x 25 cm) coupled to the controller and pump described above. A Spectroflow model 757 UV detector was utilized and all absorbances (AU setting = 2.0) were monitored at 259 nm. The <sup>3</sup>H-NMR experiments were performed on a custom built 288 MHz NMR machine equipped with Nicolet data acquisition software. CI mass spectra were obtained with an AEI MS 902S double-focus mass spectrometer equipped with a direct-inlet system and modified for chemical ionization. The reagent gas was isobutane at a pressure of 0.5 to 1.0 torr. The optical purity of (S)-5-bromonornicotine was determined by capillary column (5% methylphenylsilicone) gas chromatography (HP 5889A, temperature program 90-275°C at 25°/min) of the camphanic acid amide derivative.<sup>11</sup>

### Syntheses (Performed in Collaboration with Dr. Peyton Jacob III)

#### (S)-5-Bromonicotine (46)

Sodium borohydride (1 g, 26.5 mmol) was added portionwise with vigorous stirring over a period of 10 min to a solution of the (S)-5-bromonornicotine (54) as its (+)  $\alpha$ -methoxy- $\alpha$ -trifluoromethylphenylacetic acid salt<sup>11</sup> (1 g, 2.2 mmol >98%

enantiomeric purity) and 5 ml of 30% aqueous formaldehyde in 40 ml 10:1 isopropyl alcohol:acetic acid. Following the addition, most of the solvent was removed on a rotary evaporator and the crude product was dissolved in 100 ml of 5% aqueous sulfuric acid. After washing twice with 50 ml portions of methylene chloride, the aqueous phase was made basic with sodium hydroxide and extracted with methylene chloride (2 x 50 ml). The extracts were combined, dried, evaporated and the residue distilled (Kugelrohr oven, 90-100°C at 10 mm) to give 0.35 g (67%) of a colorless liquid displaying identical physical and spectral properties of those reported for the racemic material.<sup>19</sup>

### (S)-3',3',5-Tribromocotinine (55)

Bromine (1.35 ml, 26.3 mmol) was added to a solution of **46** (0.7 g, 2.9 mmol) in 10 ml of 80% aqueous acetic acid. The solution was heated at 80°C for 15 min, diluted with 25 ml ethanol to reduce excess bromine and allowed to stand overnight. Most of the solvent was removed on a rotary evaporator and the residue in 100 ml water, pH adjusted to 7-8 with potassium bicarbonate, was extracted with methylene chloride (2 x 50 ml). Evaporation of the solvent yielded an orange gum which was purified by column chromatography on silica (1 x 20 cm column) eluting with ethyl acetate to give 0.8 g of solid. This material had an R<sub>f</sub> value on silica gel TLC [ethylacetate:methanol:58% ammonia (85:10:1)] identical with that of racemic 3',3'-5-tribromocotinine prepared in the same manner and recrystallized from ethanol (fine white needles): mp 145-150°C (dec); <sup>1</sup>H NMR (CDCl<sub>3</sub>) δ 2.75 (s, CH<sub>3</sub>), 3.25 (ABX, J<sub>AB</sub> = 16 Hz, C<sub>4</sub>H<sub>2</sub>), 4.62 (m, C<sub>5</sub>H), 7.70 (t, C<sub>4</sub>H), 8.45 (δ, C<sub>2</sub>H), and 8.7 ppm (d, C<sub>6</sub>H).

*Anal.* Calculated for C<sub>10</sub>H<sub>9</sub>N<sub>2</sub>Br<sub>3</sub>O: C, 29.07; H, 2.22 ; N, 6.79. Found: C, 29.22; H, 2.25; N, 6.88

### (S)-5-Bromocotinine (53)

Zinc dust (2 g, 31 mmol) was added to a vigorously stirred solution of **55** (0.4 g, 1 mmol) in 20 ml of 95% aqueous acetic acid with external ice bath cooling. After 7

min the mixture was filtered through Celite and the filter cake was washed with 10 ml glacial acetic acid. The filtrate was diluted with 50 ml water and the resulting solution was made basic with aqueous ammonia and extracted with methylene chloride (2 x 50 ml). The combined extracts were dried, evaporated on a rotary evaporator, and the residue distilled (Kugelrohr oven, 140-150°C at 0.1 mm Hg) to give 0.24 g of a light yellow liquid that crystallized on standing: mp 89-92°C. Recrystallization from 3:1 methylcyclohexane-toluene provided 0.15 g (0.59 mmol, 59%) of a white crystalline solid which melted at 94.5-95.4°C: <sup>1</sup>H NMR (CDCl<sub>3</sub>) δ 2.25-2.5 (m, C<sub>3</sub>H<sub>2</sub> + C<sub>4</sub>H<sub>2</sub>), 2.65 (s, CH<sub>3</sub>), 4.40 (m, C<sub>5</sub>H), 7.60 (t, C<sub>4</sub>H), 8.3 (d, C<sub>2</sub>H), and 8.65 ppm (d, C<sub>6</sub>H).

*Anal.* Calculated for C<sub>10</sub>H<sub>11</sub>N<sub>2</sub>BrO: C, 47.06; H, 4.35; N, 10.99. Found: C, 47.18; H, 4.36; N, 11.17.

Interestingly, racemic 5-bromocotinine prepared in the same manner melted at 81.5-82.5 °C after two recrystallizations. Both the racemate and the (S)-isomer had identical R<sub>f</sub> values on silica gel TLC [ethyl acetate:methanol:58% ammonia (85:10:2)] and contained traces of (S)-cotinine.

### (S)-5-<sup>2</sup>H-Nicotine (1b)

A septum stoppered two-necked reaction vessel (10 ml) containing 1.0 ml anhydrous ethanol, 5.3 mg anhydrous triethylamine (52 μmol), and 6.3 mg of 10% Pd/C was flushed 4 times with 100% deuterium gas. Compound **46** (12.5 mg, 52 μmol) was introduced neat by syringe and the resulting mixture was stirred vigorously in the presence of approximately 5 mmol of deuterium gas. During the course of the reaction 5 μl aliquots were withdrawn at 5 min intervals through the septum and resuspended in acetonitrile (72 μl) to give a total final concentration of reactant plus product of approximately 0.8 μg/ml. The samples were analyzed by HPLC on an Alltech 5 μm silica column using a mobile phase consisting of 1% n-propylamine in acetonitrile. The eluent was monitored at 254 nm with a Beckman model 330 fixed wavelength UV detector. Peak heights of the starting compound **46** and the product **1b**

were compared to peak heights of standard calibration curves to estimate relative amounts of reactant and product. These results as well as those of additional deuteration studies are summarized in Table II.1. The above reaction mixture was worked up after 30 min by filtration, concentration and column chromatography on silica (methanol:ethylacetate).

### (S)-5-<sup>3</sup>H-Nicotine (1a)

The tritiation apparatus was arranged with a glass dual manifold which allowed us to carry out two tritiation reactions with the same tritium source. To one reaction vessel (25 ml) was added **46** (43.4 mg, 0.18 mmol) in 1 ml anhydrous ethanol containing 18.2 mg (0.18 mmol) of anhydrous triethylamine and 20 mg of 10% Pd/C. To the second reaction vessel (10 ml) was added **46** (150 mg, 0.62 mmol) in 2.5 ml anhydrous tetrahydrofuran containing 83 mg (0.82 mmol) anhydrous triethylamine and 40 mg of 10% Pd/C. The flasks, under nitrogen, were cooled with liquid nitrogen and placed under vacuum (30 mtorr). The flasks were flushed an additional two times in this way. The vapor pressure of water measured on a Varian Model 810 tc vacuum gauge was less than 10 mtorr following this procedure. Carrier free tritium gas (58 Ci/mmol) was introduced into the reaction vessels to a pressure of 735 and 670 torr for the ethanol and tetrahydrofuran solutions, respectively. The liquid nitrogen baths were removed and the progress of the tritiation monitored by noting the decrease in the partial pressure of tritium gas (Fig.II.2). After 25 min the partial pressure of tritium had plateaued at about 677 and 413 torr, respectively. The vessels were cooled once again in liquid nitrogen following which remaining tritium gas was removed by flushing with nitrogen gas. The reaction mixtures were concentrated to about 1/2 initial volume under vacuum (50 mtorr for the ethanol and 90 mtorr for the tetrahydrofuran mixture). In order to insure complete degassing, 5 ml of anhydrous ethanol was added to the ethanol reaction mixture which again was concentrated to 1/2 initial volume at 30 mtorr. Additional anhydrous ethanol or tetrahydrofuran (2 ml)



was added to the respective reaction mixture which was then filtered through 0.2  $\mu\text{m}$  nylon to remove the Pd/C catalyst. The reaction flasks were rinsed with ethanol (2 ml) which was filtered and combined with the appropriate initial filtrate.

#### Purification of (S)-5-<sup>3</sup>H-Nicotine (1a)

The reaction mixtures were analyzed initially by UV diode array and radiochemical detection following separation on a Porasil 10  $\mu\text{m}$  silica HPLC cartridge (Whatman). By both UV and radiochemical criteria the product obtained from the ethanol reaction appeared to be pure while the tetrahydrofuran reaction mixture contained approximately 10% starting material. To insure UV and radiochemical purity the following procedure was adopted. From each stock reaction mixture injections equivalent to approximately 650  $\mu\text{g}$  of the product were made on a semipreparative silica HPLC column (Rainin) with acetonitrile 1% n-propylamine as the mobile phase. Fractions corresponding to the elution time of (S)-nicotine were collected, reanalyzed by HPLC and pooled. The pooled fractions (50 ml) were concentrated to 5 ml under a slight vacuum at 48°C. To this concentrate was added 10 ml of 0.05 N HCl. Most of the remaining acetonitrile was removed by rotary evaporation. The remaining solution was transferred to a 25 ml volumetric flask. Ethanol (2.5 ml) was added to the aqueous solution of radiolabeled product as a radical trapping agent. At a concentration of 1 mCi/ml in the ethanolic solution, (S)-5-<sup>3</sup>H-nicotine decomposed at a rate of approximately 1% per month. Final UV and radiochemical purity were confirmed by HPLC on silica employing a combined UV diode-array/radiochemical flow detector. The UV purity was estimated at 99.4 and 100% for the ethanol and tetrahydrofuran reaction products, respectively, by comparison of absorption ratios at 260 nm ( $\lambda_{\text{max}}$ ) to 240 and 280 nm. Radiochemical purity in both instances was >99.0%. The final specific activity for the preparations were 32 Ci/mmol for the ethanol reaction product and 28 Ci/mmol for the tetrahydrofuran reaction product. For <sup>3</sup>H NMR analysis, approximately 100 mCi of 1a purified from the tetrahydrofuran reaction was

evaporated to dryness under vacuum and then dissolved in CDCl<sub>3</sub>. The 288 spectrum displayed a singlet signal at  $\delta$  7.33 ppm.

- 
1. Bock, F.G., "Cocarcinogenic properties of nicotine," In: Banbury Report: A safe cigarette? (G.B. Gori and R.G. Buck, Eds.) pp. 129-138 Cold Spring Harbor Laboratory, New York (1980).
  2. Booyse, F.M., G. Osikowicz and A.J. Quarfoot, "Effects of chronic oral consumption of nicotine on the rabbit aortic endothelium," *Amer. J. Path.* **102**, 229-238 (1981).
  3. Boyd, M.R., "Biochemical mechanisms in chemical induced lung injury: Roles of metabolic activation," *CRC Crit. Rev. Toxicol.* **9**, 103-176 (1980).
  4. Nguyen, T-L., L.D. Gruenke and N. Castagnoli Jr., "Metabolic oxidation of nicotine to chemically reactive intermediates," *J. Med. Chem.* **22**, 259-263 (1979).
  5. Commercial Nicotine, D or L-[N-methyl-<sup>3</sup>H] Du Pont New England Nuclear, Boston
  6. Vincek, W.C., B.R. Martin, M.D. Aceto and E.R. Bowman, "Synthesis and preliminary binding studies of 4,4-ditritio(-)-nicotine of high specific activity," *J. Med. Chem.* **23**, 960-962 (1980).
  7. Papadopoulos, N.M., "Formation of nornicotine and other metabolites from nicotine *in vitro* and *in vivo*," *Can. J. Biochem.* **42**, 435-442 (1964).
  8. Brandange, S. and L. Lindblom, "Synthesis, structure and stability of nicotine  $\Delta^{1'}$ -(5') iminium ion, an intermediary metabolite of nicotine," *Acta Chem. Scand. B* **33**, 187-191 (1979).
  9. Peterson, L.A., "Stereochemical studies of the cytochrome P-450 catalyzed oxidation of (S)-nicotine to nicotine  $\Delta^{1'}$ -(5')-iminium ion," - Ph.D. Dissertation. University of California, San Francisco (1986).
  10. Gorrod, J.W. and P. Jenner, "The metabolism of tobacco alkaloids," In: Essays in Toxicology (W.J. Hayes Jr., Ed), Vol 6, pp. 35-78 Academic Press, New York (1975).
  11. Jacob, P., "Resolution of (+)-5-bromonornicotine, synthesis of (R)-and (S)-nornicotine of high enantiomeric purity," *J. Org. Chem.* **47**, 4165-4167 (1982).
  12. Evans, E.A., "Tritium and its compounds," John Wiley and Sons, Inc., New York (1974).
  13. Nguyen, T.L. and N. Castagnoli Jr., "The syntheses of deuterium labelled tobacco alkaloids: Nicotine, nornicotine and cotinine," *J. Labelled compds.* **14**, 919-934 (1978).
  14. Whidby, J.F. and Seeman, "The configuration of nicotine. A nuclear magnetic resonance study," *J. Org. Chem.* **41**, 1585-1590 (1976).
  15. Bayly, R.J. and H. Weigel, "Self-decomposition of compounds labelled with radioactive isotopes," *Nature (London)* **188**, 384-387 (1960).

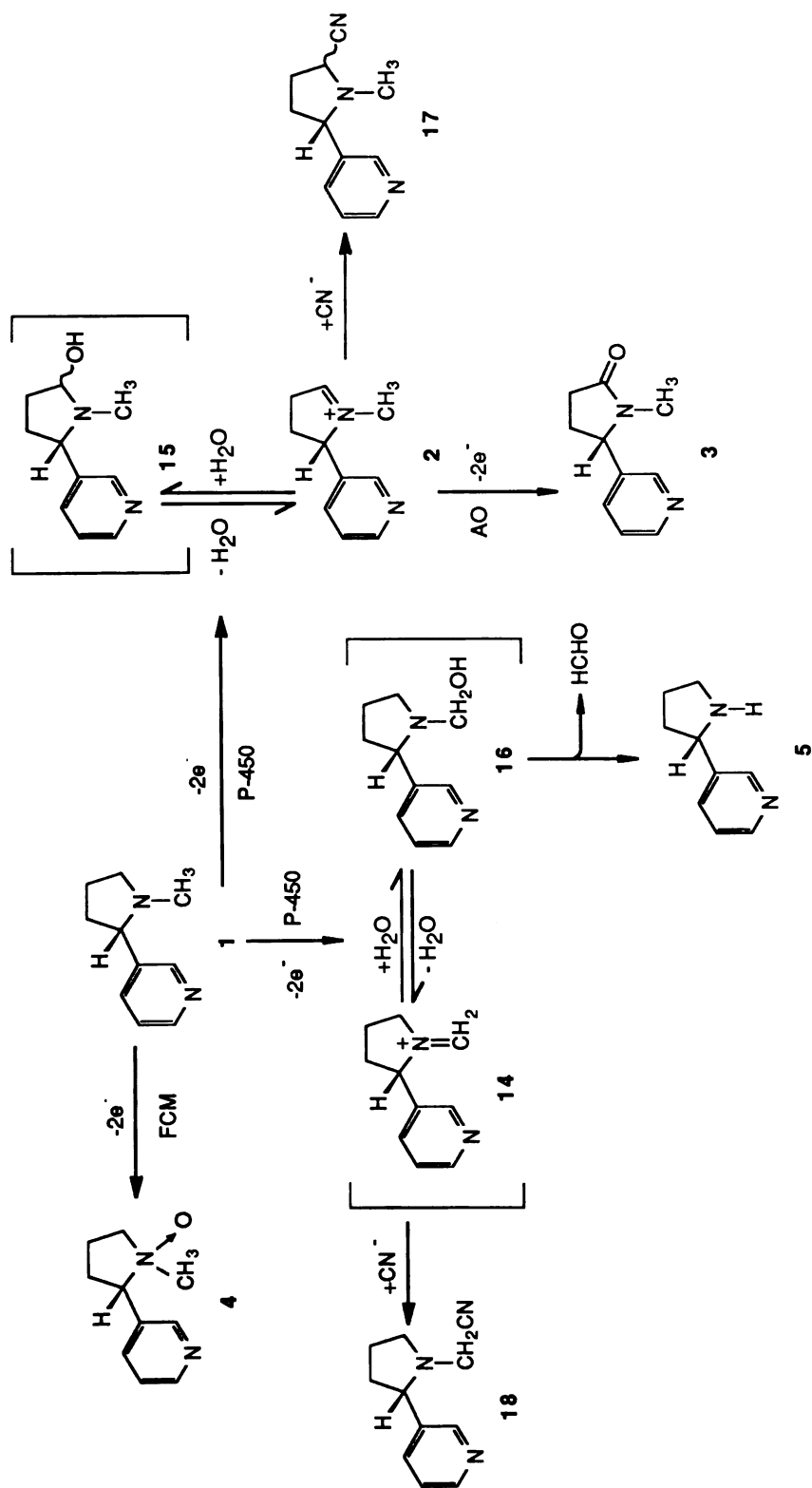
- 
16. Scholes, G., P. Shaw, R.L. Wilson and M. Ebert, "Pulse radiolysis studies of aqueous solutions of nucleic acid and related substances," In: Pulse Radiolysis (M. Ebert, J.P. Keene, A.J. Swallow and J.H. Baxendale, Eds.), pp. 151-164 Academic Press, London (1965).
  17. Baco, Z.M. and P. Alexander, "Fundamentals of Radiobiology," Pergamon Press, London (1961).
  18. Evans, E.A. and F.G. Stanford, "Stability of thymidine labeled with tritium or carbon-14," *Nature (London)* **199**, 762-765 (1963).
  19. Rondahl, L., "Synthetic analogues of nicotine VI," *Acta Pharmaceutica Suecica* **14**, 113-118 (1977).

**Chapter III**  
**Metabolism Dependent Covalent Binding of**  
**(S)-5-<sup>3</sup>H-Nicotine**

## Introduction

As described in Chapter I, (S)-nicotine (1) is suspected of contributing to some of the irreversible tissue lesions and other toxic effects observed in humans and animals who are exposed chronically to tobacco products.<sup>1, 2</sup> Although the metabolic fate of (S)-nicotine has been examined extensively,<sup>3</sup> the possibility that it may be biotransformed to chemically reactive intermediates capable of forming covalent bonds to tissue macromolecules has not been investigated.

Previous studies have shown that (S)-nicotine undergoes cytochrome P-450 dependent oxidative metabolism principally at the 5'-carbon atom of the pyrrolidine ring and, to a minor extent, at the N-methyl carbon atom.<sup>4, 5</sup> These 2-electron  $\alpha$ -carbon oxidations generate the electrophilic iminium species (S)-nicotine  $\Delta^{1',5'}$ -iminium ion (2) and nicotine methyleneiminium ion (14) which are in equilibrium with the corresponding  $\alpha$ -carbinolamines (S)-5'-hydroxynicotine (15) and (S)-N-methylhydroxynornicotine (16), respectively (Scheme III.I). The spontaneous breakdown of 16 yields nornicotine (5). The (S)-nicotine- $\Delta^{1',5'}$ -iminium species undergoes further oxidation *in vivo* in a reaction catalyzed by aldehyde oxidase<sup>6</sup> to yield the lactam (S)-cotinine (3), a major urinary metabolite of (S)-nicotine in mammals.<sup>3</sup> Characterization of the reactive electrophilic iminium intermediates has been achieved via the corresponding  $\alpha$ -cyanoamines (S)-5'-cyanonicotine (17) and (S)-N-cyanomethylnornicotine (18) which have been isolated from liver microsomal incubation mixtures of (S)-nicotine containing NaCN. Furthermore, since (S)-nicotine  $\Delta^{1',5'}$ -iminium ion (2) can be trapped as the 5'-cyanoamine 17 in post-liver perfusates of (S)-nicotine (M. Halldin, personal communication), it would appear that this iminium intermediate has more than a transient biological lifetime. These considerations encouraged us to examine the possible metabolic dependent covalent binding of (S)-nicotine to biomacromolecules under conditions favorable for cytochrome P-450 monooxygenase activity. Since the phenobarbital inducible form(s) of



Scheme III.1 Major Pathways for the Metabolic Oxidation of (S)-Nicotine

cytochrome P-450 is (are) involved in the oxidative metabolism of (S)-nicotine,<sup>7</sup> we employed liver microsomes isolated from phenobarbital pretreated rabbits. The resulting data were compared to those obtained with control rabbit liver and lung microsomes and human liver microsomes.

## **Results**

### ***In vitro* Metabolism of (S)-Nicotine**

In order to quantitate the extent of (S)-nicotine metabolism by microsomal preparations, an analytical method based on HPLC with UV detection was developed. This method, which employed a normal phase silica HPLC column, permitted the detection of methylene chloride extractable metabolites from metabolic incubations. The formation of (S)-nicotine metabolites generated in incubation mixtures containing liver microsomes prepared from phenobarbital induced rabbits revealed the formation of one major metabolite with chromatographic characteristics identical to those of synthetic (S)-nicotine- $\Delta^{1',5'}$ -iminium bisperchlorate (**Fig.III.1A**). When the post-incubation mixture was treated with excess NaCN, the HPLC peak corresponding to the iminium species was replaced by a peak with a retention time corresponding to the  $\alpha$ -cyanoamines **17** (**Fig.III.1B**), thus confirming the identity of this metabolite. The original chromatogram also showed a peak corresponding to (S)-cotinine (**3**). Since the chromatographic conditions were less than satisfactory for the detection of nornicotine, levels of this minor metabolite were not detected. In addition, because of the highly polar nature of (S)-nicotine N'-oxide, this compound was not extractable under these conditions and therefore could not be quantitated. In the absence of NADPH, (S)-nicotine was recovered essentially quantitatively (**Fig.III.1C**). Qualitatively similar results were obtained with rabbit lung microsomes and human liver microsomes.



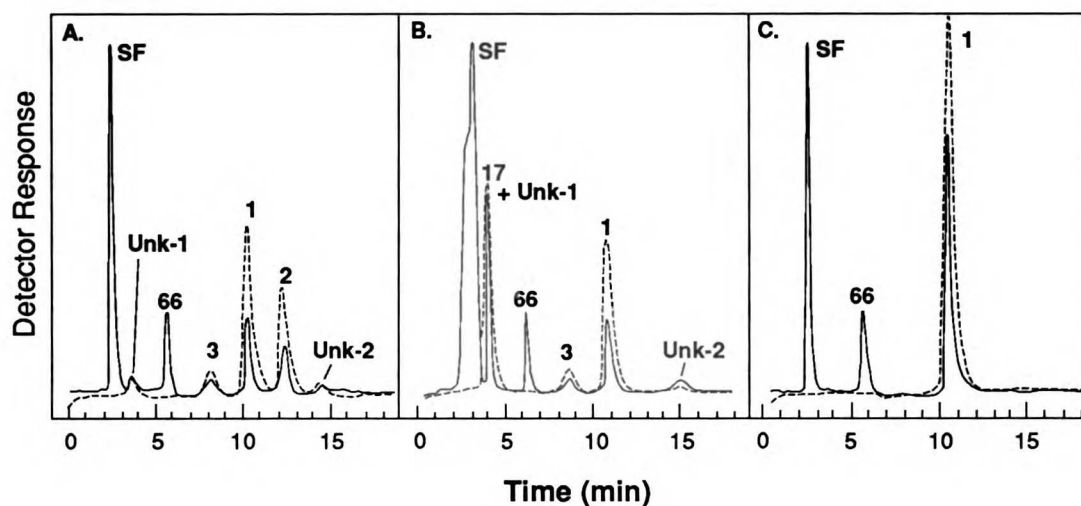


**Fig.III.1** HPLC Analysis of (S)-5-<sup>3</sup>H-Nicotine Metabolism by Rabbit Liver Microsomes. (S)-5-<sup>3</sup>H-Nicotine (0.5 mM, 1.1  $\mu$ Ci) was incubated at 37°C with liver microsomes (2 mg protein/ml) isolated from phenobarbital treated rabbits in HEPES buffer, pH 7.6, with or without NADP<sup>+</sup> and a regenerating system and analyzed by HPLC as described in Materials and Methods. (S)-5-<sup>3</sup>H-Nicotine and its base extractable metabolites were detected by UV [260 nm (—)] and radioactivity monitoring (---). A. (S)-5-<sup>3</sup>H-Nicotine metabolism after 1 hr in the presence of NADP<sup>+</sup> and a regenerating system. B. (S)-5-<sup>3</sup>H-Nicotine metabolism as above (panel A.) but treated with NaCN (0.1 mmoles) at the end of the incubation. C. (S)-5-<sup>3</sup>H-nicotine metabolism either at time zero or after 1 hr in the absence of NADP<sup>+</sup> and a regenerating system.

Quantitative estimations (Table III.1) showed that liver microsomes isolated from phenobarbital treated rabbits metabolize (S)-nicotine more efficiently than liver microsomes isolated from control rabbits. Similar results have been reported with liver microsomes prepared from treated and control rats.<sup>7</sup> The rates of disappearance of (S)-nicotine in metabolic incubations employing human liver microsomes and rabbit lung microsomes were considerably slower on a per mg microsomal protein basis than that observed with the rabbit liver microsomes (Table III.1). Estimates of the percent conversion to the various metabolites employing microsomes from phenobarbital treated rabbits showed that the iminium species is by far the major product (up to 60%) while maximum yields of (S)-cotinine were 10% of the

(S)-nicotine consumed (Fig.III.2). The observed formation of (S)-cotinine (3) in the absence of a cytosolic oxidase, probably reflects an NADPH dependent conversion of 2 to 3. The higher percent yield of the iminium metabolite observed with microsomes from phenobarbital treated rabbits suggests that phenobarbital treatment leads to the selective induction of isozyme(s) which favor C-5' oxidation. Using a separate assay, the N'-oxide of (S)-nicotine was identified and at 60 min represented about 10% of the (S)-nicotine consumed. Rough estimations from the rabbit liver microsomal studies indicate a mass balance of about 80% and suggest that additional metabolites may be formed in these incubation mixtures.

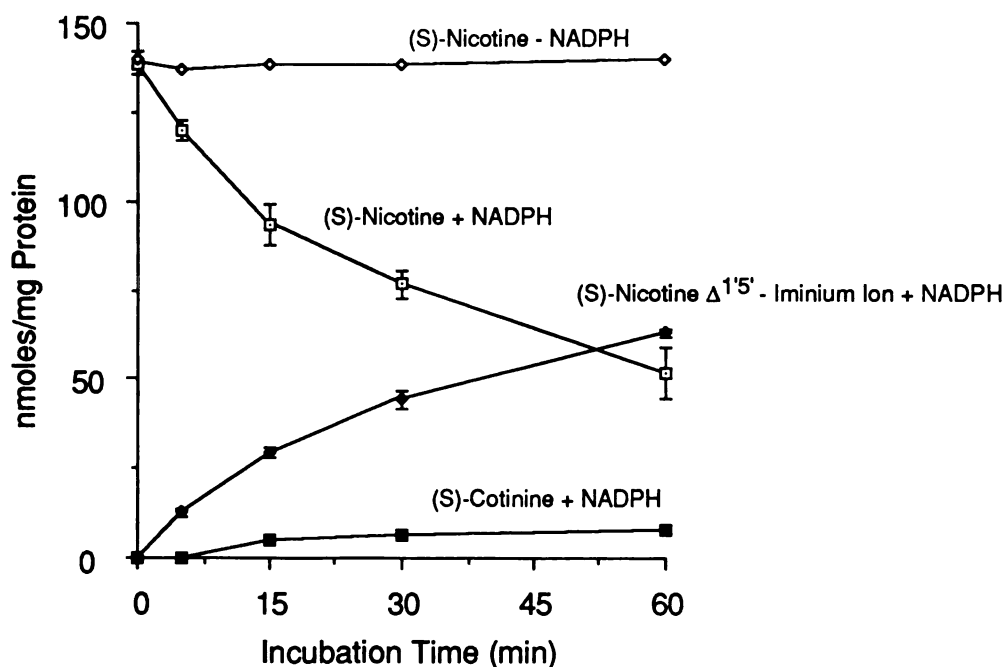


**Fig.III.2** Liver Microsomal Metabolism of (S)-Nicotine. (S)-Nicotine (0.3 mM) was incubated as described in Fig.III.1. (S)-Nicotine and the 5'-carbon oxidation products (S)-nicotine  $\Delta^{1'5'}$ -iminium ion and (S)-cotinine were analyzed by HPLC as described in Materials and Methods. Data points represent means of triplicate determinations  $\pm$  S.E. (vertical bars).

**Table III.1** NADPH Dependent Metabolism and Covalent Binding of (S)-5-<sup>3</sup>H-Nicotine in Various Tissue Preparations.

	A. (S)-Nicotine metabolized (nmol/mg protein/hr)	B. (S)-Nicotine covalently bound (nmol/mg protein/hr)	C. Ratio A:B	D. Metabolite formation (nmol/mg protein/hr) $\Delta^{1',5'}$ -iminium cotinine		E. P-450 *
-NADPH	-	-	n.d	-	-	1.14
Control Rabbit Liver Microsomes	103.5 ± 1.5	0.220 ± 0.020	472	50.5 ± 3.9	17.8 ± 0.8	1.14
PB Treated Rabbit Liver Microsomes	141.0 ± 20.2	0.550 ± 0.123	256	89.3 ± 15.4	28.4 ± 2.0	3.05
Rabbit Lung Microsomes	35.7 ± 1.8	0.160 ± 0.001	229	n.d.	n.d.	n.d.
Human Liver Microsomes	25.0 ± 0.4	0.248 ± 0.007	101	n.d.	n.d.	n.d.

\*nmoles/mg protein  
 - not detectable  
 n.d. not determined

### Metabolism Dependent Covalent Binding of (S)-5-<sup>3</sup>H-Nicotine

The incubation of (S)-5-<sup>3</sup>H-nicotine with control rabbit liver microsomal preparations resulted in the NADPH dependent covalent binding of radioactive metabolites derived from (S)-nicotine to microsomal macromolecules (Table III.1 and Fig.III.3) The binding measured after a 1 hr incubation period (220 pmoles/mg protein) was only half of that observed with liver microsomes prepared from phenobarbital treated rabbits. Lower but still measurable rates were observed with human liver and rabbit lung microsomes. Covalent binding was time dependent (Fig.III.3) and partition ratios [(S)-nicotine equivalents metabolized:(S)-nicotine equivalents bound] ranged from about 100 (human liver microsomes) to 500 (control rabbit liver microsomes). As expected, cytochrome P-450 content increased approximately 250% in liver microsomes from phenobarbital treated animals compared to controls.

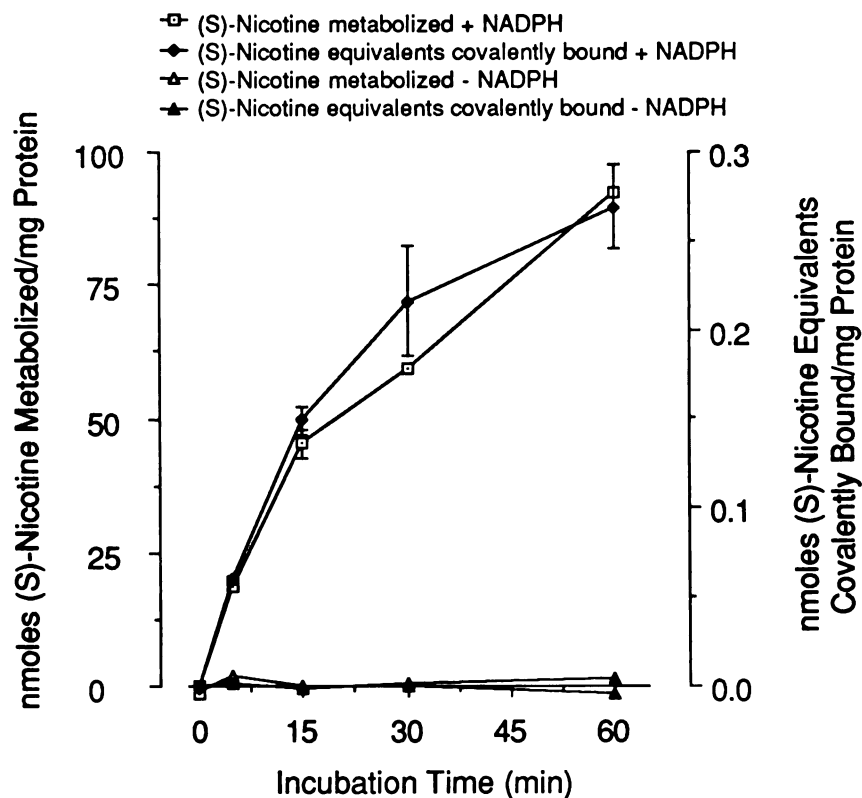


**Fig.III.3.** Metabolism Dependent Covalent Binding of (S)-5-<sup>3</sup>H-Nicotine to Liver Microsomes. (S)-5-<sup>3</sup>H-Nicotine (0.3 mM, 2.5  $\mu$ Ci) was incubated as described in Fig.III.2. Acetonitrile precipitated liver microsomal particulate material was subjected to rapid filtration and solvent washes and the remaining radioactivity determined. The radioactivity corresponding to the -NADPH control was subtracted for each data point. (S)-Nicotine was analyzed by HPLC as described in Materials and Methods. Data points are defined as the mean of triplicate determinations  $\pm$  S.E. (vertical bars).

Incubation of liver microsomes obtained from phenobarbital treated rabbits with the cytochrome P-450 monooxygenase inhibitors SKF 525-A and n-octylamine decreased both the rate of (S)-nicotine metabolism and covalent binding by approximately the same extent (Table III.2). The addition of cytochrome c, a heme containing protein which inhibits the transfer of electrons from cytochrome P-450 reductase to cytochrome P-450,<sup>4</sup> also decreased (S)-nicotine metabolism and binding. The epoxide hydratase inhibitor cyclohexene oxide inhibited the overall metabolism of (S)-nicotine, although the partition ratio decreased thus implicating a possible role of an epoxide intermediate in the covalent binding observed in these experiments.

**Table III.2** Effects of Enzyme Inhibitors on Metabolism Dependent Covalent Binding of (S)-5-<sup>3</sup>H-Nicotine to Liver Microsomes

Inhibitor	(S)-Nicotine metabolized (% of control)	(S)-5- <sup>3</sup> H-Nicotine covalently bound (% of control)
SKF 525-A (0.25 mM)	49	53
N-octylamine (3 mM)	25	36
Cytochrome c (1 mM)	30	-
Cyclohexene oxide (3 mM)	45	66
NaCN (0.5 mM)	64	54

(S)-5-<sup>3</sup>H-Nicotine (0.5 mM, 0.25  $\mu$ Ci) was incubated at 37°C for 1 hr with liver microsomes (2 mg protein/ml) from phenobarbital treated rabbits in HEPES buffer, pH 7.6, plus NADP<sup>+</sup> and a regenerating system. (S)-Nicotine concentrations were estimated by HPLC and covalent binding by radioactivity detected in the acetonitrile-precipitated particulate material which was subjected to rapid filtration and solvent washes. Values represent means of 2-3 experiments. Control data shown in Table III.1

#### Attempted Trapping of (S)-Nicotine $\Delta^{1',5'}$ -iminium ion and Inhibition of Covalent Binding by Cyanide

Previous studies using liver microsomes from male Dutch rabbits have shown that NaCN could be used to trap the metabolically generated iminium species derived from (S)-nicotine,<sup>13</sup> phencyclidine<sup>11</sup> and N-benzylpyrrolidine,<sup>8</sup> at concentrations which did not inhibit the cytochrome P-450 dependent metabolism of these substrates. Similar studies were performed in the present series of experiments using liver microsomes obtained from phenobarbital treated New Zealand White rabbits in an attempt to determine if the covalent binding of (S)-nicotine could be inhibited without affecting its metabolism. The results (Fig.III.4 and 5) show that in this species, both covalent binding and metabolism are inhibited by NaCN to about the same extent. We also observed that the addition of NaCN to liver microsomal suspensions resulted in the appearance of a Soret band with  $\lambda_{max}$  445 nm and  $\lambda_{min}$  405 nm characteristic of a type II (or modified type II) binding spectrum.<sup>9</sup> An examination of the concentration dependent characteristics of this cytochrome P-450 binding spectrum revealed multiple binding constants (Data not shown) which might reflect different affinities of cyanide

ion for the various cytochrome P-450 isozymes.<sup>10</sup> Since (S)-nicotine also exhibited a type II binding spectrum, the observed inhibition of (S)-nicotine metabolism by NaCN may be due to the competitive binding of cyanide ion and (S)-nicotine at the active site of the cytochrome P-450 isozyme present in this species. These inhibitory effects of cyanide ion were similar to those observed in incubations in which the NADPH regenerating system was replaced by excess NADPH and therefore it is unlikely that cyanide ion depletes NADP<sup>+</sup> via nucleophilic attack at the C-4 position of the pyridinium ring.<sup>10</sup>

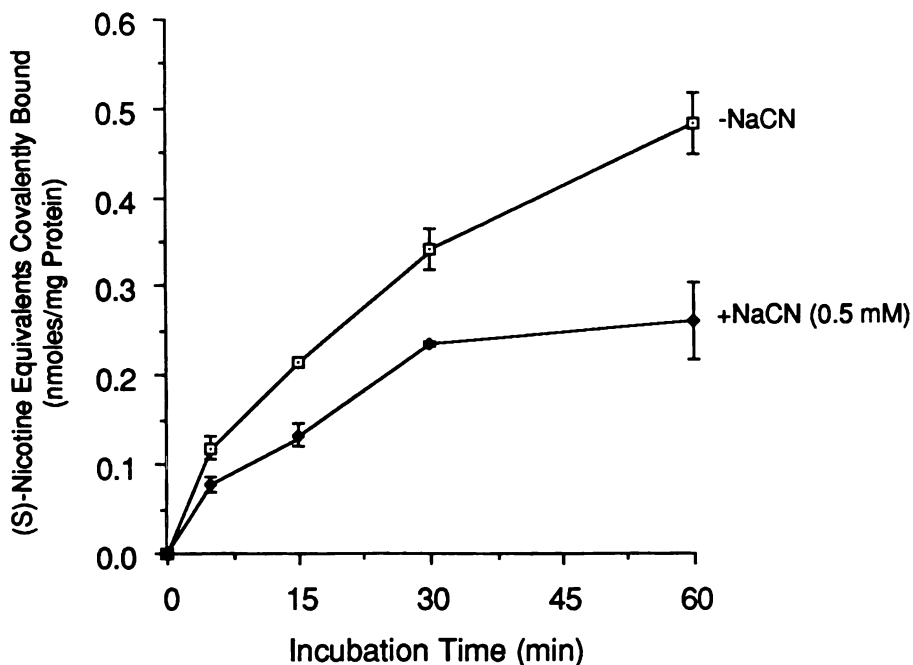


**Fig.III.4** Effect of Sodium Cyanide on the Metabolism Dependent Covalent Binding of (S)-5-<sup>3</sup>H-Nicotine to Liver Microsomes. (S)-5-<sup>3</sup>H-Nicotine (0.5 mM, 2.5  $\mu$ Ci) was incubated at 37°C with liver microsomes (2 mg protein/ml) isolated from phenobarbital treated rabbits in HEPES buffer, pH 7.6, with NADP<sup>+</sup> and a regenerating system in the presence (0.5 mM) or absence of NaCN. Acetonitrile precipitated microsomal particulate material was subjected to rapid filtration and solvent washes and the remaining radioactivity was determined. Data points represent means of triplicate determinations  $\pm$  S.E.

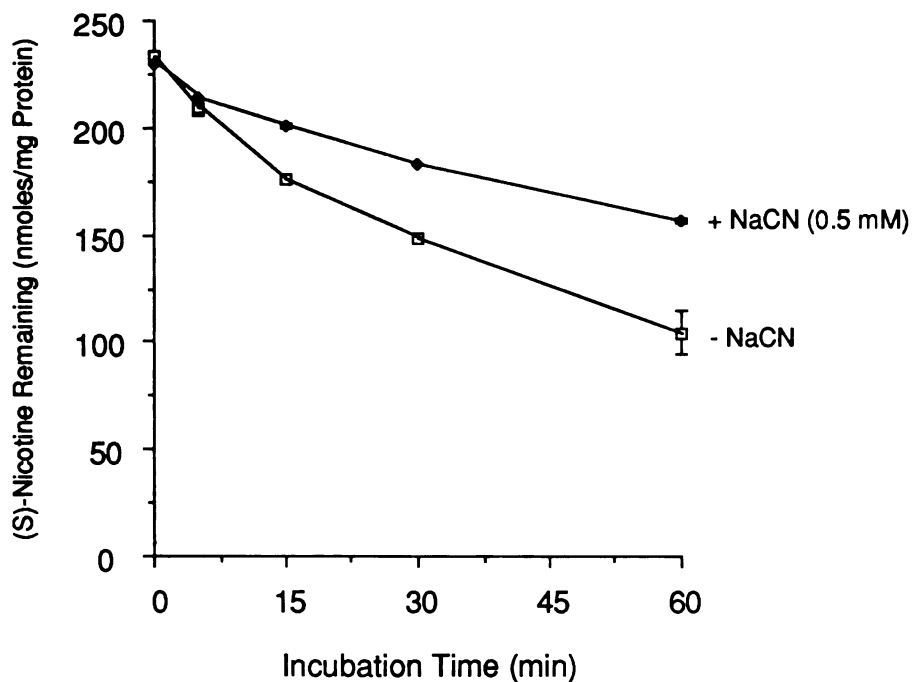


**Fig.III.5** Effect of Sodium Cyanide on Liver Microsomal Metabolism of (S)-Nicotine. (S)-Nicotine (0.5 mM) was incubated at 37°C with liver microsomes (2 mg protein/ml) from phenobarbital treated rabbits in HEPES buffer with NADP<sup>+</sup> and a regenerating system in the presence (0.5 mM) or absence of NaCN. (S)-Nicotine was analyzed by HPLC as described in Materials and Methods. Data points represent means of triplicate determinations  $\pm$  S.E.

#### Cyanide Binding to Microsomal Cytochrome P-450

A study designed to examine the concentration dependent inhibition of (S)-nicotine metabolism by sodium cyanide was performed. As shown in Fig.III.6, sodium cyanide inhibited, in a concentration dependent manner, the metabolism of (S)-nicotine (0.5 mM) catalyzed by liver microsomes prepared from untreated or phenobarbital pretreated rabbits. At a concentration of 100  $\mu$ M, sodium cyanide inhibited the metabolism of (S)-nicotine catalyzed by both preparations by approximately 50%. In order to quantitatively trap (S)-nicotine iminium ions, which are present in concentrations exceeding 150  $\mu$ M in metabolic incubation mixtures employing liver microsomes, a 2-5 fold molar excess of cyanide is required, a condition which would inhibit (S)-nicotine metabolism. Therefore, these results indicate that

sodium cyanide cannot be used to assess the involvement of (S)-nicotine iminium species in the covalent binding of metabolically activated (S)-nicotine.

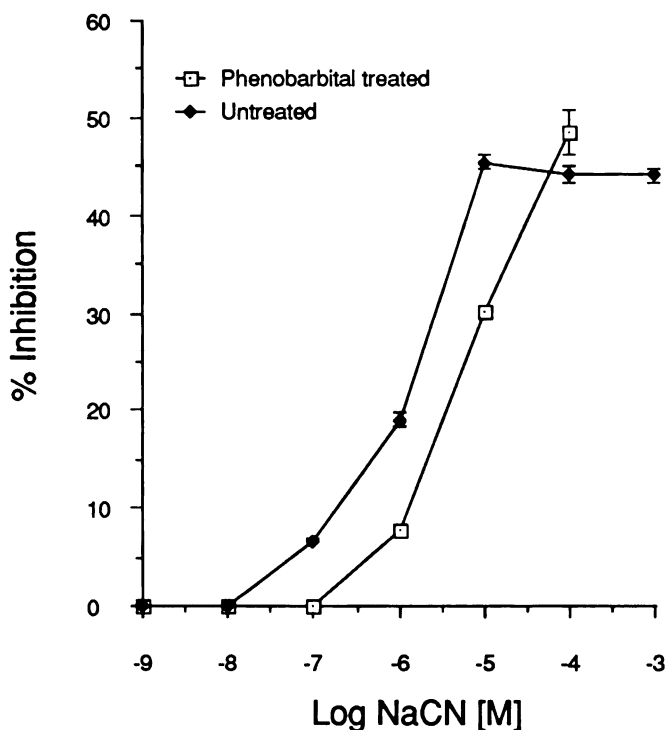


**Fig III.6** Concentration Dependent Inhibition of (S)-Nicotine Metabolism by Sodium Cyanide. (S)-Nicotine (0.5 mM) was incubated with liver microsomes (1 mg/ml) obtained from untreated and phenobarbital pretreated rabbits at 37°C for 1 hr in the presence of the indicated concentrations of sodium cyanide. (S)-Nicotine metabolism was quantitated as described in Materials and Methods.

## Discussion

The results described in this chapter show that (S)-nicotine is bioactivated by an NADPH dependent mechanism to chemically reactive intermediate(s) which bind covalently to liver and lung microsomal protein. Although the magnitude of binding is not particularly high, the relatively low partition ratio observed with microsomes obtained from untreated rabbit lung tissue suggests that the enzymes responsible for bioactivation of (S)-nicotine may be more abundant in this organ than in the liver. The even lower partition ratio observed with human liver microsomal preparations also is noteworthy. Analysis of all of the (S)-nicotine microsomal metabolic profiles demonstrated the preferential formation of the  $\Delta^{1',5'}$ -iminium ion metabolite 2,



confirming the quantitative importance of this intermediate in the metabolic pathway leading to the formation of (S)-cotinine, a major urinary metabolite of (S)-nicotine.<sup>4</sup>

Characterization of the enzyme system(s) responsible for the bioactivation of (S)-nicotine has included attempts to manipulate microsomal monooxygenase activity. N-Octylamine, an activator of microsomal flavin containing monooxygenase (FCM) and an inhibitor of cytochrome P-450, inhibited binding and metabolism. We suggest, therefore, that the FCM mediated N-oxidation of (S)-nicotine<sup>11</sup> is unlikely to result in covalent binding. Since cytochrome P-450 monooxygenase inhibitors decrease both (S)-nicotine metabolism and covalent binding to an equivalent extent, the cytochrome P-450 catalyzed oxidation pathway becomes a candidate for the bioactivation of (S)-nicotine. The 2.5 fold increase in covalent binding observed in our studies with liver microsomes prepared from phenobarbital treated rabbits compared to those from control animals is consistent with the participation of phenobarbital inducible isozymes of cytochrome P-450 (e.g. P-450 isozyme-2)<sup>7</sup> in the bioactivation process. The increased covalent binding correlates well with the increase in microsomal cytochrome P-450 content but not with the relatively modest increase observed in the overall metabolism of (S)-nicotine. A closer correlation, however, exists between the increase in covalent binding and the increase in the formation of the (S)-nicotine  $\Delta^{1',5'}$ -iminium ion metabolite.

In an effort to provide evidence for the role of (S)-nicotine  $\Delta^{1',5'}$ -iminium ion in the bioactivation process, we examined the effects of sodium cyanide on the covalent binding of (S)-nicotine to microsomal proteins. A similar approach had proven effective in the case of phencyclidine, a tertiary amine bioactivated via an obligate iminium intermediate, since metabolism dependent covalent binding of phencyclidine to proteins was blocked by concentrations of sodium cyanide which trapped the iminium intermediate but which did not inhibit its formation. This strategy proved to be less

satisfactory in the case of (S)-nicotine since sodium cyanide was found to inhibit oxidative metabolism to approximately the same extent as covalent binding.

The observation that sodium cyanide inhibits cytochrome P-450 monooxygenase activity is important with regard to experiments where this compound is used to trap electrophilic intermediates. The mechanism by which cyanide inhibits (S)-nicotine oxidation as well as other substrates is not well understood.<sup>12</sup> The present study indicates that this compound binds to unreduced (ferric) P-450 with spectral dissociation constants ranging from values as low as 35  $\mu\text{M}$  to greater than 1 mM. Studies by other groups have shown that cyanide binds to the various cytochrome P-450 isozymes with lower affinities than those reported in this study. Kitada *et al.*,<sup>12</sup> for example, have noted spectral dissociation constants ( $K_S$ ) of 0.21 and 1.05 mM for the binding of cyanide to Wistar rat liver microsomal P-450. The binding of cyanide to these microsomes resulted in a slightly modified type II binding spectra (445 nm  $\lambda_{\text{max}}$ , 410 nm  $\lambda_{\text{min}}$ ) similar to that reported in Albino male rats by Schenkman *et al.*<sup>13</sup> The possibility that cyanide competitively inhibits the binding of oxygen to the reduced form of cytochrome P-450 was suggested by Kitada *et al.*<sup>12</sup> as a mechanism for the cyanide dependent inhibition of ethylmorphine metabolism by liver microsomes. This conclusion was based on the observation that the cyanide dependent inhibition of aniline hydroxylation and ethylmorphine N-demethylation was reversible by increasing the oxygen concentration in the metabolic incubation. Additional evidence in support of this mechanism came from a study by Koop *et al.*<sup>14</sup> which described the organic hydroperoxide supported N-dealkylation of *p*-nitroanisole by *tert*-butylhydroperoxide. Enzyme kinetics indicated that the inhibition of *p*-nitroanisole N-demethylation by potassium cyanide (at concentrations ranging between 2.5-10.0 mM) was competitive with respect to the source of oxygen, *tert*-butylhydroperoxide, but uncompetitive with respect to the substrate *p*-nitroanisole. This evidence together with the reports of Kitada *et al.*<sup>12</sup> indicate that the inhibition of the liver microsomal oxidation of

(S)-nicotine by cyanide could be the result of a competition between cyanide and molecular oxygen at the cytochrome P-450 binding site.

Alternatively, the inhibition of (S)-nicotine metabolism may also be due to the cyanide sensitivity of a particular cytochrome P-450 isozyme(s) which catalyzes the oxidation of this compound. Comai and Gaylor<sup>9</sup> reported that different purified forms of rat liver cytochrome P-450 exhibit varying affinities toward cyanide. Thus, it is possible that the isozyme which is responsible for catalyzing most of the oxidation of (S)-nicotine binds cyanide with a higher affinity. More detailed studies will be required to understand better the mechanism involved in the cyanide dependent inhibition of (S)-nicotine oxidation.

Since cyanide inhibits the liver microsomal oxidation of (S)-nicotine, the experimental approach which was aimed at characterizing the bioactivation of this tertiary amine through the trapping of the reactive  $\alpha$ -carbon oxidation products with cyanide would not appear to be viable even at  $\mu\text{M}$  concentrations of this nucleophilic species. It is largely due to our inability to conclusively demonstrate the importance of the metabolic pathway leading to nicotine  $\Delta^{1',5'}$ -iminium ion in the covalent binding of (S)-nicotine that other studies were pursued. These studies will be described in the addendum to this chapter and in Chapter IV.

Despite the quantitative importance of (S)-nicotine  $\Delta^{1',5'}$ -iminium ion in the oxidative metabolism of (S)-nicotine, the present study does not provide direct evidence for its involvement as the reactive intermediate in covalent binding. Thus, it remains possible that the cytochrome P-450 dependent bioactivation process of (S)-nicotine involves the formation of an unidentified reactive intermediate that could be formed in a quantitatively minor pathway. Irrespective of the mechanistic details, however, the observed metabolic dependent alkylation of proteins by (S)-nicotine may contribute to some of the irreversible lesions reported to be caused by long term exposure to tobacco products.

## Materials and Methods

### Chemicals

Cyclohexene oxide, n-octylamine, dithiothreitol, sodium dithionite, cytochrome c, KCl, HEPES, D-glucose-6-phosphate, NADP<sup>+</sup> and tris(hydroxymethyl) aminomethane hydrochloride (TRIS) were obtained from Sigma Chemical Company (St. Louis, MO.). SKF 525-A was a generous gift of Dr. Almira Correia (University of California, San Francisco). The HPLC internal standard N-methyl-N-(3-pyridyl) methylpropanamide was a gift of Dr. Peyton Jacob III (San Francisco General Hospital). Acetonitrile and methylene chloride were HPLC grade solvents obtained from Baker (Phillipsburg, NJ). Solvents used for covalent binding studies were of practical grade. (S)-Nicotine and n-propylamine were obtained from Aldrich (Milwaukee, WI). (S)-Nicotine was distilled under vacuum prior to use. KH<sub>2</sub>PO<sub>4</sub> and sodium cyanide were purchased from Allied Chemical (Morristown, NJ) and glucose-6-phosphate dehydrogenase from Calbiochem-Behring Corporation (La Jolla, CA). Sucrose and sodium phenobarbital were obtained from Mallinckrodt, Inc. (Paris, KY). (S)-Nicotine  $\Delta^{1',5'}$ -iminium ion *bis*perchlorate,<sup>15</sup> the diastereomeric mixture of (R)- and (S)-5'-cyano-(S)-nicotine,<sup>15</sup> the diastereomeric N-oxides,<sup>16</sup> (S)-cotinine<sup>17</sup> and nornicotine<sup>18</sup> were prepared as described previously. (S)-5-<sup>3</sup>H-Nicotine was prepared by carrier free catalytic tritiation of (S)-5-bromonicotine at the National Tritiation Facility at the University of California, Berkeley.<sup>19</sup> The final product was greater than 99% pure by HPLC employing both UV and radiochemical detectors and had a specific activity of 32 Ci/mmol. Flow Scint II scintillation fluid was obtained from Radiomatic Instruments and Chemical Co. Inc. (Tampa, FL).

### Sources of Tissues

The liver and lungs of New Zealand White male rabbits (2.5-3 kg) were used for preparation of microsomes. For studies using phenobarbital treated animals, rabbits

received 0.1% (w/v) sodium phenobarbital, pH adjusted to 7.0 with 0.1 N HCl, administered in drinking water for 6 days prior to sacrifice. Human liver microsomes were obtained from liver samples of donors participating in the Stanford University Heart Transplantation Program and were provided through the courtesy of Dr. James Trudell, Department of Anesthesia, Stanford University Medical Center.

#### **Preparation of Rabbit Liver Microsomal Fractions**

Following carbon dioxide asphyxiation, the livers were perfused *in situ* via the portal vein with 250 ml of ice cold 0.25 M sucrose buffered at pH 7.4 with 0.05 M TRIS/0.05 M NaOH. Livers were minced with scissors and the pieces were homogenized in a Potter-Elvehjem apparatus in 3 volumes (w/v) of the same solution. The homogenate was centrifuged at 10,000 x g for 20 min and the resulting supernatant fraction was centrifuged at 100,000 x g for 75 min. The pellet was resuspended in 5 ml of 0.15 M KCl buffered at pH 7.4 with 0.02 M KH<sub>2</sub>PO<sub>4</sub> and this mixture was centrifuged a second time at 100,000 x g for 60 min. The resulting pellet was homogenized in this buffer at a concentration of approximately 50 mg microsomal protein/ml and stored under nitrogen at -70°C for up to 1 month. Protein concentration was determined by the method of Lowry *et al.*<sup>20</sup>

#### **Preparation of Rabbit Lung Microsomes**

Immediately after sacrificing the animal by carbon dioxide asphyxiation, the lungs were perfused via the pulmonary artery with 10-15 ml of ice cold 0.15 M KCl-0.02 M KH<sub>2</sub>PO<sub>4</sub> buffer containing 100 U/ml heparin (Elkin-Sinn, Inc. Cherry Hill, NJ). The isolated perfused lungs were coarsely minced in a solution consisting of 0.02 M TRIS, 0.15 M KCl, 0.2 mM EDTA and 0.5 mM dithiothreitol and the resulting mince homogenized in a Waring Blender with two 10 second bursts. The contents were transferred to a Potter-Elvehjem homogenizer and homogenized with 6 passes of a Teflon pestle. The resulting homogenate was centrifuged at 18,000 x g for 20 min. The post mitochondrial supernatant fraction was centrifuged for an additional 60 min at

100,000 x g. The microsomal pellet was resuspended in 5 ml of 0.02 M TRIS and 0.15 M KCl, the pH was adjusted to 7.4 with 1 N NaOH and the resulting suspension was centrifuged at 100,000 x g for an additional 60 min. The pellet was resuspended in this buffer, homogenized and stored under nitrogen at a concentration of approximately 15-25 mg/ml at -70°C for up to 1 month.

#### **Determination of Cytochrome P-450 Concentrations**

The concentrations of cytochrome P-450 were determined using an Aminco DW-2 UV-visible spectrophotometer by measuring UV absorbance differences between the dithionite reduced carbon monoxide treated sample and an unreduced carbon monoxide treated reference sample.<sup>21</sup>

#### **Binding Spectra**

All spectra were recorded with an Aminco DW-2 UV visible spectrophotometer. The frozen rabbit liver microsomal suspensions were thawed and diluted with 0.15 M KCl buffered with 0.02 M KH<sub>2</sub>PO<sub>4</sub>, pH 7.4, to yield a protein concentration of 1 mg protein/ml. Equal volumes of microsomal suspension were added to sample and reference cuvettes and baselines were recorded. Aliquots of an aqueous solution of 1 M (S)-nicotine or 1 M sodium cyanide then were added to the microsomal suspensions such that the final concentrations ranged between 0-6 mM (S)-nicotine or 0-9 mM sodium cyanide. An equal volume of buffer was added to the reference cuvette. Difference spectra were recorded at room temperature between 360 and 500 nm within 1-2 min of the addition of the compounds. All averaged data are presented as the mean ± S.E.

#### **Metabolism Studies**

Incubation mixtures (final volume 1.0 ml) consisted of 1.5 to 2.0 mg microsomal protein, 1 mM EGTA, 0.3 to 0.5 mM (S)-nicotine and where indicated, an NADPH regenerating system (0.5 mM NADP<sup>+</sup>, 8 mM glucose-6-phosphate, 1 unit/ml glucose-6-phosphate dehydrogenase and 4 mM MgCl<sub>2</sub>) in 0.1 mM HEPES buffer, pH 7.6. Binding to microsomal proteins employed (S)-5'-<sup>3</sup>H-nicotine at a specific activity of

either 83 mCi/mmol (0.3 mM) or 50 mCi/mmol (0.5 mM). Some incubation mixtures also contained 0.5 mM sodium cyanide. Incubations were carried out at 37°C under air for the time periods indicated in the text and were terminated by the addition of an equal volume of 1 M K<sub>2</sub>CO<sub>3</sub>. Sample workup followed the procedure described below for the construction of standard curves.

#### **HPLC Analysis and Standard Curves**

Standard curves for (S)-nicotine, (S)-nicotine- $\Delta^{1',5'}$ -iminium *bis*perchlorate and (S)-cotinine were constructed as follows; a mixture of the above compounds (20-80 nmoles) in 0.1 ml of 0.01 N HCl was added to a suspension of 2.0 mg of microsomal protein in 0.9 ml of 0.1 M HEPES buffer, pH 7.6. To these mixtures was added N-methyl-N-(3-pyridyl)methylpropionamide (23 nmoles) in 40  $\mu$ l HEPES buffer as internal standard followed by 1 ml of 1M K<sub>2</sub>CO<sub>3</sub>. HPLC grade methylene chloride (2 ml) was added and the resulting mixture was vortexed for 30 seconds. Centrifugation at 1000 x g for 2-3 min provided a clear organic layer which was subjected to HPLC analysis as described below. Plots of peak height ratios of analyte to internal standard against analyte concentrations gave straight lines which were used in estimating analyte concentrations in sample incubation mixtures. Recoveries were estimated to be greater than 95%. The HPLC assay employed a Beckman 110A solvent delivery system and a Hitachi 100-10 spectrophotometer/flow cell combination. The precolumn (4.6 mm x 5 cm) was packed with Lichrosorb Si 60, 30  $\mu$ m particle size (Merck, Darmstadt) and the analytical column (4.6 mm x 25 cm) with 10  $\mu$ m Lichrosorb (or 5  $\mu$ m Alltech silica). The mobile phase consisted of acetonitrile plus 1% n-propylamine (v/v) and the flow rate was 2.0 ml/min. UV absorption was monitored at 260 nm, the  $\lambda_{max}$  for (S)-nicotine. Samples were run in triplicate. This assay provided a direct measurement of the concentration of the iminium species 2 which previously had been estimated by GC and GC-MS as the corresponding diastereomeric mixture of 5'-cyano adducts. Radiochemical analysis of (S)-5-<sup>3</sup>H-nicotine and its base extractable

metabolites was accomplished by utilizing a radioactivity flow detector (Model Flo-One\Beta, Radiomatic Instruments and Chemical Co. Inc., Tampa, FL) linked post column to the HPLC system described above. Flow rates for HPLC and the Flo-Scint II scintillation fluid were 1.5 and 4.5 ml/min, respectively. The radioactivity flow detector employed a flow cell with a volume of 2.5 ml. Approximately 55 nCi of (S)-5-<sup>3</sup>H-nicotine was injected onto the HPLC-flow detector system. Estimations of the N-oxides of (S)-nicotine were achieved by the GC method reported by Jacob *et al.*<sup>22</sup>

### **Estimation of Covalent Binding**

A minor modification of a filtration method reported by Bulger *et al.*<sup>23</sup> was employed to estimate the extent of covalent binding of (S)-nicotine metabolites to microsomal proteins. Postincubation precipitates obtained by the addition of 1 ml of acetonitrile were trapped on GF/B glass microfiber filters (Whatman, Clifton, NJ) using a 10 well vacuum filtration apparatus (Biorad, Richmond, CA). In order to reduce nonspecific binding, the filters used in these experiments were pretreated by suction filtration with 2.0 ml of unlabeled 100 mM (S)-nicotine. Following filtration of the precipitates, the filters were washed with 100% ethanol (10 ml), hexane (20 ml), methanol:ether (3:1, 30 ml) and methanol:ether (1:3, 20 ml). No radioactivity was detected in the final solvent wash. The filters were transferred to scintillation vials containing 5 ml Aquasol scintillation cocktail and radioactivity was determined on a Packard Prias PLD Tri-Carb instrument. This filtration procedure, which previously had been shown to give comparable results to those obtained with the standard solvent extraction procedure,<sup>24</sup> was validated in our studies by comparing the results obtained in a parallel experiment using the solvent extraction method (See Table III.3 in the Addendum to this chapter).<sup>24</sup> The values agreed within 10% and therefore we elected to use the filtration method which is less laborious and more readily adaptable to large sample loads.



## Addendum

### NADPH Dependent Oxidation of (S)-Nicotine $\Delta^{1',5'}$ -iminium Ion

Attempts to identify either of the  $\alpha$ -carbon oxidation products of (S)-nicotine [(S)-nicotine  $\Delta^{1',5'}$ -iminium ion or (S)-nicotine methyleneiminium ion] as an intermediate in its metabolic activation were unsuccessful by the cyanide trapping approach described earlier. As an alternative to this approach, an experiment designed to saturate or mask potential sites of bioalkylation with (S)-nicotine  $\Delta^{1',5'}$ -iminium ion was performed in an attempt to block the covalent binding of metabolically activated (S)-5- $^3$ H-nicotine. However, preincubation of (S)-nicotine  $\Delta^{1',5'}$ -iminium ion at concentrations ranging between 0-500  $\mu$ M with liver microsomes (2 mg/ml) isolated

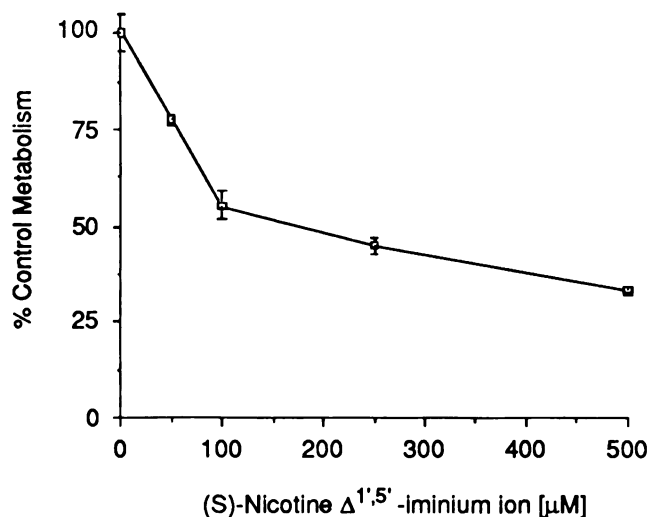


**Figure III.7** Concentration Dependent Inhibition of (S)-Nicotine Metabolism by (S)-Nicotine  $\Delta^{1',5'}$ -iminium Ion. (S)-Nicotine  $\Delta^{1',5'}$ -iminium *bis*perchlorate, at the concentrations indicated above, was preincubated with liver microsomes (2 mg/ml) isolated from phenobarbital pretreated rabbits. (S)-Nicotine (500  $\mu$ M) was added to this mixture and the concentrations remaining after a 1 hr incubation at 37°C was determined by the HPLC method described in Materials and Methods. The values indicated above are the average of triplicate determinations  $\pm$  S.E. and represent the percent of (S)-nicotine metabolized in the absence of the inhibitor (control metabolism = 183  $\mu$ M per hr).

from phenobarbital pretreated rabbits inhibited the metabolic oxidation of (S)-nicotine (500  $\mu\text{M}$ ) in a concentration dependent manner (Fig III.8). At a concentration of approximately 175  $\mu\text{M}$ , (S)-nicotine  $\Delta^{1',5'}$ -iminium ion inhibited the oxidation of (S)-nicotine by 50%.

Although the inhibitory effect of (S)-nicotine  $\Delta^{1',5'}$ -iminium ion on (S)-nicotine metabolism invalidated the experimental approach described above, these results suggest that the two compounds bind to a common microsomal enzyme. This suggestion is supported by the observation that (S)-nicotine  $\Delta^{1',5'}$ -iminium ion, in the presence of unreduced microsomal P-450, produces a type II binding spectrum (data not shown). The binding dissociation constant ( $K_s$ ), which was determined by constructing a double reciprocal plot of absorbance versus substrate concentration was estimated to be 0.1 mM, a value which was measurably lower than that recorded for (S)-nicotine ( $K_s=0.42$  mM). A candidate for the binding species is the corresponding enamine 19,

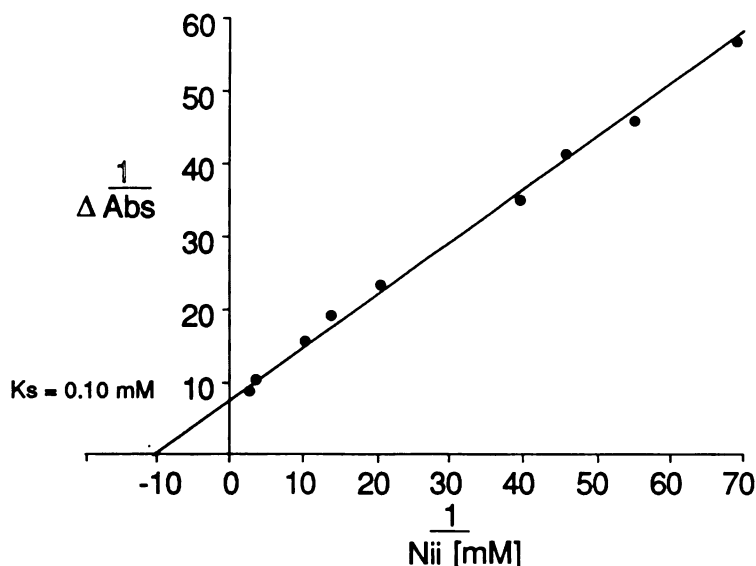


**Fig III.8** Estimation of Spectrally Detectable (S)-Nicotine  $\Delta^{1',5'}$ -Iminium Ion Binding to Liver Microsomal Cytochrome P-450.

the conjugate base of (S)-nicotine  $\Delta^{1',5'}$ -iminium ion, since this compound is more hydrophobic than the  $\Delta^{1',5'}$ -iminium ion **2** and the carbinolamine **15**.

In order to examine the substrate properties of (S)-nicotine  $\Delta^{1',5'}$ -iminium ion, this compound was incubated with liver microsomes isolated from rabbits pretreated with phenobarbital. HPLC analysis of these metabolic incubations indicated that (S)-nicotine  $\Delta^{1',5'}$ -iminium ion was converted to (S)-cotinine. The recovery of (S)-cotinine appeared to account for less than 50% of the iminium ion oxidized, although evidence for a second metabolite was not observed. In the presence of NADPH, 125 nmoles or roughly 25% of (S)-nicotine  $\Delta^{1',5'}$ -iminium ion was metabolized after a 1 hr incubation period. In the absence of NADPH, only 50 nmoles or 10% of nicotine  $\Delta^{1',5'}$ -iminium ion was metabolized during this period. Since the cytosolic enzyme aldehyde oxidase is known to catalyze the oxidation of the  $\Delta^{1',5'}$ -iminium species to (S)-cotinine, the metabolism observed in the absence of NADPH could possibly be due

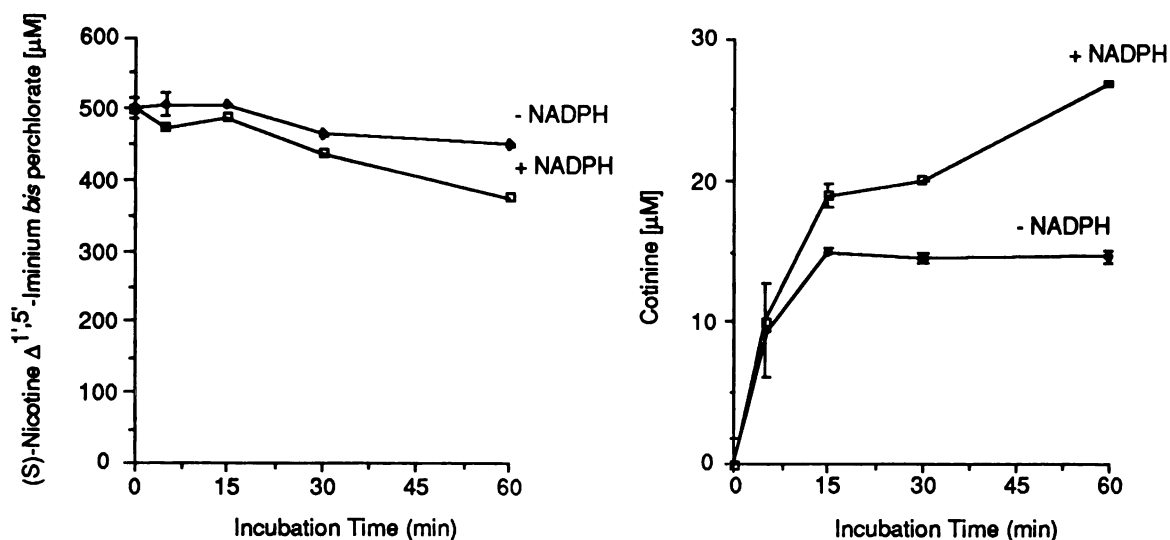


**Fig.III.9** NADPH Dependent Oxidation of (S)-Nicotine  $\Delta^{1',5'}$ -Iminium bisperchlorate. (S)-Nicotine  $\Delta^{1',5'}$ -iminium bisperchlorate ( $500 \mu\text{M}$ ) was incubated with liver microsomes ( $1 \text{ mg/ml}$ ) isolated from phenobarbital pretreated rabbits in the presence or absence of NADPH. Metabolic incubations were assayed for (S)-nicotine and (S)-cotinine by the normal phase silica HPLC method described in Materials and Methods.

to contamination of the microsomal preparation with this cytosolic enzyme. Since (S)-cotinine could not account for the (S)-nicotine  $\Delta^{1',5'}$ -iminium ion metabolized, the possibility was raised that the iminium species was being converted to a nonextractable polar metabolite and/or binding covalently with microsomal proteins. Efforts to determine the existence of nonextractable metabolites were not pursued. However, studies designed to examine the possibility that this electrophilic metabolite of (S)-nicotine binds covalently to microsomal proteins were conducted as described in the following section.

**Measurement of (S)-Nicotine Covalent Binding by SDS-Equilibrium Dialysis: Assessment of the Bioalkylating Properties of (S)-Nicotine  $\Delta^{1',5'}$ -Iminium Ion**

Due to the difficulties associated with studies aimed at determining the role of the iminium species in the covalent binding of metabolically activated (S)-nicotine, an alternate strategy was adopted. This strategy involved measuring, after extensive equilibrium dialysis, radioactivity associated covalently with SDS solubilized microsomal proteins obtained from metabolic incubation mixtures.

Estimation of covalent binding by SDS-equilibrium dialysis, a technique developed by Sun and Dent,<sup>25</sup> offers certain advantages over both the conventional extraction procedure and the filtration technique described earlier. Covalent adducts are not subjected to trichloroacetic acid precipitation or trichloroacetic acid wash steps. In addition, organic solvents are avoided. In this procedure, SDS solubilized microsomal incubation mixtures are boiled for 10 min and dialyzed extensively for up to three weeks. The radioactivity associated with a non-incubated sample (defined as background protein binding) represented approximately 25% of the radioactivity present in the samples incubated for 1 hr. The net recovery of radioactivity representing (S)-nicotine equivalents covalently bound was calculated by subtracting the background protein binding.

The application of this method has been prompted by the possible instability of covalent bonds formed between (S)-nicotine  $\Delta^{1',5'}$ -iminium ion and nucleophilic constituents present on microsomal proteins. Conventional techniques, such as those described previously, are not likely to measure this type of covalent adduct since the sample workup procedure would lead to the decomposition of the proposed adduct. For example, the acid labile nature of  $\alpha$ -aminonitriles, which are formed from the nucleophilic attack of the electrophilic iminium ions by cyanide, has been documented. The instability of these adducts is illustrated by the perchloric acid catalyzed elimination of the cyano moiety from 5'-cyanonicotine to yield the perchlorate salt of (S)-nicotine  $\Delta^{1',5'}$ -iminium ion.<sup>15</sup> Other cyanoamines such as cyano-PCP and cyano-MPTP are also sensitive to this acid catalyzed elimination reaction. We might anticipate from the behavior of these model adducts that the covalent linkage between biological nucleophiles and (S)-nicotine  $\Delta^{1',5'}$ -iminium ion would also be susceptible to acid catalyzed hydrolysis. Organic solvent treatments of microsomal incubations may also contribute to the instability of these adducts. Although poor nucleophiles, methanol and ethanol might break, by a substitution reaction, weak covalent linkages. For these reasons, the SDS equilibrium dialysis assay was performed.

The apparent NADPH dependent covalent binding of (S)-5-<sup>3</sup>H-nicotine, measured by the SDS-equilibrium dialysis method, was approximately 60-fold higher (10 nmol/mg protein/hr) than the levels detected by the filtration and solvent extraction methods (0.17 nmol/mg protein/hr)(Table III.3). These results indicate that the bulk of the covalent adducts formed between metabolically activated (S)-nicotine and microsomal proteins are unstable under conditions used for the conventional covalent binding methods (solvent extraction and filtration methods). The adduct formed between the  $\Delta^{1',5'}$ -iminium species and an endogenous nucleophile is an example of one type of covalent linkage which might be stabilized under the conditions of this SDS equilibrium dialysis method.

**Table III.3** Comparison of Three Covalent Binding Methods.

Method	N	Condition	pmol (S)-5- <sup>3</sup> H-Nicotine covalently bound/mg protein/hr†	nmol (S)-Nicotine metabolized/mg protein/hr	nmol (S)-Nicotine metabolized/nmol (S)-Nicotine covalently bound <sup>^</sup>
<b>Extraction</b>	3	+NADPH	221 ± 15	175	1,023
	3	-NADPH	49 ± 10		
<b>Filtration</b>	3	+NADPH	189 ± 21	175	1,023
	3	-NADPH	16 ± 10		
<b>Dialysis</b>					
trial-1	3	+NADPH	8440 ± 382	175	23
	3	-NADPH	757 ± 90		
*trial-2	6	+NADPH	13881 ± 660	185	15
	6	-NADPH	1148 ± 70		

†All values obtained from 1 hr metabolic incubations

Dialysis was performed for 7 days

<sup>^</sup>The amount of (S)-nicotine equivalents covalently bound was calculated by subtracting the corresponding -NADPH value.

\*A separate set of liver microsomes were used for these determinations. All other samples were performed using the same batch of liver microsomes and incubations were conducted on the same day.

If the covalent binding detected by this method is due to the interaction between the (S)-nicotine  $\Delta^{1',5'}$ -iminium ion and nucleophilic substituents present on microsomal proteins, then we might anticipate that a high concentration of a soluble nucleophile could break this covalent bond by a substitution reaction. In order to test this possibility, the reversal of this covalent linkage in the presence of excess cyanide was examined. The results (Table III.4) show that approximately 3 nmoles (nonspecific protein binding measured in the no incubation control and which was equivalent to 1.24 nmoles of (S)-5-<sup>3</sup>H-nicotine/mg protein was subtracted from the values obtained from the metabolic incubation) of (S)-5-<sup>3</sup>H-nicotine equivalents are covalently bound/mg protein/hr following a 1 hr metabolic incubation and 20 days of equilibrium dialysis (Sample B). The addition of sodium cyanide to the 1 hr metabolic incubation mixture prior to SDS equilibrium dialysis (Sample C) lowered, after the same period of dialysis, the amount of (S)-5-<sup>3</sup>H-nicotine equivalents covalently bound to a level comparable to a sample which had not been incubated (Sample A). In order to assess whether the apparent covalent binding could be attributed to ionic interactions

between the cationic iminium ion and the anionic detergent SDS, samples were dialyzed against 1 M NaCl from days 11-20. This treatment did not reduce the amount of radioactivity associated with the protein for either samples B or C, indicating that ion pairing interactions do not contribute significantly to the apparent covalent binding. These results thus further support the proposal that (S)-nicotine  $\Delta^{1',5'}$ -iminium ion binds covalently to microsomal proteins.

**Table III.4** Effect of Sodium Cyanide on the Covalent Binding of (S)-5-<sup>3</sup>H-Nicotine to Rabbit Liver Microsomal Proteins.

Assay date*	A	B.	C.
	0' + NADPH	60' + NADPH	60' + NADPH + NaCN§
	nmol (S)-5- <sup>3</sup> H-Nicotine equivalents bound/mg protein/hr <sup>‡</sup>		
8	1.15±0.45	6.83±0.30	2.22±0.10
11	0.28±0.07	3.27±0.08	0.84±0.01
20†	1.24 <sup>^</sup>	3.99±0.16	0.99±0.13

\*Radioactivity remaining in the dialysis bag was determined on the days indicated following the termination of the metabolic incubations.

†Between days 11-20 protein was dialyzed against 1 M NaCl solution.

§Sodium cyanide (100 mM final concentration) was added to the incubation mixture prior to SDS dialysis.

<sup>^</sup>lost second sample

The proposed involvement of (S)-nicotine  $\Delta^{1',5'}$ -iminium ion in the covalent binding of (S)-nicotine was examined further. This study was designed to quantitate the radioactivity released from microsomal protein following the addition of cyanide to a post-incubation mixture containing (S)-5-<sup>3</sup>H-nicotine and its radiolabeled metabolites. (S)-5-<sup>3</sup>H-Nicotine (0.5 mM) was incubated with phenobarbital treated rabbit liver microsomes for 60 min and the resulting metabolites separated by normal phase HPLC and monitored by an on-line radiochemical detector. Quantitation of each metabolite was calculated by measuring the net amount of radioactivity corresponding to the retention time of synthetic standards. The recovery of radioactivity for the 60 min +NADPH sample compared to the 0 min +NADPH or the 60 min -NADPH samples was

72%. (S)-Nicotine  $\Delta^{1',5'}$ -iminium ion accounted for 27.2% of the radioactivity used in these incubations. Radioactivity corresponding to the retention times of (S)-nicotine, (S)-cotinine and an unknown metabolite (retention time = 4 min) accounted for 34.7, 6.7 and 3.7% of the radioactivity, respectively. In order to test whether additional radioactivity associated with the  $\Delta^{1',5'}$ -iminium ion could be liberated from the microsomal mixture, excess cyanide was added to a metabolic mixture at the end of a 60 min incubation. The methylene chloride extract was analyzed as described for the control incubations. The percentage of radioactivity corresponding to (S)-nicotine and (S)-cotinine were essentially identical to the values obtained for the 60 min +NADPH incubation. The radioactivity associated with 5'-cyanonicotine (retention time = 4.3 min), the product of nucleophilic addition of cyanide to the  $\Delta^{1',5'}$ -iminium ion, accounted for 32.2% of the radioactivity (this value was calculated by subtracting the amount of radioactivity corresponding to the unknown metabolite which coelutes with 5'-cyanonicotine). Unreacted  $\Delta^{1',5'}$ -iminium ion accounted for an additional 2.9% of the radioactivity. Therefore, after the addition of excess sodium cyanide, the net amount of radioactivity corresponding to  $\Delta^{1',5'}$ -iminium ion equivalents (defined as the sum of the radioactivity corresponding to (S)-nicotine  $\Delta^{1',5'}$ -iminium ion and (S)-5'-cyanonicotine) represented 35.1% of the overall radioactivity added to the incubation. This value corresponds to a 30% increase in the amount of radioactivity recovered compared to that obtained for the 60 min +NADPH incubation. This 30% increase in recovery represents approximately 39.5 nmoles of (S)-5-<sup>3</sup>H-nicotine  $\Delta^{1',5'}$ -iminium ion equivalents released from the microsomal protein as (S)-5-<sup>3</sup>H-5'-cyanonicotine.



**Table III.5** Recovery of (S)-Nicotine  $\Delta^{1,5}$ -Iminium Ion Equivalents in the Absence and Presence of Excess Sodium Cyanide (100 mM).

Compound	0'+N or 60' - N	60'+N	60'+N; CN <sup>-</sup> added to postincubate
(S)-Nicotine	100	34.7	34.4
Unknown	-	3.7	3.7
5'-Cyanonicotine (net)	-	-	32.2
(S)-Nicotine $\Delta^{1,5}$ -iminium	-	27.2	2.9
(S)-Cotinine	-	6.7	6.3
Sum	100	72.3	79.5
(S)-5'-Cyanonicotine + (S)-Nicotine $\Delta^{1,5}$ -iminium	-	27.2	35.1

Metabolic incubations employing liver microsomes prepared from phenobarbital treated rabbits were performed as described in Materials and Methods. (S)-5-<sup>3</sup>H-Nicotine and its radiolabeled metabolites were quantitated by radiochemical detection following separation by normal phase silica HPLC of the methylene chloride extracts obtained from the metabolic incubation mixtures .

## Methods

### Substrate Binding of Nicotine $\Delta^{1,5}$ -Iminium Ion to Cytochrome P-450

Concentrated samples of substrate were delivered in a volume of 3  $\mu$ l at each concentration in a total volume of 3 ml. Rabbit liver microsomes (1.0 mg/ml) isolated from phenobarbital pretreated rabbits in 0.15 M KCl/0.02 M KH<sub>2</sub>PO<sub>4</sub> were utilized for these studies. Refer to the Chapter VI Materials and Methods section entitled "Substrate Binding of  $\beta$ -Nicotyrine to Microsomal Cytochrome P-450" for more details.

### SDS-Dialysis Covalent Binding Technique

(S)-5-<sup>3</sup>H-Nicotine was incubated with liver microsomes as described in the Materials and Methods section entitled "Estimation of Covalent Binding." Metabolic

incubations were terminated by adding 100  $\mu$ l of 20% SDS to the 1 ml incubation mixtures. The terminated incubation mixture was boiled for 10 min to allow for complete denaturation of the protein and also allowing noncovalently bound material to dissociate. Contents of the terminated incubation mixture were transferred to Spectropore dialysis tubing (cutoff pore size = 25,000 dalton MW) and dialyzed against 500-1000 fold excess of a 0.2% SDS in 0.1 M Tris-HCl buffer, pH 7.2. Dialysis was continued for several days (usually 7-8 days and in some cases up to 20 days) in the presence of the Tris-SDS buffer. After the fourth or fifth day of dialysis, a Tris buffer prepared without the detergent was used. Dialysis was continued until the radioactivity in the dialysis buffer reaches background levels. The buffer was changed on alternating days over the course of the dialysis.

1. Sudan, B.J.L. and J. Sterboul, "Nicotine: an hapten," *Br. J. Dermatol.* **104**, 349 (1981).
2. Bock, F.G., "Cocarcinogenic properties of nicotine." In: *Banbury Report: A safe cigarette?* (G.B. Gori and R.G. Buck, Eds.) pp. 129-138 Cold Spring Harbor Laboratory, New York (1980).
3. Gorrod, J.W. and P. Jenner, "The metabolism of tobacco alkaloids," In: *Essays in Toxicology* (W.J. Hayes Jr., Ed.) Vol. 6, pp. 35-78 Academic Press, New York (1975).
4. Hucker, H.B., J.R. Gillette and B.B. Brodie, "Enzymatic pathway for the formation of cotinine, a major metabolite of nicotine in rabbit liver," *J. Pharmacol. Exp. Ther.* **129**, 94-100 (1960).
5. Papadopoulos, N.M., "Formation of nornicotine and other metabolites from nicotine *in vitro* and *in vivo*," *Can. J. Biochem.* **42**, 435-442 (1964).
6. Brandange, S. and L. Lindblom, "The enzyme "aldehyde oxidase" is an iminium oxidase. Reaction with nicotine  $\Delta^{1,5}$ iminium ion," *Biochem. Biophys. Res. Comm.* **91**, 991-996 (1979).
7. Nakayama, H. T. Nakashima and Y. Kurogochi, "Participation of cytochrome P-450 in nicotine oxidation," *Biochem. Biophys. Res. Comm.* **108**, 200-205 (1982).
8. Ho, B. and N. Castagnoli Jr., "Trapping of metabolically generated electrophilic species with cyanide ion: Metabolism of 1-benzylpyrrolidine," *J. Med. Chem.* **23**, 133-139 (1980).
9. Comai, K. and J.L. Gaylor, "Existence and separation of three forms of cytochrome P-450 from rat liver microsomes," *J. Biol. Chem.* **248**, 4947-4955 (1973).
10. Eisner, V. and J. Kuthan, "The chemistry of dihydropyridines," *Chemical Reviews* **72**, 1-42 (1972).
11. Damani, L.A., W.F. Pool, P.A. Crooks, R.K. Kaderlik and D.M. Ziegler, "Stereoselectivity in the N'-oxidation of nicotine isomers by flavin-containing monooxygenase," *Mol. Pharmacol.* **33**, 702-705 (1988).
12. Kitada, M., K. Chiba, T. Kamataki and H. Kitagawa, "Inhibition by cyanide of drug oxidations in rat liver microsomes," *Japan. J. Pharmacol.* **27**, 601-608 (1977).
13. Schenkman, J.B., H. Remmer and R.W. Estabrook, "Spectral studies of drug interaction with hepatic microsomal cytochrome," *Mol. Pharmacol.* **3**, 113-123 (1967).
14. Koop, D.R. and P.F. Hollenberg, "Kinetics of the hydroperoxide-dependent dealkylation reactions catalyzed by rabbit liver microsomal cytochrome P-450," *J. Biol. Chem.* **255**, 9685-9692 (1980).

15. Peterson, L., A.J. Trevor and N. Castagnoli Jr., "Stereochemical studies on the cytochrome P-450 catalyzed oxidation of (S)-nicotine to the (S)-nicotine- $\Delta^{1'(5')}$ -iminium species," *J. Med. Chem.* **30**, 249-254 (1987).
16. Taylor, E.C. and N.E. Boyer, "Pyridine-1-oxides. IV. Nicotine-1-oxide, nicotine-1'-oxide, and nicotine 1,1'-dioxide," *J. Org. Chem.* **24**, 275-277 (1959).
17. Bowman, E.R. and H. McKennis Jr., "(-)-Cotinine," *Biochem. Prep.* **10**, 36-39 (1963).
18. Nguyen, T.L. and N. Castagnoli Jr., "The syntheses of deuterium labelled tobacco alkaloids: Nicotine, nor nicotine and cotinine," *J. Labelled Compds.* **14**, 919-934 (1978).
19. Shigenaga, M., P. Jacob III., N.L. Benowitz, N. Castagnoli Jr. and A.J. Trevor, "Synthesis of (S) 5-<sup>3</sup>H nicotine and (S)-5-<sup>3</sup>H cotinine," *J. Labelled Compds.* **24**, 713-723 (1987).
20. Lowry, O.H., N.J. Rosebrough, A.L. Farr and R.J. Randall, "Protein measurement with the Folin phenol reagent," *J. Biol. Chem.* **193**, 265-275 (1951).
21. Estabrook, R.W., J. Peterson, J. Baron and A. Hildebrandt, "The spectrophotometric measurement of turbid suspensions of cytochromes associated with drug metabolism," *Methods Pharmacol.* **2**, 303-350 (1972).
22. Jacob, P. III., N.L. Benowitz, L. Yu and A.T. Shulgin, "Determination of Nicotine N-oxide by gas chromatography following thermal conversion to 2-methyl-6-(3-pyridyl)tetrahydro-1,2,-oxime," *Anal. Chem.* **58**, 2218-2221 (1986).
23. Bulger, W.H., J.E. Temple and D. Kupfer, "Covalent binding of [<sup>14</sup>C] methoxychlor metabolite(s) to rat liver microsomal components," *Tox. Appl. Pharmacol.* **68**, 367-374 (1983).
24. Ward, D.P., A.J. Trevor, J.D. Adams, T.A. Baillie and N. Castagnoli Jr., "Metabolism of phencyclidine: The role of iminium ion formation in covalent binding of rabbit microsomal protein," *Drug Metab. Dispos.* **10**, 690-695 (1982).
25. Sun J.D. and J.G. Dent, "A new method for measuring covalent binding of chemicals to cellular macromolecules," *Chem. Biol. Interact.* **32**, 41-61(1980).

**Chapter IV**  
**Lung Microsomal Metabolism**  
**and Bioactivation of (S)-Nicotine**

## Introduction

Although the oxidation of various xenobiotics by liver enzymes is well recognized, lung enzymes have also been shown to contribute significantly to this process. The studies which describe the metabolic oxidation of foreign substances by pulmonary enzymes have been prompted in large part by the reported susceptibility of the lung to the toxic effects of a number of airborne substances.<sup>1</sup> Since the lung represents the portal of entry for such substances, metabolism and bioactivation of these compounds at this site might contribute to their numerous associated toxicities.<sup>2</sup> In this regard, it is of interest to note that lung carcinogens such as benzo(a)pyrene are bioactivated by cytochrome P-450 enzymes to metabolites which bind irreversibly with nucleophilic substituents present in DNA and protein.<sup>3,13</sup> Other lung toxicants such as the pyrrolizidine alkaloids and 4-ipomeanol are also metabolized by these enzymes to reactive intermediates which bind covalently to pulmonary tissue macromolecules.<sup>2</sup>

Lung tissue contains a significant concentration of cytochrome(s) P-450.<sup>4</sup> The highest concentration of pulmonary cytochrome P-450 appears to be localized in the smooth endoplasmic reticulum rich bronchiolar Clara cells.<sup>5</sup> The alveolar type II cells have been shown to contain lower but measurable levels of this enzyme. Of the many animals examined for lung cytochrome P-450 activity, the rabbit appears to express the highest constitutive level of this enzyme.<sup>6</sup> It is for this reason that this species has been used for the characterization of the various lung P-450 isozymes and their specific inhibitors. From these studies the rabbit pulmonary cytochrome P-450 monooxygenase system has been shown to be comprised of at least three isozymic forms; cytochromes P-450-2, P-450-5 and P-450-6.<sup>4,7</sup> The 2 major forms, cytochrome P-450 isozymes-2 and -5, are present in approximately equivalent concentrations (0.1-0.2 nmoles of P-450 isozyme/mg microsomal protein) and account for essentially all of the P-450 present in this tissue.<sup>8</sup> Cytochrome P-450 isozymes-2 and -5, previously designated P-450<sub>I</sub> and P-450<sub>II</sub>, respectively, exhibit differences in their carbon

monoxide binding spectra, substrate specificity, immunochemical characteristics, chymotrypsin and papain generated peptide fragmentation profiles, subunit molecular weight and N-terminal amino acids.<sup>9</sup> In contrast to the marked differences between these two lung isozymes, the cytochrome P-450 isozyme-2 isolated from lung and liver are found to be very similar, if not identical, when comparisons based on the criteria described above are made. With the availability of a sensitive immunofluorescence assay, semiquantitative estimations of cytochrome P-450 isozyme-2 in lung and liver have been made.<sup>10</sup> The relative fluorescent intensity generated from the binding of the P-450 isozyme-2 specific antibody has been shown to be greater in the Clara cells than in hepatocytes isolated from rabbits which had been pretreated with phenobarbital.<sup>10</sup> With this immunofluorescence assay cytochrome P-450 isozyme-2 was estimated to account for approximately 50% of the pulmonary cytochrome P-450 but only 10% of the hepatic P-450.<sup>11</sup> The principal difference between rabbit liver and lung P-450 isozyme-2 is the apparent lack of response by the lung enzyme to the inducing effects of phenobarbital. Isozyme-2 is the only lung P-450 isozyme capable of catalyzing the N-demethylation of benzphetamine.<sup>12</sup> Isozyme-5, on the other hand, is the only known pulmonary P-450 isozyme which catalyzes the oxidation of 2-aminofluorene.<sup>12</sup>

#### **Metabolism and Bioactivation of Xenobiotics by Pulmonary Cytochrome P-450 Isozymes**

Several investigators have examined the role of these isozymes in the metabolism and bioactivation of toxic substances which are inhaled. For example, studies on the biotransformation of benzo(a)pyrene by two purified isozymes of rabbit lung cytochrome P-450 have been performed in order to assess the role of each enzyme in the metabolic activation of this compound to intermediates which are proposed to be associated with its cancer inducing effects.<sup>13</sup> The results of these studies indicate that each isozyme oxidizes this compound through different metabolic pathways. Cytochrome

P-450 isozyme-5 (designated cytochrome P-450 II in their studies) was shown to transform benzo(a)pyrene to metabolites which bind covalently to DNA and which are mutagenic. In contrast, rabbit lung cytochrome P-450 isozyme-2 (designated cytochrome P-450 I in their study) catalyzed the oxidation of benzo(a)pyrene to non-mutagenic metabolites.

Studies similar to those described above indicate that the bioactivation of a number of aromatic amines by rabbit lung cytochrome P-450 is also isozyme dependent. In reconstituted systems, purified lung cytochrome P-450 isozyme-5, but not isozyme-2, oxidatively transforms 2-aminoanthracene, 2-aminofluorene and 2-acetylaminofluorene to metabolites which are mutagenic as determined by the Ames assay using the Salmonella strain TA98.<sup>14</sup> In addition, the conversion of these compounds to mutagenic metabolites by microsomal enzymes is inhibited by anti-P-450 isozyme-5 antibodies, but not by anti-P-450 isozyme-2 antibodies, results which further support the role of isozyme-5 in the bioactivation of these aromatic amines. In contrast to the isozyme specific metabolic activation of aromatic amines, aflatoxin B<sub>1</sub>, a potent hepatocarcinogen, has been shown to be activated metabolically by both isozymes-2 and -5, indicating that the bioactivation of xenobiotics by the lung monooxygenase system is not necessarily isozyme specific.

A minor form of pulmonary cytochrome P-450, isozyme-6, which to date has not been purified, is induced by 2,3,7,8-tetrachlorodibenzo-p-dioxin (TCDD), 3-methylcholanthrene (3-MC) and Aroclor 1260. This isozyme is similar to hepatic cytochrome P-450 isozyme-6 based on substrate specificities and immunological cross reactivity with antibodies prepared against purified hepatic P-450 isozyme-6.<sup>7</sup> Induction of pulmonary isozyme-6 by TCDD has been reported to increase the levels of this enzyme 10-20 fold.



### **Pulmonary Flavin Containing Monooxygenase**

Another pulmonary enzyme which may catalyze the oxidation of (S)-nicotine is the flavin containing monooxygenase (FCM). FCM, which has been isolated from rabbit lung, has been purified to homogeneity and its substrate properties characterized.<sup>15,16</sup> This enzyme, similar to the FCM isolated from the liver of various species, catalyzes the oxidation of nitrogen and sulfur containing xenobiotics to the corresponding N-oxides and sulfoxides. However, in contrast to the liver enzyme, the FCM isolated from rabbit lung does not catalyze the oxidation of imipramine and chlorpromazine, two of the better substrates for the liver enzyme. Although the purified rabbit lung FCM is found to be similar to the liver enzyme with respect to molecular weight, spectral properties and catalytic activity toward dimethylaniline, cysteamine and methimazole, this enzyme differs in its pH-activity profile and relative thermal stability. In addition, lung FCM enzyme activity is inducible by glucocorticoid pretreatment<sup>17</sup> but unlike the liver enzyme is not stimulated by n-octylamine. Furthermore, the lung enzyme is found to be immunologically distinct from rabbit and pig liver FCM.<sup>18</sup>

### **Clara Cells - The Principal Site of Pulmonary Cytochrome P-450 Monooxygenase Activity**

The Clara cells appear to be a primary target for the irreversible binding of a number of compounds which are metabolically activated in lung tissue. For example, the lung toxicant 4-ipomeanol binds covalently and causes preferential necrosis in this cell population *in vivo*.<sup>2</sup> The carcinogenic agent diethylnitrosamine (DEN) is activated metabolically by the cytochrome P-450 containing Clara cells to reactive intermediates which bind to cellular constituents and which produce lung neoplasms in rats and hamsters.<sup>19,20,21</sup>

Since Clara cells possess the enzymes required for the bioactivation of many inhaled xenobiotics it has been suggested that the origin of some bronchogenic cancers

may arise from this cell population. Recently, two cell lines derived from human lung adenocarcinomas have been isolated and characterized.<sup>19,21</sup> These cell lines, designated NCI-H322 and NCI-H358, possess xenobiotic metabolizing activities and share ultrastructural features of Clara cells (NCI-H322) or the alveolar type II cells (NCI-H358). In common with the cells from which they are thought to be derived, both tumor cell lines maintain the capacity to metabolize DEN to intermediates which bind covalently to cellular protein and DNA. Metabolism of DEN by NCI-322 is inhibited by carbon monoxide, indicating that cytochrome P-450 participates in the bioactivation of this compound. In contrast, metabolism of DEN by NCI-358 is inhibited by aspirin and indomethacin, inhibitors of the cyclooxygenase component of prostaglandin synthetase, more effectively than by carbon monoxide, evidence which indicates that the catalytic activity of prostaglandin synthetase, not cytochrome P-450, is responsible for the bioactivation of this carcinogen. Such cell lines may prove in the future to be useful for studying the metabolism and bioactivation of (S)-nicotine *in situ*.

The metabolism of (S)-nicotine by lung tissue is of interest since this organ represents the initial site of absorption<sup>22</sup> and is one of the primary target organs for diseases related to the consumption of tobacco products. The metabolism of (S)-nicotine by pulmonary tissue has been examined previously in perfused lung studies<sup>23,24</sup> and *in vitro*.<sup>25</sup> Since pulmonary cytochrome P-450 has been documented to be an effective catalyst for the bioactivation of numerous foreign compounds to their respective electrophilic and bioalkylating species,<sup>13,26,14</sup> we were led to assess the possibility of whether (S)-nicotine could be bioactivated by this pulmonary enzyme system.

A property of the rabbit lung microsomal system which makes it particularly attractive for studies on the metabolism and bioactivation of (S)-nicotine is the relatively simple composition of the cytochrome P-450 isozymes present in this subcellular fraction. In contrast to the numerous P-450 isozymes present in liver microsomes, the lung microsomes isolated from untreated rabbits contain only three

constitutively expressed isozymes which account for essentially all of the cytochrome P-450 present in this tissue.<sup>9,7</sup> As already described, rabbit lung cytochrome P-450 isozyme-2 has been shown to account for up to 50% of the cytochrome P-450 present in Clara cells and is similar, if not identical, to the phenobarbital inducible P-450 isozyme-2 present in liver.<sup>11</sup> The similarities between the two predominant cytochrome P-450 isozymes present in rabbit lung microsomal fraction and the phenobarbital inducible P-450 isozymes of liver is significant with regard to the possible role these lung enzymes play in the metabolic disposition of (S)-nicotine especially since the phenobarbital-inducible liver isozymes play a key role in the metabolic activation of this compound.

Studies have shown that phenobarbital induces the expression of a liver P-450 isozyme(s) which catalyzes the oxidation of (S)-nicotine.<sup>27</sup> The isozyme(s) induced by this pretreatment oxidizes (S)-nicotine to the electrophilic (S)-nicotine  $\Delta^{1',5'}$ -iminium ion. Two lines of evidence support this conclusion. First, phenobarbital pretreatment causes an 8-fold increase in the rate of (S)-nicotine metabolism by isolated perfused rat liver,<sup>28</sup> a metabolic event which is correlated with a parallel increase in (S)-cotinine formation. These results indicate that phenobarbital induces an isozyme which catalyzes the 5'-carbon oxidation of (S)-nicotine to produce (S)-cotinine via the intermediate metabolite (S)-nicotine  $\Delta^{1',5'}$ -iminium ion. Second, as described in Chapter III, our studies have shown that pretreatment of rabbits with phenobarbital increases the overall liver microsomal metabolism of (S)-nicotine by 35%. More dramatic, however, is the almost 2-fold increase in the formation of (S)-nicotine  $\Delta^{1',5'}$ -iminium ion, a change which compares favorably with the approximate 2.5-fold increase in the covalent binding of (S)-nicotine. In addition, this result also strongly suggests a link between the metabolism of (S)-nicotine by phenobarbital inducible enzymes, (S)-nicotine  $\Delta^{1',5'}$ -iminium ion formation and covalent binding. Evidence from other studies show that a purified phenobarbital

inducible cytochrome P-450 isozyme isolated from rat liver catalyzes the oxidation of (S)-nicotine when this enzyme, cytochrome P-450 reductase and phospholipids are reconstituted<sup>29</sup> and that antibodies prepared against a phenobarbital inducible cytochrome P-450 isozyme, purified from guinea pig liver, inhibits the oxidation of (S)-nicotine by up to 95%.<sup>27</sup>

In contrast to the inducing effects of phenobarbital on liver cytochrome P-450 catalyzed oxidation of (S)-nicotine, 3-methylcholanthrene, an inducer of a separate class of P-450 isozymes (P-448), does not appear to increase the metabolism of (S)-nicotine.<sup>30</sup> Perfused livers isolated from rats pretreated with 5,6-benzoflavone (BF), another inducer of cytochrome P-448, also metabolize (S)-nicotine to an extent similar to that of perfused livers from untreated controls, indicating that induction of the P-448 isozyme does not contribute significantly to the overall metabolism of this compound.<sup>28</sup>

The evidence obtained from these studies support the proposal that a phenobarbital inducible isozyme present in liver catalyzes the oxidation of (S)-nicotine and that the metabolic pathway which it catalyzes is associated with the bioalkylation properties of (S)-nicotine. The strong biochemical similarities between the phenobarbital inducible liver P-450 isozymes and the predominant cytochrome P-450 isozymes present in lung, together with the known association between these liver isozymes and the metabolic activation of (S)-nicotine has encouraged a detailed evaluation of the metabolism and bioactivation of (S)-nicotine by lung microsomal enzymes. In order to make these evaluations, studies were performed utilizing microsomes and soluble fractions isolated from this organ. To understand better the contribution of specific forms of lung cytochrome P-450 in the metabolism and bioactivation of (S)-nicotine, selective inhibitors of rabbit lung cytochrome P-450 isozymes and pretreatment regimens which alter the expression of these isozymes were employed.

## Results

### Lung Microsomal Metabolism of (S)-Nicotine: Comparison of Lung and Liver Microsomal Oxidation of (S)-Nicotine

Initial studies of the lung microsomal metabolism of (S)-nicotine involved determining the time course of its oxidation. (S)-Nicotine (100  $\mu\text{M}$ ) was added to metabolic incubation mixtures consisting of microsomes isolated from untreated New Zealand White rabbits (1-2 mg/ml, final concentration), and appropriate cofactors, including NADP<sup>+</sup> and a regenerating system. The lung microsomal metabolism of (S)-nicotine was assayed by analyzing methylene chloride extracts of metabolic incubations by HPLC with UV detection at 260 nm. This method was described in detail in Chapter III. The rate of metabolism was estimated to be 1.28 nmoles (S)-nicotine oxidized·mg protein<sup>-1</sup>·min<sup>-1</sup> and was linear over the first 20 min. Metabolism was not observed in incubations performed in the absence of NADP<sup>+</sup> and a regenerating system. For comparison, rabbit liver microsomal metabolism of 100  $\mu\text{M}$  (S)-nicotine appeared linear over the first 15 min and proceeded at a rate of approximately 2.11 nmoles (S)-nicotine oxidized·mg protein<sup>-1</sup>·min<sup>-1</sup> (Fig.IV.1). On the basis of microsomal protein content, the rate of (S)-nicotine oxidation was approximately 39% lower in the lung microsomal incubations compared to that observed with the liver preparations. However, when expressed on the basis of cytochrome P-450 content (liver and lung microsomes = 1.28  $\pm$  0.14 nmoles P-450/mg protein and 0.20  $\pm$  0.02 nmoles P-450/mg protein, respectively), the rate of (S)-nicotine oxidation catalyzed by the lung enzyme system was approximately 4 times greater than the rate observed with the liver preparation (6.4 vs.1.7 nmoles (S)-nicotine oxidized·nmole cytochrome P-450<sup>-1</sup>·min<sup>-1</sup>). These results suggest that, compared to liver, pulmonary microsomes

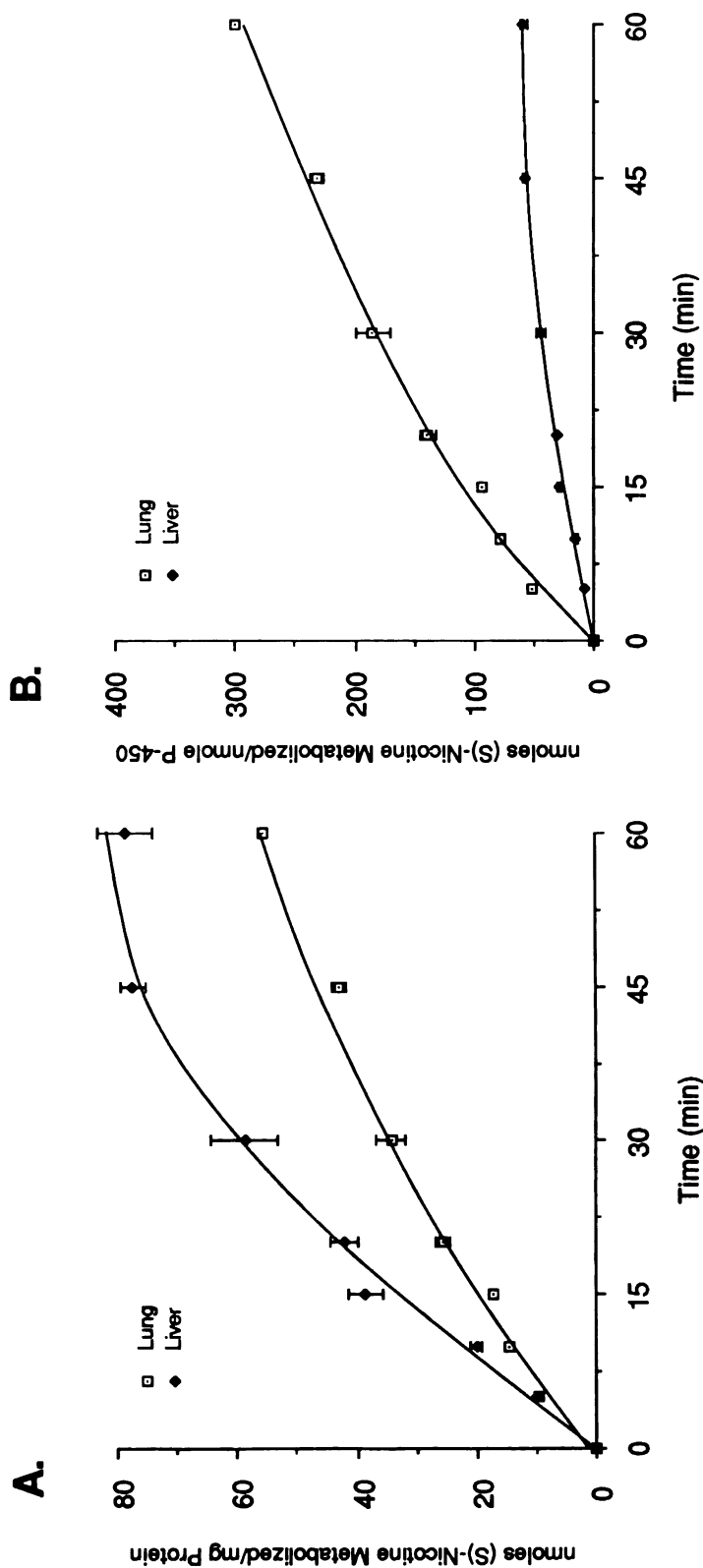


Fig. IV.1 A Comparison Between the Lung and Liver Microsomal Metabolism of (S)-Nicotine. (S)-Nicotine (100  $\mu$ M) was incubated with lung (1 mg/ml) or liver (0.5 mg/ml) microsomes for the time periods indicated. (S)-Nicotine metabolism was measured by the normal phase HPLC method described in Chapter III and was normalized to (A) protein and (B) cytochrome P-450 content.

contain a higher proportion of the cytochrome P-450 isozyme(s) which catalyzes the oxidation of (S)-nicotine.

### **Effects of Cytochrome P-450 Inhibitors on the Lung Microsomal Metabolism of (S)-Nicotine**

The role of cytochrome P-450 in the rabbit lung microsomal oxidation of (S)-nicotine was examined by performing metabolic incubations in the presence of cyanide ion and SKF 525-A, two known inhibitors of liver cytochrome P-450.<sup>31</sup> Incubation of (S)-nicotine (100  $\mu$ M) in the presence of 1.9 mg/ml microsomal protein and the required cofactors necessary for monooxygenase activity resulted in the oxidation of approximately 68% of (S)-nicotine after a 1 hr incubation at 37°C (**Fig.IV.2C**). Metabolites of (S)-nicotine (1), which included (S)-nicotine  $\Delta^{1',5'}$ -iminium ion (2), (S)-cotinine (3) and an unidentified compound which eluted near the solvent front **Unk**, were estimated to account for approximately two thirds of the 68 nmoles of (S)-nicotine oxidized. Since methylene chloride was used for the extraction of the lung microsomal incubation mixtures, it was not possible to detect (S)-nicotine N'-oxide or other polar metabolites. In the absence of NADPH, metabolism of (S)-nicotine was not observed (**Fig.IV.2B**). Sodium cyanide (500  $\mu$ M), a compound which was shown in Chapter III to inhibit the liver microsomal metabolism of (S)-nicotine, inhibited the lung microsomal oxidation of this compound by approximately 40% (**Fig.IV.2D**). In addition, the peak corresponding to (S)-nicotine  $\Delta^{1',5'}$ -iminium ion (2) was absent in this incubation and instead a peak which coeluted with synthetic 5'-cyanonicotine (17) was observed. The formation of 17 provides additional support for the metabolic formation of the (S)-nicotine  $\Delta^{1',5'}$ -iminium ion by lung microsomes. Furthermore, in this incubation (S)-cotinine was the major metabolite suggesting that 5'-cyanonicotine was being oxidized further by an NADPH dependent

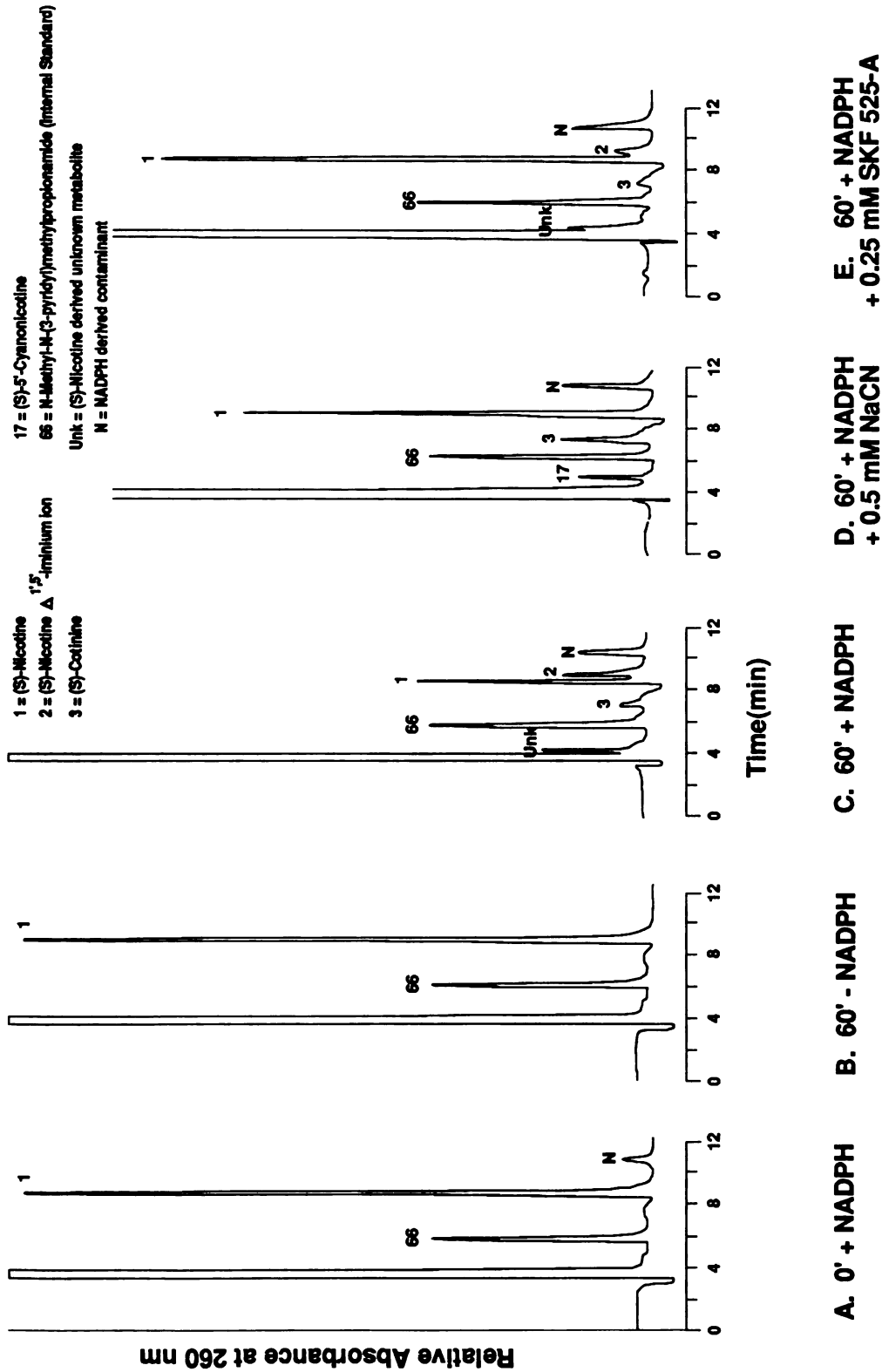


Figure IV.2 A-E HPLC Chromatograms of (S)-Nicotine and its Metabolites Following Incubation with Lung Microsomes Under Various Conditions. F.R. = 1 ml/min 1% n-PA in ACN



process to the lactam (S)-cotinine. The unknown peak observed in the 60 min control incubation was absent in the incubation containing sodium cyanide indicating that the metabolite is either trapped directly by this nucleophile or is derived from a cyanide trappable species such as (S)-nicotine  $\Delta^{1',5'}$ -iminium ion or (S)-nicotine methyleneiminium ion. Finally the cytochrome P-450 inhibitor, SKF 525-A (0.25 mM) was found to inhibit the overall metabolism of (S)-nicotine by approximately 50% (Fig.IV.2E). The metabolites (S)-nicotine  $\Delta^{1',5'}$ -iminium ion (2), (S)-cotinine (3) and the unknown metabolite **Unk** decreased in proportion to the degree of inhibition. These results are consistent with the role of lung cytochrome P-450 in the oxidative metabolism of (S)-nicotine.

#### Detection of an Unknown Metabolite Produced by Lung Microsomal Oxidation of (S)-Nicotine

Using HPLC with UV detection at 260 nm and a mobile phase consisting of 1% n-propylamine in acetonitrile at a flow rate of 1.5 ml/min, (S)-nicotine  $\Delta^{1',5'}$ -iminium ion, which accounted for approximately 50% of the (S)-nicotine equivalents metabolized, eluted with a retention time of 11 min. (S)-Cotinine, which eluted with a retention time of 8.5 min, accounted for approximately 11% of the metabolites formed. In addition to the 5'-carbon oxidation products, an unidentified peak was observed. This peak eluted at approximately 4 min and exhibited a UV absorbance similar to that observed for (S)-cotinine (Fig.IV.3A). None of the available (S)-nicotine related synthetic standards were found to coelute with this peak. Of the standards which were tested,  $\beta$ -nicotyrine (6) was found to exhibit chromatographic properties most similar to the unknown metabolite. However, coinjection of  $\beta$ -nicotyrine with the methylene chloride extract of the lung microsomal incubation indicated that the retention times of the two compounds were not identical (data not shown). The synthetic  $\beta$ -nicotyrine standard eluted approximately 0.15 min earlier than the unknown metabolite.

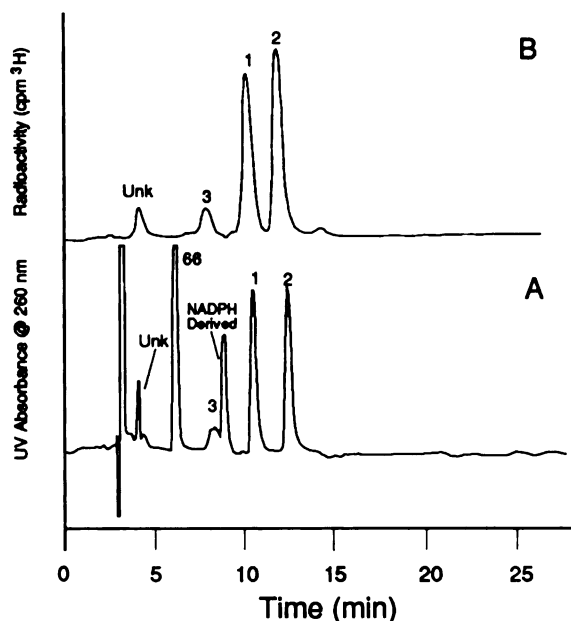


**Fig.IV.3 A and B.** Analysis of the Lung Microsomal Metabolism of (S)-5-<sup>3</sup>H-Nicotine by HPLC with (A) UV and (B) Radiochemical Detection.

In an attempt to demonstrate unambiguously that the unknown metabolite was (S)-nicotine derived, lung microsomal incubations, containing either unlabeled or (S)-5-<sup>3</sup>H-nicotine (100  $\mu$ M, 1  $\mu$ Ci) as substrate, were analyzed separately by UV and radiochemical detection, respectively, following a 1 hr incubation at 37°. The radiochemical chromatogram of a lung microsomal incubation of (S)-5-<sup>3</sup>H-nicotine exhibited four prominent peaks corresponding to (S)-nicotine, (S)-cotinine, (S)-nicotine  $\Delta^{1',5'}$ -iminium ion and the unknown with retention times essentially identical to those described above (Fig.IV.3B). The unknown substance which eluted at 4.1 min was estimated to account for approximately 5% of the total radioactivity present in the incubation mixture. The existence of this radioactive peak co-migrating with the unknown substance observed in the UV chromatogram provides good evidence that it is (S)-nicotine derived. HPLC analysis of metabolic samples which were either incubated in the absence of NADPH or quenched immediately after the addition of radiolabeled (S)-nicotine did not produce this peak, thus demonstrating that the formation of the unknown <sup>3</sup>H-labeled metabolite is NADPH and time dependent. The same

conclusion was reached following the analysis of parallel incubation mixtures by UV detection.

The UV spectrum corresponding to the unknown peak exhibited a  $\lambda_{\max}$  at 286 nm as determined by diode array UV analysis of a lung microsomal incubation mixture. The absorbance maxima for this spectrum and its overall shape was very similar to the diode array UV spectrum obtained for synthetic  $\beta$ -nicotyrine tartrate (Fig.IV.4).

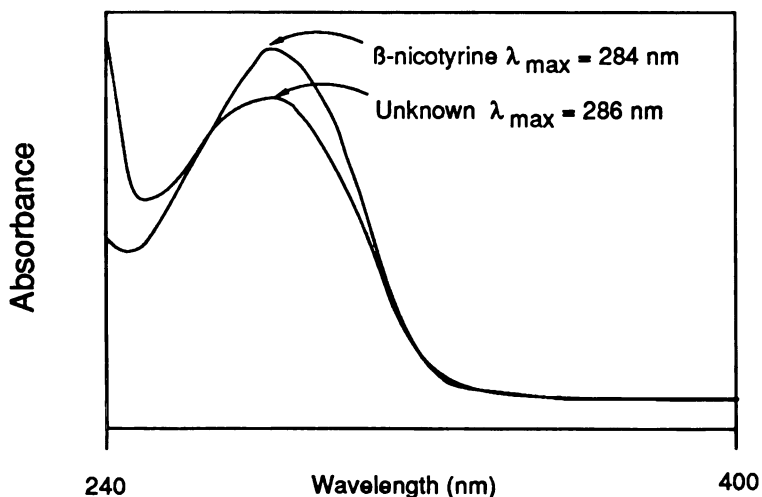


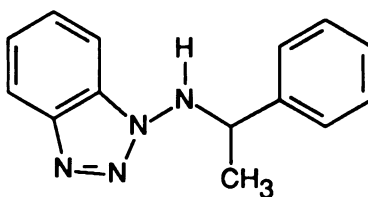
**Fig.IV.4** UV Spectra of the Unknown Metabolite Derived from the Lung Microsomal Metabolism of (S)-Nicotine and Synthetic  $\beta$ -Nicotyrine Tartrate

Further efforts to identify the unknown compound involved the analysis of methylene chloride extracts of lung microsomal incubations of (S)-nicotine by GC-EIMS. To facilitate the identification of fragment ions derived from (S)-nicotine, a 1:1  $d_0$  and 3',3'  $d_2$  mixture of (S)-nicotine (100  $\mu$ M) was incubated with rabbit lung microsomes (2 mg/ml). The methylene chloride extract was purified by normal phase silica HPLC and the fraction corresponding to the unknown metabolite was extracted back into aqueous 1M  $H_2SO_4$ . The pH of the acidic aqueous layer was raised to alkaline pH with 50%  $K_2CO_3$  and the resulting solution was extracted with toluene/butanol 9:1 (0.3 ml). GC-EIMS of the toluene/butanol extract produced over a dozen peaks on the total ion chromatogram, several of which contained the expected doublet peaks corresponding

to fragment ions derived from (S)-nicotine and the dideuterated derivative. Unfortunately, the ions obtained from this array of peaks were difficult to interpret. In view of the reported acid labile nature of pyrrole compounds<sup>32</sup> and considering the possibility that the unknown may contain a pyrrole substituent (as suggested by the UV spectrum described above), back extraction of (S)-nicotine from an organic phase to an acidic aqueous phase containing 1M H<sub>2</sub>SO<sub>4</sub> may have led to the decomposition of this metabolite.

Further attempts to characterize the identity of the unknown metabolite were unsuccessful since this compound was not observed in subsequent analyses. The formation of this metabolite was observed a total of five times using lung microsomes from three separate preparations. Therefore, it is unlikely that the compound is an artifact. In summary, the formation of the metabolite was time, NADPH and cytochrome P-450 dependent. Metabolic incubations containing (S)-5-<sup>3</sup>H-nicotine also produced a peak coeluting with the unknown, demonstrating unambiguously that the metabolite was (S)-nicotine derived. The reasons for our failure to reproduce these earlier observations are not known. The initial observations suggesting the possible formation of a metabolite containing a pyrrole substituent from the lung microsomal oxidation of (S)-nicotine is of toxicological interest since such an electron rich compound might be metabolized to an intermediate possessing bioalkylating properties. Further studies will need to be performed in order to confirm the formation of this compound.

### Characterization of Lung Cytochrome P-450 Isozymes Participating in the Oxidation of (S)-Nicotine



65

Initial studies aimed at identifying the lung cytochrome P-450 isozyme responsible for catalyzing the oxidation and bioactivation of (S)-nicotine used  $\alpha$ -methylbenzylaminobenzotriazole (65) in metabolic incubations containing rabbit lung microsomes and (S)-nicotine.  $\alpha$ -Methylbenzylaminobenzotriazole is a suicide inhibitor which has been shown at low micromolar concentrations to inactivate almost

**Table IV.1** Inhibitory Effects of  $\alpha$ -Methylbenzylaminobenzotriazole on (S)-Nicotine Metabolism by Rabbit Lung Microsomes

Condition	Incubation Time (min)	(S)-Nicotine metab. nmoles/mg avg $\pm$ S.E.	% Inhibition
No inhibitor	20	12.7 $\pm$ 0.1	0
1 $\mu$ M	20	2.2 $\pm$ 0.1	83
2.5 $\mu$ M	20	0.9 $\pm$ 0.1	93
No inhibitor	60	50.4 $\pm$ 2.3	0
1 $\mu$ M	60	13.6 $\pm$ 0.7	73
2.5 $\mu$ M	60	6.5 $\pm$ 0.2	87

(S)-Nicotine concentration was 100  $\mu$ M for all determinations  
n=3 for all determinations

completely rabbit lung cytochrome P-450 isozyme-2 and to a lesser degree rabbit lung P-450 isozyme-6.<sup>33</sup> In this study we show that at concentrations of 1  $\mu$ M and 2.5  $\mu$ M,  $\alpha$ -methylbenzylaminobenzotriazole inhibits the lung microsomal oxidation of (S)-nicotine by 74.5 and 96.1%, respectively (Table IV.1). This concentration of

inhibitor has previously been reported to inhibit 74.5 and 93% of the rabbit lung isozyme-2 catalyzed N-demethylation of benzphetamine and 41 and 70% of the isozyme-6 catalyzed O-deethylation of ethoxyresorufin.<sup>33</sup> Essentially the same degrees of inhibition were observed for the benzphetamine N-demethylation (78 and 90%) and ethoxyresorufin deethylation (50 and 85%) reactions performed in our

**Table IV.2** Effect of  $\alpha$ -Methylbenzylaminobenzotriazole on P-450 Isozyme-2 and -6 Catalyzed Oxidations

Pretreatment	Benzphetamine N-demethylation		Ethoxyresorufin O-deethylation	
	nmol HCHO formed/mg/min	% inhibition	pmol resorufin formed/mg/min	% inhibition
no inhibitor	5.1 $\pm$ 0.5	0.0	5.2 $\pm$ 0.6	0.0
1 $\mu$ M	1.3 $\pm$ 0.3	74.5	2.6 $\pm$ 0.6	50.0
2.5 $\mu$ M	0.2 $\pm$ 0.1	96.1	0.8 $\pm$ 0.4	84.6

Each value represents the average of 3 (Benzphetamine N-demethylation) or 6 (ethoxyresorufin O-deethylase) determinations  $\pm$  S.D.

studies (Table IV.2). Since  $\alpha$ -methylbenzylaminobenzotriazole also inhibits rabbit lung P-450 isozyme-6 in addition to lung P-450 isozyme-2, it is not possible with this single inhibitor to exclude the involvement of isozyme-6 in the lung microsomal oxidation of (S)-nicotine.

#### **Effect of Various Pretreatments on the Lung Microsomal Metabolism of (S)-Nicotine**

In order to assess further the participation of specific lung P-450 isozymes in the metabolic oxidation of (S)-nicotine, we utilized lung microsomes isolated from rabbits pretreated with phenobarbital, TCDD and Aroclor 1260.<sup>12</sup> The metabolism of (S)-nicotine by lung microsomes isolated from phenobarbital pretreated rabbits was essentially the same as that catalyzed by untreated control rabbit lung microsomes

(Fig.IV.5). The extent of benzphetamine N-demethylation was slightly lower in this study but essentially identical in another study when the catalytic activity of lung microsomes isolated from phenobarbital pretreated and untreated rabbits were compared (Table IV.3). Therefore, in contrast to its P-450 inducing properties in the liver, phenobarbital does not appear to induce lung P-450 isozymes-2 and -5. Despite its apparent lack of effect on (S)-nicotine and benzphetamine metabolism, it has been reported previously that pretreatment of rabbits with phenobarbital decreases the activity of lung P-450 isozyme-6 catalyzed O-deethylation of 7-ethoxyresorufin by approximately 60% compared to that observed with control lung microsomes.<sup>12</sup> Therefore, it is unlikely that lung P-450 isozyme-6 catalyzes the oxidation of (S)-nicotine.

**Table IV.3** Lung microsome catalyzed Benzphetamine N-demethylation

Pretreatment	Present Study			Literature values*
	n	nmol HCHO/mg/min average $\pm$ S.D.	% untreated	nmol HCHO/mg/min average $\pm$ S.D.
Untreated	8	10.4 $\pm$ 1.3	100	8.9 $\pm$ 2.6
Phenobarbital	5	7.2 $\pm$ 0.1	69	8.9 $\pm$ 3.4
Aroclor-1260	5	1.9 $\pm$ 0.1	18	2.0 $\pm$ 1.6
TCDD	5	5.0 $\pm$ 2.2	48	6.7 $\pm$ 1.3

\*C.J. Serabjit-Singh, P.W. Albro, I.G.C. Robertson and R.M. Philpot, *J. Biol. Chem.* **258** 12827-12834 (1983)

TCDD pretreatment has been shown previously by others to induce rabbit lung P-450 isozyme-6 10-20 fold without appreciably affecting the levels or catalytic activity of lung P-450 isozymes-2 and 5.<sup>12</sup> Results of incubations which employed lung microsomes from rabbits pretreated with TCDD showed that the extent of (S)-nicotine oxidation was comparable to that observed with control lung microsomes (Fig.IV.5) while the O-deethylation of ethoxyresorufin, a reaction catalyzed

specifically by lung P-450 isozyme-6, was induced approximately 4-fold (data not shown). The failure of TCDD and phenobarbital pretreatments to affect the lung microsomal oxidation of (S)-nicotine indicates that lung P-450 isozyme-6 probably does not contribute significantly to the lung microsomal oxidation of (S)-nicotine.

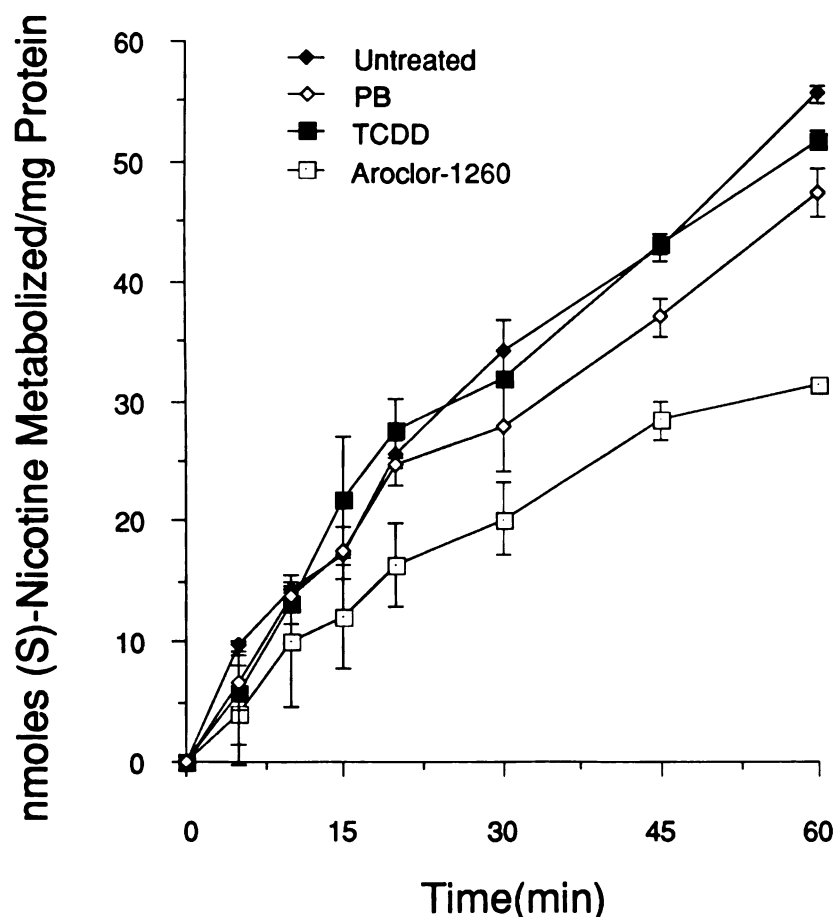


**Fig. IV.5** Lung Microsomal Oxidation of (S)-Nicotine: Effects of Phenobarbital, TCDD and Aroclor 1260 Pretreatments. The metabolism of (S)-nicotine (100  $\mu$ M) by lung microsomes (1 mg/ml for all preparations) isolated from rabbits pretreated with phenobarbital, TCDD or Aroclor 1260 were compared with the activity of lung microsomes isolated from untreated rabbits. (S)-Nicotine oxidase activity was assayed by measuring the UV 260 nm peak height of (S)-nicotine following separation of methylene chloride extracts of microsomal incubations by normal phase silica HPLC.



Furthermore, these observations also suggest that the inhibitory effect of the suicide substrate  $\alpha$ -methylbenzylaminobenzotriazole on the lung microsomal oxidation of (S)-nicotine is due to the inactivation of lung P-450 isozyme-2 not isozyme-6. The apparent lack of lung P-450 isozyme-6 catalyzed oxidation of (S)-nicotine is supported further by studies performed by others with liver microsomes prepared from rats pretreated with 3-methylcholanthrene, a compound demonstrated to induce the same subset of P-450 isozymes as TCDD. This pretreatment produced little change in the overall oxidation of (S)-nicotine.<sup>30</sup>

To test further the hypothesis that P-450 isozyme-2 catalyzes the oxidation of (S)-nicotine, lung microsomes prepared from rabbits pretreated with Aroclor 1260 were incubated with (S)-nicotine. Aroclor 1260, a mixture of polychlorinated biphenyls, has been demonstrated previously to induce rabbit lung P-450 isozyme-6 but, by an unknown mechanism, repress lung P-450 isozyme-2. The induction of P-450 isozyme-6 has been attributed to the co-planar polychlorinated biphenyls and dibenzofurans present in this mixture, since removal of these components by fractionation results in the loss of this inducing property. The removal of these components apparently has no effect on the repression of rabbit lung P-450 isozyme-2 by the remaining components of Aroclor 1260.

Results of this study indicate that the metabolism of (S)-nicotine is inhibited by 35% compared to metabolic incubations which used lung microsomes isolated from untreated, phenobarbital pretreated or TCDD pretreated rabbits. Since Aroclor 1260 selectively decreases the content of lung P-450 isozyme-2, the inhibition of (S)-nicotine metabolism may be attributable to a decrease in the metabolic oxidation pathway catalyzed by this enzyme.

In order to gain a better understanding of the effects of Aroclor 1260 on the metabolism of (S)-nicotine, a reversed phase C-18 HPLC separation method for (S)-

$5\text{-}^3\text{H}$ -nicotine and its major radiolabeled metabolites (S)-nicotine N'-oxide, nornicotine, (S)-cotinine and (S)-nicotine  $\Delta^{1',5'}$ -iminium ion was developed. This assay is based on the reversed phase HPLC separation of supernatants of acetonitrile precipitated microsomal incubates followed by radiochemical detection of the tritium labeled metabolites. By this method, (S)-nicotine metabolite formation was quantitatively estimated directly by measuring the amount of radioactivity corres-

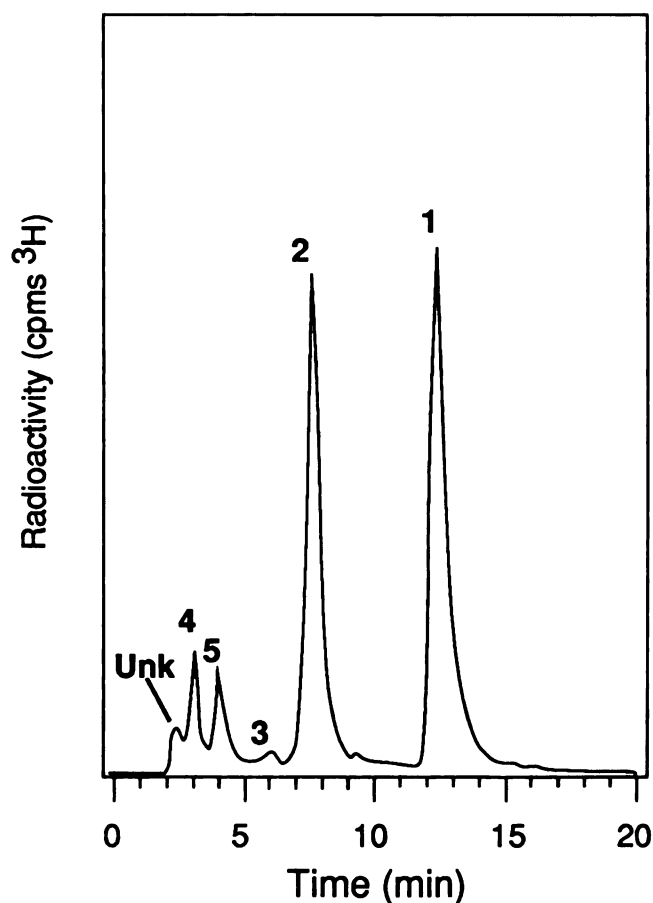


**Fig.IV.6** Reversed Phase HPLC Analysis of the Lung Microsomal Metabolism of (S)-Nicotine (S)- $5\text{-}^3\text{H}$ -Nicotine (1a) and its radiolabeled metabolite analogs (S)-nicotine  $\Delta^{1',5'}$ -iminium ion (2), (S)-cotinine (3), (S)-nicotine N'-oxide (4) and (S)-nornicotine (5) were analyzed by radiochemical detection following separation of aqueous filtrates of lung microsomal incubates by reversed phase C-18 HPLC.

ponding to each (S)-nicotine metabolite. Incubation of  $100\ \mu\text{M}$  (S)- $5\text{-}^3\text{H}$ -nicotine with lung microsomes from untreated rabbits followed by radiochromatographic

analysis of these incubation mixtures indicated that approximately 65% of the metabolites formed were the 5'-carbon oxidation products (S)-nicotine  $\Delta^{1',5'}$ -iminium ion and (S)-cotinine (Fig.IV.6). This value is comparable to previous estimates based on silica HPLC with UV detection. The reversed phase HPLC separation provides an advantage over silica HPLC; it permits the analysis of aqueous filtrates of the lung microsomal incubates and thus the detection of all components present in these filtrates, including polar metabolites such as (S)-nicotine N'-oxide. In addition, this separation technique provides a more accurate way to measure the formation of nornicotine which, due to its poor chromatographic properties, was difficult to assess by the normal phase silica HPLC method described in Chapter III. We determined after a 1 hr incubation at 37°C, that (S)-nicotine N'-oxide and nornicotine each accounted for approximately 15% of the (S)-5-<sup>3</sup>H-nicotine equivalents metabolized. An unknown peak which eluted before (S)-nicotine N'-oxide accounted for the remaining 5%. It was not determined whether this unknown peak was related to the unidentified compound described earlier (See Fig.IV.3).

#### **Effects of Various Inhibitors and Pretreatments on the (S)-Nicotine Metabolite Profile**

In order to assess further the role of cytochrome P-450 isozyme-2 in the metabolism of (S)-nicotine, (S)-5-<sup>3</sup>H-nicotine (100  $\mu$ M) was incubated with lung microsomes (1 mg/ml) and various agents which influence cytochrome P-450 content and/or function.

Metabolism of (S)-nicotine to its metabolites was measured in metabolic incubation mixtures containing lung microsomes isolated from rabbits pretreated with Aroclor 1260. As mentioned above, pretreatment of rabbits with Aroclor 1260 inhibits the lung P-450 isozyme-2 catalyzed N-demethylation of benzphetamine by 70% but inhibits (S)-nicotine oxidation by only 35%. However, upon examination of the

metabolite profile generated in incubations containing (S)-nicotine and these microsomes, a 57% reduction in the formation of (S)-nicotine  $\Delta^{1',5'}$ -iminium ion was observed (Fig.IV.7). In contrast, the formation of nornicotine and nicotine N'-oxide did not differ significantly from metabolic incubations employing control lung microsomes. The inhibitory effects of Aroclor 1260 pretreatment on the lung microsomal N-demethylation of benzphetamine and formation of (S)-nicotine  $\Delta^{1',5'}$ -iminium ion provides further evidence that lung P-450 isozyme 2 is responsible for oxidizing (S)-nicotine to this metabolite.

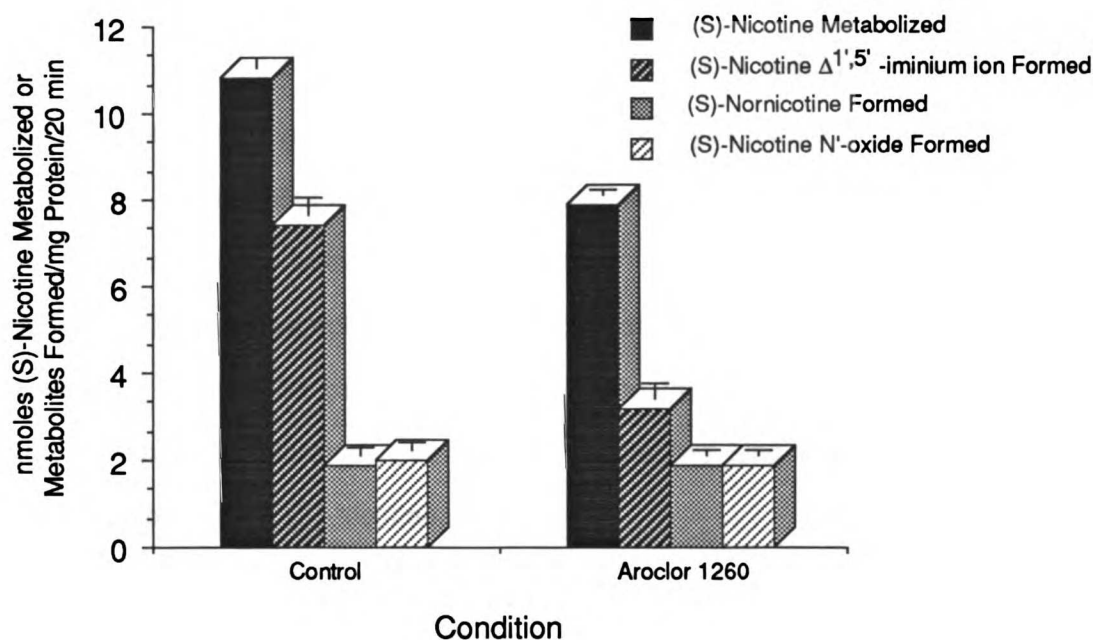
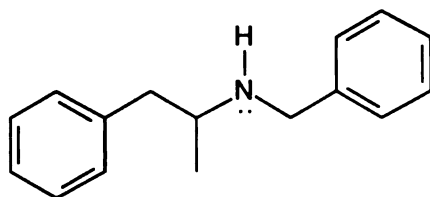


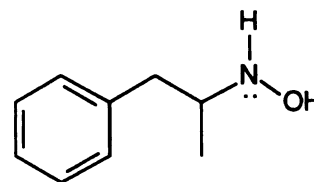
**Fig.IV.7** Comparison of the Metabolic Profiles of the Control and Aroclor 1260 Pretreated Rabbit Lung Microsomal Oxidation of (S)-Nicotine

Incubations containing 2.5  $\mu\text{M}$  of the rabbit lung P-450 isozyme-2 suicide inhibitor  $\alpha$ -methylbenzylaminobenzotriazole completely inhibited the formation of (S)-nicotine  $\Delta^{1',5'}$ -iminium ion and (S)-cotinine, whereas the formation of (S)-nicotine N'-oxide was inhibited by only 41% (Fig.IV.8 and Table IV.4)  $\alpha$ -Methylbenzylaminobenzotriazole did not inhibit the oxidation of (S)-nicotine to

nornicotine. These results are qualitatively similar to the effects observed with lung microsomes isolated from rabbits pretreated with Aroclor 1260.



63



64

To evaluate further the effect of lung cytochrome P-450 isozymes-2 and -5 on the metabolism of (S)-nicotine, the metabolic intermediate (MI) complex forming agents norbenzphetamine (63) and N-hydroxyamphetamine (64) were used. These inhibitors, which are metabolically transformed in a process requiring NADPH and O<sub>2</sub>, form stable noncovalent complexes with the heme of cytochrome P-450.<sup>34</sup> Oxidative metabolism of norbenzphetamine by lung microsomes results in the formation of an intermediate which selectively inhibits rabbit lung P-450 isozyme-2.<sup>35</sup> The metabolism of N-hydroxyamphetamine produces an intermediate which forms stable complexes with lung P-450 isozymes-2 and -5. Together, the use of each of these two inhibitors can provide information on the role of the two lung P-450 isozymes in the oxidative metabolism of (S)-nicotine.

In this study norbenzphetamine was found to inhibit the lung microsomal oxidation of (S)-nicotine by 76%. The formation of (S)-nicotine  $\Delta^{1',5'}$ -iminium ion and nicotine N'-oxide were inhibited by 84% and 59%, respectively while the formation of nornicotine was inhibited by only 28%. In comparison, the inhibition of (S)-nicotine metabolism by N-hydroxyamphetamine was almost complete (97%), suggesting that lung P-450 isozyme-5 also participates in the metabolic oxidation of (S)-nicotine. N-hydroxyamphetamine inhibited the formation of (S)-nicotine  $\Delta^{1',5'}$ -iminium ion by greater than 98%, while the formation of nicotine N'-oxide was

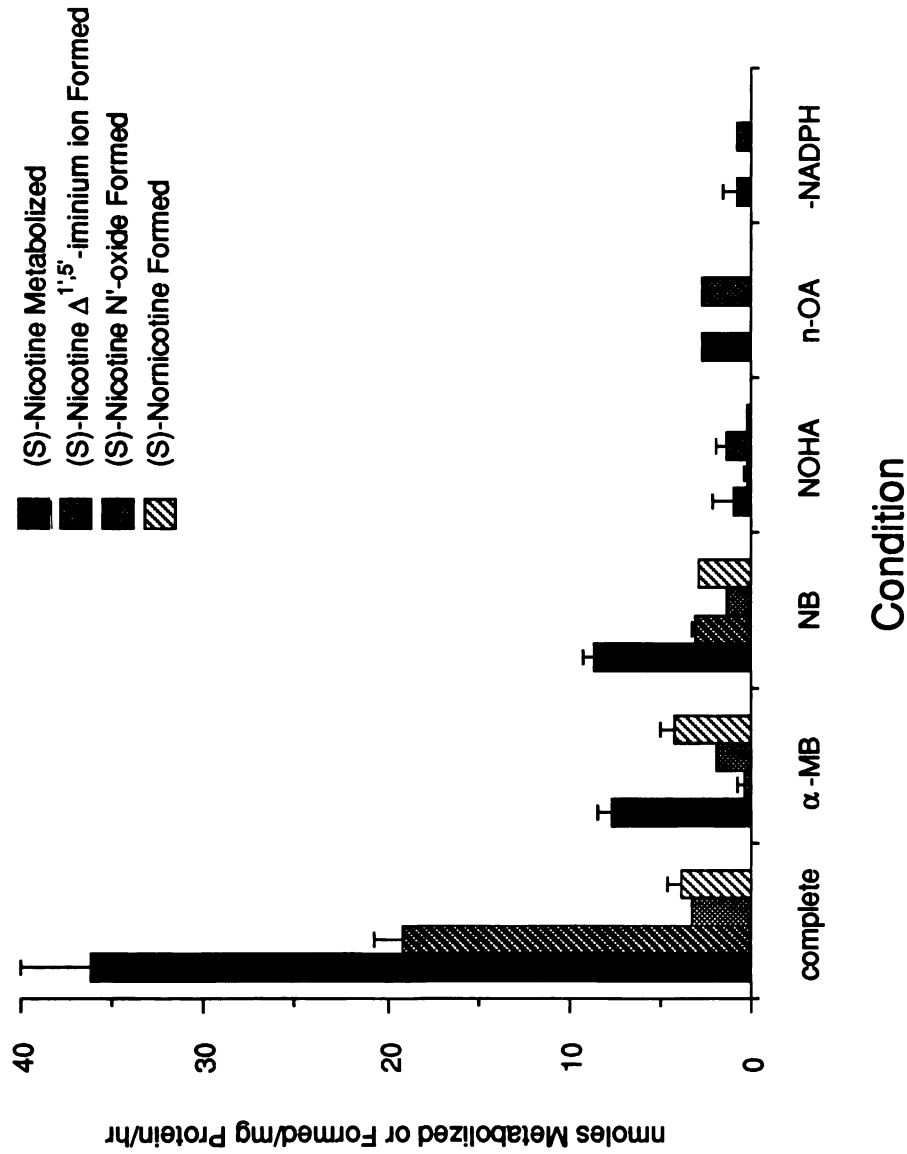


Fig. IV.8 Effect of Selective and Nonselective Lung P-450 Inhibitors on the Lung Microsomal Oxidation of (S)-Nicotine to its Major Metabolites (S)-Nicotine  $\Delta^{1,5}$ -iminium ion, (S)-Nicotine N'-oxide and (S)-Normicotine.  $\alpha$ -MB =  $\alpha$ -methylaminobenzylaminobenzotriazole; NB = norbenzphetamine; NOHA = N-Hydroxyamphetamine; n-OA = n-Octylamine. Values represent the average of two determinations  $\pm$  S.E.

Condition	Nicotine	Nicotine $\Delta^{1,5}$ - -Iminium	Cotinine	N'-oxide	Nornicotine	Unknown	% Recovery of $^3\text{H}$
Complete	63.8 $\pm$ 3.8	19.2 $\pm$ 1.5	0.7 $\pm$ 0.3	3.2 $\pm$ 0.1	3.9 $\pm$ 0.6	0.9 $\pm$ 0.1	91.6
No Incubation	99.8 $\pm$ 1.9 (99)	ND (100)	ND (100)	ND (100)	ND (100)	ND (100)	99.8
$\alpha$ -MB (2.5 $\mu\text{M}$ )	92.3 $\pm$ 0.8 (79)	0.3 $\pm$ 0.5 (98)	ND (100)	1.9 $\pm$ 0.1 (41)	4.3 $\pm$ 0.6 (-12)	ND (100)	98.8
NB (100 $\mu\text{M}$ )	91.4 $\pm$ 0.6 (76)	3.0 $\pm$ 0.3 (84)	ND (100)	1.3 $\pm$ 0.1 (59)	2.8 $\pm$ 0.1 (98.5)	ND (100)	98.5
NOHA (0.67 mM)	99.1 $\pm$ 1.3 (98)	0.2 $\pm$ 0.2 (99)	ND (100)	1.4 $\pm$ 0.5 (57)	0.1 $\pm$ 0.1 (98)	ND (100)	100.7
n-OA (3.0 mM)	99.6 $\pm$ 0.1 (99)	ND (100)	ND (100)	2.6 $\pm$ 0.1 (18)	ND (100)	ND (100)	102.2
NADPH omitted	99.3 $\pm$ 0.9 (98)	ND (100)	ND (100)	0.7 $\pm$ 0.1 (78)	ND (100)	ND (100)	100.0

n=2 for each condition  $\pm$  S.E.

ND = not detected.

Values in parentheses ( ) represent percent inhibition relative to the condition "complete"

**Table IV.4** Effect of Selective and Nonselective Lung P-450 Inhibitors on the Lung Microsomal Oxidation of (S)-Nicotine to its Major Metabolites (S)-Nicotine  $\Delta^{1,5}$ -Iminium Ion, (S)-Nicotine N'-Oxide, (S)-Cotinine and (S)-Nornicotine.  $\alpha$ -MB =  $\alpha$ -Methylbenzylaminobenzotriazole; NB = Norbenzphetamine; NOHA = N-Hydroxyamphetamine; n-OA = n-Octylamine.

inhibited to essentially the same degree (57%) observed with norbenzphetamine. This result suggests that the P-450 catalyzed N'-oxidation is mediated by isozyme-2 since N-hydroxyamphetamine, which inhibits P-450 isozyme-5 in addition to isozyme-2, does not inhibit the formation of this metabolite any further than that produced by norbenzphetamine. The nonselective P-450 inhibitor n-octylamine completely inhibited the metabolic conversion of (S)-nicotine to (S)-nicotine  $\Delta^{1',5'}$ -iminium ion and nornicotine but inhibited nicotine N'-oxide formation by only 18%. These results suggest that together with lung P-450 isozyme-2, the lung flavin containing monooxygenase (FCM) catalyzes the formation of this metabolite since this enzyme is less susceptible to the inhibitory effects of this P-450 inhibitor. In view of the suggested involvement of lung cytochrome P-450 in the N'-oxidation of (S)-nicotine, the relatively minor inhibition of N'-oxidation in lung microsomal incubations supplemented with n-octylamine is surprising. It is possible that lung FCM is activated by n-octylamine. Although it has been shown that liver FCM activity is induced by n-octylamine<sup>36</sup> such a role for this compound has not been described for the lung enzyme. Since nornicotine formation appears to be inhibited completely by N-hydroxyamphetamine and n-octylamine but not by the isozyme-2 selective inhibitors  $\alpha$ -methylbenzylaminobenzotriazole and norbenzphetamine, the metabolic conversion of (S)-nicotine to nornicotine is likely to be catalyzed by lung cytochrome P-450 isozyme-5.

#### **Effects of Lung P-450 Isozyme-2 Inhibition on the Covalent Binding of (S)-5-<sup>3</sup>H-Nicotine to Lung Microsomal Proteins**

Since certain pretreatment regimens and inhibitors were shown to alter the metabolic oxidation pathways of (S)-nicotine, it became possible to study in greater detail those routes which are involved in the bioactivation of this alkaloid. As described above, the enzymatic conversion of (S)-nicotine to (S)-nicotine  $\Delta^{1',5'}$ -iminium ion, a



metabolic pathway which we propose is related to the bioactivation of this tertiary amine, appears to be catalyzed almost exclusively by lung cytochrome P-450 isozyme-2. In order to examine whether this pathway is linked to the bioactivation of (S)-nicotine, covalent binding of (S)-5-<sup>3</sup>H-nicotine to lung microsomal proteins was assessed in metabolic incubations containing microsomes isolated from untreated or Aroclor 1260-pretreated rabbit lung or untreated rabbit lung microsomes supplemented with  $\alpha$ -methylbenzylaminobenzotriazole, a suicide inhibitor of lung P-450 isozyme-2.

Compared to lung microsomes obtained from untreated rabbits, lung microsomes isolated from Aroclor 1260-pretreated rabbits catalyzed the bioactivation of (S)-5-<sup>3</sup>H-nicotine much less effectively (0.035 versus 0.11 nmoles (S)-5-<sup>3</sup>H-nicotine equivalents covalently bound/mg protein/hr, respectively) (Table IV.5). This 68% decrease in covalent binding closely paralleled the 57% decrease in the lung P-450 isozyme-2 catalyzed oxidation of (S)-nicotine to (S)-nicotine  $\Delta^{1',5'}$ -iminium ion. In contrast, the decrease in covalent binding did not correlate with the formation of

**Table IV.5** Effect of Lung P-450 Isozyme-2 Inhibition on the Covalent Binding of (S)-5-<sup>3</sup>H-Nicotine to Rabbit Lung Microsomal Protein

Condition	(n)	nmoles (S)-5- <sup>3</sup> H-nicotine equivalents covalently bound/ mg protein/hr
complete	5	0.113 $\pm$ 0.036
Aroclor 1260	3	0.036 $\pm$ 0.006
+ $\alpha$ -mb†	2	N.D.*
-NADPH	5	N.D.*

\*amount of radioactivity measured was essentially equivalent to nonspecific binding.

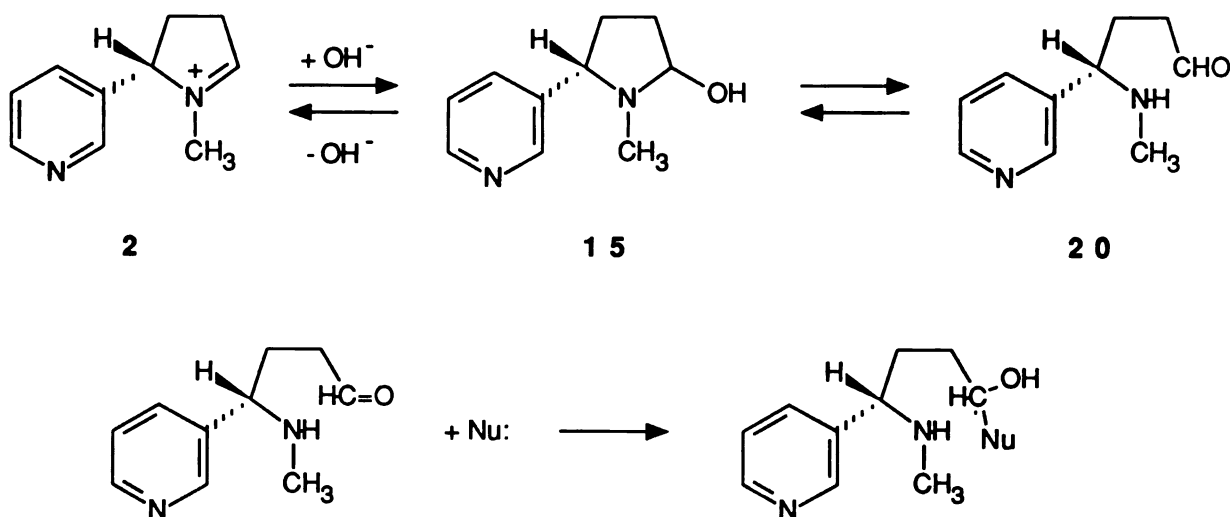
† $\alpha$ -mb =  $\alpha$ -methylbenzylaminobenzotriazole

Values represent mean  $\pm$  S.E.

normicotine and nicotine N'-oxide, the levels of which were essentially the same as that produced by control lung microsomes. Preincubation of lung microsomes for 15 min with 2.5  $\mu\text{M}$   $\alpha$ -methylbenzylaminobenzotriazole completely inhibited the covalent binding of (S)-5- $^3\text{H}$ -nicotine to lung microsomal proteins (Table IV.5). This result indicates that P-450 isozyme-2 is responsible for catalyzing the bioactivation of (S)-nicotine. The results of these two experiments suggest strongly that the lung cytochrome P-450 isozyme-2 catalyzed oxidation of (S)-nicotine to (S)-nicotine  $\Delta^{1',5'}$ -iminium ion is necessary to produce the reactive intermediate(s) which bind covalently to lung microsomal protein.

#### Metabolic Oxidation of (S)-Nicotine $\Delta^{1',5'}$ -Iminium Ion: Investigation of the Relationship Between its Further Oxidation and the Bioactivation of (S)-Nicotine

The evidence that the major metabolic pathway of (S)-nicotine involves its biotransformation to the electrophilic and potential bioalkylating species (S)-nicotine



**Scheme IV.1** Equilibrium Among the Isoelectronic Species 2, 15 and 20 and Proposed Trapping of 20 by a soluble nucleophile (i.e. Semicarbazide)

$\Delta^{1',5'}$ -iminium ion has prompted us to test directly the relationship between this species and its role in the covalent binding of (S)-nicotine. Subsequent to its formation, (S)-nicotine  $\Delta^{1',5'}$ -iminium ion is oxidized further to (S)-cotinine. This biotransformation reaction is catalyzed *in vitro* by the liver enzyme aldehyde oxidase.<sup>37</sup> In addition to being oxidized metabolically, (S)-nicotine  $\Delta^{1',5'}$ -iminium ion may also react directly with nucleophilic substituents present in biological macromolecules to form covalent adducts at the 5'-carbon atom. Alternatively, since the iminium ion exists in equilibrium with the corresponding ring opened aldehyde derivative (4-methylamino-4-(3-pyridyl)butanal **20**, via (S)-5'-hydroxynicotine **15**, nucleophilic attack at the carbonyl carbon atom of **20** may also lead to alkylated biomacromolecules (Scheme IV.1)

#### **Comparison of the (S)-Nicotine $\Delta^{1',5'}$ -Iminium Oxidase Activity of Lung and Liver 100,000 x g Soluble Fraction**

Due to the bioalkylating potential of (S)-nicotine  $\Delta^{1',5'}$ -iminium ion, its further oxidation is likely to serve a protective mechanism for the cell. Since the aldehyde oxidase present in the cytosolic fraction of liver tissue catalyzes the conversion of (S)-nicotine  $\Delta^{1',5'}$ -iminium ion to (S)-cotinine,<sup>37</sup> we decided to assess the relative iminium oxidase activity present in the lung cytosolic fraction. Experiments were designed to measure the enzymatic conversion of the aldehyde oxidase substrate 3-aminocarbonyl-1-methylpyridinium ion (NMN, **61**) to the corresponding 2-pyridone derivative (**62**) and (S)-nicotine  $\Delta^{1',5'}$ -iminium ion to (S)-cotinine. The activities measured in incubations containing cytosolic fractions obtained from lung were compared to the activities present in the cytosolic fraction obtained from rabbit liver.

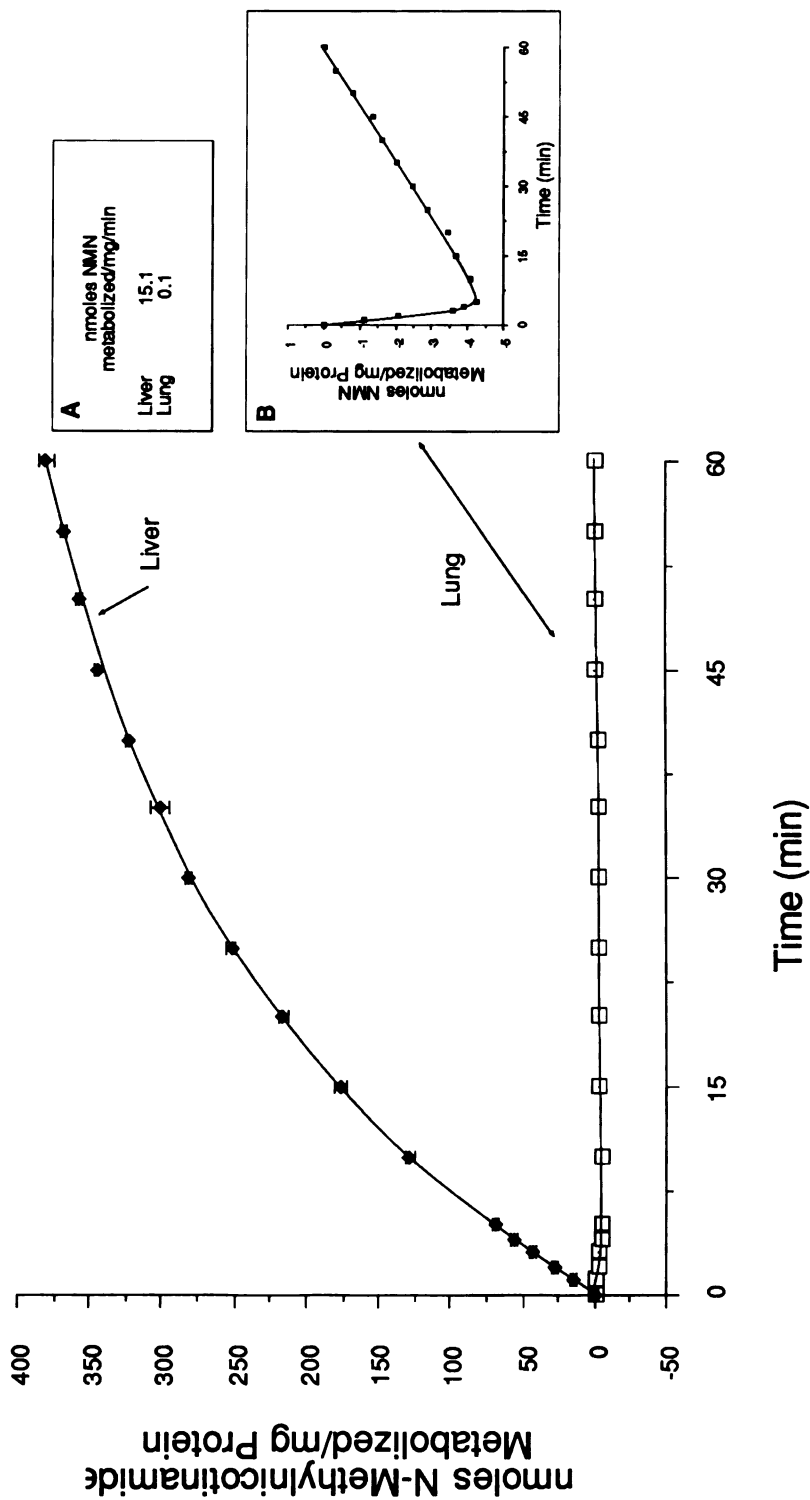
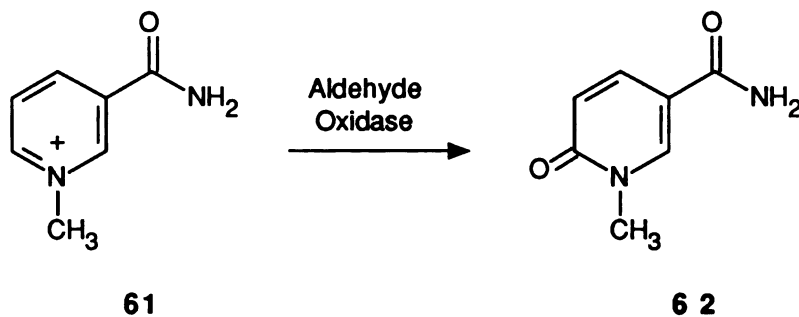


Fig. IV.9 A Comparison of the Lung and Liver Aldehyde Oxidase (AO) Activities Present in the Rabbit 100,000 x g Soluble Fraction. N-Methylnicotinamide (NMN) (5 mM) was incubated with the soluble fractions (1 mg/ml) isolated from the respective tissues and AO activity was estimated by monitoring the formation of the 2-pyridone derivative, the product of NMN oxidation, at 300 nm. An extinction coefficient of 4170 was used to calculate the amount of product formed. Insets: A). Comparison of the rates of AO catalyzed oxidation of NMN by liver and lung 100,000 x g soluble fraction. B). Scale for lung AO activity has been expanded to show details.



The cytosolic fraction of rabbit lung tissue was incubated with N-methylnicotinamide (NMN, **61**). Enzyme activity was measured by monitoring the rate at which the 2-pyridone derivative **62** was formed. Oxidation of NMN (5 mM) by the lung soluble fraction (1 mg/ml) proceeded at a rate of 0.1 nmole/mg protein/min (Fig. IV.9). Formation of the pyridone **62**, which was determined by monitoring the increase in UV absorbance at 300 nm, was linear over the course of a 60 min incubation at 37°C, although a slight decrease in absorbance was observed during the initial 6 min. In contrast, the 100,000 x g soluble fraction isolated from rabbit liver tissue catalyzed the oxidation of NMN at a rate of 15.1 nmoles/mg protein/min, a value approximately 150 fold greater than that observed for the corresponding lung activity (Fig. IV.9). In addition, the formation of **62** was linear during the first 5 min only, reflecting the rapid oxidation and turnover of **61** by the liver soluble fraction. These results indicate that the apparent lung NMN oxidase activity is much lower than the corresponding activity present in liver.

The (S)-nicotine  $\Delta^{1',5'}$ -iminium ion oxidase activities present in the same cellular subfractions were also compared. This activity was measured by monitoring the formation of (S)-cotinine by UV absorbance at 260 nm following separation on silica HPLC of methylene chloride extracts obtained from incubation mixtures containing the respective soluble fractions and synthetic (S)-nicotine  $\Delta^{1',5'}$ -iminium *bis*perchlorate. The lung soluble fraction catalyzed the oxidation of (S)-nicotine  $\Delta^{1',5'}$ -iminium *bis*perchlorate (1 mM) to (S)-cotinine at a rate of 0.35 nmoles·mg protein<sup>-1</sup>·min<sup>-1</sup> (Fig. IV.10). After a 1 hr incubation, 7.4 nmoles of (S)-nicotine  $\Delta^{1',5'}$ -iminium ion,

or <1% of the substrate, was converted to (S)-cotinine. Addition of the aldehyde oxidase inhibitor menadione (10  $\mu\text{M}$ ) inhibited this enzymatic reaction by only 30%. The oxidation of the iminium species (1mM) by liver 100,000 x g soluble fraction (1 mg/ml) was linear over the first 5 min and proceeded at a rate of 12.6 nmoles-mg protein<sup>-1</sup>·min<sup>-1</sup>, a rate comparable to the oxidation of NMN catalyzed by liver 100,000 x g soluble fraction and approximately 36 fold greater than the rate catalyzed by lung 100,000 x g soluble fraction (Fig.IV.10). The oxidation of (S)-nicotine  $\Delta^{1',5'}$ -iminium ion to (S)-cotinine by liver 100,000 x g soluble fraction was inhibited by 67% in the presence of 10  $\mu\text{M}$  menadione, a result consistent with the participation of aldehyde oxidase in this metabolic conversion.

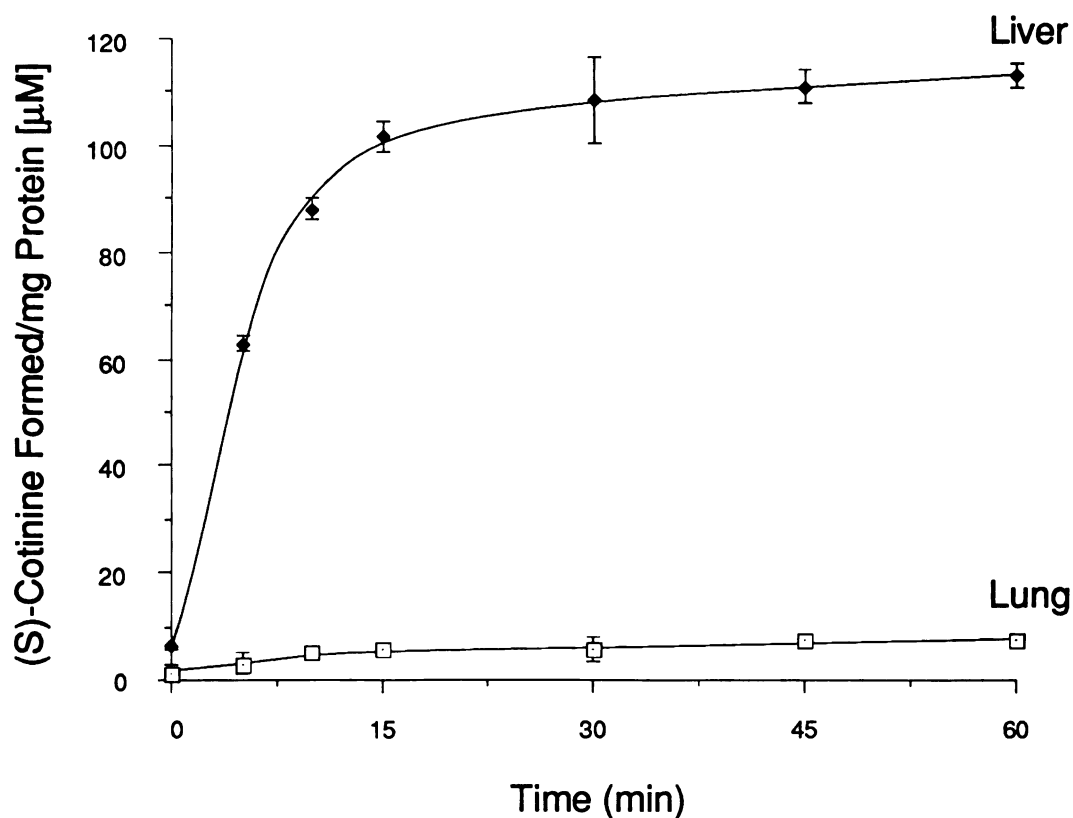


**Fig.IV.10** Lung and Liver 100,000 x g Soluble Fraction Catalyzed Oxidation of (S)-Nicotine  $\Delta^{1',5'}$ -iminium Ion. (S)-Nicotine  $\Delta^{1',5'}$ -iminium *bis* perchlorate (0.5 mM) was incubated with 100,000 x g soluble fraction (1 mg/ml) isolated from the respective tissues. (S)-Cotinine was quantitatively estimated by the normal phase silica HPLC method described in Materials and Methods.

The comparatively low rates of NMN and (S)-nicotine  $\Delta^{1',5'}$ -iminium bisperchlorate oxidation catalyzed by rabbit lung 100,000 x g soluble fraction indicates that the level of aldehyde oxidase in this tissue is substantially lower than that present in liver. The much less efficient conversion of (S)-nicotine  $\Delta^{1',5'}$ -iminium ion to (S)-cotinine by lung soluble enzymes might therefore be expected to favor the accumulation of the iminium species in this tissue.

If the iminium species is involved in the bioactivation of (S)-nicotine, then the covalent binding of (S)-nicotine in lung tissue would be expected to be higher than that in liver tissue, since the rate at which the  $\Delta^{1',5'}$ -iminium ion species is removed by lung soluble enzymes is comparatively slow. In order to address this possibility, the effect of the two soluble fractions on the covalent binding of (S)-nicotine following metabolic activation by lung microsomes was measured. Addition of 0.1 mg/ml of liver 100,000 x g soluble fraction inhibited the covalent binding of (S)-5-<sup>3</sup>H-nicotine by greater than 90% [0.016 nmoles (S)-nicotine equivalents bound/mg protein/hr vs 0.218 nmoles/mg protein/hr in the control incubation (Table IV.6)]. However, in

**Table IV.6** Bioactivation of (S)-5-<sup>3</sup>H-Nicotine: Effect of Treatments Which Modify the Level of (S)-Nicotine  $\Delta^{1',5'}$ -Iminium Ion in Lung Microsomal Incubations.

Condition	(n)	nmoles (S)-5- <sup>3</sup> H-nicotine equivalents covalently bound/ mg protein/hr
Complete System	5	0.214 ± 0.020 <sup>§</sup>
+ 0.1 mg/ml liver 100,000 x g soluble fraction	3	0.016 ± 0.002
+ 0.1 mg/ml lung 100,000 x g soluble fraction	3	0.203 ± 0.012
+ 1 mM semicarbazide	3	0.195 ± 0.016
+ 2.5 μM α-mb <sup>†</sup>	2	0.027 ± 0.001
- NADPH	2	0.012 ± 0.002

<sup>§</sup>Nonspecific binding observed at the zero time point control (equivalent to 0.057 nmoles) was subtracted to yield the values presented above.

<sup>†</sup>α-mb = α-methylbenzylaminobenzotriazole

Values represent the mean ± S.E.

metabolic incubations containing 0.1 mg/ml of lung 100,000 x g soluble fraction the amount of (S)-5-<sup>3</sup>H-nicotine bound covalently to lung microsomal proteins was essentially the same as that obtained in the control incubation (0.203 vs. 0.218 nmoles/mg protein/hr, respectively). The much lower iminium oxidase activity present in lung soluble fraction compared to that detected in the corresponding fraction of liver (see Fig.IV.11 A and B), together with the failure of the lung soluble fraction to block covalent binding indicates that the reactive (S)-nicotine  $\Delta^{1',5'}$ -iminium ion is involved in the covalent binding of (S)-nicotine to lung microsomal protein. These results imply that the lung may be more susceptible than the liver to bioalkylation reactions involving this electrophilic species.

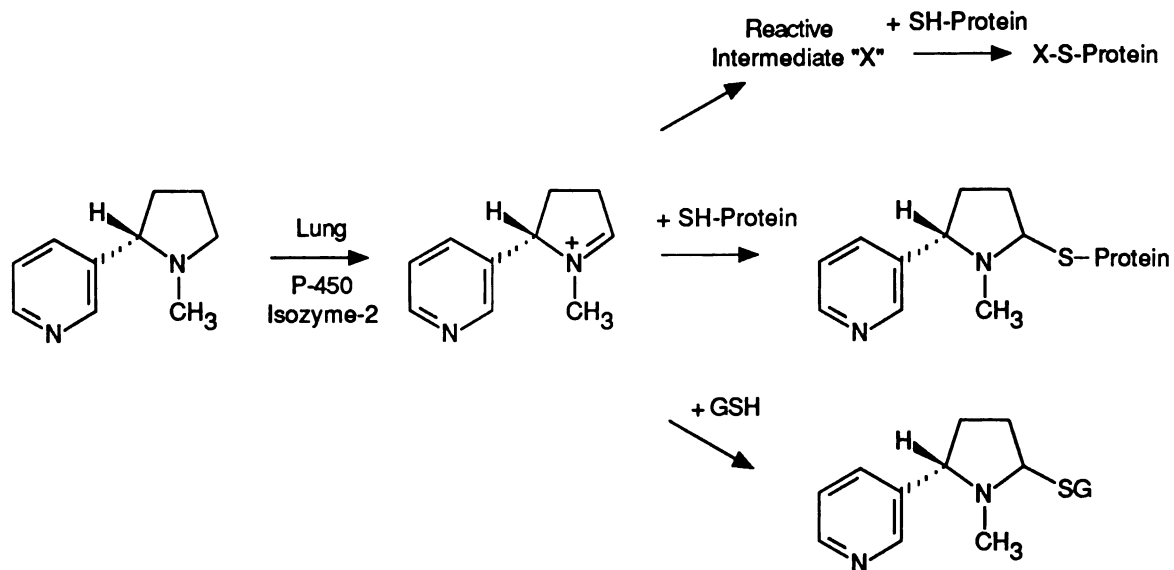
Although (S)-nicotine  $\Delta^{1',5'}$ -iminium ion is implicated in the bioalkylation of metabolically activated (S)-nicotine, other compounds which exist in equilibrium with this metabolic intermediate could conceivably contribute to the covalent binding observed. One such compound is the ring opened form of 5'-hydroxynicotine, 4-methylamino-4-(3-pyridyl)butanal (**20**) which may also be reactive towards nucleophilic constituents present in biomacromolecules (See Scheme IV.1). To test this possibility, metabolic incubation mixtures were supplemented with 1 mM semicarbazide, a soluble nucleophile which traps aldehyde containing compounds, such as **20**, to produce the nonreactive semicarbazone derivative. Semicarbazide did not produce a significant decrease in covalent binding and therefore we conclude that the ring opened form of (S)-5'-hydroxynicotine is probably not acting as the ultimate electrophilic species in these experiments.

To determine whether a soluble nucleophile could block the covalent binding of (S)-nicotine to nucleophilic substituents present in lung microsomal protein, glutathione was added to incubation mixtures containing (S)-5-<sup>3</sup>H-nicotine. Glutathione (2 mM) inhibited the covalent binding of (S)-5-<sup>3</sup>H-nicotine by 84 %



	Metabolism	Covalent Binding
	nmoles/mg/hr	nmoles/mg/hr
no incubation	N.D.	N.D.
complete	39.1 ± 2.1	0.099 ± 0.004
complete + 2 mM Glutathione	39.6 ± 4.2	0.015 ± 0.002
-NADPH	N.D.	0.016 ± 0.001

**Table IV.7** Effect of Glutathione (GSH) on the Rabbit Lung Microsomal Oxidation and Covalent Binding of (S)-5-<sup>3</sup>H-Nicotine. (S)-Nicotine or (S)-5-<sup>3</sup>H-nicotine (0.1 mM, 23  $\mu$ Ci/ $\mu$ mole) was incubated with 1 mg/ml lung microsomes in a total volume of 0.4 ml. GSH was added at a final concentration of 2 mM. Following the termination of the incubation, metabolism and covalent binding of (S)-nicotine was determined by the assays described in the Materials and Methods section. The net values obtained for covalent binding was obtained by subtracting the amount of (S)-nicotine associated with the microsomal protein in the no incubation condition (0.024 nmoles (S)-nicotine equivalents/mg protein/hr) from the remaining three conditions. Results are expressed as the average of triplicate determinations  $\pm$  S.E. N.D. = not detectable



**Scheme IV.2** Lung Cytochrome P-450 Isozyme-2 Catalyzed Metabolic Activation of (S)-Nicotine and Trapping of the Proposed Reactive Intermediate(s) by Glutathione and Tissue Protein

(Table IV.7) without affecting its metabolism. These results therefore are consistent with the trapping of the reactive (S)-nicotine metabolite by glutathione (Scheme IV.2).

## Discussion

Previous studies have demonstrated the persistent localization of (S)-nicotine in lung and other extrahepatic tissues.<sup>38,39,40</sup> Autoradiographic examination of the lung following intravenous administration of radiolabeled nicotine reveal the localization of radioactivity in the bronchial epithelium. Other foreign compounds which preferentially localize at this site following administration include 4-ipomeanol, a potent lung toxicant which is metabolically activated by cytochrome P-450 present in the Clara cells. This cell type, which has been shown in *in vitro* cell culture studies to metabolize a number of acutely toxic or carcinogenic foreign compounds, has been proposed as the cell of origin of many lung carcinomas including those induced by metabolically activated substances. For these reasons, we postulate that the bioactivation of (S)-nicotine by cytochrome P-450 present in lung cells such as the bronchiolar Clara cells may be responsible for the long term localization of this compound in the lung. The studies presented in this chapter are aimed at characterizing the metabolic disposition and bioactivation of this compound in incubation mixtures employing microsomes and cytosolic fractions obtained from rabbit lung tissue.

We show in the present study that (S)-nicotine is metabolized by lung microsomes to the same major metabolites detected previously in studies which employed enzymes or cellular homogenates isolated from liver tissue of various animals. The metabolic oxidation of (S)-nicotine by rabbit lung microsomes is time, NADPH and cytochrome P-450 dependent. These results indicate that the lung microsomal enzymes which catalyze the oxidation of (S)-nicotine are qualitatively similar to the corresponding family of enzymes found in the liver, findings consistent with the known

similarities between the liver and lung P-450 isozymes found in rabbit. In addition to these observations, lung microsomes catalyzed the oxidation of (S)-nicotine to an unknown metabolite possessing chromatographic and UV spectral characteristics similar, but not identical, to those of  $\beta$ -nicotyrine. Several attempts to isolate and characterize this compound were not successful. Obviously, the similarities between the unknown compound and  $\beta$ -nicotyrine are quite intriguing since the later compound, whose metabolic fate will be described in Chapter VI, may be metabolically activated to reactive intermediates.

Two of the principal P-450 enzymes present in rabbit lung, isozymes-2 and -5, have been characterized extensively and shown to be essentially identical to the phenobarbital inducible liver cytochrome P-450 isozymes-2 and -5 based on a number of biochemical and immunochemical criteria.<sup>11</sup> Recent studies by others have shown (S)-nicotine to be a good substrate for phenobarbital inducible isozymes in rat and guinea pig liver.<sup>29,27</sup> In addition, studies described in Chapter III have indicated that liver microsomes isolated from rabbits pretreated with phenobarbital metabolically activate (S)-nicotine approximately 2.5 fold faster than control rabbit liver microsomes. Together, these observations encouraged us to examine whether the corresponding lung cytochrome P-450 isozymes catalyze the oxidation and bioactivation of (S)-nicotine.

The major metabolite detected in rabbit lung microsomal incubations was the electrophilic species (S)-nicotine  $\Delta^{1',5'}$ -iminium ion. This compound, which represented approximately 40% of all the metabolites generated from the oxidative metabolism of (S)-nicotine, was proposed in Chapter III to be involved in the metabolism dependent covalent binding of (S)-nicotine to liver microsomal protein. Attempts to define the route of metabolism and to identify the reactive species involved in the covalent binding process were unsuccessful.

A comparison of the liver and lung microsomal metabolism of (S)-nicotine revealed, on the basis of P-450 content, that lung microsomes oxidize this compound at a rate 4-fold higher than that observed with liver microsomes. This higher rate of metabolism suggests that lung P-450 isozymes-2 and/or -5 catalyze its oxidation since 80-90% of the P-450 present in lung is comprised of these two isozymes. In contrast, P-450 isozymes-2 and -5 together account for a small proportion (<20%) of the total P-450 present in liver which is comprised of at least 9 different isozymic forms.<sup>41</sup> Both of the lung P-450 isozymes are thought to be similar to the phenobarbital inducible liver P-450 isozyme(s) which we propose catalyzes the bioactivation of (S)-nicotine. The relatively high concentration of cytochrome P-450 present in lung tissue is significant since bioactivation of foreign compounds such as (S)-nicotine in the P-450 rich Clara cells could lead to irreversible lesions to DNA and possibly tumorigenesis.

The use of pretreatment regimens which alter the activity of lung cytochrome P-450 isozymes offered an opportunity to assess the involvement of lung P-450 isozymes in the overall oxidation of (S)-nicotine. Pretreatment of rabbits with Aroclor 1260 significantly inhibited the lung microsomal oxidation of (S)-nicotine while pretreatment with phenobarbital and TCDD had no measurable effect. Use of Aroclor 1260 pretreatment and selective and nonselective inhibitors of lung cytochrome P-450 isozymes, together with a new reversed phase HPLC assay (developed to measure the individual metabolites), permitted us to evaluate the relationship between each isozyme and specific metabolic pathways. From the results of these studies, the oxidation of (S)-nicotine to (S)-nicotine  $\Delta^{1',5'}$ -iminium ion was found to be catalyzed almost exclusively by lung P-450 isozyme-2. Evidence was also provided for the participation of this enzyme in the oxidation of (S)-nicotine to the N'-oxide. The metabolic pathway leading to the formation of normicotine was not affected by treatments which decreased or increased the activity of isozymes-2 and -6, respectively, whereas compounds which

also inhibit P-450 isozyme-5 (N-hydroxyamphetamine and n-octylamine) almost completely blocked this pathway. It is concluded therefore that the oxidation of (S)-nicotine at the N-methyl carbon is catalyzed by lung cytochrome P-450 isozyme-5.

The results of the isozyme studies together with the rationale described above encouraged us to examine which metabolic pathway(s) is/are responsible for the bioactivation of (S)-nicotine. The studies described in Chapter III suggest the involvement of a phenobarbital inducible liver isozyme of P-450 in the bioactivation of this compound. The lung contains P-450 isozymes-2 and -5 both of which are inducible in the liver by phenobarbital. Therefore these isozymes are reasonable candidates for catalyzing the bioactivation of (S)-nicotine in the lung. The above studies indicate that the oxidation of (S)-nicotine to the electrophilic (S)-nicotine  $\Delta^{1',5'}$ -iminium ion and (S)-nicotine methyleneiminium ion are catalyzed by P-450 isozyme-2 and -5, respectively. Since P-450 isozyme-2 can be selectively inhibited, it is possible to evaluate its contribution to the bioactivation of (S)-nicotine. In order to make this assessment, covalent binding experiments were performed with either rabbit lung microsomes after Aroclor 1260 pretreatment (which is known to lower isozyme-2 levels), or control lung microsomes preincubated with the isozyme-2 selective inhibitor  $\alpha$ -methylbenzylaminobenzotriazole. The substantial and almost complete inhibition of covalent binding under conditions where oxidation at the 5'-carbon atom is blocked suggests that the metabolic pathway leading to the formation and/or further oxidation of (S)-nicotine  $\Delta^{1',5'}$ -iminium ion is involved in the bioactivation of (S)-nicotine. Further studies with semicarbazide revealed that the ring opened aldehyde form of (S)-5'-hydroxynicotine is not responsible for the covalent binding of (S)-nicotine. In addition, the soluble nucleophile glutathione was shown to be an effective inhibitor of this binding.

The strong correlation between the formation of (S)-nicotine  $\Delta^{1',5'}$ -iminium ion and covalent binding prompted us to test whether the  $\Delta^{1',5'}$ -iminium species is involved in the covalent binding of bioactivated (S)-nicotine. To address this question, the aldehyde oxidase containing cytosolic fraction obtained from liver was added to lung microsomal incubations of (S)-5-<sup>3</sup>H-nicotine and the extent of covalent binding was compared to that in control incubations. The covalent binding of (S)-nicotine was reduced by > 90% in the presence of the cytosolic fraction [which catalyzes the oxidation of the iminium ion to the unreactive lactam (S)-cotinine] suggesting that the  $\Delta^{1',5'}$ -iminium ion is linked directly to the covalent binding. In contrast, addition of the cytosolic fraction obtained from lung tissue did not have a significant effect on the lung microsomal bioactivation of (S)-nicotine. The results of these experiments are consistent with the earlier study which showed that liver cytosolic fraction catalyzed the oxidation of (S)-nicotine  $\Delta^{1',5'}$ -iminium ion to (S)-cotinine efficiently whereas the lung cytosolic fractions possessed relatively little activity.

The removal of the electrophilic and potentially reactive  $\Delta^{1',5'}$ -iminium species from the cellular environment by liver aldehyde oxidase is consistent with this enzyme serving a protective role. In contrast, the corresponding lung enzyme appears to be much less efficient in catalyzing the oxidation of (S)-nicotine  $\Delta^{1',5'}$  iminium ion. Because of the poor iminium oxidase activity in lung tissue, the intracellular concentration of (S)-nicotine  $\Delta^{1',5'}$ -iminium ion, particularly in the P-450 rich Clara cells, is likely to be much greater than its concentration in hepatocytes. High intracellular concentrations of the iminium species may result in an increase in its direct covalent binding or, via further metabolism, to an ultimate bioalkylating species. One such further metabolic oxidation pathway involves the conversion of (S)-nicotine  $\Delta^{1',5'}$ -iminium ion to  $\beta$ -nicotyrine, a reaction catalyzed by monoamine oxidase B. This metabolic pathway is described in greater detail in Chapter V.

These *in vitro* experiments have shown that lung cytochrome P-450 isozyme-2 metabolically activates (S)-nicotine via oxidation at the 5'-carbon atom and that the covalent binding which results can be lowered or eliminated by the enzymatic removal of (S)-nicotine  $\Delta^{1',5'}$ -iminium ion from the incubation mixture. Our observations raise the question of whether the bioactivation of (S)-nicotine would occur to a greater extent in lung versus liver tissue. In view of the relatively high concentration of P-450 isozyme-2 present in the lung microsomal fraction and considering that this enzyme is enriched in Clara cells (1 of an estimated 40 cell types in the lung), the oxidative conversion of (S)-nicotine to (S)-nicotine  $\Delta^{1',5'}$ -iminium ion would most likely represent the principal metabolic pathway for this alkaloid. In addition, the rate at which (S)-nicotine  $\Delta^{1',5'}$ -iminium ion is converted to (S)-cotinine in this tissue is likely to be much slower than in liver, since the iminium oxidase activity measured in the lung cytosolic fraction is estimated to be <3% the activity present in the corresponding liver fraction. Viewed in another way, the potential for bioalkylation may be expressed as a function of the ratio of the rates of (S)-nicotine  $\Delta^{1',5'}$ -iminium ion formation:aldehyde oxidase catalyzed (S)-nicotine  $\Delta^{1',5'}$ -iminium ion oxidation.

Although the metabolic pathway involved in the formation of (S)-nicotine  $\Delta^{1',5'}$ -iminium ion is necessary for the covalent binding of (S)-nicotine, it is not clear whether the ultimate reactive species is the iminium ion or possibly a further oxidation product which is difficult to characterize. Bioactivation of (S)-nicotine via oxidation at its 5'-carbon atom is similar to the metabolic activation pathway described for the tertiary amine phencyclidine. In the later case, it has been shown conclusively that the  $\alpha$ -carbon oxidation of PCP is necessary for the covalent binding of this compound to microsomal protein. The oxidation of PCP at this position produces the PCP iminium ion, which is itself metabolically activated further to produce the ultimate bioalkylating species. Adapting this model of tertiary amine bioactivation to (S)-nicotine raises the

possibility that the  $\Delta^{1',5'}$ -iminium ion may not be the ultimate reactive component. Further studies will need to be performed to address this question.

## Materials and Methods

### Chemicals

3-(Aminocarbonyl)-1-methylpyridinium chloride (NMN) was obtained from W.A. Taylor and Co. (Baltimore, MD). Chemicals used in metabolic incubations were described in the Materials and Methods section of Chapter III. Acetonitrile, methanol and methylene chloride were HPLC grade solvents obtained from Fisher Scientific Co. (Plainview, NJ). Triethylamine and n-propylamine were obtained from Aldrich (Milwaukee, WI).  $\alpha$ -Methylbenzylaminobenzotriazole ( $\alpha$ -mb) and Aroclor 1260 were the generous gifts of Dr. James M. Mathews (Research Triangle Institute, North Carolina). Norbenzphetamine and N-hydroxyamphetamine were kindly provided by Dr. Michael Franklin (University of Utah). Benzphetamine, 7-ethoxyresorufin and resorufin were generously provided by Dr. Almira Correia (University of California, San Francisco). (S)-Nicotine- $\Delta^{1',5'}$ -iminium ion *bis*perchlorate,<sup>42</sup> the diastereomeric (S)-nicotine N-oxides,<sup>43</sup> (S)-cotinine,<sup>44</sup> and nornicotine<sup>45</sup> were prepared as described previously. (S)-5-<sup>3</sup>H-Nicotine was prepared as described in Chapter II. Flow Scint II scintillation fluid was obtained from Radiomatic Instruments and Chemical Co. Inc. (Tampa, FL). 3 mm Nylon 66 filters were obtained from Micron Separations Inc. [MSI] Cameo (Honeoye Falls, NY).

### Treatment of Animals

A 1mg/ml solution of TCDD (2,3,7,8-tetrachlorodibenzo-p-dioxin) was prepared by dissolving 2.3 mg of this compound in 2.3 ml corn oil. The stock solution was diluted with corn oil to a final concentration of 100  $\mu$ g/ml. Injections were made in the lower left caudal portion of the abdomen of three New Zealand White rabbits (3 kg)



with 0.75 ml of the 100 µg/ml solution via a 20 gauge needle. A neat solution of Aroclor 1260 (200 mg/kg) was injected as described for TCDD. Animals pretreated with TCDD and Aroclor 1260 were sacrificed 72 hours later. Rabbits which were pretreated with phenobarbital received sodium phenobarbital 0.1% (w/v), pH adjusted to pH 6.9 with HCl, in their drinking water for 1 week prior to the isolation of the lung microsomes.

#### **Preparation of Lung Tissue Fractions**

Male New Zealand White Rabbits (3-4 kg), were sacrificed by carbon dioxide asphyxiation and the lung tissue processed as follows: The lungs were perfused with approximately 30 ml of heparinized 0.15 M KCl buffer (100 units of heparin/ml), removed, blotted with tissue to remove excess buffer and weighed. The lung tissue was finely minced with surgical scissors in three volumes of a buffer consisting of 0.02 M TRIS, 0.15 M KCl, 0.2 mM EDTA and 0.5 mM dithiothreitol in 20% glycerol, pH 7.4. The resulting suspension was placed in a Potter-Elvehjem homogenizer and homogenized with 6 passes of a Teflon pestle. Because the homogenizing buffer contained glycerol, centrifugation was performed at a higher speed. To obtain a supernatant containing microsomes and soluble proteins, the lung homogenate was centrifuged at 18,000 x g for 20 min. The resulting 18,000 x g supernatant was centrifuged at 100,000x g in order to obtain the microsomal pellet. The 100,000 x g supernatant was removed with a Pasteur pipet and stored at -70°C until used. The remaining pellet was washed with buffer and recentrifuged at 100,000 x g for 60 min. The resulting microsomal pellet was resuspended in buffer to a concentration of approximately 10 mg/ml and stored at -70°C until used.

#### **Incubation Conditions**

(S)-Nicotine was incubated in the presence of a mixture which included EGTA (1.0 mM), NADP<sup>+</sup> (0.5 mM) and a glucose 6-phosphate based regenerating system (glucose 6-phosphate [8.0 mM], glucose 6-phosphate dehydrogenase [1 unit/ml], and magnesium chloride [4.0 mM]), and lung microsomes from untreated male New Zealand

White rabbits (1mg/ml) in a final incubation volume of 0.4 ml. This mixture was preincubated for 5 min at 37°C before addition of the substrate.

#### **Comparison of Liver and Lung Microsomal Oxidation of (S)-Nicotine**

Microsomes were isolated from untreated New Zealand White rabbits. (S)-Nicotine (100 $\mu$ M) was added to metabolic incubation mixtures consisting of either liver (0.5 mg/ml) or lung microsomes (1 mg/ml) and the appropriate cofactors. Incubations were conducted over a period of 60 min at 37°C. Separate incubations (0.4 ml) were used for each time point. Incubations were terminated by the addition of an equal volume of ice cold 1 M K<sub>2</sub>CO<sub>3</sub> followed by the addition of the internal standard, N-methyl-N-(3-pyridyl)methylpropionamide. Methylene chloride (0.8 ml) was added to the incubation mixture and vortexed for 1-2 min. The phases were separated by centrifugation at 1000 x g for 3-5 min. The methylene chloride extract was separated by normal phase HPLC and the amount of (S)-nicotine metabolized was quantitated by determining the peak height ratio of (S)-nicotine to the internal standard and determining the corresponding amounts from a standard calibration curve.

#### **Normal Phase Silica HPLC Analysis**

To examine the overall lung and liver microsomal metabolism of (S)-nicotine, an HPLC assay based on normal phase silica was used. This assay, which was described in detail in Chapter III, detects (S)-nicotine and the methylene chloride extractable metabolites (S)-nicotine  $\Delta^{1',5'}$ -iminium ion and (S)-cotinine. Lung microsomal incubations (0.4 ml) were terminated by adding 0.4 ml 1M K<sub>2</sub>CO<sub>3</sub>. The internal standard N-methyl-N-(3-pyridyl)methylpropionamide (20 nmoles) and 1 ml of HPLC grade methylene chloride were added to this quenched incubation mixture. This mixture was extracted by vortexing vigorously for 1 min. The phases were separated by centrifuging this emulsion at 1000 x g for 2-3 min. A volume of 50  $\mu$ l of the resulting methylene chloride extract was analyzed by HPLC. The HPLC system consisted of a Beckman 110A solvent delivery system and a Hitachi 100-10 spectrophotometer/flow

cell combination. The precolumn consisted of a direct-connect precolumn assembly and a 5  $\mu\text{m}$  Adsorbosphere silica precolumn cartridge, Alltech (State College, PA). A 3  $\mu\text{m}$  Chemco silica column (75 mm x 4.6 mm) (Dychrom, Sunnyvale CA) was used for the analytical separation of (S)-nicotine and its metabolites. The mobile phase consisted of 0.3% n-propylamine in acetonitrile. UV absorbance was monitored at 260 nm, the  $\lambda_{\text{max}}$  for nicotine.

#### **$\alpha$ -Methylbenzylaminobenzotriazole Studies**

In experiments which used  $\alpha$ -methylbenzylaminobenzotriazole as an inhibitor of (S)-nicotine metabolism, concentrations of 1  $\mu\text{M}$  and 2.5  $\mu\text{M}$  were employed. Dilutions of a 10 mM  $\alpha$ -methylbenzylaminobenzotriazole stock solution prepared in methanol were made and appropriate volumes of this solution were transferred such that 0.4 or 1 nmoles of the inhibitor were delivered to the sample tubes. Methanol was evaporated with a gentle stream of nitrogen prior to the addition of other components of the incubation mixture. The incubation mixtures were preincubated with this inhibitor for 30 min at 37°C prior to the addition of (S)-nicotine (100  $\mu\text{M}$ ). Samples were processed for HPLC analysis as described above. Each condition was performed a minimum of three times.

#### **The Effect of MI Complex Formation on the Lung Microsomal Oxidation of (S)-Nicotine**

The metabolic intermediate complex inhibitors N-hydroxyamphetamine (667  $\mu\text{M}$ ) or norbenzphetamine (100  $\mu\text{M}$ ) were preincubated with lung microsomes isolated from untreated New Zealand White rabbits (4 mg/ml). The concentrations used in these experiments were derived from studies which established maximal rates of MI complex formation.<sup>35</sup> For maximal inhibition, these compounds were preincubated with NADPH (0.8 mM) and lung microsomes for 30 min at room temperature. Microsomes treated in this manner were subsequently transferred to incubation tubes, which included the components/cofactors necessary for cytochrome P-450 monooxygenase activity. The

resulting incubation mixture containing 1 mg/ml of the preincubated lung microsomes, were incubated with (S)-nicotine (100  $\mu$ M) for an additional 20 min at 37°C.

#### **Radiochemical Analysis**

Radiochemical analysis of (S)-5-<sup>3</sup>H-nicotine and its metabolites was accomplished by utilizing a radioactivity flow detector (Model Flo-one\betaeta, Radiomatic Instruments and Chemical Co. Inc., Tampa, FL) linked post column to a reversed phase HPLC system described below. Flow rates for HPLC and the Flo-Scint II scintillation fluid were 1 and 3 ml/min, respectively. Updates were obtained at 6 sec intervals. The radioactivity flow detector employed a flow cell with a volume of 0.2 ml. Approximately 0.5  $\mu$ Ci of (S)-5-<sup>3</sup>H-nicotine equivalents were injected onto the HPLC-flow detector system.

#### **Reversed Phase HPLC Analysis**

To characterize better the metabolite profile of (S)-nicotine following lung microsomal incubations, an analytical system which utilized reversed phase HPLC with radiochemical detection was developed. The analytical system used for much of the work described earlier consisted of a normal phase silica HPLC column with a mobile phase of 0.5-1.0% n-propylamine in acetonitrile. This analytical system is an effective and simple method for separating (S)-nicotine from its 5'-carbon oxidation products (S)-nicotine  $\Delta^{1',5'}$ -iminium ion and (S)-cotinine, but is not appropriate for measuring the N'-oxide or nornicotine, two of the quantitatively important metabolites of (S)-nicotine. Since silica is deactivated in water, this bonded phase, which is used in the normal phase HPLC method, is inappropriate for analyzing polar compounds (i.e. Nicotine N'-oxide) which partition into the aqueous phase. Furthermore, because the chromatographic properties and the detection sensitivity for nornicotine were poor, the normal phase silica HPLC method was judged to be an inadequate method for quantitating this compound. Due to these two major limitations, a method based on C-18 reversed phase HPLC was developed to separate (S)-nicotine N'-oxide, (S)-cotinine, nornicotine

and (S)-nicotine  $\Delta^{1',5'}$ -iminium ion from the parent compound (S)-nicotine. Among the various mobile phases tried, those consisting of a mixture of a buffered aqueous phase containing triethylamine and organic solvents such as methanol and/or acetonitrile produced the best separations. Other aqueous mobile phases such as acetate buffer were not as effective and did not provide adequate resolution of the peaks. The mobile phase used for the reversed phase separation of (S)-nicotine from its major metabolites consisted of an aqueous and an organic phase in a ratio of 4:1. The aqueous phase consisted of 30 mM sodium phosphate, pH 6.5, with 0.1% triethylamine added as a modifying agent. The final pH of the buffer was adjusted to 7.0 as needed with 0.1 N NaOH. The aqueous buffer was filtered (0.2  $\mu$ m nylon) under vacuum and mixed vigorously with magnetic stirring for a period of 10-15 min to remove air bubbles. The organic phase consisted of an acetonitrile/methanol mixture in a ratio of 7:3 and was filtered under vacuum through a 0.2  $\mu$ m nylon filter. The precolumn consisted of an Alltech direct-connect precolumn assembly and a precolumn cartridge containing 5  $\mu$ m Adsorbosphere C-18. A 5  $\mu$ m C-18 Beckman Ultrasphere analytical column (25 cm x 4.6 mm) was used for the separation of (S)-nicotine and its metabolites. The flow rate was 1.0 ml/min.

Sample workup for the reversed phase HPLC analysis of (S)-nicotine metabolism by lung microsomes included the following steps: Microsomal incubations containing 1 mg microsomal protein/ml, (S)-5-<sup>3</sup>H-nicotine (100  $\mu$ M, 2.5  $\mu$ Ci) and the appropriate cofactors in a total of 0.4 ml were terminated by adding 0.4 ml acetonitrile. The quenched incubation mixture was placed on ice for approximately 30 min to precipitate microsomal proteins. The incubation mixture was carefully transferred to a 1.5 ml microfuge tube and centrifuged at 10,000 x g for 5 min. The supernatant was carefully transferred by Pasteur pipet to a plastic disposable 1 ml tuberculin syringe fitted with a disposable Micron Separations filter (3 mm, 0.22  $\mu$ m

Nylon 66) and filtered. A volume of 0.1 ml of the resulting filtrate was injected onto the HPLC system and analyzed by a Flo-One $\beta$  radiochemical flow detector.

### Enzymatic Assays

In order to estimate the aldehyde oxidase activity present in lung 100,000 x g soluble fraction, oxidation of 3-aminocarbonyl-1-methylpyridinium ion (5 mM) was measured. 3-Aminocarbonyl-1-methylpyridinium ion (N-methylnicotinamide, NMN), a pyridinium compound, is metabolized by liver aldehyde oxidase principally at the C-2 carbon atom to yield the corresponding 2-pyridone derivative.<sup>46</sup> Lung and liver 100,000 x g soluble fraction isolated from untreated New Zealand White rabbits (1 mg protein) were added separately to quartz cuvettes containing 1 mM EGTA and 0.1 M sodium phosphate buffer, pH 7.4, in a volume of 1 ml. NMN was added to the cuvette to yield a final concentration of 5 mM. Upon addition of NMN, the solution was mixed carefully by resuspension with a pasteur pipet. Aldehyde oxidase catalyzed oxidation of NMN was measured by monitoring the increase in absorbance at 300 nm ( $\lambda_{max}$  for the 2-pyridone derivative) over a period of 1 hr at 37°C in a DU-50 UV/VIS spectrophotometer. Since the buffers used to prepare the lung 100,000 x g soluble fraction differed from those used to prepare the liver soluble fraction, control studies were performed in order to test whether heparin or glycerol influence the oxidation of NMN, which proved not to be the case.

Similar incubations were used to evaluate the effect of these preparations on the oxidative metabolism of (S)-nicotine  $\Delta^{1',5'}$ -iminium ion. Following incubations in a metabolic shaker for various periods of time, metabolism was quenched by adding an equal volume of ice-cold 1 M  $K_2CO_3$ . The internal standard, N-methyl-N-(3-pyridyl)methylpropionamide, was added to the quenched mixture. The quenched mixture containing (S)-nicotine  $\Delta^{1',5'}$ -iminium ion and the product (S)-cotinine were extracted with methylene chloride and assayed by normal phase silica HPLC with UV detection at 260 nm. (S)-Nicotine  $\Delta^{1',5'}$ -iminium ion and (S)-cotinine were

quantitated by determining the peak height ratio of each compound to the internal standard and determining the corresponding amounts from a calibration curve constructed from known concentrations of each component and the internal standard.

Cytochrome P-450 content was determined by the method of Estabrook *et al.*<sup>47</sup> Benzphetamine N-demethylation was determined by quantitating the amount of formaldehyde produced in 15 min at 37°C with the Nash assay.<sup>48</sup> A Beckman DU-50 with Data capture software was used for this determination. 7-Ethoxyresorufin O-deethylase activity was measured by quantitating the amount of resorufin produced in a 5-10 min incubation at 25°C using the method of Burke *et al.*<sup>49</sup> A Perkin Elmer 650-40 Fluorescence spectrophotometer (Norwalk, CT) was used for the determination of ethoxyresorufin O-deethylase activity.

#### **Covalent Binding of (S)-5-<sup>3</sup>H-Nicotine to Rabbit Microsomal Protein**

To estimate the extent of covalent binding, (S)-5-<sup>3</sup>H-nicotine (40 nmoles, 2.5 µCi) was incubated with the appropriate cofactors required for cytochrome P-450 monooxygenase activity (see above) and lung microsomes isolated from untreated or Aroclor 1260 pretreated rabbits in a total volume of 0.4 ml. In studies which utilized  $\alpha$ -methylbenzylaminobenzotriazole, the method which employed this inhibitor was used except that (S)-5-<sup>3</sup>H-nicotine was substituted. In studies which used liver or lung 100,000 x g soluble fraction, 40 µl of a 1 mg/ml solution was added to a 0.4 ml incubation volume yielding a final concentration of 0.1 mg/ml. Metabolic incubations containing (S)-5-<sup>3</sup>H-nicotine were terminated by adding 4 ml of 20% trichloroacetic acid in H<sub>2</sub>O (w/v). The precipitated sample was vortexed for 5 min, centrifuged and the supernatant removed. This step was repeated a total of three times. This step was followed by washing the precipitate three times with 70% methanol (4 ml each). Finally, the protein was washed with 100% methanol until no radioactivity could be detected in the solvent wash. To the final protein pellet was added 1N NaOH (1 ml); this

mixture was heated at 50°C overnight. The hydrolyzed protein mixture was neutralized with 0.25 ml of 4 N HCl. The neutralized solution (0.5 ml) was counted using a Packard Trias, PLD Tri-Carb liquid scintillation counter. A portion of the remaining solution (0.1 ml) was assayed for protein by the method of Lowry.<sup>50</sup>

#### **Analysis of the Lung Microsomal Metabolite of (S)-Nicotine by GC-EIMS**

To facilitate the identification of ions derived from (S)-nicotine, a 1:1  $d_0$  and 3',3'  $d_2$  mixture of (S)-nicotine (100  $\mu$ M) was incubated with rabbit lung microsomes (2 mg/ml) for 30 min. The methylene chloride extract was purified by HPLC and the fraction corresponding to the unknown metabolite was extracted back into aqueous 1 M  $H_2SO_4$ . The pH of the acidic aqueous layer was raised to alkaline pH with 50%  $K_2CO_3$  and the resulting solution was extracted with toluene/butanol 9:1 (0.3 ml). The conditions for GC-EIMS analysis are described in greater detail in the Materials and Methods section of Chapter V.



- 
1. DePierre, J.W. and L. Ernster, "The metabolism of polycyclic hydrocarbons and its relationship to cancer," *Biochim. Biophys. Acta.* **473**, 149-186 (1978).
  2. Boyd, M.R., "Biochemical mechanisms in chemical induced lung injury: Roles of metabolic activation," *CRC Crit. Rev. Toxicol.* **9**, 103-176 (1980).
  3. Grover, P.L. and P. Sims, "Enzyme-catalyzed reactions of polycyclic hydrocarbons with deoxyribonucleic acid and protein *in vitro*," *Biochem. J.* **110**, 159-160 (1969).
  4. Guengerich, F.P., "Preparation and properties of highly purified cytochrome P-450 and NADPH cytochrome P-450 reductase from pulmonary microsomes of untreated rabbits," *Mol. Pharmacol.* **13**, 911-923 (1977).
  5. Hook, G.E.R., J.R. Bend, D. Hoel, J.R. Fouts and T.E. Gram, "Preparation of lung microsomes and a comparison of the distribution of enzymes between subcellular fractions of rabbit lung and liver," *J. Pharmacol. Exp. Ther.*, **182**, 474-490 (1972).
  6. Oppelt, W.W., M. Zange, W.E. Ross and H. Remmer, "Comparison of microsomal drug hydroxylation in lung and liver of various species," *Res. Commun. Chem. Pathol. Pharmacol.* **1**, 43-56 (1970).
  7. Liem, H.H., U. Muller-Eberhard and E.F. Johnson, "Differential induction by 2,3,7,8-tetrachlorodibenzo-p-dioxin of multiple forms of rabbit microsomal cytochrome P-450: Evidence for tissue specificity," *Mol. Pharmacol.* **18**, 565-570 (1980).
  8. Wolf, C.R., M.M. Szutowski, L.M. Ball and R.M. Philpot, "The rabbit pulmonary monooxygenase system: Characteristics and activities of two forms of pulmonary cytochrome P-450," *Chem-Biol. Interact.* **21**, 29-43 (1978).
  9. Slaughter, S.R., C.R. Wolf, J.P. Marciniszyn and R.M. Philpot, "The rabbit pulmonary monooxygenase system: Partial structural characterization of the cytochrome P-450 components and comparison to the hepatic cytochrome P-450," *J. Biol. Chem.* **256**, 2499-2503 (1981).
  10. Serabjit-Singh, C.J., C.R. Wolf, G.C. Plopper and R.M. Philpot, "Cytochrome P-450: Localization in rabbit lung," *Science* **207**, 1469-1470 (1980).
  11. Serabjit-Singh, C.J., C.R. Wolfe and R.M. Philpot, "The rabbit pulmonary monooxygenase system: Immunochemical and biochemical characterization of the enzyme components," *J. Biol. Chem.* **254**, 9901-9907 (1979).
  12. Serabjit-Singh, C.J., P.W. Albro, I.G.C. Robertson and R.M. Philpot, "Interactions between xenobiotics that increase or decrease the levels of cytochrome P-450 isozymes in rabbit lung and liver," *J. Biol. Chem.* **258**, 12827-12834 (1983).
  13. Wolf, C.R., B.R. Smith, L.M. Ball, C. Serabjit-Singh, J.R. Bend and R.M. Philpot, "The rabbit pulmonary monooxygenase system: Catalytic differences between two purified forms of cytochrome P-450 in the metabolism of benzo(a)pyrene," *J. Biol. Chem.* **254**, 3658-3663 (1979).

- 
14. Robertson, I.G.C., R.M. Philpot, E. Zeiger and C.R. Wolf, "Specificity of rabbit pulmonary cytochrome P-450 isozymes in the activation of several aromatic amines and aflatoxin B1," *Mol. Pharmacol.* **20**, 662-668 (1981).
  15. Williams, D.E., S.E. Hale, A.S. Muerhoff and B.S.S. Masters, "Rabbit lung flavin-containing monooxygenase. Purification, characterization, and induction during pregnancy," *Mol. Pharmacol.* **28**, 381-390 (1985).
  16. Poulsen, L.L., K. Taylor, D.E. Williams, B.S.S. Masters and D.M. Ziegler, "Substrate specificity of the rabbit lung flavin-containing monooxygenase for amines: Oxidation products of primary alkylamines," *Mol. Pharmacol.* **30**, 680-685 (1986).
  17. Devereux, T.R. and J.R. Fouts, "Effect of pregnancy or treatment with certain steroids on N,N-dimethylaniline demethylation and N-oxidation by rabbit liver or lung microsomes," *Drug Metab. Dispos.* **3**, 254-258 (1975).
  18. Williams, D.E., D.M. Ziegler, D.J. Nordin, S.E. Hale and B.S.S. Masters, "Rabbit lung flavin-containing monooxygenase is immunochemically and catalytically distinct from the liver enzyme," *Biochem. Biophys. Res. Comm.* **125**, 116-122 (1984).
  19. Falzon, M., J.B. McMahon, A.F. Gadzar and H.M. Schuller, "Preferential metabolism of N-nitroso diethylamine by two cell lines derived from human pulmonary adenocarcinomas," *Carcinogenesis* **7**, 17-22 (1986).
  20. Boyd, M.R. and H.M. Reznik-Schuller, "Metabolic basis for the pulmonary Clara cell as a target for pulmonary carcinogenesis," *Toxicol. Pathol.* **12**, 56-61 (1984).
  21. Falzon, M., J.B. McMahon and H.M. Schuller, "Xenobiotic metabolizing enzyme activity in human non-small-cell derived lung cancer cell lines," *Biochem. Pharmacol.* **35**, 563-568. (1986).
  22. Armitage, A.K., C.T. Dollery, C.F. George, T.H. Houseman, P.J. Lewis and D.M. Turner, "Absorption and metabolism of nicotine from cigarettes," *Br. Med. J.* **4**, 313-316 (1975).
  23. Turner, D.M., A.K. Armitage, R.H. Briant and C.T. Dollery, "Metabolism of nicotine by the isolated perfused dog lung," *Xenobiotica* **5**, 539-551 (1975).
  24. McGovren, J.P., W.C. Lubawy and H.B. Kostenbauder, "Uptake and metabolism of nicotine by the isolated perfused rabbit lung," *J. Pharmacol. Exp. Ther.* **199**, 198-207 (1976).
  25. Booth, J. and E. Boyland, "Enzymatic oxidation of (-)-nicotine by guinea-pig tissues *in vitro*," *Biochem. Pharmacol.* **20**, 407-415 (1971).
  26. Boyd, M.R., "Evidence for the Clara cell as a site of cytochrome P-450 dependent mixed-function oxidase activity in lung," *Nature (London)* **269**, 713-715 (1977).

- 
27. Nakayama, H., T. Nakashima and Y. Kurogochi, "Cytochrome P-450-dependent nicotine oxidation by liver microsomes of guinea pigs: Immunochemical evidence with antibody against phenobarbital-inducible cytochrome P-450," *Biochem. Pharmacol.* **34**, 2281-2286 (1985).
  28. Rüdell, U., H. Foth and G.F. Kahl, "Eightfold induction of nicotine elimination in perfused rat liver by pretreatment with phenobarbital," *Biochem. Biophys. Res. Commun.* **148**, 192-198 (1987).
  29. Nakayama, H., T. Nakashima and Y. Kurogochi, "Participation of cytochrome P-450 in nicotine oxidation," *Biochem. Biophys. Res. Comm.* **108**, 200-205 (1982).
  30. Nakayama, H., T. Nakashima and Y. Kurogochi, "Heterogeneity of hepatic nicotine oxidase," *Biochim. Biophys. Acta* **715**, 254-257 (1982).
  31. Buening, M.K. and M.R. Franklin, "SKF 525-A inhibition, induction, and 452-nm complex formation," *Drug Metab. Dispos.* **4**, 244-255 (1976).
  32. The Chemistry of Pyrroles (R.A. Jones and G.P. Bean, Eds.) In the Series: Organic Chemistry. A series of monographs. Vol. 34, Academic Press, London (1977).
  33. Mathews, J.M. and J.R. Bend, "N-alkylaminobenzotriazoles as isozyme-selective suicide inhibitors of rabbit pulmonary microsomal cytochrome P-450," *Mol. Pharmacol.* **30**, 25-32 (1986).
  34. Mansuy, D., P. Gans, J.-C. Chottard and J.F. Bartoli, "Nitrosoalkanes as Fe (II) ligands in the 455 nm absorbing cytochrome P-450 complexes formed from nitroalkanes in reducing conditions," *Eur. J. Biochem.* **76**, 607-615 (1977).
  35. Franklin, M.R., C.R. Wolf, C. Serabjit-Singh and R.M. Philpot, "Quantitation of two forms of pulmonary cytochrome P-450 in microsomes, using substrate specificities," *Mol. Pharmacol.* **17**, 415-420 (1980).
  36. Ziegler, D.M. and L.L. Poulson, "Hepatic microsomal mixed-function amine oxidase," In: *Methods in Enzymology*, (S. Fleischer and L. Packer, Eds.) Vol. 52, pp. 142-151 Academic Press, New York (1978).
  37. Brandange, S. and L. Lindbloom, "The enzyme "aldehyde oxidase" is an iminium oxidase. Reaction with nicotine  $\Delta^{1'-(5)}$  iminium ion," *Biochem. Biophys. Res. Comm.* **91**, 991-996 (1979).
  38. Lindquist N.G. and S. Ullberg, "Autoradiography of intravenously injected  $^{14}\text{C}$ -nicotine indicates long-term retention in the respiratory tract," *Nature* **248**, 600-601 (1974).
  39. Waddell, W. and C. Marlowe, "Localization of nicotine- $^{14}\text{C}$  cotinine- $^{14}\text{C}$  and nicotine 1'-N-oxide- $^{14}\text{C}$  in tissues of the mouse," *Drug Metab. Dispos.* **4**, 530-539 (1976).
  40. Szüts, T., S. Olsson, N.G. Lindquist, S. Ullbert, A. Pilotti and C. Enzell, "Long-term fate of [ $^{14}\text{C}$ ]Nicotine in the mouse: Retention in the bronchi, melanin-containing tissues and urinary bladder wall," *Toxicology* **10**, 207-220 (1978).

- 
41. Lu, A.Y.H. and S.B. West, "Multiplicity of mammalian microsomal cytochromes P-450," *Pharmacol. Rev.* **31**, 277-295 (1980).
  42. Peterson, L., A.J. Trevor and N. Castagnoli Jr., "Stereochemical studies on the cytochrome P-450 catalyzed oxidation of (S)-nicotine to the (S)-nicotine- $\Delta^{1'(5')}$ -iminium species," *J. Med. Chem.* **30**, 249-254 (1987).
  43. Taylor, E.C. and N.E. Boyer, "Pyridine-1-oxides. IV. Nicotine-1-oxide, nicotine-1'-oxide, and nicotine 1,1'-dioxide," *J. Org. Chem.* **24**, 275-277 (1959).
  44. Bowman, E.R. and H. McKennis Jr., "(-)-Cotinine," *Biochem. Prep.* **10**, 36-39 (1963).
  45. Nguyen, T.L. and N. Castagnoli, Jr., "The syntheses of deuterium labelled tobacco alkaloids: Nicotine, nor nicotine and cotinine," *J. Labelled compds.* **14**, 919-934 (1978).
  46. Felsted, R.L., A.E.-Y. Chu and S. Chaykin, "Purification and properties of the aldehyde oxidases from hog and rabbit livers," *J. Biol. Chem.* **248**, 2580-2587 (1973).
  47. Estabrook, R.W., J. Peterson, J. Baron and A. Hildebrandt, "The spectrophotometric measurement of turbid suspension of microsomes associated with drug metabolism," *Methods Pharmacol.* **2**, 303-350 (1972).
  48. Nash, T., "The colorimetric estimation of formaldehyde by means of the Hantzsch reaction," *Biochem. J.* **55**, 416-421 (1953).
  49. Burke, M.D. and R.T. Mayer, "Ethoxyresorufin: Direct fluorometric assay of a microsomal O-deethylation which is preferentially inducible by 3-methylcholanthrene," *Drug Metab. Disp.* **2**, 583-588 (1974).
  50. Lowry, O.H., N.J. Rosebrough, A.L. Farr and R.J. Randall, "Protein measurement with the Folin phenol reagent," *J. Biol. Chem.* **193**, 265-275 (1951).

**Chapter V**  
**Monoamine Oxidase B**  
**and (S)-Nicotine  $\Delta^{1',5'}$ -Iminium Ion:**  
**Identification of  $\beta$ -Nicotyrine as a**  
 **$\Delta^{1',5'}$ -Iminium Ion Derived Metabolite**

## Introduction

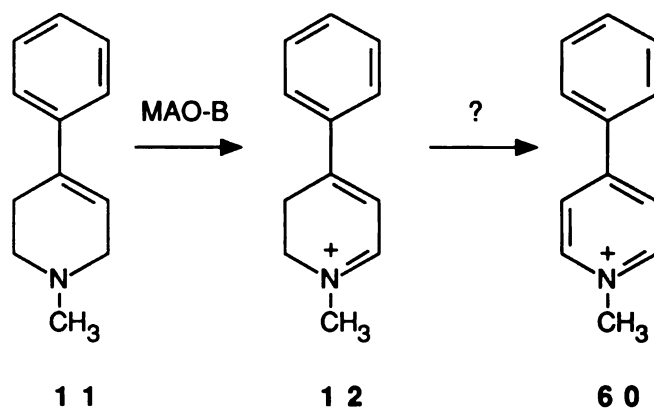
A number of epidemiological studies has shown an inverse correlation between smoking and Parkinson's disease.<sup>1,2</sup> For example, a study of 300,000 United States military veterans showed that the risk of death from Parkinson's disease was significantly lower in smokers and ex-smokers than in nonsmokers.<sup>3</sup> The factor(s) responsible for the decreased incidence of Parkinson's disease in smokers is not known. Several hypotheses to explain this inverse correlation include changes in pre-morbid behavior or selective mortality in individuals who smoke. It has also been proposed that (S)-nicotine could be an agent responsible for inhibiting the progress of this disease.<sup>4</sup> However, none of the epidemiological findings to date have provided strong evidence to support these hypotheses.

1-Methyl-4-phenyl-1,2,3,6-tetrahydropyridine (MPTP, 11), a tertiary allylamine (Scheme V.1), is bioactivated by MAO-B to species capable of irreversibly lesioning the cells of the substantia nigra and of producing symptoms such as rigidity and tremor which are characteristic of idiopathic Parkinson's disease.<sup>5</sup> The metabolic activation of MPTP (11) to the ultimate neurotoxic species MPP<sup>+</sup> (60) proceeds via an initial two electron oxidation catalyzed by MAO-B which yields the corresponding dihydropyridinium species MPDP<sup>+</sup> (12). The further two electron oxidation of MPDP<sup>+</sup> yields MPP<sup>+</sup> in a process which is not well characterized. Bioaccumulation of MPP<sup>+</sup> by the dopaminergic neurons results in irreversible cell damage and loss of neuronal function. Thus, the MAO-B catalyzed oxidation of MPTP is necessary for the expression of neurotoxicity in MPTP-induced Parkinsonism.

The etiology of Parkinson's disease is not known. It is possible, however, that this disease is caused by foreign or endogenous compounds which resemble MPTP and which require the catalytic activity of MAO-B to produce the neurotoxic species which lesion the nigrostriatal neurons. Evidence consistent with such a proposal include the recent demonstration that an inhibitor of MAO-B activity, Deprenyl, is effective in

slowing the progress of this disease in individuals who are in the early stages of its development.<sup>6</sup> Thus, the inhibition of MAO-B by various compounds, including those present in tobacco, could slow the progress of this disease by preventing the conversion of a putative protoxin to the ultimate neurotoxic species. In one recent study, platelet MAO-B activity was shown to be much lower in heavy cigarette smokers compared to platelet MAO-B activity of control subjects.<sup>7</sup> In this same report, *in vivo* administration of the tobacco component hydrazine protected the dopaminergic nigrostriatal neurons of mice from MPTP-induced damage.

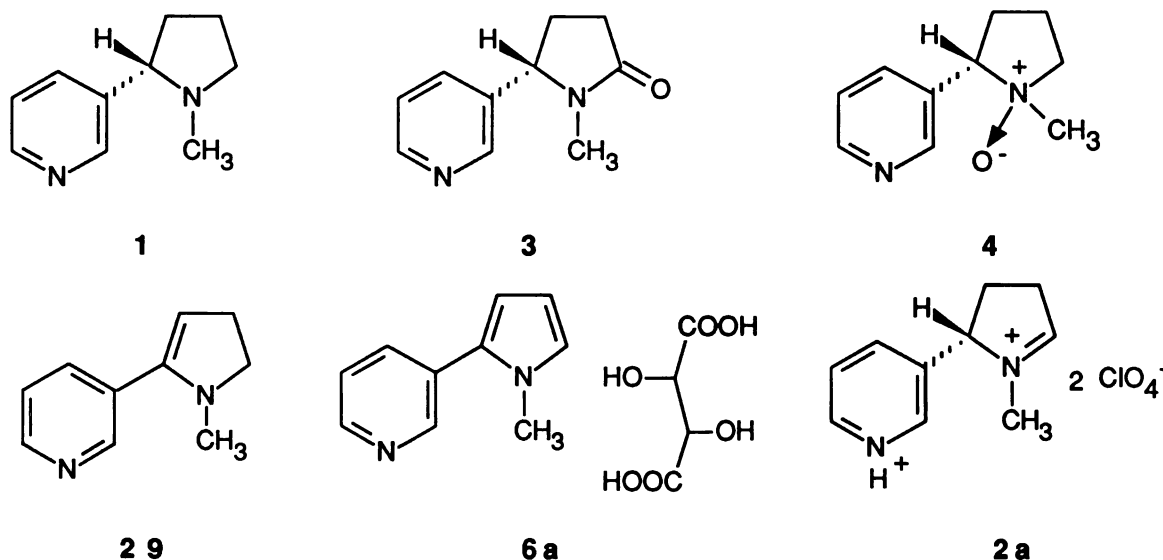
The strong epidemiological evidence linking smoking to a lower incidence of Parkinson's disease together with the known Parkinson's inducing effects of MPTP have prompted us to investigate the inhibitory properties of (S)-nicotine and its key metabolites on the bioactivation of MPTP by semipurified MAO-B. In the present study, evidence is presented for the inhibition of the MAO-B catalyzed oxidation of MPTP by the principal intermediary metabolite of (S)-nicotine, (S)-nicotine  $\Delta^{1',5'}$ -iminium ion, the two electron oxidation product of (S)-nicotine formed from a reaction catalyzed by cytochrome P-450. In addition, we have demonstrated that this electrophilic intermediate is converted to  $\beta$ -nicotyrine in the presence of MAO-B in a time and enzyme concentration dependent process which is inhibited by pargyline. The metabolism of (S)-nicotine to  $\beta$ -nicotyrine by rabbit liver enzymes has been reported previously.<sup>8</sup> In the present report, evidence is presented for the enzymatic conversion of (S)-nicotine  $\Delta^{1',5'}$ -iminium ion to  $\beta$ -nicotyrine by semipurified MAO-B. The identification of (S)-nicotine  $\Delta^{1',5'}$ -iminium ion as a substrate for MAO-B implicates enamines, which in the present case exist in equilibrium with the isoelectronic iminium species, as a new class of substrates for this enzyme.



Scheme V.1

## Results

### Effects of (S)-Nicotine and Related Compounds on the MAO-B Catalyzed Oxidation of MPTP



The effects of (S)-nicotine (1), (S)-cotinine (3), (S)-nicotine N'-oxide (4), myosmine (29),  $\beta$ -nicotyrine tartrate (6a) and (S)-nicotine  $\Delta^{1',5'}$ -iminium bisperchlorate (2a) on the MAO-B catalyzed oxidation of MPTP were examined. Preincubation of (S)-nicotine, (S)-cotinine and (S)-nicotine N'-oxide with MAO-B, at a concentration of 0.5 mM each, had no effect on MPTP oxidation (Table V.1). The



Table V.1

## Inhibition of the MAO-B Catalyzed Oxidation of MPTP by Various Agents.

Compound	[mM]	% Control $\pm$ S.E.
Control	—	100.0 $\pm$ 1.8
(S)-Nicotine	0.5	93.8 $\pm$ 1.5
(S)-Cotinine	0.5	96.2 $\pm$ 0.7
(S)-Nicotine N'-oxide	0.5	100.1 $\pm$ 1.1
$\beta$ -Nicotyrine tartrate	0.5	84.8 $\pm$ 1.6
Myosmine	0.5	86.9 $\pm$ 1.5
(S)-Nicotine $\Delta^{1',5'}$ -iminium <i>bis</i> perchlorate	0.5	51.0 $\pm$ 1.4
Sodium perchlorate	1.0	104.1 $\pm$ 5.4
Sodium tartrate	0.5	101.4 $\pm$ 1.4

Each compound was preincubated with 0.02 units of MAO-B at 30°C for 15 min in 0.2% Triton/0.05 M sodium phosphate, pH 7.2, prior to the addition of MPTP. Upon addition of MPTP (3.2 mM) to the cuvettes containing the enzyme and compound, formation of MPDP<sup>+</sup> was determined by monitoring the increase in absorbance at 343 nm. All values are expressed as a percentage of MPTP oxidation observed in the absence of added compound. N = 3 for all determinations.

minor tobacco alkaloids  $\beta$ -nicotyrine and myosmine inhibited the MAO-B catalyzed oxidation of MPTP by <16%. In contrast, preincubation of 0.5 mM (S)-nicotine  $\Delta^{1',5'}$ -iminium *bis*perchlorate with semipurified MAO-B led to a 50% decrease in the rate of oxidation of MPTP to MPDP<sup>+</sup>. Sodium perchlorate at a concentration of 0.5 mM did not exhibit any inhibitory effects on this enzymatic reaction.

### Time and Concentration Dependent Inhibition of the MAO-B Catalyzed Oxidation of MPTP by (S)-Nicotine $\Delta^{1',5'}$ -iminium Ion

Preincubation of (S)-nicotine  $\Delta^{1',5'}$ -iminium *bis*perchlorate with semipurified MAO-B for periods ranging from 0 to 60 min, led to a preincubation time dependent decrease in the rate of MPTP oxidation (Fig.V.1A). When (S)-nicotine  $\Delta^{1',5'}$ -iminium *bis*perchlorate and MPTP were added concurrently, the initial rate of MPTP oxidation was inhibited by 12%. Preincubation of MAO-B with (S)-nicotine  $\Delta^{1',5'}$ -iminium *bis*perchlorate for 15 min inhibited the initial rate of MPTP oxidation by 53%. Extending this preincubation time beyond 15 min did not significantly inhibit further the rate of MPTP oxidation. Although the time dependent inhibition suggested the possibility of a mechanism-based inactivation, a semilog plot of MPTP oxidase activity versus time did not yield a first order kinetics plot characteristic of this type of inhibition (data not shown). (S)-Nicotine  $\Delta^{1',5'}$ -iminium *bis*perchlorate also inhibited MPTP oxidation by MAO-B in a concentration dependent manner. At a concentration of approximately 400  $\mu$ M, (S)-nicotine  $\Delta^{1',5'}$ -iminium *bis*perchlorate inhibited the initial rate of this reaction by 50% (Fig.V.1B). At an inhibitor concentration of 4 mM, MPTP oxidation was inhibited by approximately 90%.

### Enzyme Kinetics of the (S)-Nicotine $\Delta^{1',5'}$ -iminium Ion Dependent Inhibition of the MAO-B Catalyzed Oxidation of MPTP

In order to understand better the nature of the interaction between the iminium species and MAO-B, enzyme kinetic analyses were performed. These studies were prompted by the time and concentration dependent inhibition of the MAO-B catalyzed oxidation of MPTP by (S)-nicotine  $\Delta^{1',5'}$ -iminium *bis*perchlorate. In order to perform this study, various concentrations of (S)-nicotine  $\Delta^{1',5'}$ -iminium *bis*perchlorate were added to incubation mixtures containing semipurified MAO-B. These incubation mixtures were either coincubated with MPTP or preincubated for 15

min prior to the addition of this substrate. Oxidation of MPTP was monitored as described above. Results of these two analyses were evaluated by constructing double reciprocal plots of velocity (rate of MPTP oxidation) vs. substrate concentration (MPTP concentration [mM]), at inhibitor concentrations ranging from 0 to 1 mM. Analysis of this data, derived from the experiment where (S)-nicotine  $\Delta^{1',5'}$ -iminium *bis*perchlorate and MPTP were coincubated, indicated an intersection of the lines of the double reciprocal plot between the x- and y-axis. This result is consistent with the interpretation that the inhibition of the MAO-B catalyzed oxidation of MPTP by the  $\Delta^{1',5'}$ -iminium ion proceeds through a combination of competitive and noncompetitive components or linear mixed-type inhibition<sup>9</sup> (Fig.V.2A). Preincubation of the inhibitor with the enzyme for 15 min followed by addition of MPTP produced lines which intersected closer to the x-axis (Fig.V.2B). This shift indicates that the noncompetitive component of the linear mixed-type inhibition is preincubation time dependent. The slopes of each line (defined as  $K_m/V_{max}$ ), obtained from the double reciprocal plots described above, were also plotted as a function of the inhibitor concentration [(S)-nicotine  $\Delta^{1',5'}$ -iminium *bis*perchlorate]. The  $K_i$  values, which were calculated from the absolute value obtained from the x-axis intersection of the  $K_m/V_{max}$  vs [(S)-nicotine  $\Delta^{1',5'}$ -iminium *bis*perchlorate (mM)] plot, were estimated to be 1.1 mM and 375  $\mu$ M for the coincubation and preincubation conditions, respectively (Fig.V.2 Inset). These results are in accord with the preincubation time dependent inhibition described in Fig V.1A. Similar studies employing benzylamine as the substrate produced qualitatively similar results (Fig.V.3), indicating a generalized inhibitory effect of (S)-nicotine  $\Delta^{1',5'}$ -iminium *bis*perchlorate on the catalytic activity of MAO-B.

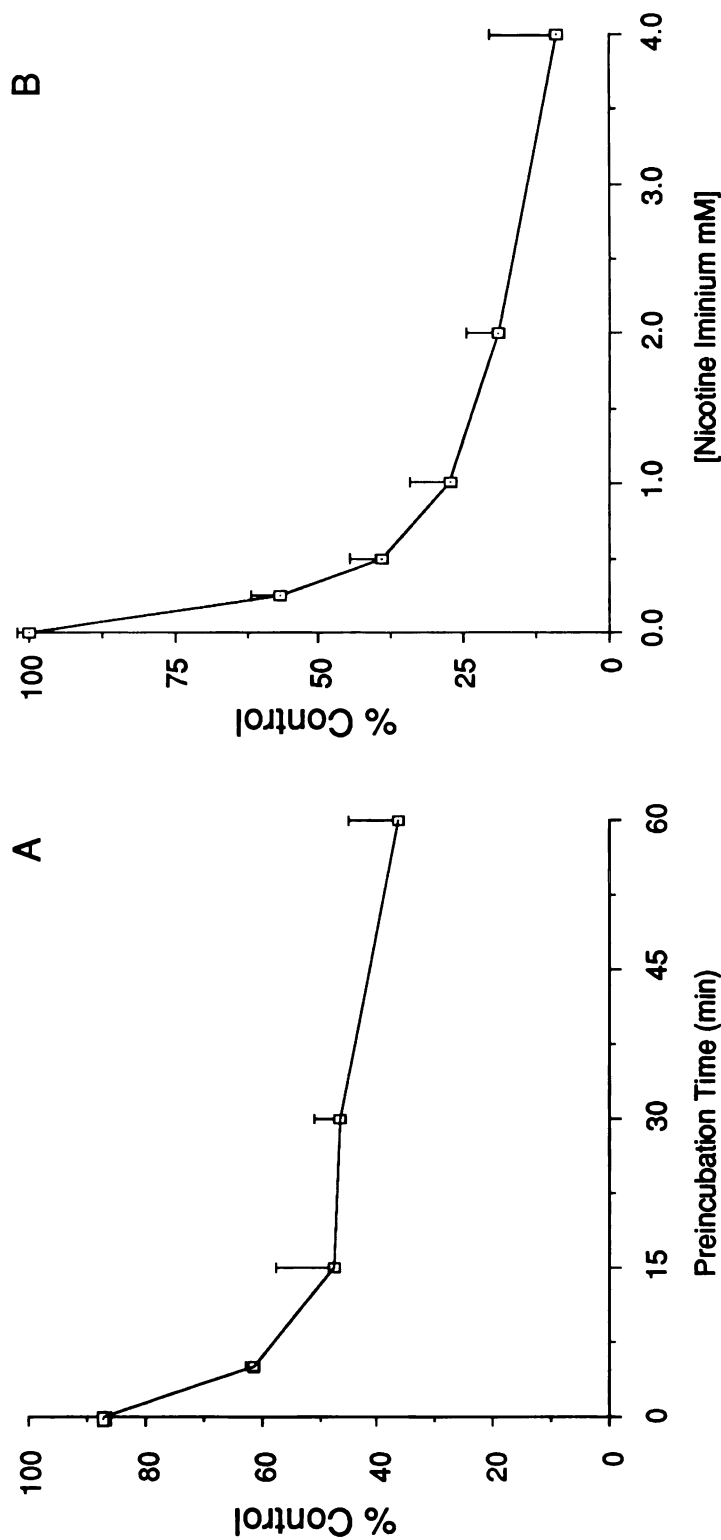


**Fig.V.1 A and B.** Preincubation Time Dependent and Concentration Dependent Inhibition of the MAO-B catalyzed Oxidation of MPTP by (S)-Nicotine  $\Delta^{1',5'}$ -iminium *Bis perchlorate*. (A). (S)-Nicotine  $\Delta^{1',5'}$ -iminium *bis perchlorate* (0.5 mM) was preincubated with 0.02 units of MAO-B for the time period indicated and the initial rates of MPTP (3.2 mM) metabolism compared. (B). (S)-Nicotine  $\Delta^{1',5'}$ -iminium *bis perchlorate* was preincubated for 15 min with 0.02 units of enzyme at the concentrations indicated above prior to the addition of MPTP (3.2 mM)

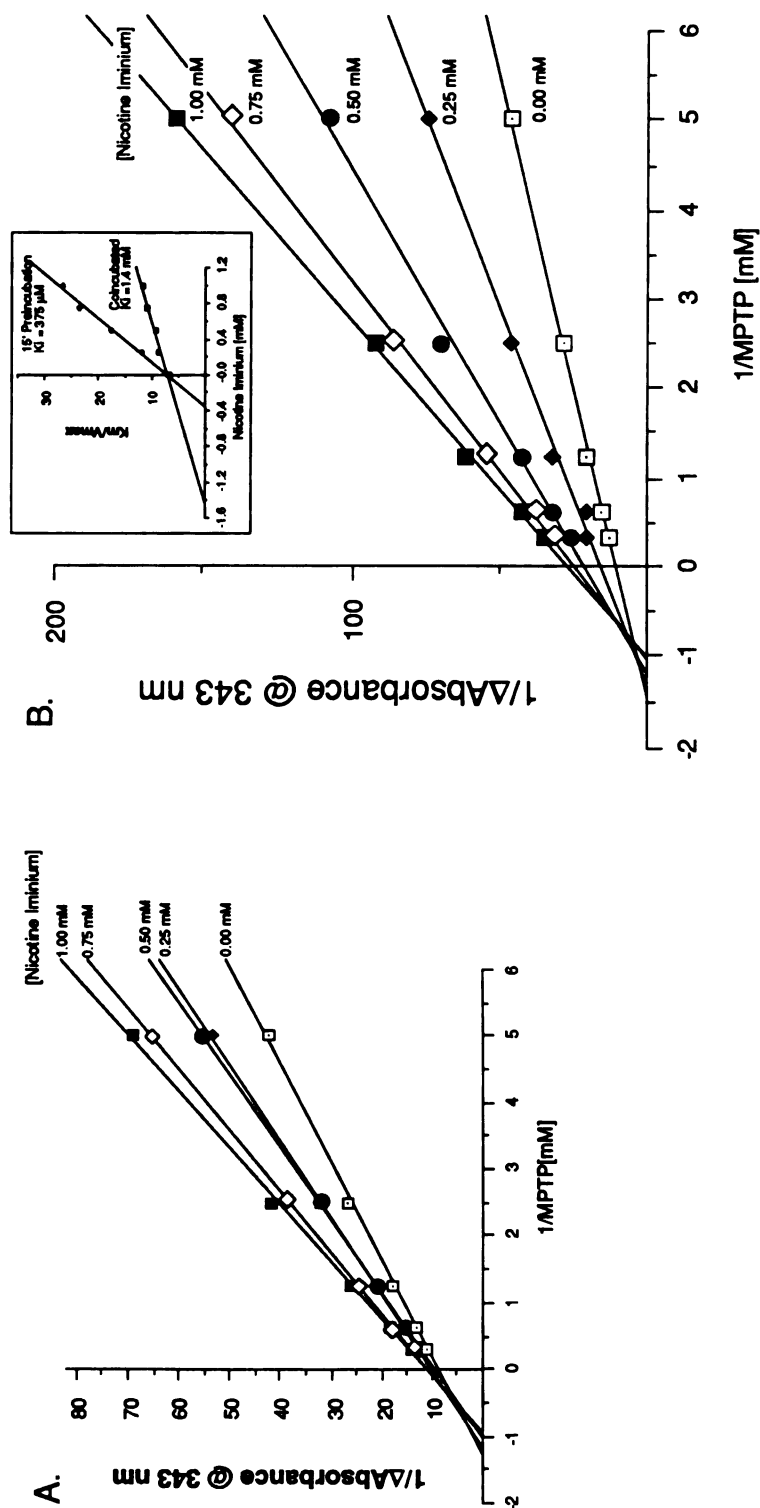


**Fig. V.2 A and B.** Enzyme Kinetic Analyses of the (S)-Nicotine  $\Delta^{1',5'}$ -Iminium Ion Dependent Inhibition of the MAO-B Catalyzed Oxidation of MPTP. (A). Coincubation of inhibitor with MPTP. (B). Preincubation of inhibitor for 15' at 30°C prior to the addition of MPTP. (Inset). Estimation of  $K_i$  for the conditions (A) and (B).

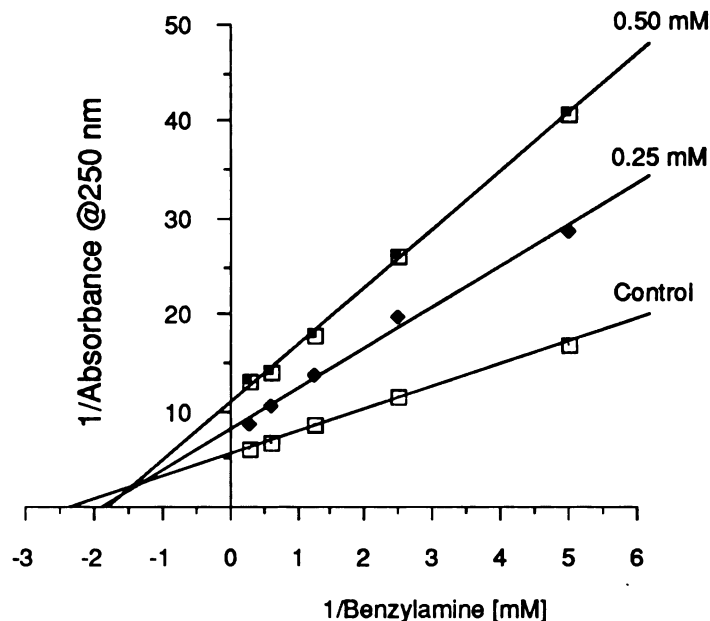


**Fig.V.3** Enzyme Kinetic Analysis of the (S)-Nicotine  $\Delta^{1',5'}$ -Iminium *bis*perchlorate Dependent Inhibition of the MAO-B Catalyzed Oxidation of Benzylamine

The results of these experiments indicate that (S)-nicotine  $\Delta^{1',5'}$ -iminium *bis*perchlorate inhibits the MAO-B catalyzed oxidation of MPTP by at least two different mechanisms. The competitive component of the linear mixed-type inhibition observed above could be due to the (S)-nicotine  $\Delta^{1',5'}$ -iminium ion occupying the MPTP binding site in the catalytic domain of MAO-B. The noncompetitive component of the linear mixed-type inhibition may be due to a covalent modification of MAO-B by (S)-nicotine  $\Delta^{1',5'}$ -iminium ion. Such a modification could alter the catalytic activity of this enzyme by binding to sites which alter its conformation.

#### **Inhibition of MAO-B Activity by Phencyclidine Iminium Ion**

In order to address whether iminium ion species, in general, inhibit MAO-B activity, the inhibitory effect of phencyclidine iminium perchlorate was examined. Phencyclidine iminium perchlorate (0.5 mM), preincubated for 15 min with MAO-B,

inhibited the catalytic activity of this enzyme better than that observed with (S)-nicotine  $\Delta^{1',5'}$ -iminium ion (Table V.2). The phencyclidine iminium ion inhibited the oxidation of MPTP and benzylamine by approximately 65%. For comparison, phencyclidine (PCP) itself was found to inhibit the MAO-B catalyzed oxidation of MPTP by only 13%. The  $\alpha$ -cyanoamine derivative, cyano-PCP, inhibited the oxidation of benzylamine and MPTP by 9% and 33%, respectively. The reason for the greater inhibition of MPTP oxidation by cyano-PCP is not clear. Cyanide ion derived from the cyano-PCP preparation could trap the enzymatic product of MAO-B, MPDP<sup>+</sup>, to produce the corresponding cyano-MPTP derivative which absorbs maximally at a different wavelength. This sequence of events would be consistent with the apparent inhibitory effects of cyano-PCP shown in Table V.2. Sodium cyanide, at concentrations of 1 and 10 mM inhibited the oxidation of benzylamine by 44 and 95%, respectively.

**Table V.2** Inhibition of the MAO-B Catalyzed Oxidation of MPTP and Benzylamine by Phencyclidine Iminium Perchlorate, Structurally Related Analogs and Sodium Cyanide

Compound	[mM]	% Control $\pm$ S.D.	
		MPTP	benzylamine
Control	—	100.0 $\pm$ 1.4	100.0 $\pm$ 1.1
Phencyclidine (PCP)	0.5	86.7 $\pm$ 0.3	N.D.*
PCP iminium perchlorate	0.5	34.9 $\pm$ 0.8	35.0 $\pm$ 5.2
Cyano-PCP	0.5	67.4 $\pm$ 2.7	91.6 $\pm$ 0.3
Sodium cyanide	1.0	N.D.	66.2 $\pm$ 1.4
Sodium cyanide	10.0	N.D.	4.5 $\pm$ 0.5

Because of the poor water solubility of phencyclidine and its structural analogs DMSO was used to prepare stock solutions for each of these compounds. The amount of DMSO present in the incubation mixture (4% final concentration) did not inhibit MAO-B activity.

\*N.D. not determined; n = 3 for all determinations

The mechanism of the inhibition produced by phencyclidine iminium perchlorate was examined by enzyme kinetic analysis. The results of this analysis (Fig.V.4) suggested that the inhibition of the MAO-B catalyzed oxidation of benzylamine by phencyclidine iminium ion was noncompetitive.

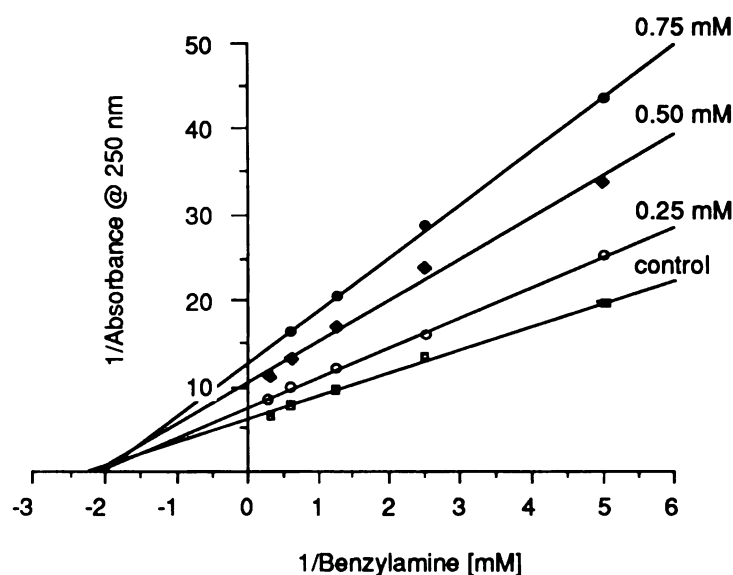


**Fig.V.4.** Enzyme Kinetic Analysis of Phencyclidine Iminium Perchlorate Inhibition of the MAO-B Catalyzed Oxidation of Benzylamine

#### Identification of $\beta$ -Nicotyrine as a MAO-B Catalyzed Oxidation Product of (S)-Nicotine $\Delta^{1',5'}$ -Iminium Ion

The enzyme kinetic analysis shown in Fig.V.2 suggested that the competitive component of the mixed-type of inhibition produced by (S)-nicotine  $\Delta^{1',5'}$ -iminium bisperchlorate could be due to its affinity for the active site of MAO-B. This possibility encouraged us to test the substrate properties of the iminium species. In order to examine this possibility, (S)-nicotine  $\Delta^{1',5'}$ -iminium bisperchlorate was incubated with semipurified MAO-B and analyzed by normal phase silica HPLC with UV detection at



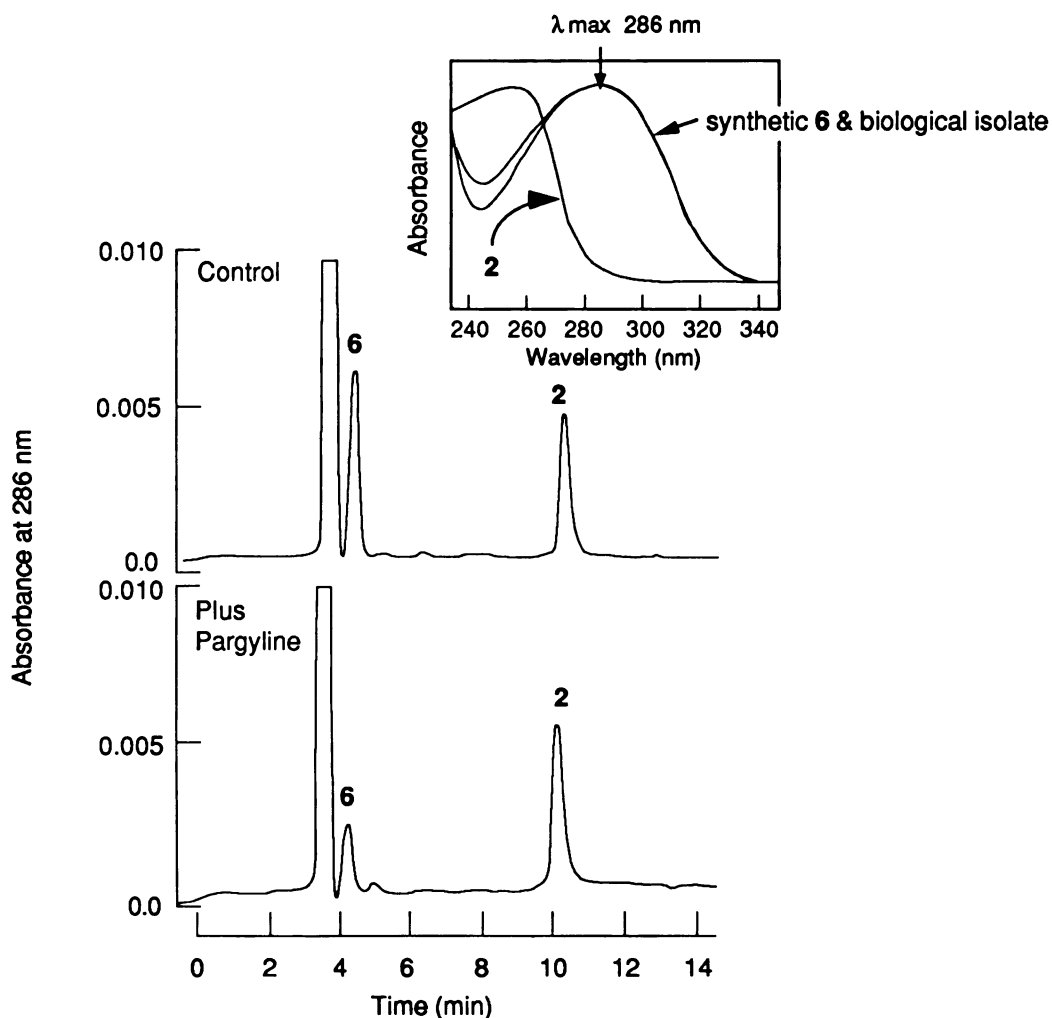


**Fig.V.5** HPLC Diode Array UV Analysis of the MAO-B Catalyzed Oxidation of (S)-Nicotine  $\Delta^{1',5'}$ -Iminium Ion *bis*perchlorate in the Presence or Absence of Pargyline (10  $\mu$ M). Inset: UV spectra of (S)-nicotine  $\Delta^{1',5'}$ -iminium ion (2), synthetic  $\beta$ -nicotyrine (6) and putative 6 derived from the MAO-B catalyzed oxidation of 2.

260 nm. The results of this analysis revealed a peak eluting near the solvent front (retention time=4.2 min) consistent with a compound possessing less polar characteristics compared to the  $\Delta^{1',5'}$ -iminium species. HPLC diode array UV analysis of this peak produced a UV absorbance spectrum exhibiting a  $\lambda_{max}$  at 286 nm, similar to that reported for the tobacco alkaloid  $\beta$ -nicotyrine.<sup>10</sup> The HPLC retention time and diode array UV spectral characteristics of synthetic  $\beta$ -nicotyrine were essentially identical to this metabolite. Capillary GC electron impact mass spectral analysis of this

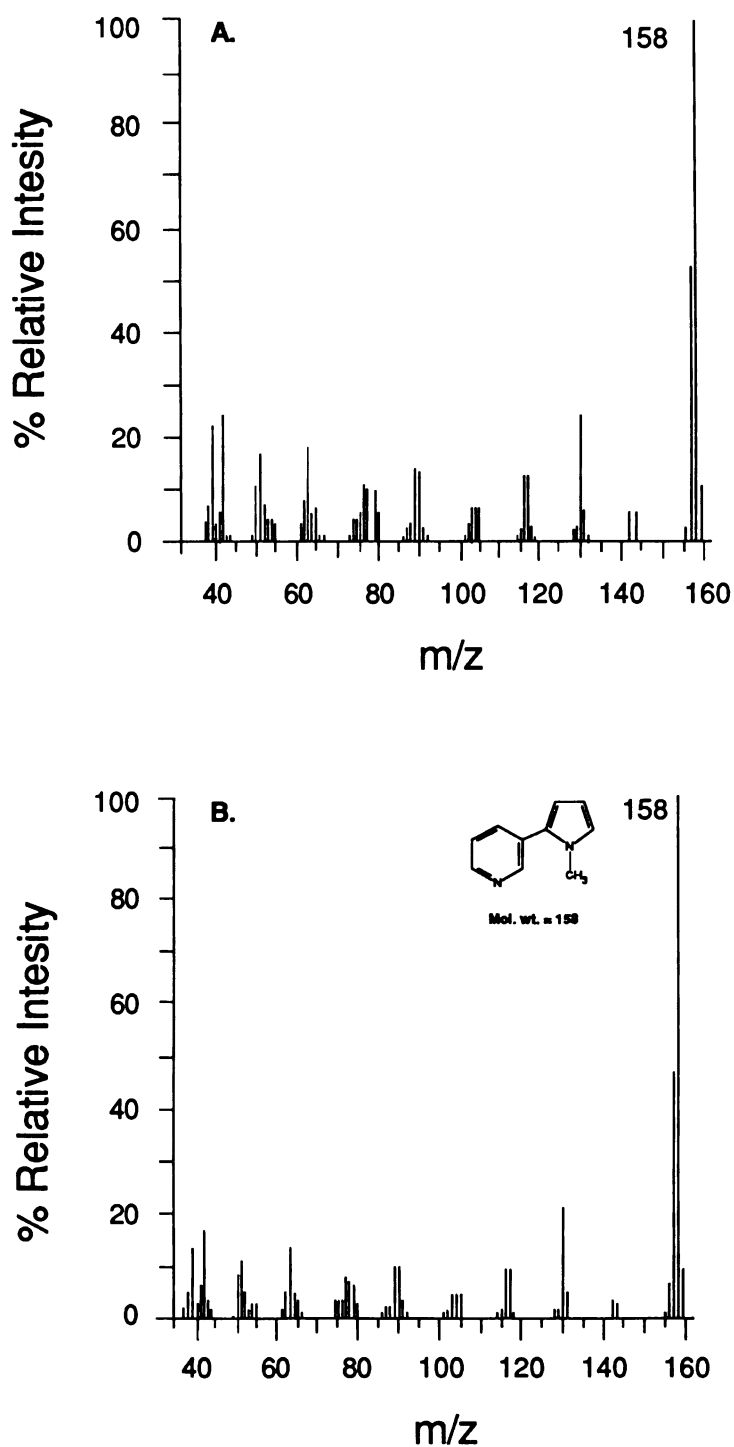


**Fig.V.6** Capillary GC-EI Mass Spectra Obtained from (A). the HPLC Purified Product Derived from the MAO-B Catalyzed Oxidation of (S)-Nicotine  $\Delta^{1',5'}$ -Iminium bisperchlorate and Comparison to (B). Synthetic  $\beta$ -Nicotryne Tartrate.

peak produced a total ion chromatogram which contained a peak (retention time 8.654-8.731 min) with a parent ion at  $m/z$  158 which corresponds to the molecular mass of  $\beta$ -nicotyrine. The mass fragmentation profiles obtained from the GC-EIMS analysis of both the metabolite and synthetic  $\beta$ -nicotyrine were compared and found to be the same (Fig.V.6). Based on these results, we assign the structure of the product derived from the MAO-B catalyzed oxidation of (S)-nicotine  $\Delta^{1',5'}$ -iminium ion as  $\beta$ -nicotyrine.

#### MAO-B Catalyzed Oxidation of (S)-Nicotine $\Delta^{1',5'}$ -Iminium *bis*perchlorate to $\beta$ -Nicotyrine

Metabolic incubations were carried out in order to characterize further the MAO-B catalyzed oxidation of (S)-nicotine  $\Delta^{1',5'}$ -iminium ion to  $\beta$ -nicotyrine. As shown in Fig.V.7, MAO-B catalyzed this reaction at a rate of approximately 0.3 nmoles/nmole MAO-B/min. The formation of  $\beta$ -nicotyrine was linear over the initial

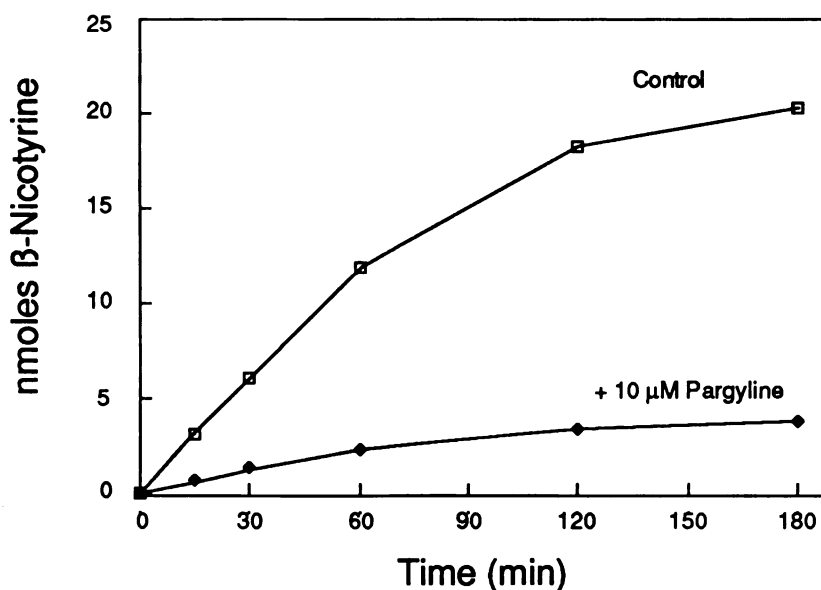


**Fig.V.7** Kinetics of the MAO-B Catalyzed Oxidation of (S)-Nicotine  $\Delta^{1',5'}$ -Iminium *Bis* perchlorate to  $\beta$ -Nicotyrine in the Presence or Absence of Pargyline. (S)-Nicotine  $\Delta^{1',5'}$ -iminium ion (0.5 mM) was incubated at 30°C with MAO-B (0.7 nmoles) in the presence or absence of pargyline (10  $\mu$ M). Formation of  $\beta$ -nicotyrine was monitored by the normal phase silica HPLC method described in Materials and Methods.

30 min of the incubation. Preincubation of the mechanism based inhibitor pargyline (10  $\mu$ M) and MAO-B for 15 min, prior to the addition of substrate, inhibited the formation of  $\beta$ -nicotyrine by approximately 80%. The oxidation of (S)-nicotine  $\Delta^{1',5'}$ -iminium *bis*perchlorate to  $\beta$ -nicotyrine was also dependent upon the concentration of MAO-B (Fig.V.8).

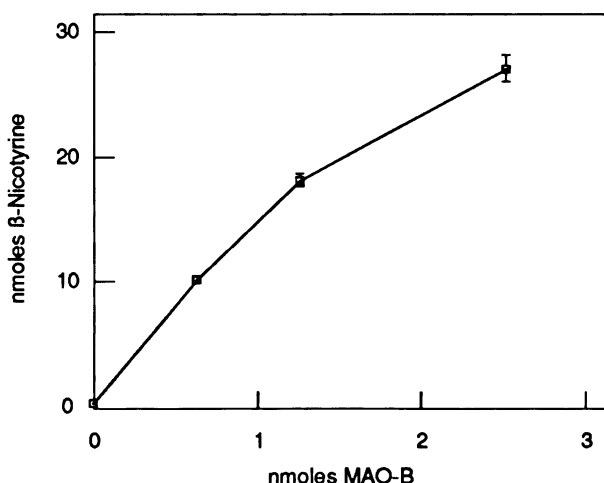


**Fig.V.8** MAO-B Concentration Dependent Oxidation of (S)-Nicotine  $\Delta^{1',5'}$ -Iminium *Bis* perchlorate to  $\beta$ -Nicotyrine. (S)-Nicotine  $\Delta^{1',5'}$ -iminium *bis*perchlorate (500 nmoles) was incubated at 30°C for 3 hr with MAO-B at the concentrations indicated.  $\beta$ -Nicotyrine formation was measured by HPLC analysis as described in Materials and Methods.

NMR studies have shown previously that (S)-nicotine  $\Delta^{1',5'}$ -iminium ion (2) exists in equilibrium with the corresponding carbinolamine 15, at pH 7.4 (Scheme IV.2).<sup>11</sup> These studies, however, failed to demonstrate the presence of the enamine species 19, which has been proposed to exist in equilibrium with the  $\Delta^{1',5'}$ -iminium ion species. Indeed, the protons attached to the C-4' position of (S)-nicotine  $\Delta^{1',5'}$ -iminium ion have been shown to be susceptible to deuterium exchange in the presence of



was the highest at pH 9.0. As the pH of a solution containing (S)-nicotine  $\Delta^{1',5'}$ -iminium ion is increased beyond pH 7.4, the relative proportion of the carbinolamine species **15** increases; previous studies have shown that at pH 8.9, (S)-nicotine  $\Delta^{1',5'}$ -iminium ion is converted almost exclusively to this form.<sup>11</sup> The formation of  $\beta$ -nicotyrine as a function of buffer pH indicates that the iminium species **2** and the carbinolamine **15** are unlikely substrates for MAO-B since the pH conditions which favor their existence yield lower amounts of product. These measurements, albeit indirect, support the suggestion of the enamine species as the likely substrate for MAO-B.

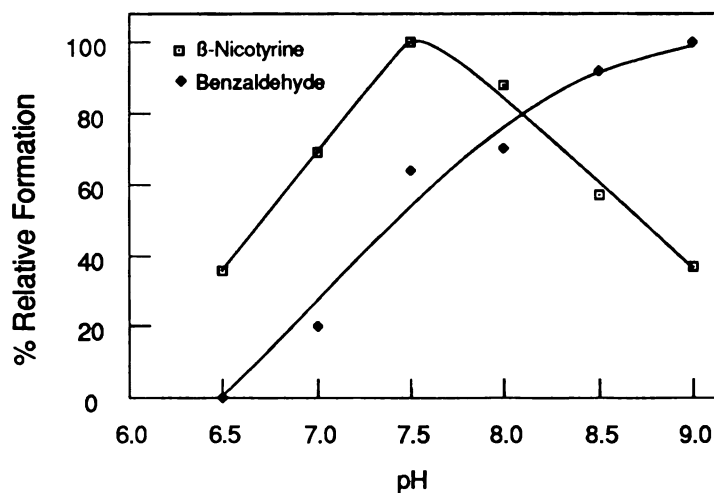


**Fig.V.9** MAO-B Catalyzed Oxidation of (S)-Nicotine  $\Delta^{1',5'}$ -Iminium Ion to  $\beta$ -Nicotyrine as a Function of pH.  $\beta$ -Nicotyrine formation was monitored by HPLC with UV detection as described in Materials and Methods. For comparison, the MAO-B catalyzed oxidation of benzylamine to benzaldehyde was measured spectrophotometrically as described in Materials and Methods.

## Discussion

The epidemiological studies which indicate an inverse correlation between cigarette smoking and Parkinson's disease has led some investigators to speculate that a constituent of tobacco maybe responsible for inhibiting the development of this disease. Recently, studies on the tertiary allylamine MPTP has revealed that this compound is

bioactivated by MAO-B to metabolites which selectively lesion the cells of the substantia nigra to produce symptoms indistinguishable from idiopathic Parkinsonism. Because of the similarities between idiopathic Parkinson's disease and the neurotoxicities induced by MPTP, this compound has become a useful tool for studying the molecular mechanisms involved in the development of this disease.

In the present study, the inhibitory effects of (S)-nicotine and related alkaloids on the rate of oxidation of MPTP catalyzed by the mitochondrial enzyme monoamine oxidase B (MAO-B) was examined. (S)-Nicotine  $\Delta^{1',5'}$ -iminium ion (2), was shown *in vitro* to inhibit the MAO-B catalyzed oxidation of MPTP to its two electron oxidation product MPDP<sup>+</sup>. This inhibition was both concentration and preincubation time dependent. Other major metabolites of (S)-nicotine, including (S)-cotinine and (S)-nicotine N'-oxide as well as (S)-nicotine itself, did not appear to exhibit any significant inhibitory effects. The inhibitory effects of  $\beta$ -nicotyrine and myosmine were moderate. Based on the reactive nature of iminium ions,<sup>14,15</sup> we speculated that this inhibition could be mediated by interactions occurring between this electrophilic species and nucleophilic functionalities present on this enzyme. In this regard, nucleophilic attack by the enzyme's sulfhydryl groups on the iminium species may result in the formation of adducts which could alter the enzymatic activity of this enzyme.

In order to determine the nature of this inhibition, enzyme kinetic studies were performed. Results of these studies revealed that the  $\Delta^{1',5'}$ -iminium species inhibited MAO-B activity by a linear mixed-type mechanism, indicating that the inhibition was due to noncompetitive and competitive components. One interpretation of the noncompetitive component of this inhibition was that the iminium ion, as an electrophilic reactive species, interacts covalently with nucleophilic sulfhydryl containing amino acids present in MAO-B. Presumably, if the electrophilic iminium were to interact in this manner, cyanide ion would cleave the (S)-nicotine-thiol linkage

at the 5' position with the concomitant formation of the stable (S)-5'-cyanonicotine derivative. This approach is analogous to the one described in the addendum of Chapter III, which showed that cyanide ion can reverse the apparent covalent binding of bioactivated (S)-5-<sup>3</sup>H-nicotine when measured by SDS equilibrium dialysis. Unfortunately this experiment could not be carried out since it was found that 1 mM cyanide inhibited the MAO-B catalyzed oxidation of benzylamine by 60%. As an alternative to the approach described above, inhibition of the MAO-B catalyzed reactions by phencyclidine iminium ion was attempted. Results of this experiment showed that the iminium ion of phencyclidine was a good inhibitor of this enzyme activity, whereas, the inhibitory properties of the parent compound phencyclidine were poor. In contrast to the complex enzyme kinetics exhibited by the  $\Delta^{1',5'}$ -iminium ion, the inhibition produced by the phencyclidine iminium species appeared to be due to a noncompetitive component only. The results obtained from the enzyme kinetic analyses of the  $\Delta^{1',5'}$ -iminium ion and phencyclidine iminium ion indicate that the reactive electrophilic nature of these compounds may contribute to the inhibition of MAO-B activity.

Despite these positive findings, the relative concentration of (S)-nicotine  $\Delta^{1',5'}$ -iminium ion required to inhibit MAO-B activity is much higher than one could reasonably expect to find *in vivo*. For example, although the iminium species has never been directly assayed in human biological fluids, a plasma concentration of 0.5  $\mu$ M would be the most liberal estimate one could make based on the assumption that the plasma concentration of (S)-nicotine  $\Delta^{1',5'}$ -iminium species was equivalent to that of (S)-nicotine. This consideration alone makes it difficult to accept the inhibition of MAO-B by (S)-nicotine  $\Delta^{1',5'}$ -iminium ion as a mechanism for the protective effect of smoking on Parkinson's disease. Nevertheless, localized intracellular concentrations of compounds can be generated, as illustrated by the active concentration of certain xenobiotics, such as the cationic neurotoxicant MPP<sup>+</sup>, by synaptosomal membrane preparations.<sup>16</sup> The positively charged (S)-nicotine  $\Delta^{1',5'}$ -iminium ion could

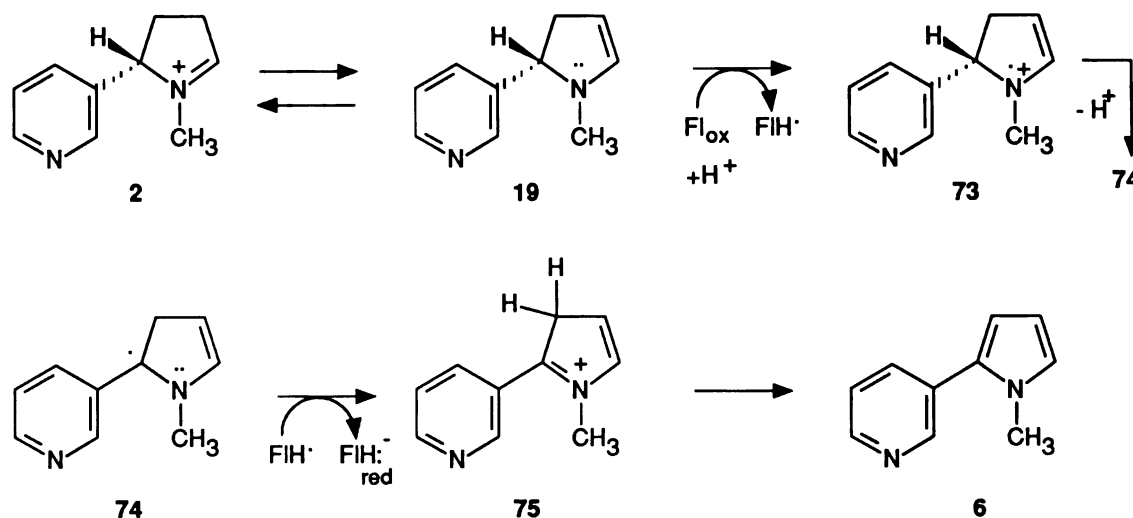


conceivably be bioconcentrated by a similar mechanism, although such an effect has never been tested. Furthermore, the long term exposure to (S)-nicotine by smokers could be a significant factor in the expression of this protective effect. The lack of detectable aldehyde oxidase activity, the enzyme which catalyzes the oxidation of the (S)-nicotine  $\Delta^{1',5'}$ -iminium ion to (S)-cotinine, in mice and rat brains<sup>17</sup> is an additional factor which could also contribute favorably to the persistent localization of (S)-nicotine  $\Delta^{1',5'}$ -iminium ion in this tissue.

The enzyme kinetic data described above which suggest that the  $\Delta^{1',5'}$ -iminium ion dependent inhibition of the MAO-B catalyzed oxidation of MPTP and benzylamine was, in part, competitive in nature, prompted us to investigate whether (S)-nicotine  $\Delta^{1',5'}$ -iminium ion could be a substrate for this enzyme. Incubations of MAO-B and (S)-nicotine  $\Delta^{1',5'}$ -iminium *bis*perchlorate led to the formation of an unknown metabolite which was detected by HPLC-UV analysis. The formation of this metabolite was shown to be time and enzyme concentration dependent and was inhibited by the MAO-B inhibitor pargyline. With the aid of HPLC-UV diode array analysis, UV spectral data were obtained which revealed a compound with a  $\lambda_{\text{max}}$  at 286 nm. The UV spectral characteristic of the metabolite was similar to that reported for the substituted pyrrole  $\beta$ -nicotyrine,<sup>18</sup> a tobacco alkaloid which previously had been tentatively identified as a metabolite of the rabbit liver oxidation of (S)-nicotine.<sup>8</sup> GC-EIMS analysis of putative  $\beta$ -nicotyrine confirmed this structure.

We propose that this product is formed via oxidation of the corresponding enamine free base **19** (See **Scheme V.3**) since much of the current evidence on the catalytic mechanism of MAO-B catalyzed oxidations supports an initial abstraction of one of the lone pair electrons present on the nitrogen atom of the substrate.<sup>13</sup> The effects of buffer pH on the oxidation of the iminium species by MAO-B is consistent with this notion, since physiological pH conditions would be expected to increase the likelihood of the enamine free base in solution.

As shown in **Scheme V.3** we envision the MAO-B catalyzed oxidation of (S)-nicotine  $\Delta^{1',5'}$ -iminium ion proceeding via the enamine species **19** as described



**Scheme V.3** Proposed Mechanism for the MAO-B Catalyzed Oxidation of (S)-Nicotine  $\Delta^{1',5'}$ -Iminium Ion to  $\beta$ -Nicotyrine.

previously. The oxidized flavin of MAO-B abstracts one electron from the pyrrolidine nitrogen yielding the aminium cation radical intermediate **73** which spontaneously rearranges to afford the carbon centered radical species **74**. Abstraction of the second electron by the one electron reduced flavin of MAO-B yields a fully reduced flavin and the cationic intermediate **75**. Spontaneous rearrangement of **75** yields the pyrrole containing end product  $\beta$ -nicotyrine (**6**).

The relatively poor turnover of (S)-nicotine  $\Delta^{1',5'}$ -iminium ion by MAO-B compared to that observed with MPTP and benzylamine (197 and 530 mole substrate/mole enzyme/min, respectively)<sup>19</sup> may be attributed to at least two factors. First, (S)-nicotine  $\Delta^{1',5'}$ -iminium ion inhibits the MAO-B catalyzed oxidation of both MPTP and its classic substrate benzylamine, in part, by a noncompetitive mechanism and therefore it might inhibit its own oxidation. Secondly, the enamine, which we

propose to be the favored substrate for this oxidation, is present in relatively small amounts compared to the other compounds with which it is in equilibrium, (S)-nicotine  $\Delta^{1',5'}$ -iminium ion (2), (S)-5'-hydroxynicotine (15) and the ring opened aldehyde species 4-methylamino-4-(3-pyridyl)butanal (20). The failure to observe the free base enamine form by NMR at physiological pH indicates that it contributes little to the overall equilibria of the various isoelectronic forms. Based on this evidence, the absolute concentration of enamine would appear to be relatively low. This consideration alone could account for the low turnover of (S)-nicotine  $\Delta^{1',5'}$ -iminium ion to  $\beta$ -nicotyrine.

These findings point to a new pathway for the metabolism and disposition of the principal two electron oxidation product of (S)-nicotine, (S)-nicotine  $\Delta^{1',5'}$ -iminium ion, and a catalytic role for MAO-B in the metabolism of enamines in general. This extends the catalytic role of MAO-B from that previously observed for tertiary allylamines such as MPTP to include enamines such as that formed from the cytochrome P-450 catalyzed oxidation of (S)-nicotine.  $\beta$ -Nicotyrine itself is of potential toxicological interest since this electron rich aromatic system may be bioactivated to toxic species by cytochrome P-450 as has been observed with related cyclopentadienoid heterocycles, including the well studied lung toxicant 4-ipomeanol.<sup>20</sup> Therefore, documenting the enzymatic conversion of (S)-nicotine to the pyrrole derivative via the iminium/enamine species would demonstrate an intimate association between MAO-B and cytochrome P-450 in its bioactivation to potentially toxic species. In this regard, studies which will be presented in Chapter VI were pursued in order to evaluate the further metabolism of  $\beta$ -nicotyrine as it may relate to the chronic toxicology of (S)-nicotine.

**Notes:**

The effect of (S)-chronic nicotine administration on dopaminergic function of MPTP treated mice has recently been described.<sup>21</sup> In that study, the effect of chronic

(S)-nicotine administration on the rate of recovery of striatal dopaminergic neuron terminals lesioned by MPTP was assessed. The rate of terminal recovery, as measured by the level of striatal dopamine, in mice treated chronically with (S)-nicotine (16 weeks, 5 mg/kg via drinking water) was not significantly different from control mice. In addition, the MAO-B activity in striatal homogenates was comparable to that in control mice.

## Materials and Methods

### Synthesis

#### $\beta$ -Nicotyrine Tartrate (6a)

(S)-Nicotine (25 g, 154 mmol) was added neat to a reaction flask containing 10% Pd/C (3 g) and which had been purged with nitrogen gas. Under magnetic stirring, the contents were mixed under a nitrogen atmosphere and heated slowly to a final temperature of 250°C. After 3 hr the reaction mixture was filtered and  $\beta$ -nicotyrine was purified by vacuum distillation (112-114°C/3 mtorr). Addition of 95% ethanol and tartaric acid to the distillate provided oily yellow crystals.  $\beta$ -Nicotyrine tartrate was recrystallized 5 times from ethanol to yield 1.7 g (3.6%) of slightly yellow crystals (m.p. 86-88°C) UV  $\lambda_{\text{max}}$  = 282 nm in 0.1 M HEPES pH 7.6.  $^1\text{H-NMR}$ : 80 MHz ( $\text{D}_2\text{O}$ )  $\delta$  3.75 (s, 3H, N-CH<sub>3</sub>), 6.32 (d of d, 1H, C4'), 6.59 (d of d, 1H, C3'), 7.03 (t, 1H, C5'), 8.06 (m, 1H, C5), 8.60 (m, 2H C4, C6), and 8.83 (bs 1H, C2).

#### (S)-5'-Cyanonicotine (17)

A 70% solution of REDAL [sodium dihydrobis (2-methoxyethoxy) aluminate] (3.6 g, 11.9 mmol) in dry ether (50 ml) was added to an ice-cooled, magnetically stirred solution of (S)-cotinine (2.9 g, 16.4 mmol) in ether (60 ml) in a flame dried flask over 30 min. The reaction mixture was allowed to stir for 105 min, although time course sampling of the reaction revealed completion of the reaction by 30 min. An aqueous solution (50 ml) of KCN (6 g, 91.2 mmol) was added over 15 min followed by

adjusting the pH to 5-6 with glacial acetic acid (20 ml). The reaction mixture was allowed to warm to 25°C, made basic with a saturated K<sub>2</sub>CO<sub>3</sub> solution (50 ml), followed by extraction with ether (50 ml x 3). After drying the extracts, filtration and removal of the solvent, a yellow oil was obtained. The oil was purified on a silica gel column using a step gradient employing methylene chloride/acetonitrile/n-propylamine (90:9.9:0.1/50:49.5:0.5). The product was isolated as a pale yellow oil (66.5% yield). <sup>1</sup>H NMR: 80 MHz (CDCl<sub>3</sub>):  $\delta$  1.5-2.5 (complex m, 4H, C3' and C4'), 2.3 and 2.32 (2s, 3H, N-CH<sub>3</sub> of the (E)- and (Z)-isomers), 3.5 (complex m, 1.4 H, C2' and 5'H of the (E)-isomer), 4.1 (d of d, 0.6 H, 5'-H of the (Z)-isomer), 7.28 (m, 1H, C5), 7.6 (m, 1H, C4), and 8.55 (m, 2H, C2 and C6).

#### (S)-Nicotine $\Delta^{1',5'}$ -Iminium b/sperchlorate (2a)

A 70% perchloric acid solution (2.05 ml, 23.8 mmol) was diluted with ethanol (7.9 ml) and added slowly to an ice-cooled ethanolic solution (15.8 ml) of (S)-5'-cyanonicotine (2.05 g, 11.0 mmol). The white crystals were filtered, washed with methanol (10-20 ml) containing a few drops of 70% perchloric acid and recrystallized 2 times with acidic methanol to provide 1.2 g (31% yield) of product: (m.p. 233-235°C with decomposition). <sup>1</sup>H NMR: 80 MHz <sup>1</sup>H NMR analysis (10% DCI in D<sub>2</sub>O) agreed with that reported previously:  $\delta$  2.0 - 2.35 (complex multiplets, 4H, C3' and C4'), 3.28 (br s, 3H, N-CH<sub>3</sub>), 7.5-9.0 (m, 5H, 4 aromatic pyridine H and C5').<sup>22</sup>

#### Other Chemicals

Pargyline were obtained from Aldrich Chemical Company (Milwaukee, WI.). (S)-Nicotine and structurally related compounds were obtained from sources described in the Materials and Methods section of Chapter III. Phencyclidine (PCP), PCP iminium perchlorate and cyano-PCP were obtained as described.<sup>23</sup> N-2-hydroxyethyl-piperzaine-2-ethanesulfonic acid (HEPES) and Triton X-100 were purchased from Sigma Chemical Co.(St. Louis, MO). All other chemicals were reagent grade. HPLC grade solvents were used throughout these studies when required and were purchased from

Fisher Scientific Co. (Plainview, NJ). Partially purified bovine MAO-B was prepared by the method of Salach.<sup>24</sup>

#### **Inhibition of MPTP Oxidation by (S)-Nicotine $\Delta^{1',5'}$ -Iminium Ion**

MAO-B (0.02 units, 0.042 nmoles) was preincubated with (S)-nicotine  $\Delta^{1',5'}$ -iminium *bis*perchlorate (0.5 mM, unless stated otherwise) in 0.2% Triton/0.05 M sodium phosphate buffer, pH 7.2, for 15 min at 30°C. Upon addition of MPTP (to a final concentration of 3.2 mM, unless stated otherwise) the contents were mixed by resuspension with a Pasteur pipette followed by UV spectrophotometric measurements. Formation of the two electron oxidation product of MPTP, MPDP<sup>+</sup>, was monitored at 343 nm every 15 or 30 seconds in a Beckman DU-50 UV/VIS spectrophotometer equipped with kinetic data acquisition software. Initial rates of oxidation were determined over the first three minutes. The linearity of the rate of oxidation (R) was calculated by the kinetic data acquisition program and found to be  $\geq 0.995$ . Benzylamine oxidation was measured in an essentially identical manner by monitoring the increase in absorbance at 250 nm.

#### **Enzyme Kinetic Analyses**

Enzyme kinetic analysis of the (S)-nicotine  $\Delta^{1',5'}$ -iminium ion dependent inhibition of MPTP oxidation by MAO-B involved determining the initial rates of oxidation of MPTP at varying concentrations to its product MPDP<sup>+</sup>. Concentrations of the inhibitor, (S)-nicotine  $\Delta^{1',5'}$ -iminium *bis*perchlorate, ranging from 0-1.0 mM were used and double reciprocal plots of oxidation rates versus MPTP concentration were determined. (S)-Nicotine  $\Delta^{1',5'}$ -iminium *bis*perchlorate at concentrations of 0, 0.25, 0.5, 0.75 and 1.0 mM was preincubated for 15 min with approximately 0.013 units of MAO-B in a pH 7.2, 0.2% Triton buffer. Preparation of enzyme (10  $\mu$ l of a stock solution of semipurified MAO-B with a specific activity of 32 units/ml was diluted with 990  $\mu$ l of a 0.05 M Tris 0.2% Triton buffer, pH 7.2, to obtain a dilute stock solution. 140  $\mu$ l of this dilute stock was added to 6.496 ml of the buffer described above

plus 20  $\mu\text{l}$  of the appropriate stock solution of (S)-nicotine  $\Delta^{1',5'}$ -iminium bisperchlorate (stock solutions of 12.5, 25, 37.5 and 50 mM were prepared with the Tris-Triton buffer). The mixture which contained the enzyme, buffer and (S)-nicotine  $\Delta^{1',5'}$ -iminium bisperchlorate, was preincubated for 15 min at 30°C. Aliquots of 968  $\mu\text{l}$  were transferred from this pooled preincubation mixture to each of 6 standard size quartz cuvettes (1 ml capacity, 10 mm path length). To each of the cuvettes was added 32  $\mu\text{l}$  of an appropriate stock solution of MPTP (ranging in concentrations of between 3.125-100 mM) followed by rapid resuspension of the cuvette contents with a Pasteur pipet. Following this step, the sample compartment was closed and the DU-50 spectrophotometer calibrated (10 sec elapsed time) followed by spectrophotometric monitoring at 343 nm. The rates of oxidation were calculated from the change in absorbance at 343 nm over the first 2-3 min. Parallel experiments were performed in which the iminium species was omitted from the preincubation step. In this experiment (S)-nicotine  $\Delta^{1',5'}$ -iminium bisperchlorate and MPTP were added to the cuvette after the 15 min preincubation period. MPTP hydrochloride was made up as a stock solution of 0.1 M and serially diluted a total of five times to obtain stock solutions of 0.1, 0.05, 0.025, 0.0125, 0.00625, and 0.003125M. The same approach was used to measure the enzyme kinetics of benzylamine oxidation in the presence and absence of (S)-nicotine  $\Delta^{1',5'}$ -iminium ion and PCP iminium ion. Where benzylamine was used as the MAO-B substrate, the initial rate of oxidation was measured by monitoring the increase in absorbance at 250 nm.

#### **Analysis of $\beta$ -Nicotyrine by HPLC with UV Diode Array Detection**

(S)-Nicotine  $\Delta^{1',5'}$ -iminium bisperchlorate (0.5 mM) was incubated with MAO-B (0.7 units, as determined by benzylamine oxidation) at 30°C for 60 min in 0.5 ml of HEPES buffer [0.1 M, pH 7.6, in the presence or absence of pargyline (10  $\mu\text{M}$ )]. Incubations were terminated by the addition of an equal volume of saturated  $\text{K}_2\text{CO}_3$  followed by the addition of the internal standard N-methyl-N-(3-pyridyl)

methylpropanamide. Methylene chloride (1 ml) was added and the resulting mixture was vortexed vigorously and then centrifuged at 1000 x g. The resulting methylene chloride extracts were analyzed by HPLC, which utilized a Beckman Model 330 liquid chromatographic system equipped with an Alltech silica Econosphere column (5  $\mu$ m, 4.6 mm x 25 cm), and monitored at either 254 or 286 nm. The mobile phase consisted of 1% n-propylamine in acetonitrile and the flow rate was 1.0 ml/min. HPLC separation followed by UV-diode array detection was accomplished by using conditions described above in conjunction with a Beckman model 114 M liquid chromatographic system equipped with a Hewlett Packard 1040A UV detector. The online UV scans were performed between 190-400 nm.

#### GC-EIMS Analysis of $\beta$ -Nicotyrine

A large scale incubation [3.3 units (7 nmoles) of MAO-B and 2.5  $\mu$ moles of (S)-nicotine  $\Delta^{1',5'}$ -iminium bisperchlorate in 5.0 ml of 0.2% Triton/0.1 M sodium phosphate buffer pH 7.2] was used to generate large quantities of enzymatically derived  $\beta$ -nicotyrine. Following a 2 hr incubation at 30°C, the metabolic incubation was quenched by the addition of an equal volume of 1 M  $K_2CO_3$  followed by extraction of the metabolites with methylene chloride (10 ml). The methylene chloride extract was concentrated and injected onto the HPLC system described above (The mobile phase consisted of 1% n-propylamine in acetonitrile at a flow rate of 1.0 ml/min. UV absorbance was monitored at 254 nm) and the peak corresponding to the retention time of synthetic  $\beta$ -nicotyrine was collected. Pooled fractions were concentrated *in vacuo* and resuspended in toluene followed by GC-EIMS analysis (HP 5970 Series mass selective detector, 5890 A gas chromatograph, 12 M x 0.2 mm diam. methylsilicone capillary column) 70-200°C, 4.0 min solvent delay, 20°C/min temperature gradient. The detector was set at 70 eV. Splitter ratio was 20:1. Injection port temperature was 200°C.



- 
- 1 Nefzger, M.D., F.A. Quadfasel and V.C. Karl, "A retrospective study of smoking in Parkinson's disease," *Am. J. Epidemiol.* **88**, 149-158 (1968).
  - 2 Kessler, I.I., "Epidemiologic studies of Parkinson's disease. II. A hospital-based survey," *Am. J. Epidemiol.* **95**, 308-318 (1972).
  - 3 Kahn, H.A. In: Epidemiological approaches to the study of cancer and other chronic diseases, Monograph No. 19 pp. 1-125 National Cancer Institute, U.S. Government printing office, Washington, D.C. (1966).
  - 4 Kessler, I.I. and E. Diamond, "Epidemiologic studies of Parkinson's disease I. Smoking and Parkinson's disease: A survey and explanatory hypothesis," *Am. J. Epidemiol.* **94**, 16-25 (1971).
  - 5 Langston, J.W., "MPTP: Insights into the etiology of Parkinson's disease," *Eur. Neurol.* **26 Suppl 1**, 2-10 (1987).
  - 6 Tetrad, J.W. and J.W. Langston, "The effect of deprenyl (selegiline) on the natural history of Parkinson's disease," *Science* **245**, 519-522 (1989).
  - 7 Yong, V.W. and T.L. Perry, "Monoamine oxidase B, smoking, and Parkinson's disease," *J. Neurol. Sci.* **72**, 265-272 (1986).
  - 8 Takeuchi, M., "The metabolic change of nicotine in rabbit liver extract," *Folia Pharmacol Japon* **51**, 62-69 (1955).
  - 9 Segel, I. H., "Behavior and analysis of rapid equilibrium and steady-state enzyme systems," In: *Enzyme Kinetics* pp.125-130, John Wiley & Sons, New York (1975).
  - 10 Swain, M.L., A. Eisner, C.F. Woodward and B.A. Brice, "Ultraviolet absorption spectra of nicotine, nor nicotine and some of their derivatives," *J. Am. Chem. Soc.* **71**, 1341-1345 (1949).
  - 11 Brandange, S. and L. Lindblom, "Synthesis, structure and stability of nicotine  $\Delta^{1',5'}$  iminium ion, an intermediary metabolite of nicotine," *Acta Chem. Scand. B* **33**, 187-191 (1979).
  - 12 Peterson, L.A., "Stereochemical studies of the cytochrome P-450 catalyzed oxidation of (S)-nicotine to nicotine  $\Delta^{1',5'}$ -iminium ion," Ph.D. Dissertation. University of California, San Francisco (1986).
  - 13 Silverman, R.B., S.J. Hoffman and W.B. Catus III, "A mechanism for mitochondrial monoamine oxidase catalyzed amine oxidation," *J. Am. Chem. Soc.* **102**, 7126-7128 (1980).
  - 14 Nguyen, T-L., L.D. Gruenke and N. Castagnoli Jr., "Metabolic oxidation of nicotine to chemically reactive intermediates," *J. Med. Chem.* **22**, 259-263 (1979).

- 
- 15 Ward, D.P., A.J. Trevor, J.D. Adams, T.A. Baillie and N. Castagnoli Jr., "Metabolism of phencyclidine: The role of iminium ion formation in covalent binding of rabbit microsomal protein," *Drug Metab. Dispos.* **10**, 690-695 (1982).
  - 16 Chiba, K., A.J. Trevor and N. Castagnoli Jr., "Active uptake of MPP+, a metabolite of MPTP, by brain synaptosomes," *Biochem. Biophys. Res. Commun.* **128**, 1228-32 (1985).
  - 17 Wu, E., T. Shinka, P. Caldera-Munoz, H. Yoshizumi, A. Trevor and N. Castagnoli Jr., "Metabolic studies on the nigrostriatal toxin MPTP and its MAO B generated dihydropyridinium metabolite MPDP+," *Chem. Res. Toxicol.* **1**, 186-194 (1988).
  - 18 Woodward, C.F., A. Eisner and P.G. Haines, "Pyrolysis of nicotine to myosmine," *J. Am. Chem. Soc.* **66**, 911-914 (1944).
  - 19 Salach, J.I., T.P. Singer, N. Castagnoli Jr. and A. Trevor, "Oxidation of the neurotoxic amine 1-methyl-4-phenyl-1,2,3,6-tetrahydropyridine (MPTP) by monoamine oxidases A and B and suicide inactivation of the enzymes by MPTP," *Biochem. Biophys. Res. Comm.* **125**, 831-835 (1984).
  - 20 Boyd, M.R., "Biochemical mechanisms in chemical induced lung injury: Roles of metabolic activation," *CRC Crit. Rev. Toxicol.* **9**, 103-176 (1980).
  - 21 Sershen, H., A. Hashim, H.L. Wiener and A. Lajtha, "Effect of chronic oral nicotine on dopaminergic function in the MPTP-treated mouse," *Neurosci. Lett.* **93** 270-274 (1988).
  - 22 Peterson, L.A., A.J. Trevor and N. Castagnoli Jr., "Stereochemical studies on the cytochrome P-450 catalyzed oxidation of (S)-nicotine to the (S)-nicotine  $\Delta^{1'(5')}$ -iminium species," *J. Med. Chem.* **30**, 249-253 (1987).
  - 23 Hoag, M.K.P., A.J. Trevor, A. Kalir and N. Castagnoli Jr., "Phencyclidine iminium ion: NADPH dependent metabolism, covalent binding to macromolecules and inactivation of cytochrome(s) P-450," *Drug Metab. Dispos.*, **15** 485-490 (1987).
  - 24 Salach, J.I. and W. Weyler, "Preparation of the flavin-containing aromatic amine oxidases of human placenta and beef liver," *Methods Enzymol.* **142**, 627-37 (1987).

**Chapter VI**  
**Metabolic Fate of  $\beta$ -Nicotyrine**

## Introduction

$\beta$ -Nicotyrine is a member of the cyclopentadienoid heterocycle family of compounds. These electron rich compounds have been implicated in numerous organ specific toxicities. Previous studies, some of which are described in the following section, have documented, for a number of model cyclopentadienoid heterocyclic compounds, the requirement for metabolic activation of the parent compound to produce intermediates with bioalkylating properties. Studies performed *in vivo* indicate that similar metabolic processes are required to elicit toxic responses.

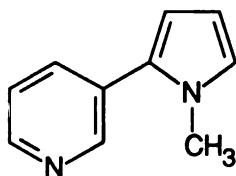
In the previous chapter, the mitochondrial enzyme MAO-B was shown to catalyze the two electron oxidation of (S)-nicotine  $\Delta^{1',5'}$ -iminium ion (2) to  $\beta$ -nicotyrine (6). This observation supports the results of a previous report which showed that  $\beta$ -nicotyrine was formed metabolically from (S)-nicotine by rabbit liver enzymes.<sup>1</sup>  $\beta$ -Nicotyrine has been reported as a urinary metabolite of intraperitoneally injected (S)-nicotine in dogs and rats.<sup>2</sup> In addition to its metabolism dependent formation,  $\beta$ -nicotyrine is also present in tobacco<sup>3</sup> and cigarette smoke condensates.<sup>4</sup> Pyrolysis and autoxidation of (S)-nicotine also gives rise to this product.<sup>5,6</sup>

The recent studies on the metabolism dependent formation of  $\beta$ -nicotyrine and our overall interest in (S)-nicotine bioactivation and toxicity of tobacco alkaloids in general, have encouraged us to characterize the rabbit liver and lung microsomal metabolism of  $\beta$ -nicotyrine. The structural characterization of its principal metabolite and one of the subsequently formed autoxidation products suggest the formation of reactive intermediates which may produce toxic responses similar to those described for other members of the cyclopentadienoid heterocycle family of compounds.

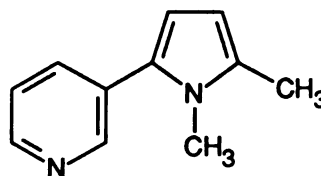
## Background

### Pharmacology of $\beta$ -Nicotyrine

$\beta$ -Nicotyrine exhibits cholinergic stimulating properties similar to those of (S)-nicotine but possesses only about 1% of its potency.<sup>7</sup> The effects induced by  $\beta$ -nicotyrine include the contraction of guinea pig ileum and the elicitation of the pressor response which, as a consequence of sympathetic ganglion stimulation and adrenal medulla release of catecholamines, results in vasoconstriction. Because of the skeletal muscle relaxing effects of  $\beta$ -nicotyrine this compound was at one time under consideration as a potentially useful therapeutic agent. Gaskell *et al.*<sup>8</sup> submitted a patent describing this property for  $\beta$ -nicotyrine and the 5'-methyl derivative 1,5-dimethyl-2-(3-pyridyl)pyrrole (26). The muscle relaxing effects observed in these studies led these authors to promote the use of the two compounds in the treatment of pathological states characterized by hyperactivity of the spinal reflex arc. However, at minimally toxic doses both compounds caused a general depression in respiratory and central nervous system activities.



6



26

More recently, Stalhandske *et al.*<sup>9</sup> described the effects of  $\beta$ -nicotyrine on the acute toxicities and metabolism of (S)-nicotine *in vivo*. The key finding in this study centered on the observation that infusions of  $\beta$ -nicotyrine, at concentrations between 8.8 - 140 mg/kg, led to a significant inhibition of (S)-nicotine metabolism *in vivo*. This study was carried out by analyzing the concentration of (S)-nicotine and (S)-cotinine present in the liver following pretreatment of these animals with

$\beta$ -nicotyrine. The treated animals were administered  $\beta$ -nicotyrine by intraperitoneal injection and 5 min later N-[methyl- $^{14}\text{C}$ ]-nicotine was injected by the same route. Samples of liver were isolated 5 min after the injection of N-[methyl- $^{14}\text{C}$ ]-nicotine and analyzed for (S)-nicotine and (S)-cotinine. In addition to the marked inhibition of (S)-nicotine metabolism, a dramatic increase in the brain and blood concentrations of (S)-nicotine was noted. Despite the increased concentration of (S)-nicotine in the brain, the  $\text{LD}_{50}$  of intraperitoneally administered (S)-nicotine was not altered significantly. These results indicate that the cholinergic stimulating properties of (S)-nicotine are inhibited by  $\beta$ -nicotyrine. It was postulated that  $\beta$ -nicotyrine could inhibit this activity by acting as a competitive ligand for nicotinic acetylcholine receptor binding sites in the central nervous system. Consistent with this view was the observation in chickens and cats that the central nervous system responses, such as the central spinal reflexes, could be inhibited by this compound.<sup>7</sup> More recently, Copland has shown that  $\beta$ -nicotyrine blocks (S)-nicotine induced constriction of vascular smooth muscle.<sup>10</sup>

Therefore, from these various reports,  $\beta$ -nicotyrine appears to evoke a number of physiological responses. In some instances, the physiological effects induced are similar although not as pronounced as those elicited by (S)-nicotine. The ability of  $\beta$ -nicotyrine to produce responses similar to those of (S)-nicotine suggests indirectly that these two compounds share similar binding sites in the central nervous system.

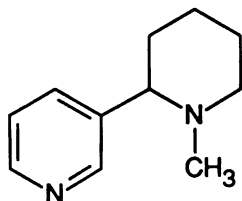
#### **Sources of $\beta$ -Nicotyrine and Its Absorption**

$\beta$ -Nicotyrine is an alkaloid which is present in smaller quantities than (S)-nicotine in tobacco.<sup>11</sup> Pyrolysis of (S)-nicotine during smoking also contributes to the  $\beta$ -nicotyrine absorbed by the individual.<sup>3</sup> In addition to these sources,  $\beta$ -nicotyrine may be formed *in vivo* from (S)-nicotine via the MAO-B catalyzed oxidation of (S)-nicotine  $\Delta^{1,5}$ -iminium ion.

Absorption of  $\beta$ -nicotyrine in the oral cavity (buccal absorption) is estimated to be approximately 23% at pH 5.0 and only 27% at pH 7.4.<sup>12</sup> The percent of  $\beta$ -nicotyrine unionized at these pH values has been reported to be 66.6 and 99.8%, respectively.<sup>13</sup> Despite being unprotonated at physiological pH,  $\beta$ -nicotyrine is poorly absorbed in the oral cavity. Most of the  $\beta$ -nicotyrine which enters the body is apparently absorbed by the lung.

### $\beta$ -Nicotyrine Metabolism

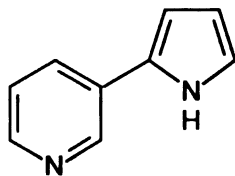
The *in vitro* metabolism of  $\beta$ -nicotyrine by liver tissues has been demonstrated. In one study, the oxidative metabolism of (S)-nicotine (1), (S)-methylanabasine (27) and  $\beta$ -nicotyrine (6) were compared. Of these three compounds,  $\beta$ -nicotyrine appeared



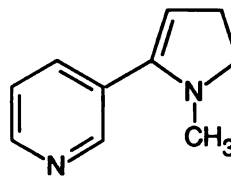
27

to be the most extensively metabolized.<sup>14</sup> In fact, the liver 10,000 x g supernatant fraction isolated from hamster and guinea pig completely metabolized 5  $\mu$ moles of this compound (volume was not stated) after an 80 min incubation. Rabbit, mouse and rat liver 10,000 x g supernatant also metabolized  $\beta$ -nicotyrine better than either (S)-nicotine or (S)-methylanabasine. Following oral administration of  $\beta$ -nicotyrine to human subjects unchanged  $\beta$ -nicotyrine could not be detected in urine indicating that this compound was metabolized completely.<sup>12</sup> The lipophilic and unsaturated pyrrolidine containing tobacco alkaloids  $\beta$ -nornicotyrine (28) and myosmine (29), were probably also rapidly and completely metabolized since neither of these compounds could be detected in urine, whereas 12% of the dose of (S)-nicotine which was

administered orally was recovered intact. The comparatively higher lipid solubility of  $\beta$ -nicotyrine is likely to contribute to its more rapid metabolism<sup>12</sup>



28



29

### Metabolic Activation of Cyclopentadienoid Heterocyclic Compounds

Many substituted cyclopentadienoid heterocycles, including several clinical drugs, are converted enzymatically to reactive intermediates which may be associated with liver, lung and kidney toxicities in human and experimental animals exposed to these compounds.<sup>15,16</sup> These electron rich compounds include substituted derivatives of pyrrole (42), thiophene (43) and furan (44). Support for the formation of reactive intermediates such as an arene oxide has come from the structural identification of adducts formed through nucleophilic attack of the putative epoxide species.<sup>17</sup>



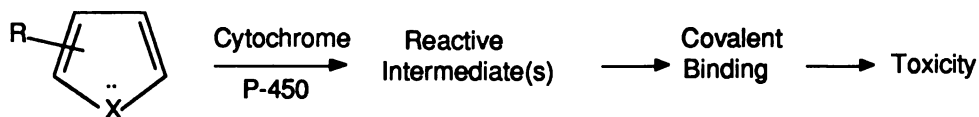
42



43



44



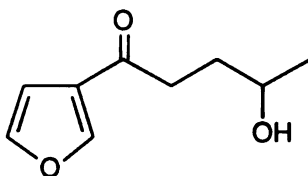
X = O, S or N

---

**Scheme VI.1** Proposed Sequence of Events Leading to the Toxicity of Cyclopentadienoid Heterocyclic Compounds.



The toxic furanoterpenoid 4-ipomeanol [1-(3-furyl)-4-hydroxypentanone (25)] is the best studied compound of this class and serves as a good model for other cyclopentadienoid heterocycles such as  $\beta$ -nicotyrine. 4-Ipomeanol is produced in mold-damaged sweet potatoes and is the major component of "lung edema factor".<sup>18</sup> Natural outbreaks of poisoning in cattle have been associated with the ingestion of this compound, resulting in many cases in severe and sometimes fatal respiratory distress.



25

A characteristic cellular lesion produced by 4-ipomeanol is necrosis of the cytochrome P-450 rich Clara cells.<sup>19</sup> Experimentally, it has been shown that cattle which have received toxic doses of this compound develop pulmonary edema and emphysema.<sup>20</sup> Other animals including rats, rabbits, mice and guinea pigs express similar lung pathologies when exposed to this compound. Interestingly, chickens and Japanese quails, which lack both the ciliated and nonciliated (Clara) airway lining cells, do not appear to be susceptible to these pneumotoxic effects. Instead, 4-ipomeanol induced toxicity is localized primarily in the liver of these avian species.<sup>21</sup>

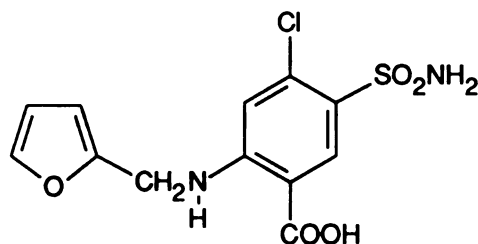
Studies utilizing radiolabeled 4-ipomeanol have shown that covalent binding occurs preferentially in tissues which are susceptible to its toxic actions. For example, in rabbits and rats 4-ipomeanol binds covalently primarily to lung tissue,<sup>22</sup> whereas in chickens and Japanese quail the principal target is liver tissue.<sup>21</sup> The lung tissue of these avian species does not appear to be a target for the irreversible binding of this compound. Therefore, a good correlation exists between tissue sites which are susceptible to irreversible modification by reactive metabolites of 4-ipomeanol and

those which display pathological changes. In addition, studies in which the time course of covalent binding and the initial signs of toxicity (i.e. accumulation of lung fluid) have been measured indicate that covalent binding of 4-ipomeanol, which peaks at 40 min following its administration, always precedes the changes in lung pathology which occur typically between 16-24 hr.<sup>23</sup>

Bioactivation studies of 4-ipomeanol performed *in vitro* have demonstrated that oxidative metabolism is necessary for covalent binding. The bioactivation process requires NADPH and oxygen and is inhibited by carbon monoxide, cytochrome c and heat denaturation of microsomal protein. The organ specific toxicities associated with 4-ipomeanol appear to correlate well with the ability of microsomes isolated from those organs to metabolically activate this compound. In contrast, microsomes isolated from organs not susceptible to the toxic effects of 4-ipomeanol (i.e. chicken lung) do not catalyze this biotransformation.

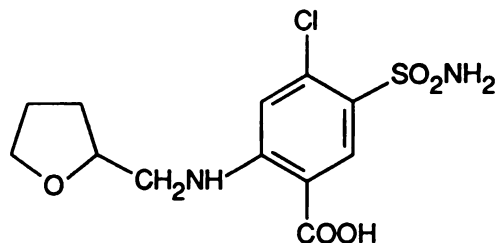
In an attempt to identify the toxiphor of this compound, the bioactivation of radiolabeled analogs of 4-ipomeanol, in which the furan ring is substituted with either phenyl or methyl substituents, has been examined. In contrast to 4-ipomeanol, these compounds do not undergo NADPH dependent covalent binding *in vitro*<sup>24</sup> or *in vivo*<sup>23</sup> and are non toxic at doses of up to 800 mg/kg. The bioalkylation properties of 4-ipomeanol are therefore most likely mediated by metabolites generated from the oxidation of the furan ring.

Furosemide (38), a clinically important drug used in the treatment of hypertension, is metabolically activated to reactive species which may contribute to the hepatotoxicities observed in mice given a high dose of this drug.<sup>25</sup> Similar metabolic processes may be responsible for the furosemide induced hepatotoxicities reported in man.<sup>26</sup> *In vitro* studies in mice have shown that the cytochrome P-450 catalyzed oxidation of this compound results in the formation of intermediates which bind covalently to liver protein.<sup>15</sup> In addition, the severity of hepatic necrosis is correlated



38

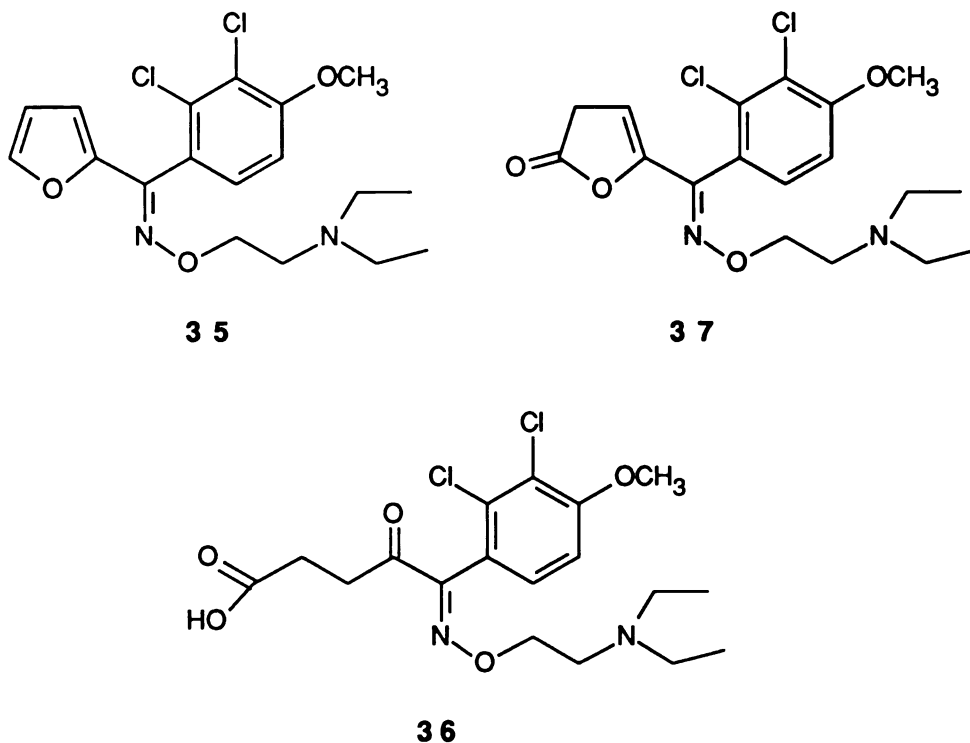
with the extent of covalent binding.<sup>15</sup> Evidence supporting the involvement of the furan moiety in the covalent binding and resulting toxicities include the following: 1) Studies showing that radioactivity associated with the furan ring of covalently bound furosemide is stable to acid hydrolysis but not when the radioactivity is bound to the anthranilic acid portion of this molecule; this suggests that the reactive intermediate which binds covalently is derived from the furanyl substituent, not the anthranilic acid moiety,<sup>27</sup> 2) the failure to demonstrate covalent binding of a radiolabeled tetrahydrofuran analog, compound 59, of furosemide to microsomal preparations and the lack of hepatotoxicity of this analog in animals,<sup>27</sup> 3) the demonstration that the epoxide hydratase inhibitor 1,2-epoxy 3,3,3-trichloropropane enhances the covalent binding of radiolabeled furosemide; this finding suggests the formation of a reactive arene oxide intermediate.<sup>27</sup> These observations are consistent with the proposal that the toxic effects of furosemide are dependent on the metabolic activation of its furan substituent to the reactive arene oxide.



59

The calcium inhibitor, dichlofurime, (2,3-Dichloro-4 methoxy)phenyl-furyl-2, O-(diethyl-amino-ethyl)ketone-oxime, methanesulphonate (35), undergoes exten-

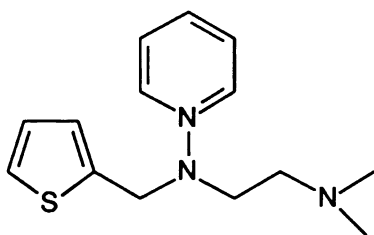
sive first pass metabolism when administered orally to dogs or pigs.<sup>28</sup> Identification of the metabolites isolated from plasma or urine indicate that the furan substituent of the parent compound is metabolized extensively. The ring opened species **36**, is the major



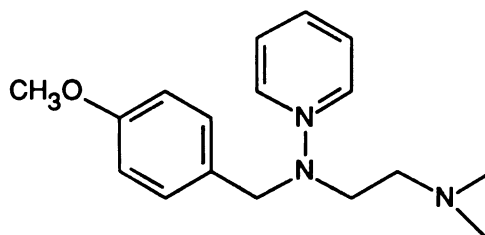
metabolite observed in dogs administered this compound. The lactone **37**, was observed as a mass spectral fragment of **36**. Similar biotransformation reactions occur with 8-methoxypsoralen when administered to humans.<sup>29</sup> Metabolism of this bisubstituted furan yields 3 different ring opened metabolites, including an aryl diol and aryl-acetic acid. These studies support previous observations which have documented the susceptibility of the furan substituent to metabolic oxidations.

Methapyrilene (**13**), a thiophene containing compound and an H<sub>1</sub> antagonist drug is a hepatocarcinogen in experimental animals.<sup>30</sup> Chronic toxicity studies indicate that the thiophene containing antihistaminic drug methapyrilene (**13**) is a potent hepatocarcinogen.<sup>31</sup> Despite the carcinogenic activity of this compound *in vivo*, attempts to demonstrate its genotoxicity in short term tests such as bacterial

mutagenicity<sup>32</sup> and sister chromatid exchange<sup>33</sup> have not been successful. Nevertheless, a recent study by Lampe *et al.*<sup>34</sup> has demonstrated that radiolabeled methapyrilene (thienyl methylene-<sup>14</sup>C) is bioactivated by cytochrome P-450 to reactive intermediates which bind covalently to DNA. The identity of this reactive metabolite has not been elucidated.



13

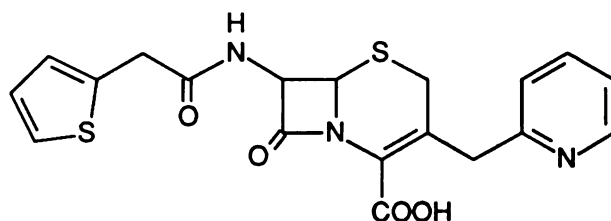


30

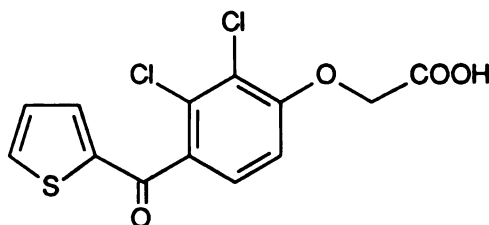
In an effort to determine the toxiphor of methapyrilene, structural analogs of this drug **13** were tested for their hepatocarcinogenicity and compared to the toxicities produced by the parent compound. Mepyramine (**30**), one of the drugs which was developed as a replacement for methapyrilene, is a structural analog in which the thiophene ring is substituted with methoxybenzene. When compared to **13** this compound was found to be much less carcinogenic in rats. Pyribenzamine (**31**), an analog in which the thiophene ring is substituted with benzene, was reported to lack hepatocarcinogenic activity. These findings are consistent with the proposal that the thiophene ring is required for the genotoxicity of **13**.<sup>30</sup> Furthermore, the observation that the metabolic oxidation of thiophene itself produces intermediates which yield stable and isolable mercapturic acid adducts<sup>35</sup> lends further support for the suggestion that the oxidation of the thiophene ring of **13** is responsible for the formation of the hepatocarcinomas observed in animals administered this compound.

Cephaloridine (**40**), a renal toxicant in man, appears to cause renal tubular necrosis in rats by a cytochrome P-450 mediated process.<sup>15</sup> The demise of ticrynafen

(41), a diuretic-uricosuric agent, was related to several occurrences of hepatic and renal injury in patients receiving this drug.<sup>36</sup> Although the exact mechanism of toxicity mediated by these drugs is not known, it has been speculated that the oxidation of the thiophene ring is involved. Oxidation of unsubstituted thiophene to an arene oxide intermediate has been implicated through studies in which mercapturic acid adducts of thiophene from the urine of animals administered this compound were isolated.<sup>17</sup>



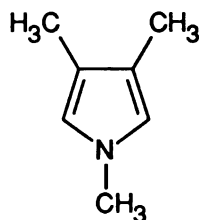
40



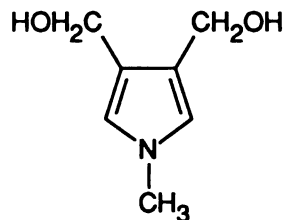
41

### Activation of Pyrrole

In order to understand better the bioactivation of compounds containing pyrrole substituents, Guengerich *et al.*<sup>37</sup> studied the covalent binding of the model pyrroles 1,3,4-trimethylpyrrole (32) and 1-methyl-3,4-*bis*(hydroxymethyl)pyrrole (39). Following administration to rats of the tritium labeled pyrrole derivatives covalent binding of their reactive metabolites to protein, DNA and RNA was observed. The extent to which 1,3,4-trimethylpyrrole (32) was found to bind covalently was approximately an order of magnitude greater than the more hydrophilic derivative 1-methyl-3,4-*bis*(hydroxymethyl)pyrrole (39).



32



39

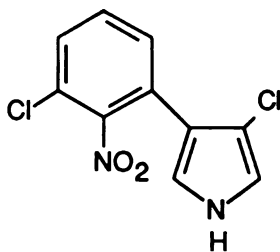
The proposal that the covalent binding of these pyrrole derivatives is due to cytochrome P-450 dependent bioactivation is supported by *in vitro* studies which showed that the covalent binding of **32** to liver microsomal fractions was inhibited by SKF 525-A, carbon monoxide, anaerobiosis and glutathione. Furthermore, reconstituted vesicles containing cytochrome P-450 and cytochrome P-450 reductase also catalyze the bioactivation of the trimethyl compound **32**.

To estimate the overall chemical reactivity of the metabolites of [ $^3\text{H}$ ]1,3,4-trimethylpyrrole, the half-life of this intermediate was determined. Following the removal of metabolically activated **32** from the incubation mixture by filtration through Celite, the reactive metabolite(s) was incubated with albumin and the irreversible binding determined. Under these conditions, the half-life of the reactive intermediate(s) was estimated to be approximately 90 min. This experiment suggests that reactive metabolites of **32** are stable enough to migrate through aqueous solutions before reacting with target nucleophiles. At concentrations up to 500 mg/kg, the trimethylpyrrole compound was not lethal when administered to rats. However, histological analysis revealed that **32** produced centrilobular necrosis in 3 out of 6 rats examined.

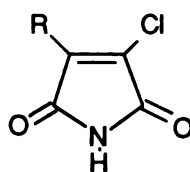
The cytochrome P-450 catalyzed bioactivation of **32** and **39** supports the view that oxidative metabolism of pyrrole containing compounds may lead to the formation of reactive and potentially cytotoxic metabolites. Guengerich *et al.*<sup>37</sup> postulates that

pyrrolizidine alkaloids may be subject to further metabolic activation through oxidation of the pyrrole substituent, a process which may contribute to its overall hepato- and pulmonary toxicities.

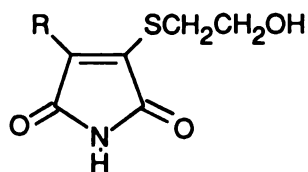
Pyrronitrin, 3-chloro-4-[2-nitro-3-chlorophenyl]pyrrole (33), is a broad-spectrum antifungal agent which is degraded metabolically *in vivo* and *in vitro*.<sup>38</sup> This compound is not recovered intact from either urine or bile following intraperitoneal administration to rats. The pyrrole ring of pyrronitrin is metabolized rapidly in a NADPH dependent manner by microsomal enzymes.<sup>38</sup> One of the key metabolites identified in this study was 4-chloro-3-(3-chloro-2-nitrophenyl)maleimide (67). Since maleimide derivatives are, in general, chemically reactive it was anticipated that covalent binding of 67 to protein might occur. To test this hypothesis, synthetic 67 was incubated with  $\beta$ -mercaptoethanol and found to form the thiol adduct 68, evidence which illustrates the bioalkylating potential of the maleimide 67.



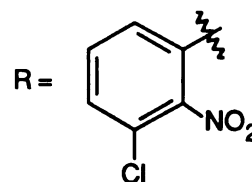
33



67



68





As suggested by the examples described above, oxidative metabolism of cyclopentadienoid heterocycles may lead to organ specific toxicities in individuals exposed to these compounds. The mechanism and the site of ring oxidation for this class of compounds is not well understood, although it has been proposed that the double bond adjacent to the heteroatom may be oxidized to a highly reactive arene oxide intermediate.<sup>27</sup> The difficulty in characterizing such a metabolite is consistent with the generally unstable and reactive nature of these intermediates. Because of the apparent reactivity and/or chemical instability of the bioactivated compounds, direct evidence for the existence of the ultimate reactive species has been difficult to obtain. As indicated above, attempts to identify the nature of the reactive species have employed various methods including the identification of the products formed between the ultimate reactive species and soluble nucleophiles such as glutathione,<sup>39</sup> characterization of the effects of epoxide hydratase inhibitors on the level of bioactivated intermediates which bind covalently to biomacromolecules,<sup>27</sup> and the structural characterization of the stable rearrangement products of these reactive intermediates.<sup>38</sup>

Although  $\beta$ -nicotyrine has been identified as a component of tobacco,<sup>3</sup> the relationship between its oxidative metabolism and the toxicities associated with tobacco use has not been explored. If the intermediates formed from the oxidative metabolism of  $\beta$ -nicotyrine are similar to those generated from the cyclopentadienoid species described above, it is possible that  $\beta$ -nicotyrine may also be toxic. In an effort to understand better its metabolic fate, the liver and lung microsomal metabolism of  $\beta$ -nicotyrine was examined. The chemical characterization of the principal metabolite of  $\beta$ -nicotyrine was also performed. Various analytical techniques including HPLC with mass spectral detection (LC-MS) coupled with collisional activated dissociation (CAD) mass spectrometry, GC-EIMS and diode array UV spectral analyses and chemical synthesis of the proposed metabolite were employed in order to elucidate the structure of

this enzymatically generated product. Characterization of one of the base catalyzed decomposition products is also described.

## Results

### Binding of $\beta$ -Nicotyrine to Unreduced Liver Cytochrome P-450: Characterization of Substrate Binding

Addition of  $\beta$ -nicotyrine tartrate to liver microsomes isolated from phenobarbital pretreated rabbits led to the formation of a type II binding spectra. At substrate concentrations less than 0.25 mM, the binding of  $\beta$ -nicotyrine to microsomal protein produced an absorption spectrum displaying a  $\lambda_{\max}$  at 427 nm and a  $\lambda_{\min}$  at 390 nm. As the concentration of substrate was raised above 0.25 mM, the  $\lambda_{\max}$  and  $\lambda_{\min}$  each shifted approximately 3 nm to 430 and 393 nm, respectively. The binding dissociation constant ( $K_S$ ) of 5.6  $\mu$ M, derived from the binding of  $\beta$ -nicotyrine to this unreduced microsomal preparation, was estimated by constructing a double reciprocal plot of  $1/\Delta$  Absorbance (426-393 nm) vs.  $1/[\beta\text{-nicotyrine } (\mu\text{M})]$  (Fig. VI.1.). This binding dissociation constant represents a high affinity binding of cytochrome P-450 by  $\beta$ -nicotyrine and is comparable to the binding dissociation constant values reported for endogenous cytochrome P-450 substrates (i.e. estrogens).<sup>40</sup> In comparison, (S)-nicotine has a much lower binding affinity ( $K_S = 400 \mu\text{M}$ ), characteristic of most type II substrates.<sup>41</sup>

### NADPH Dependent Formation of a $\beta$ -Nicotyrine Derived Metabolite

In order to study its microsomal metabolism,  $\beta$ -nicotyrine (500  $\mu$ M) was incubated in the presence or absence of NADPH with liver microsomes (2 mg/ml) isolated from rabbits pretreated with phenobarbital. Quantitative analysis by HPLC with UV detection at 284 nm revealed that approximately 80% of the starting material was consumed after 1 hr in the presence of NADPH. In the absence of NADPH, no meta-

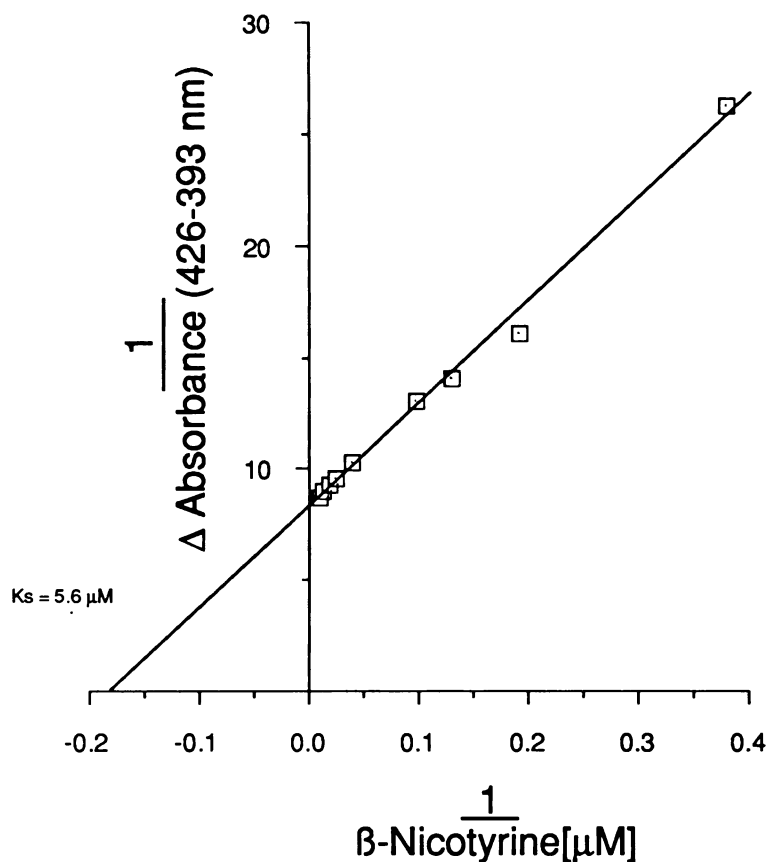


**Fig.VI.1.**  $\beta$ -Nicotyrine Binding to Unreduced Rabbit Liver Microsomes (1 mg/ml) Isolated from Phenobarbital Pretreated Rabbits. The binding dissociation constant ( $K_s$ ) was estimated by constructing a double reciprocal plot of  $1/\Delta$  Absorbance (426-393 nm) vs  $1/[\beta\text{-nicotyrine } (\mu\text{M})]$  and calculating the negative value of the x-intercept.

bolism was observed. Paralleling the time and NADPH dependent decrease in  $\beta$ -nicotyrine (retention time = 1.9-2.1 min) was the formation of a new peak arising at approximately 2.8 min (Fig.VI.2 and 3). Diode array UV spectral analysis of the metabolically formed peak revealed a UV spectrum with a  $\lambda_{\text{max}}$  at 232 nm indicating the loss of the pyrrolic moiety of  $\beta$ -nicotyrine which absorbs maximally at 284 nm (Fig.VI.3 Inset).

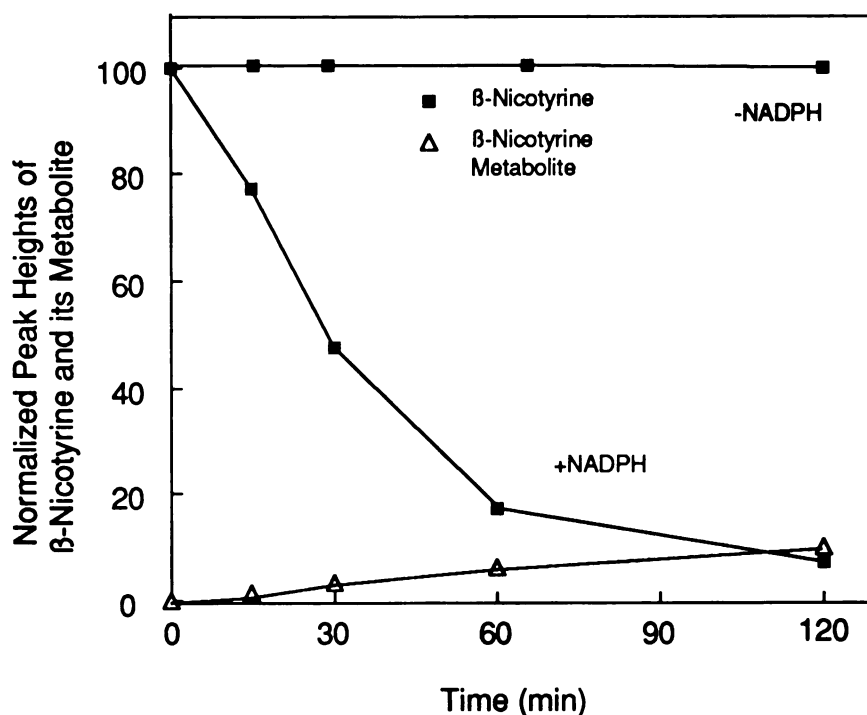
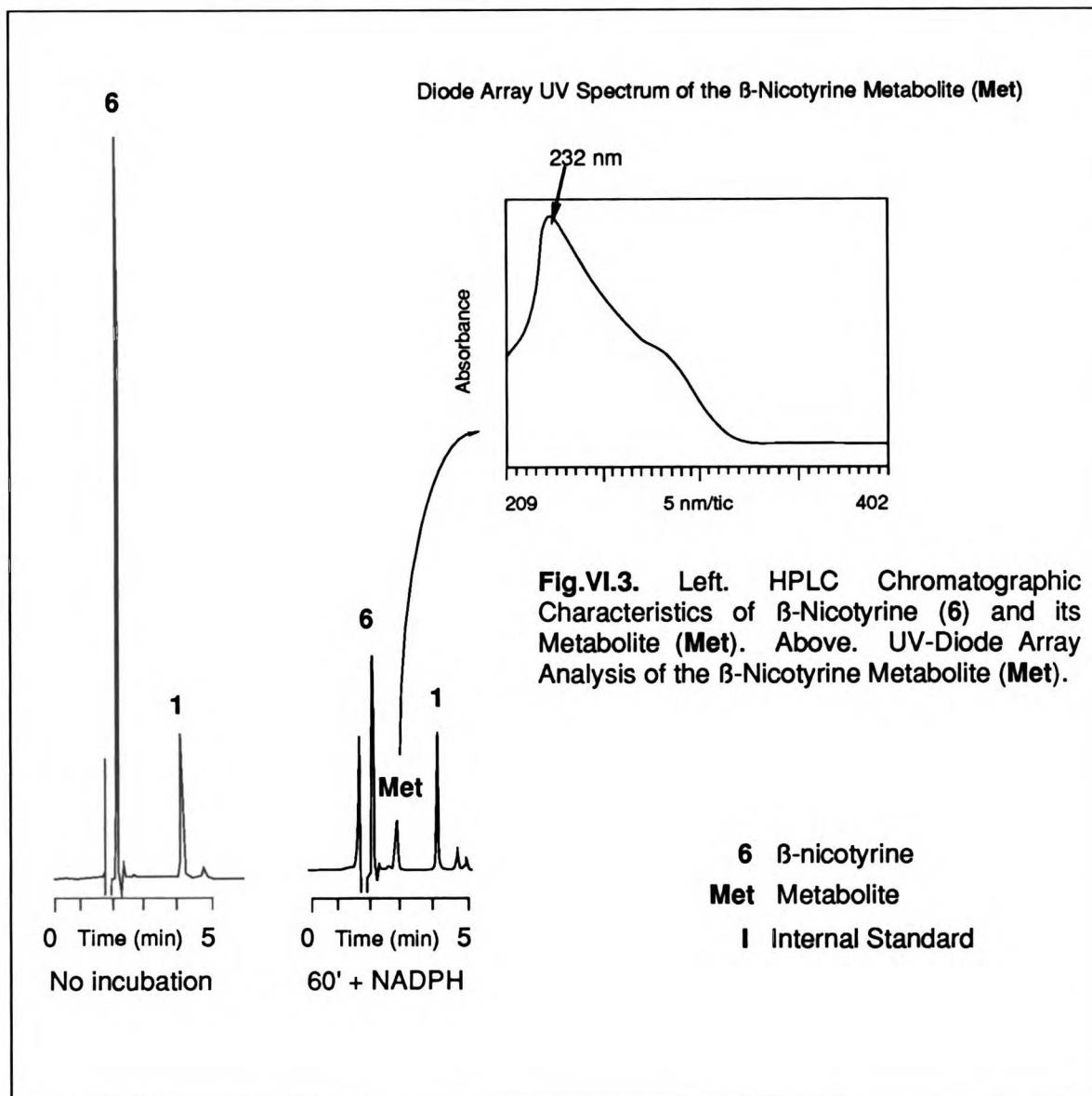


**Fig.VI.2** Liver Microsomal Metabolism of  $\beta$ -Nicotyrine.  $\beta$ -Nicotyrine (0.5 mM) was incubated with liver microsomes (2 mg protein/ml) for the indicated time periods. Metabolism of  $\beta$ -nicotyrine was monitored by HPLC with UV detection at 284 nm with (S)-nicotine as an internal standard. The formation of the metabolite could not be quantitated although the relative amount formed was estimated by the ratios of peak height of the metabolite vs. (S)-nicotine.

### $\beta$ -Nicotyrine Metabolism by Lung Microsomes

The role of lung microsomal enzymes in the metabolism of  $\beta$ -nicotyrine was examined next.  $\beta$ -Nicotyrine (100  $\mu$ M) was incubated with lung microsomes (1 mg/ml) prepared from New Zealand White rabbits and the extent of oxidation was measured over a 1 hr period (Fig.VI.4). For comparison,  $\beta$ -nicotyrine metabolism by liver microsomes prepared from these animals was also assessed. Oxidative metabolism of  $\beta$ -nicotyrine, which for both preparations was linear over the initial 15 min, proceeded at a rate of 1.7 and 2.7 nmoles $\cdot$ mg protein $^{-1}\cdot$ min $^{-1}$  for the lung and liver



microsomal incubations, respectively. However, when these rates were expressed as a function of cytochrome P-450 content, the specific activity of the metabolic oxidation catalyzed by lung (8.3 nmoles  $\beta$ -nicotyrine oxidized  $\cdot$  nmole cytochrome P-450<sup>-1</sup>  $\cdot$  min<sup>-1</sup>) was approximately 4-fold greater than the corresponding rate with liver microsomes (2.3 nmoles  $\beta$ -nicotyrine oxidized  $\cdot$  nmole cytochrome P-450<sup>-1</sup>

$\cdot\text{min}^{-1}$ ). The difference in the specific activities of the two microsomal preparations indicates that compared to liver the lung contains a higher proportion of the cytochrome P-450 isozyme which catalyzes the oxidation of this compound. Based on the reported composition of rabbit lung cytochrome P-450, it is likely that isozyme-2 and/or -5 catalyzes this oxidation.<sup>42</sup> Studies described in the addendum of this chapter will examine the role of these isozymes in the oxidation of  $\beta$ -nicotyrine.

#### **Inhibition of $\beta$ -Nicotyrine Oxidase: Role of Cytochrome P-450 In the Oxidation of $\beta$ -Nicotyrine**

The role of liver and lung cytochrome(s) P-450 in the oxidative metabolism of  $\beta$ -nicotyrine was examined under various conditions (Table VI.1). The substrate was recovered quantitatively when the incubations were performed at 4°C or in the absence of NADPH. N-Octylamine (3.0 mM), an inhibitor of cytochrome P-450 oxidases but an activator of the NADPH dependent flavin containing monooxygenase (FCM),<sup>43</sup> inhibited the oxidation of  $\beta$ -nicotyrine in both microsomal preparations by approximately 80%. Somewhat unexpected was the weak inhibitory properties of SKF 525-A (0.25 mM).  $\beta$ -Nicotyrine metabolism was inhibited in the presence of this cytochrome P-450 inhibitor by only 27 and 12% for the liver and lung preparations, respectively. On the other hand, N-hydroxyamphetamine (NOHA), a compound which inhibits cytochrome P-450 isozymes through the formation of metabolic intermediate complexes,<sup>44</sup> also blocked the liver and lung microsomal oxidation of  $\beta$ -nicotyrine by 85 and 93%, respectively. Incubations performed in the presence of argon inhibited the liver microsomal metabolism by approximately 90% but the lung microsomal activity by only 46%. The relatively poor inhibition of  $\beta$ -nicotyrine metabolism in the lung microsomal incubations may be due to the difficulty of completely removing oxygen from this oxygen rich tissue. NaCN (0.5 mM), an inhibitor of the cytochrome P-450 catalyzed oxidation of (S)-nicotine, did not inhibit  $\beta$ -nicotyrine metabolism. In both

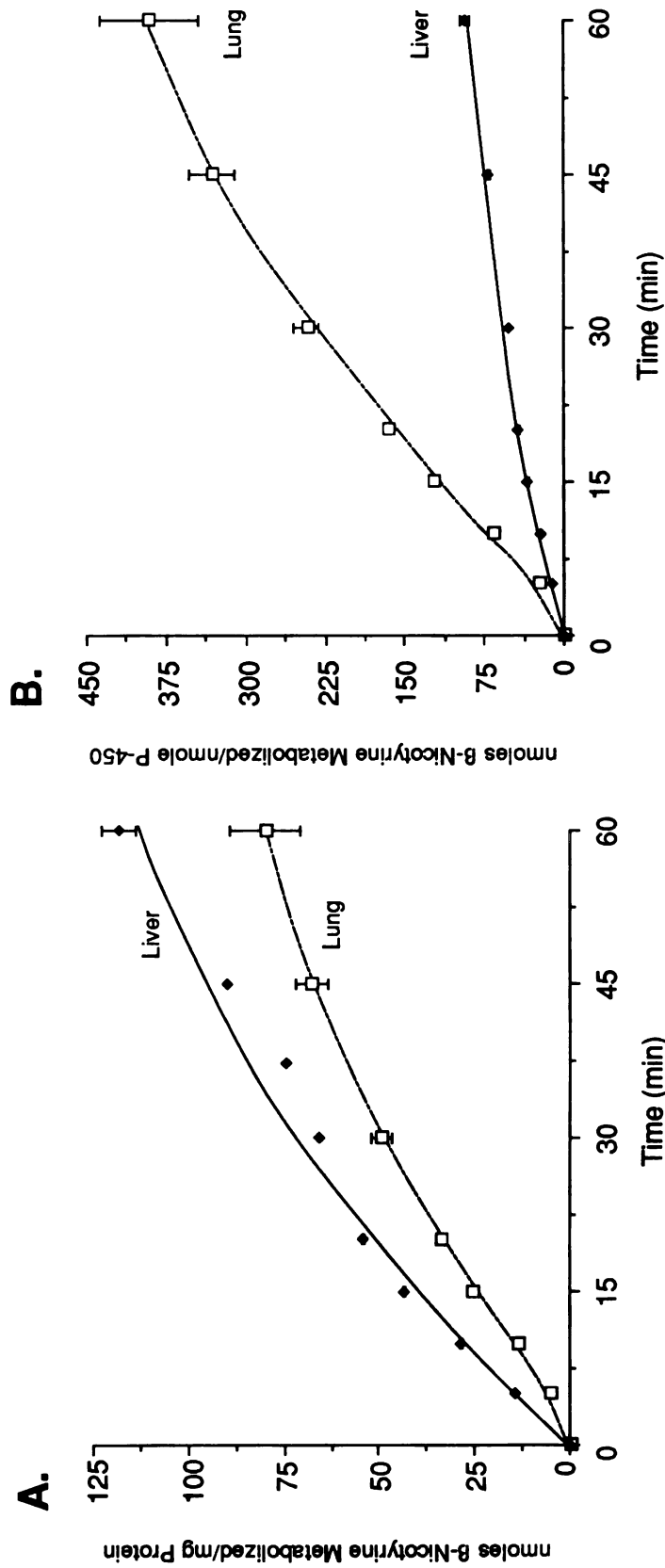


**Fig. VI.4** Comparison Between the Liver and Lung Microsomal Metabolism of  $\beta$ -Nicotyrine per (A). mg of Microsomal Protein or (B). nmol Cytochrome P-450.

microsomal preparations, formation of the  $\beta$ -nicotyrine metabolite was inhibited by approximately the same extent as the metabolism of the parent compound (data not shown). These data support the proposal that the microsomal metabolism of  $\beta$ -nicotyrine is cytochrome P-450 mediated.

**Table VI.1** Effect of Various Treatments on the Microsomal Metabolism of  $\beta$ -Nicotyrine.  $\beta$ -Nicotyrine tartrate (0.5 or 0.1 mM) was incubated with untreated liver or lung rabbit microsomes, respectively, for 20 min at 37°C .

Treatment	Liver		Lung	
	$\beta$ -Nicotyrine <sup>1</sup> Metabolized	% Control	$\beta$ -Nicotyrine <sup>1</sup> Metabolized	% Control
Complete (control)	96.8 $\pm$ 11.8	100	31.6 $\pm$ 1.1	100
NADPH omitted	3.6 $\pm$ 1.8	4	ND	0
4°C	101.7 $\pm$ 4.3	- 5	0.9 $\pm$ 1.2	3
n-Octylamine (3.0 mM) <sup>2</sup>	18.5 $\pm$ 2.0	19	5.8 $\pm$ 0.4	18
NOHA (0.67mM) <sup>2</sup>	14.7 $\pm$ 2.7	15	2.3 $\pm$ 0.1	7
SKF 525-A (0.25 mM)	70.3 $\pm$ 3.3	73	27.7 $\pm$ 0.5	88
Argon	9.4 $\pm$ 9.3	10	17.0 $\pm$ 3.0	54
NaCN (0.5 mM)	96.3 $\pm$ 4.9	99	33.1 $\pm$ 1.8	105

<sup>1</sup> nmoles  $\beta$ -nicotyrine metabolized/mg protein/20 min

<sup>2</sup> preincubated for 30 min at room temperature

ND-not detected

Values are expressed as the mean (n = 2-4)  $\pm$  S.E.

### $\beta$ -Nicotyrine Metabolite: Stability Studies

Attempts to isolate the liver and lung microsomal metabolite of  $\beta$ -nicotyrine using the 0.5% n-propylamine/acetonitrile mobile phase proved unsuccessful because of its tendency to undergo autoxidation. The attempted isolation of the  $\beta$ -nicotyrine metabolite involved HPLC purification of the methylene chloride extract obtained from a potassium carbonate terminated incubation mixture. The peak corresponding to the metabolite was collected and pooled with other fractions obtained from multiple injections of this extract. Reanalysis of this pooled material within hours of collection showed that the metabolite peak had decomposed by approximately 30%. By day 2, the



metabolite peak was undetectable indicating the unstable nature of this molecule under the conditions used for its isolation. The possibility of base-catalyzed decomposition led us, in a second attempt, to freeze the incubation mixture at  $-20^{\circ}\text{C}$  in the incubation buffer, pH 7.6. However, after 6 weeks of storage under these conditions the metabolite had undergone complete decomposition.

The chemical stability of the metabolite under basic, acidic and physiological pH conditions was examined in an effort to obtain clues which could explain the chemical nature of the decomposition process. The stability of the metabolite under basic conditions was tested by adding an equal volume of 1 M  $\text{K}_2\text{CO}_3$  to metabolic incubation mixtures containing the metabolite. This mixture was extracted at various time points and analyzed by HPLC with UV detection. Under these conditions, the metabolite decomposed rapidly with a half-life of approximately 5 min (Fig.VI.5). Exposure of the metabolite to 1 N HCl for various periods of time prior to extraction and HPLC analysis led to a less rapid rate of decomposition. The half-life of the metabolite under these conditions was approximately 100 min. The metabolite did not undergo measurable decomposition over a 180 min period at pH 7.6.

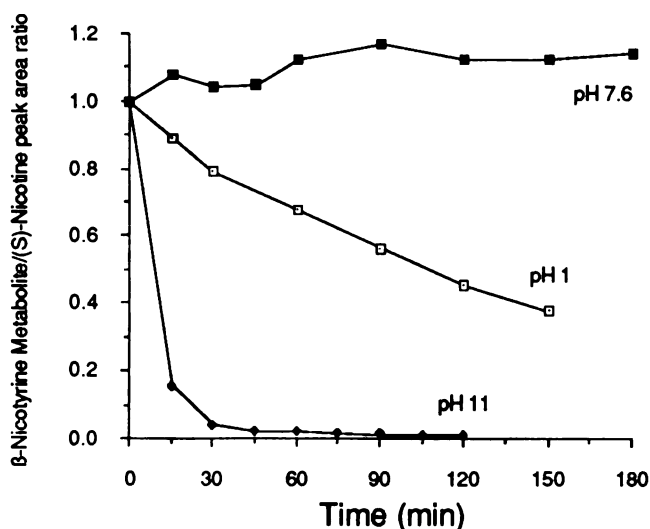
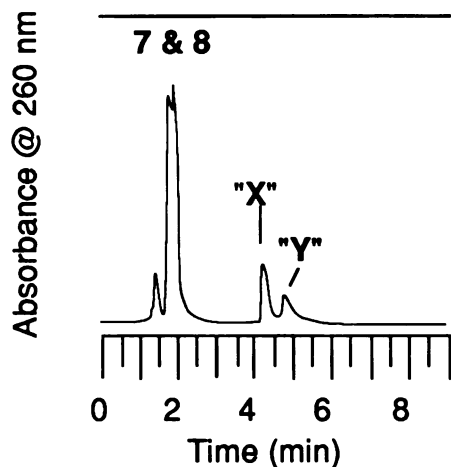


Fig.VI.5 Stability of the  $\beta$ -Nicotyrine Derived Metabolite at pH 1, 7.6 and 11

One of the limitations of the study described above was the inability to trace the decomposition of the metabolite. In an effort to understand this process better, studies aimed at identifying the unextractable decomposition products of the metabolite were performed. Methylene chloride extracts of potassium carbonate terminated reaction mixtures were spiked with the internal standard (S)-nicotine, concentrated *in vacuo*



**Fig.VI.6** HPLC analysis of the  $\beta$ -Nicotyrine Metabolite and its Two Base-Catalyzed Decomposition Products "X" and "Y". The internal standard (S)-nicotine was not included in the sample which yielded this chromatogram.

and passed through a normal phase silica HPLC column. The HPLC effluent corresponding to the elution times of the metabolite (1.03 min) and (S)-nicotine (2.3 min) was collected. At various time points following this collection, aliquots were reanalyzed by HPLC and the peak area ratios (metabolite/(S)-nicotine) calculated (Fig.VI.6 and 7). In less than 2 hr following the initial collection, the metabolite peak had decreased in intensity by greater than 50%. An increase in a second peak eluting with a retention time of 4.3 min paralleled the decrease in the metabolite peak indicating that it was derived from this metabolite. UV diode array analysis of this decomposition product "X" revealed a UV spectrum with a  $\lambda_{\max}$  at 256 nm (Fig.VI.8). This compound apparently was also unstable since it too disappeared with time giving rise to a third peak (decomposition product "Y") which exhibited a retention time of 4.8 min. UV diode array analysis of this decomposition product "Y" revealed a UV spectrum with a  $\lambda_{\max}$  at

256 nm. Although more stable than either the metabolite or decomposition product "X", this compound also decomposed with time (See Inset Fig.VI.7).

### HPLC-Mass Spectral Characterization of the $\beta$ -Nicotyrine Metabolite

In our initial attempts at characterizing the chemical structure of the principal metabolite of  $\beta$ -nicotyrine, a methylene chloride extract of a liver microsomal incubation of  $\beta$ -nicotyrine was analyzed by HPLC with mass spectral detection (LC-MS). Prior to the analysis of the  $\beta$ -nicotyrine metabolite and its decomposition products, the HPLC-CI/MS and HPLC-collision activated dissociation (CAD)/MS of  $\beta$ -nicotyrine tartrate were performed in order to obtain reference spectra. The ion current corresponding to  $\beta$ -nicotyrine appeared on the HPLC chromatogram at approximately 15 min. CI/MS analysis of this peak using methane as the reagent gas yielded a base peak at  $m/z$  159, corresponding to the protonated molecular ion  $[MH]^+$ . Ions corresponding to  $m/z$  at 187 and 199, which were present at a relative abundance of less than 10% each, are consistent with the methane adduct species  $[M + 29]^+$  and  $[M + 41]^+$ , respectively. CAD/MS was performed next on  $\beta$ -nicotyrine tartrate. This technique involves the bombardment of a selected precursor ion (e.g. the molecular ion) with a collisional gas such as argon, resulting in its dissociation to daughter ions which are then detected by the third quadrupole. HPLC-CAD/MS analysis of this reference standard produced prominent ions at  $m/z$  of 159, 144, 117 and 91 (Fig.VI.9). HPLC-MS analysis of the methylene chloride extract of a metabolic incubation containing  $\beta$ -nicotyrine and liver microsomes isolated from rabbits pretreated with phenobarbital, produced a total ion chromatogram with peaks corresponding to the retention times of  $\beta$ -nicotyrine (16.9 min) and the metabolite (26.7 min) (Fig.VI.10). The peaks eluting at 11.2 and 14.4 min were artifacts of the metabolic incubation or workup procedure since the same two peaks were observed in methylene chloride extracts of incubations performed in the absence of substrate. HPLC-CI/MS of

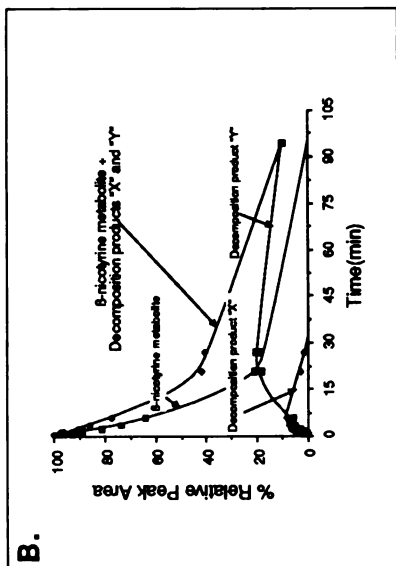
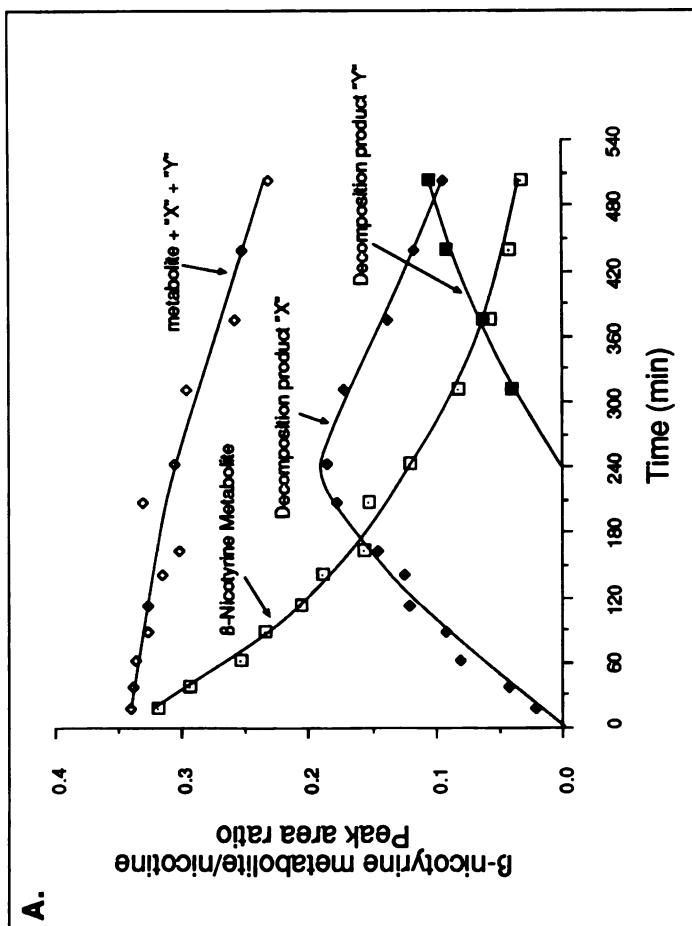
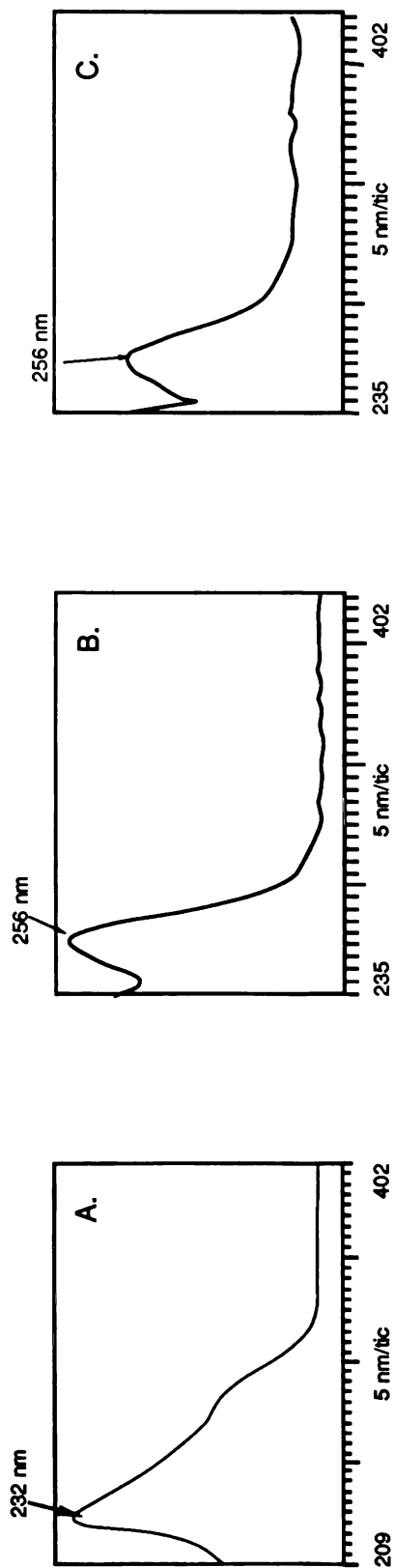
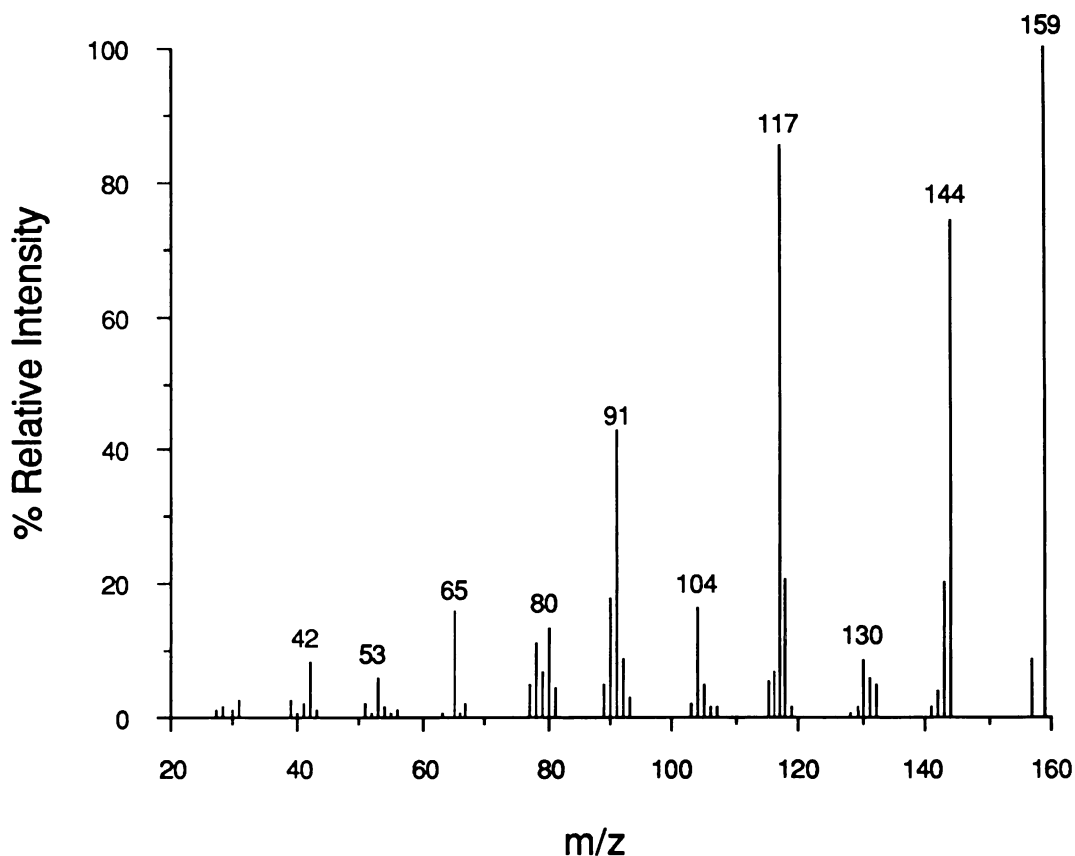


Fig. VI.7 Stability of the  $\beta$ -Nicotyrine Metabolite in the Presence of A) 0.5% n-Propylamine/Acetonitrile B) 3.0% n-Propylamine/Acetonitrile; Formation of Two Base-Catalyzed Decomposition Products vs. Time.





**Fig. VI.8** UV Diode Array Spectra of (A). the  $\beta$ -Nicotyrine Metabolite and (B). the Base-Catalyzed Decomposition Product "X" and (C). Decomposition Product "Y".



**Fig.VI.9** HPLC-CAD/MS of the  $m/z$  159 Precursor Ion Derived from  $\beta$ -Nicotyrine

the metabolite peak yielded a base ion at  $m/z$  175 (Fig.VI.11). Ions at  $m/z$  189, 203, and 215, which were present at a relative abundance of less than 5%, are most likely attributed to the formation of the corresponding methane adduct species  $[M + 15]^+$ ,  $[M + 29]^+$  and  $[M + 41]^+$ , respectively. In the absence of NADPH, the ion current at  $m/z$  175 was negligible, indicating that the appearance of this peak was metabolism dependent.

The molecular ion at  $m/z$  175 is consistent with the net addition of one oxygen atom to  $\beta$ -nicotyrine. Candidate compounds which are consistent with this addition include the pyridine N-oxide analog 47, the arene oxide analog 48, 2'-hydroxy  $\beta$ -nicotyrine (49) or the dehydrocotinine species 7 and 8 (Fig.VI.12). The absence of any significant fragment ions in this spectrum led us to examine the daughter ion

spectrum of the protonated parent ion by argon induced CAD/MS. This spectrum (Fig.VI.13) revealed a series of daughter ions some of which were tentatively assigned as shown in Table VI.2. Of these daughter ions,  $m/z$  117, 104 and 78 were also observed when  $\beta$ -nicotyrine tartrate was analyzed by LC-CAD/MS and are consistent

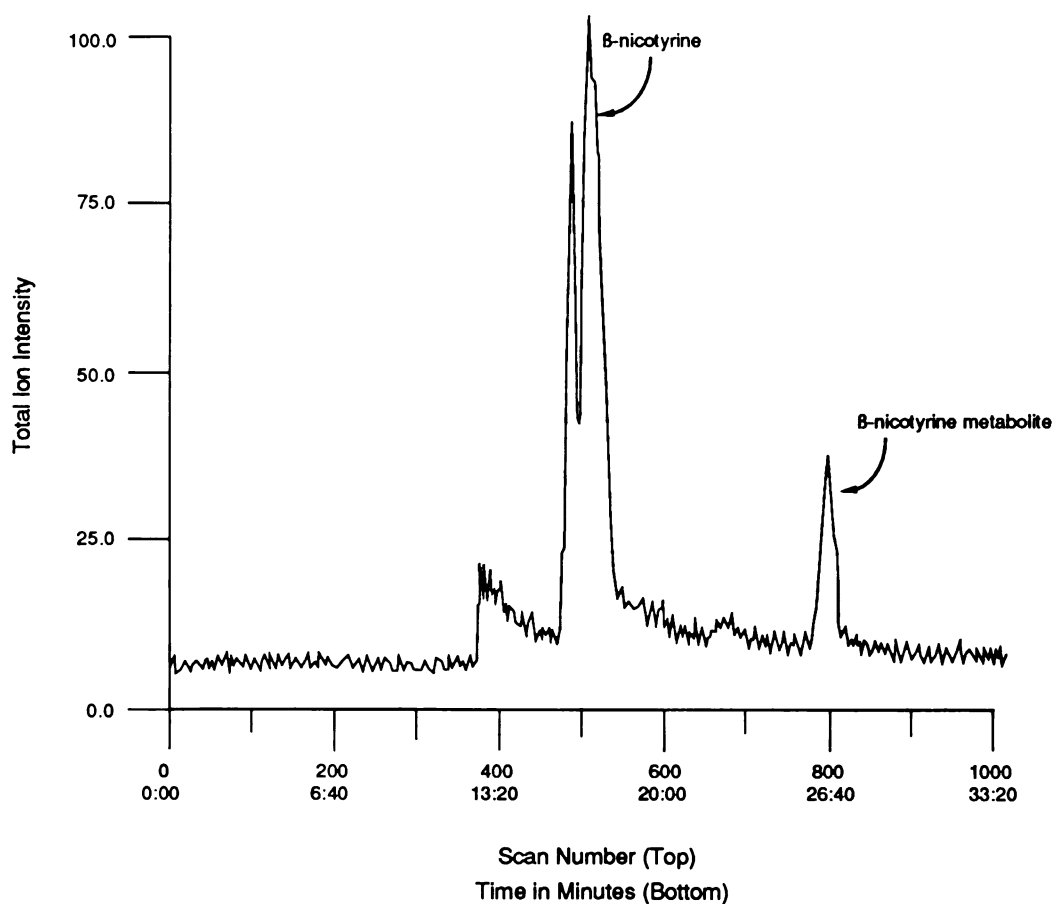


**Fig.VI.10** Total Ion Chromatogram Obtained from the HPLC-CI/MS Analysis of  $\beta$ -Nicotyrine and its Metabolite

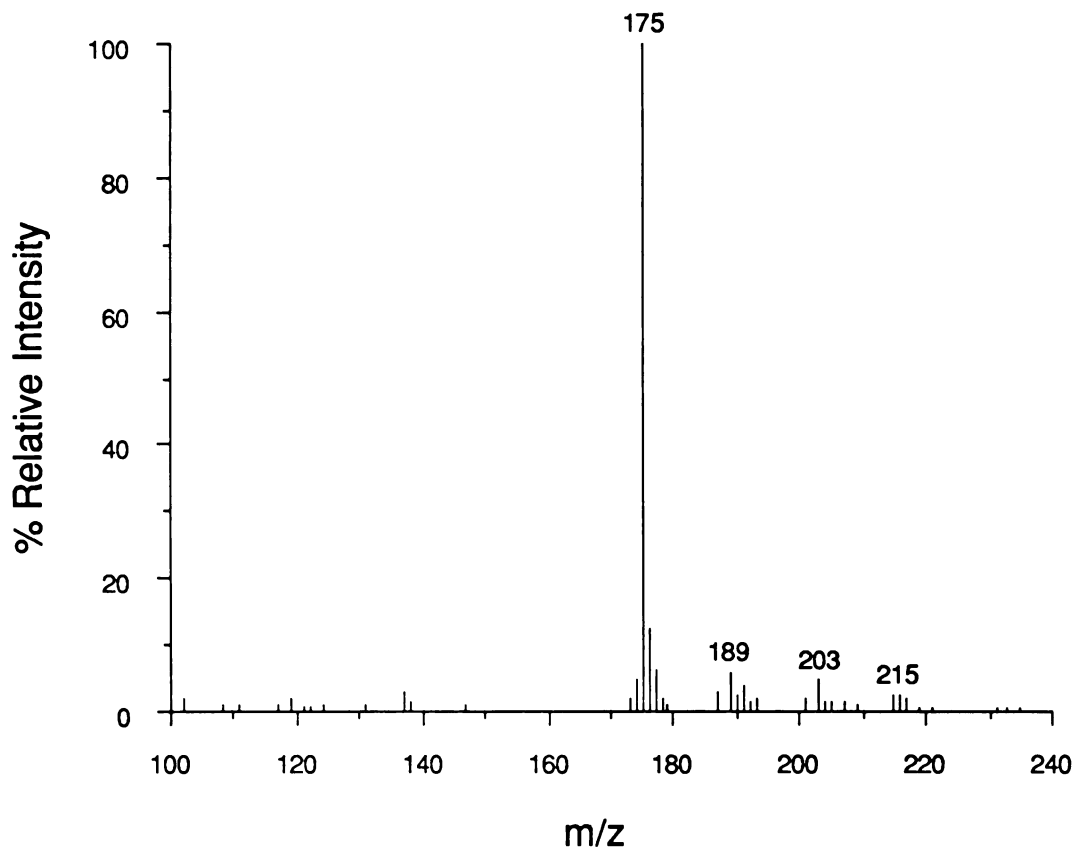


Fig.VI.11 HPLC-Cl/MS of the  $\beta$ -Nicotyrine Metabolite

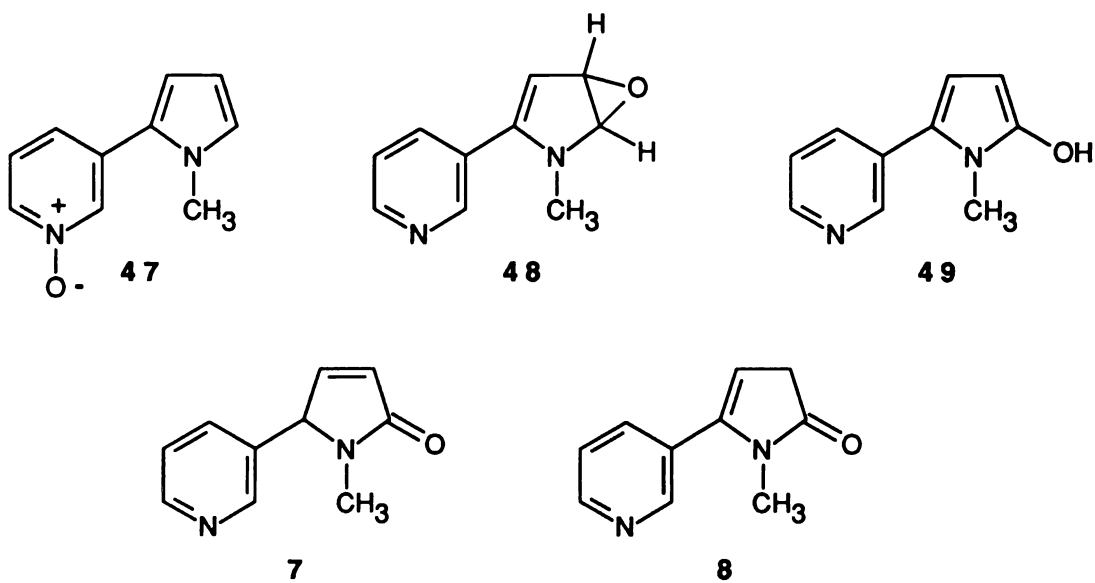
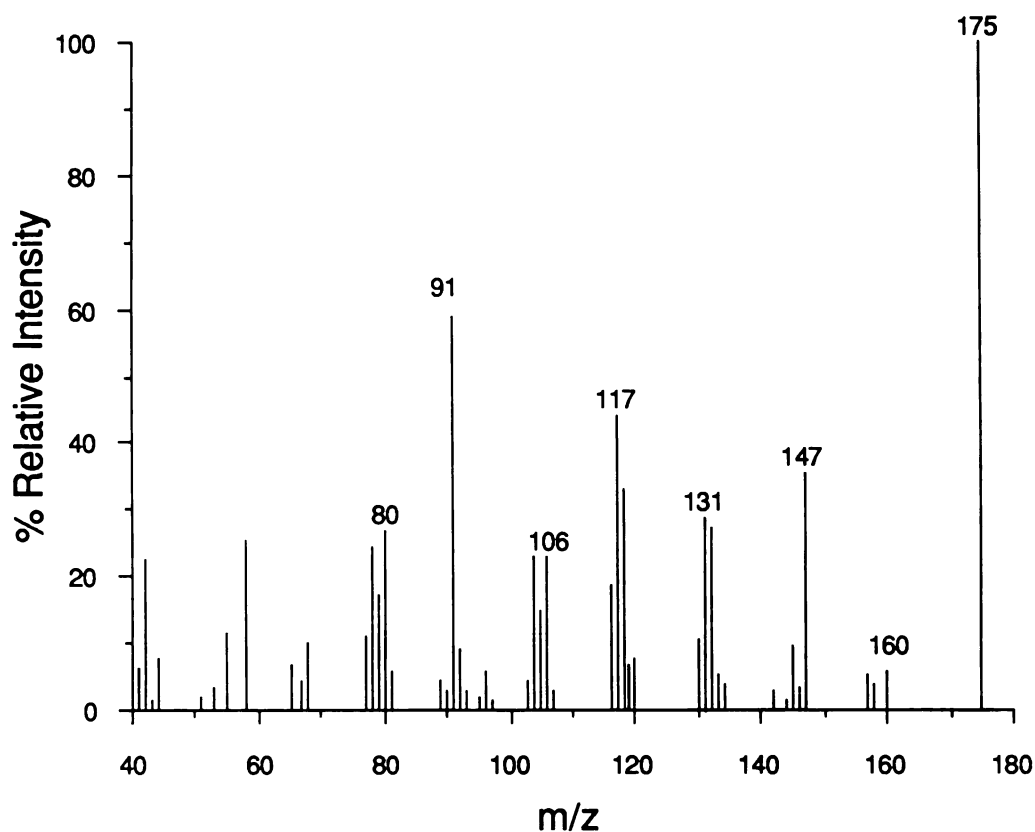


Fig.VI.12 Candidate Structures for the  $\beta$ -Nicotyrine Metabolite





**Fig.VI.13** CAD/MS of the  $m/z$  175 Precursor Ion Derived from the  $\beta$ -Nicotyrine Metabolite

with the assignments  $[\text{PyCH}_3\text{H}_3^+]$ ,  $[\text{PyCH}_2\text{H}_2^+]$  and  $[\text{Py}^+]$ , respectively, made for the daughter ion spectrum of the protonated parent ion of the metabolite. This interpretation of the spectrum ruled out modification of the pyridyl group in this structure since the assignments of most of the fragment ions (i.e.  $m/z$  117, 104 and 78) required the presence of a  $\text{C}_6\text{H}_4\text{N}$  (unmodified pyridyl) moiety. The assignments for product ions involving loss of CO (Table VI.2.iii, iv, v) and NCO (Table VI.2.vi, vii, x) indicated the presence of an NCO moiety that would result from the introduction of an oxygen atom at C-2 or C-5 of the  $\beta$ -nicotyrine N-methylpyrrole system. Although arene oxides such as 48 (See Scheme VI.3) are possible structures,  $\alpha$ -amino epoxides, if formed, are likely to be only transient intermediates that would undergo spontaneous cleavage of the epoxide ring. Based on these considerations, the

pyrrolinones **7** and **8** (Scheme VI.2) appeared to be the most likely structures for the metabolite.

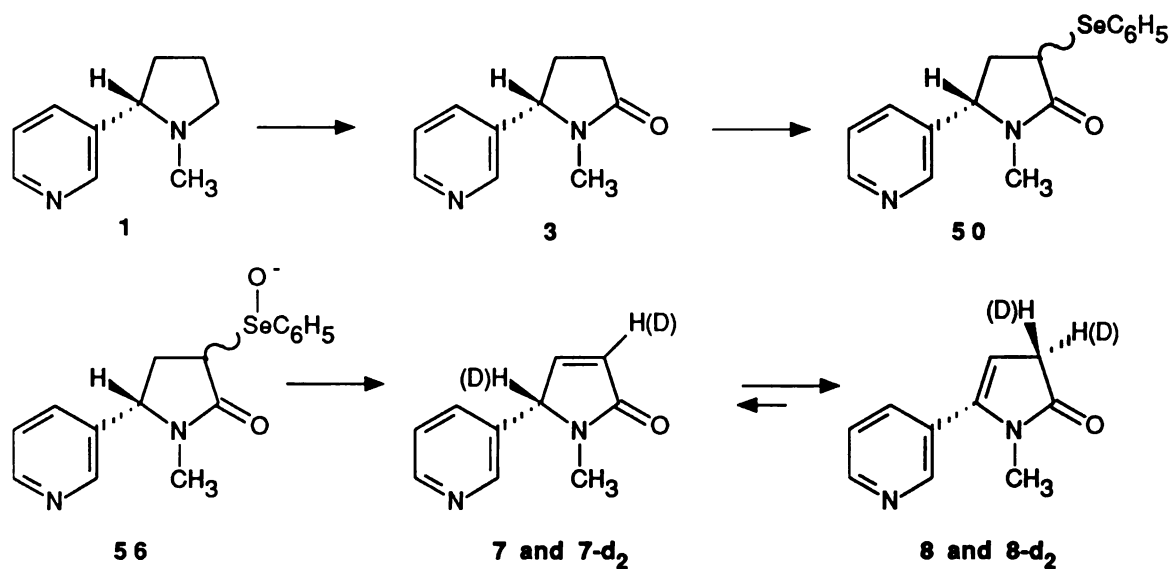
**Table VI.2** Daughter ions from the m/z 175 Precursor Ion Derived from the  $\beta$ -Nicotyrine Metabolite

Ion	m/z	%	Ion Composition	Fragment Lost
i	175	100	(PyC <sub>5</sub> H <sub>6</sub> NO)H <sup>+</sup>	- - - -
ii	160	15	(PyC <sub>4</sub> H <sub>3</sub> NO)H <sup>+</sup>	<sup>•</sup> CH <sub>3</sub>
iii	147	40	(PyC <sub>4</sub> H <sub>6</sub> N)H <sup>+</sup>	CO
iv	132	30	(PyC <sub>3</sub> H <sub>3</sub> N)H <sup>+</sup>	CH <sub>3</sub> , CO
v	131	30	(PyC <sub>3</sub> H <sub>2</sub> N)H <sup>+</sup>	H <sup>•</sup> <sup>•</sup> CH <sub>3</sub> , CO
vi	118	35	PyC <sub>3</sub> H <sub>4</sub> <sup>+</sup>	CH <sub>3</sub> NCO
vii	117	50	PyC <sub>3</sub> H <sub>3</sub> <sup>•+</sup>	CH <sub>3</sub> NHC <sup>•</sup> O
viii	106	25	??	??
ix	104	25	PyC <sub>2</sub> H <sub>2</sub> <sup>+</sup>	CH <sub>3</sub> NCOC <sup>•</sup> H <sub>2</sub>
x	80	30	Ar <sup>+</sup>	- - - -
xi	78	30	Py <sup>+</sup>	CH <sub>3</sub> NC <sub>4</sub> H <sub>4</sub> O

### Synthesis of $\Delta^{3',4'}$ - and $\Delta^{4',5'}$ -Dehydrocotinine

These conclusions prompted us to undertake the synthesis of the pyrrolinone **7** which we expected could be prepared from (S)-nicotine (**1**) via (S)-cotinine (**3**) according to the route shown in Scheme VI.2. The conversion of (S)-cotinine to the corresponding phenylselenenyl derivative **50** was achieved according to a literature report.<sup>45</sup> Oxidation of **50** with hydrogen peroxide yielded the corresponding selenenyl oxide derivative **56** which underwent spontaneous elimination. The mixture resulting from this reaction proved to be difficult to purify. Column chromatography led to a poor yield of a pure, crystalline product. The HPLC retention time, HPLC-diode array UV spectrum (Fig.VI.14) and HPLC-Cl/MS-CAD/MS of the protonated molecular ion (m/z 175) of this synthetic product were essentially identical to those observed for the  $\beta$ -nicotyrine metabolite. Upon storage in 0.5% n-propylamine/acetonitrile, the

synthetic material also underwent autoxidation to the same decomposition products (unknown "X" and unknown "Y") observed with the metabolite.



Scheme VI.2 Synthesis of Pyrrolinones 7 and 8

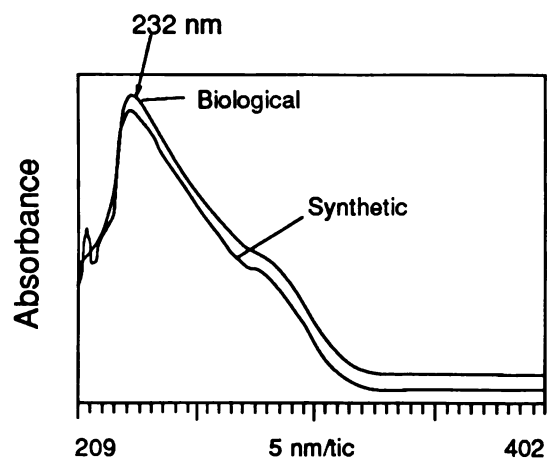


Fig.VI.14 Diode-Array UV Spectra of Synthetic 8 and the  $\beta$ -Nicotyrine Metabolite

The  $^1\text{H}$  NMR spectrum of this synthetic product displayed only one olefinic proton signal as a triplet centered at  $\delta$  5.4 ppm. Decoupling experiments established that this

signal was coupled to a 2-proton doublet centered at  $\delta$  3.18 ppm. These spectral data established the structure of this product as the 4,5-pyrrolinone **8**. Since the 3,4-pyrrolinone **7** must be the initial product formed following elimination of PhSeOH from **56**, **8** must be formed via rearrangement of **7**. Consistent with this sequence,  $^1\text{H}$  NMR analysis showed that the remaining oily fractions obtained from the column were mixtures of **8** and up to 30% of a second compound which was assigned the structure of the 3,4-pyrrolinone isomer **7**. The presence of two, coupled olefinic proton signals centered at  $\delta$  6.25 [C(4)-H] and 7.00 ppm [C(3)-H] were taken as definitive structural evidence for this assignment.

#### Deuterium Exchange Experiment

GC-EIMS analysis of toluene:butanol (7:3) extracts obtained from  $\text{D}_2\text{O}$  incubation mixtures of synthetic **8** showed that **7** and **8** are in equilibrium in aqueous solution. The total ion chromatogram revealed two peaks in a ratio of approximately 1:3 with retention times of 9.406 and 9.581 min, respectively (Fig.VI.15). The EI mass spectrum of the minor product displayed ions at  $m/z$  176 (100%), 175 (25%) and

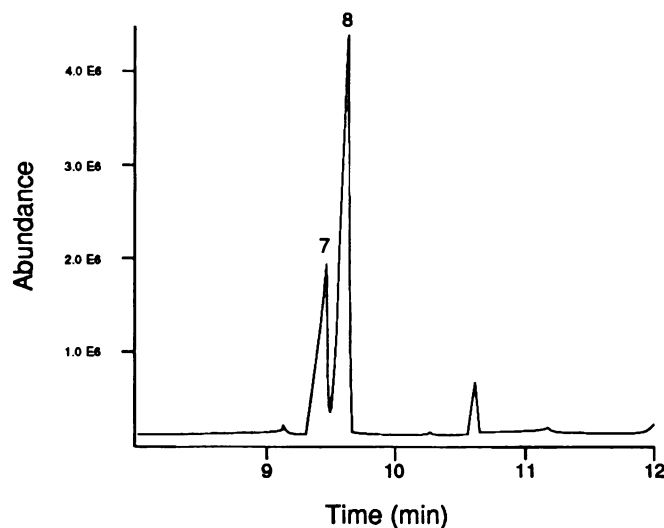


**Fig.VI.15** Total Ion Chromatogram Obtained from the Capillary GC-EIMS Analysis of Synthetic **7** and **8** Incubated in Deuterated Phosphate Buffer

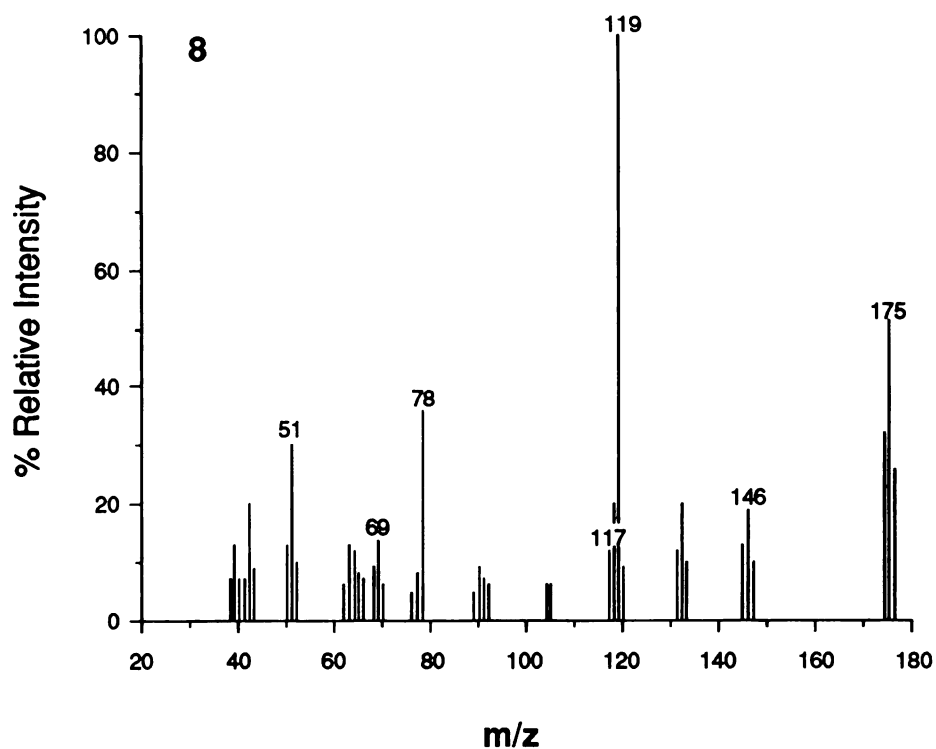
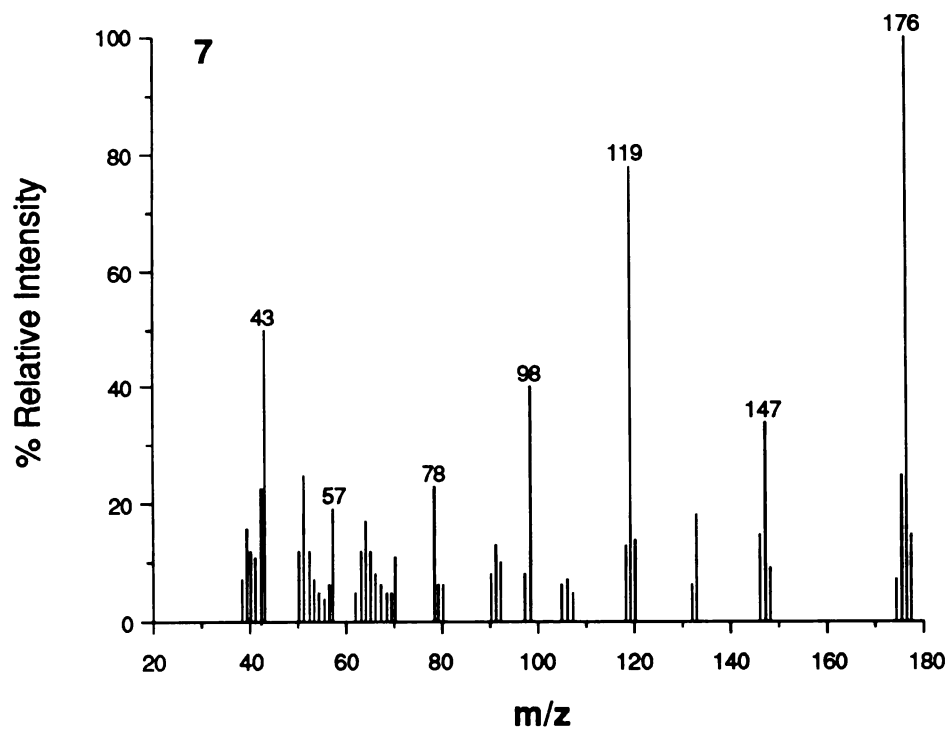


**Fig.VI.16** Electron Impact Mass Spectra of 7 (Top) and 8 (Bottom) Following Incubation in Deuterated Phosphate Buffer

174 (7%) corresponding to the parent ions of the  $d_2$ ,  $d_1$  and  $d_0$  containing species, respectively (Fig.VI.16). Fragment ions corresponding to the loss of  $\text{CH}_3$  [ $m/z$  161 (40%)],  $\text{CH}_3\text{NCO}$  [ $m/z$  119 (80%)] and pyridyl [ $m/z$  98 (40%)] have led us to assign the structure of this compound to the  $\Delta^{3',4'}$ -isomer 7. The corresponding spectrum of the major product [ $m/z$  176 (26%)], 175 (51%) and 174 (32%)] lacked the fragment

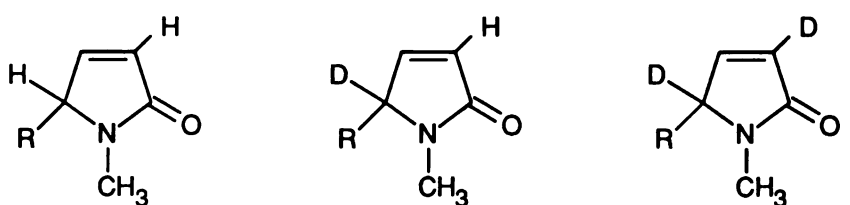
**Table VI.3** Deuterium Exchange and Back-Exchange Experiment

Incorporation of deuterium into the  $\Delta^{3',4'}$ -isomer 7 and  $\Delta^{4',5'}$ -isomer 8 in deuterated 0.05 M sodium phosphate buffer: Evidence for equilibrium between 7 and 8 and back-exchange of deuterium with protons derived from the extracting solvent toluene/butanol (7:3).

m/z	Day 1 analyzed 15 min post extraction		Day 2 analyzed 24 hr post extraction	
	(relative ion intensities)		(relative ion intensities)	
	7	8	7	8
174 $d_0$	7	32	54	73
175 $d_1$	25	51	89	38
176 $d_2$	100	26	64	7

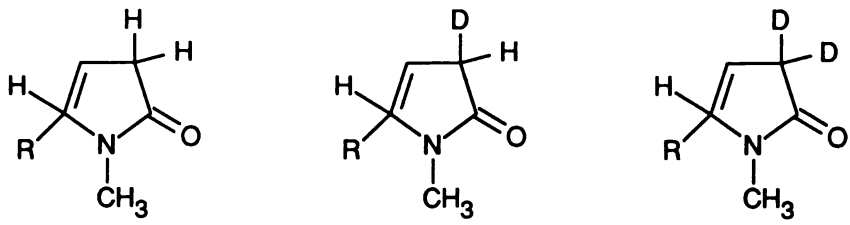
7



R = Pyridyl

8



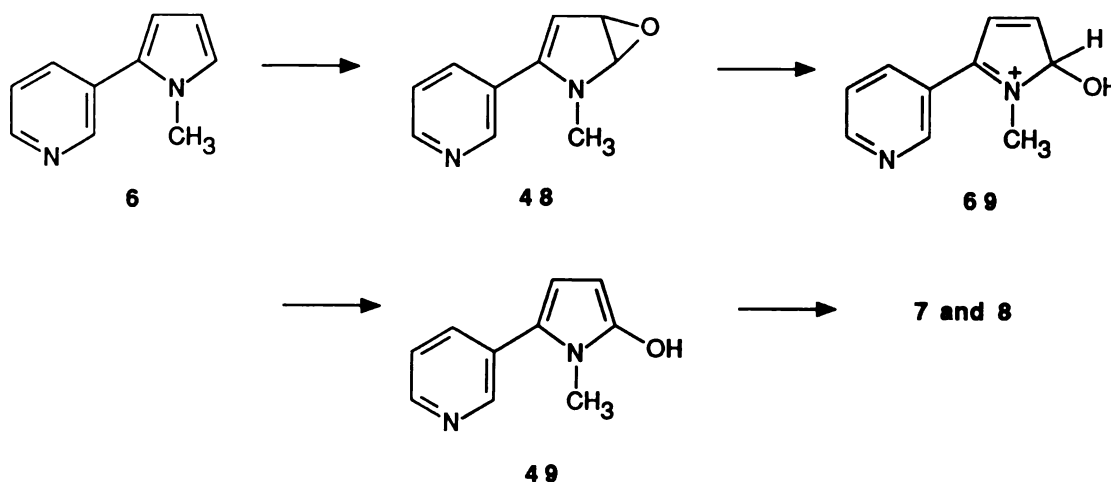
174

175

176

ion corresponding to pyridyl ( $m/z$  98), fully consistent with the  $\Delta^{4',5'}$ -isomer **8**. The structures of the dideutero isomers are therefore designated as **7-d<sub>2</sub>** and **8-d<sub>2</sub>**. Upon standing for 24 hr in the toluene:butanol extract, the deuterium content of the  $\Delta^{4',5'}$ -isomer [ $m/z$  176 (7%), 175 (38%) and 174 (73%)] decreased more than that of the  $\Delta^{3',4'}$ -isomer [ $m/z$  176 (64%), 175 (89%) and 174 (54%)] probably due to the more rapid back-exchange of the  $\Delta^{4',5'}$ -isomer in the toluene:butanol extract. These data, which are summarized in **Table VI.3**, indicate that the pyrrolinone isomers **7** and **8** exist in equilibrium in aqueous solutions, which may explain some of the difficulties encountered in the isolation and recrystallization of synthetic **8** described earlier.

Based on these results the cytochrome P-450 catalyzed oxidation of  $\beta$ -nicotyrine can be visualized as proceeding via a pathway that leads to an unstable intermediate such as the arene oxide **48**. This intermediate rearranges to 1-methyl-2-(3-pyridyl)-5-



**Scheme VI.3** Proposed Cytochrome P-450 Catalyzed Oxidation Pathway of  $\beta$ -Nicotyrine

hydroxypyrrrole (49) via the charged species 69. Subsequent tautomerization of the hydroxypyrrrole derivative 49 yields the final products 7 and 8.

The instability of the  $\beta$ -nicotyrine metabolite discussed earlier (Fig.VI.7) also may be rationalized in terms of Scheme VI.3. The hydroxypyrrrole 49 is a highly electron rich aromatic system which would be expected to undergo autoxidation. The corresponding anion 70 (Scheme VI.4) would be even more unstable, a property which would explain the catalytic effect of base on the decomposition of the metabolite.

In an effort to characterize the two decomposition products, HPLC-CI/MS and HPLC-CAD/MS were performed on the  $\beta$ -nicotyrine metabolite which had been purified approximately 16 hr earlier by HPLC. The total ion chromatogram obtained from the HPLC-CI/MS analysis of this sample is shown in Fig.VI.17. The methane CI/mass

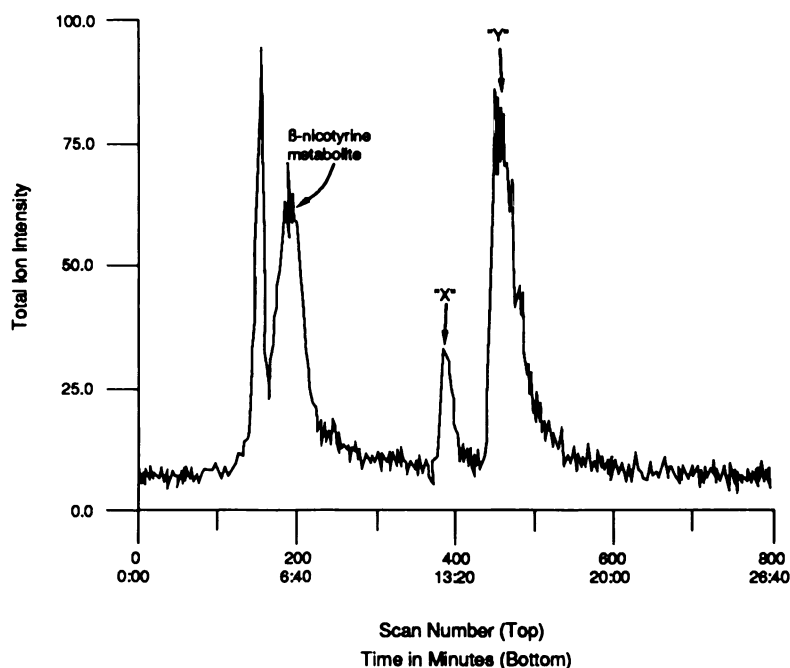


**Fig.VI.17** Total Ion Chromatogram Obtained from the CI/MS of the  $\beta$ -Nicotyrine Metabolite and its Base-Catalyzed Decomposition Products. Samples were prepared by collecting the peak corresponding to the  $\beta$ -nicotyrine metabolite and storing it for approximately 16 hr in the HPLC mobile phase (0.5% n-propylamine/acetonitrile). The decomposition products "X" and "Y" were separated on a 3 $\mu$ m particle size silica column (75 x 4.6 mm) using the mobile phase described above at a flow rate of 0.35 ml/min.



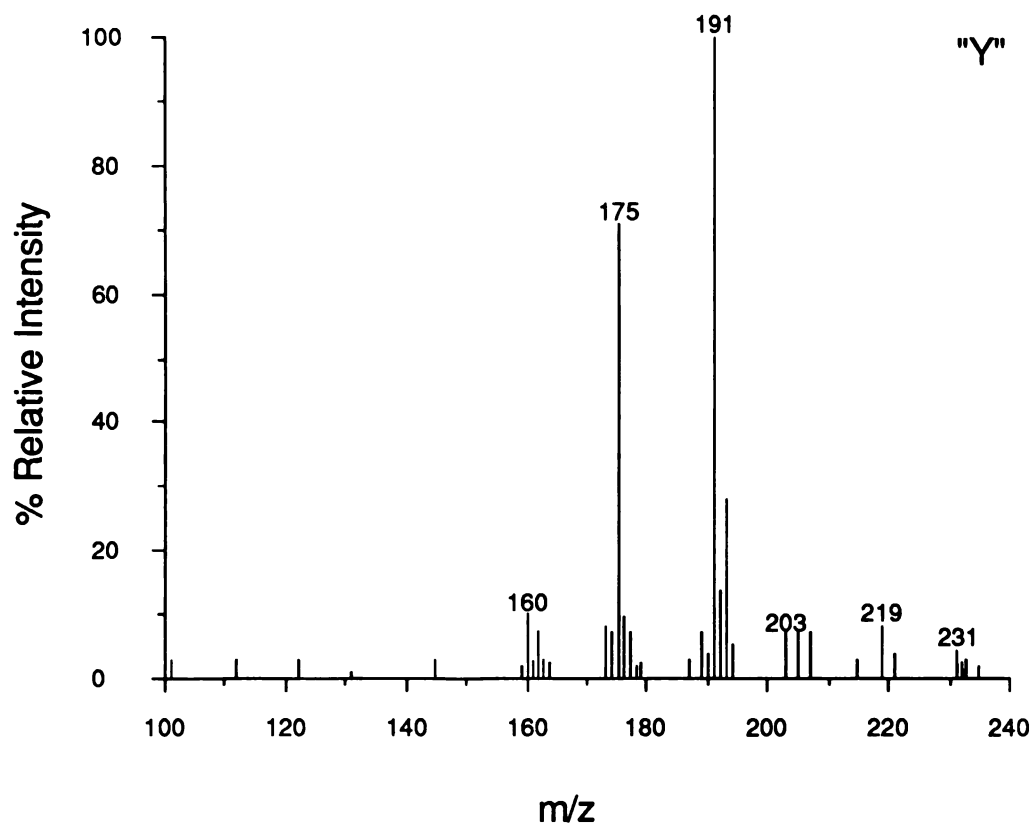
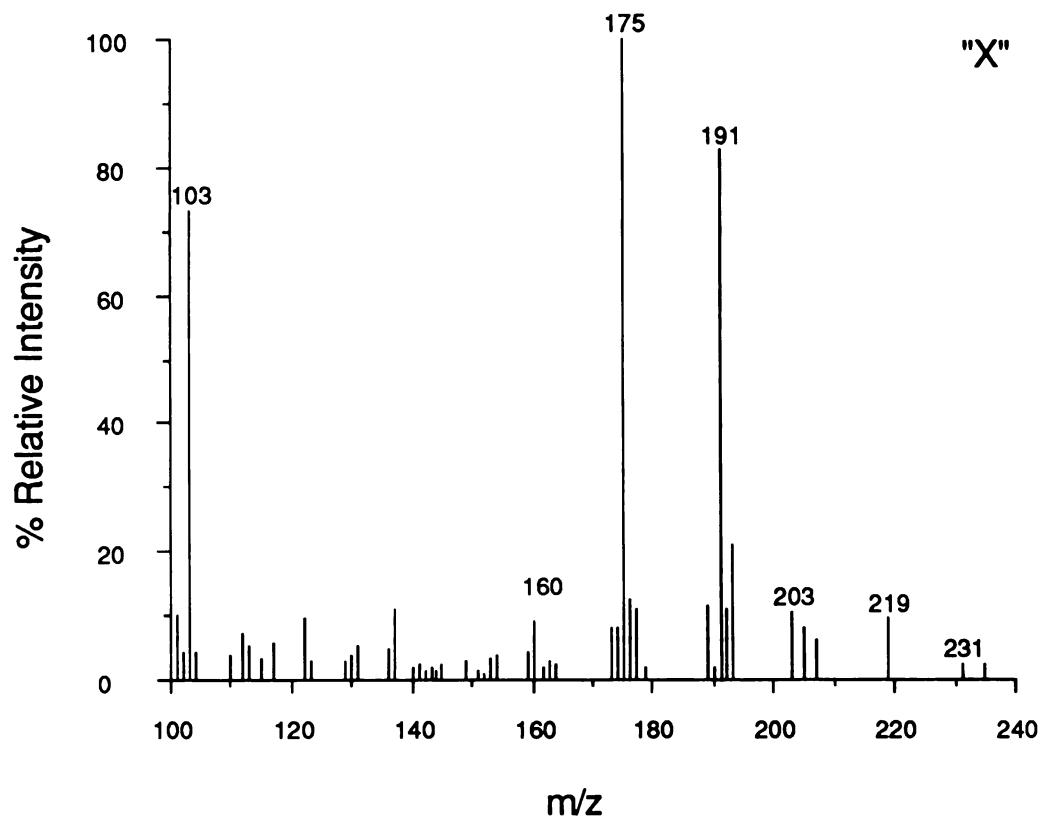


Fig VI.18 CI/MS of Base-Catalyzed Decomposition Products "X" and "Y"

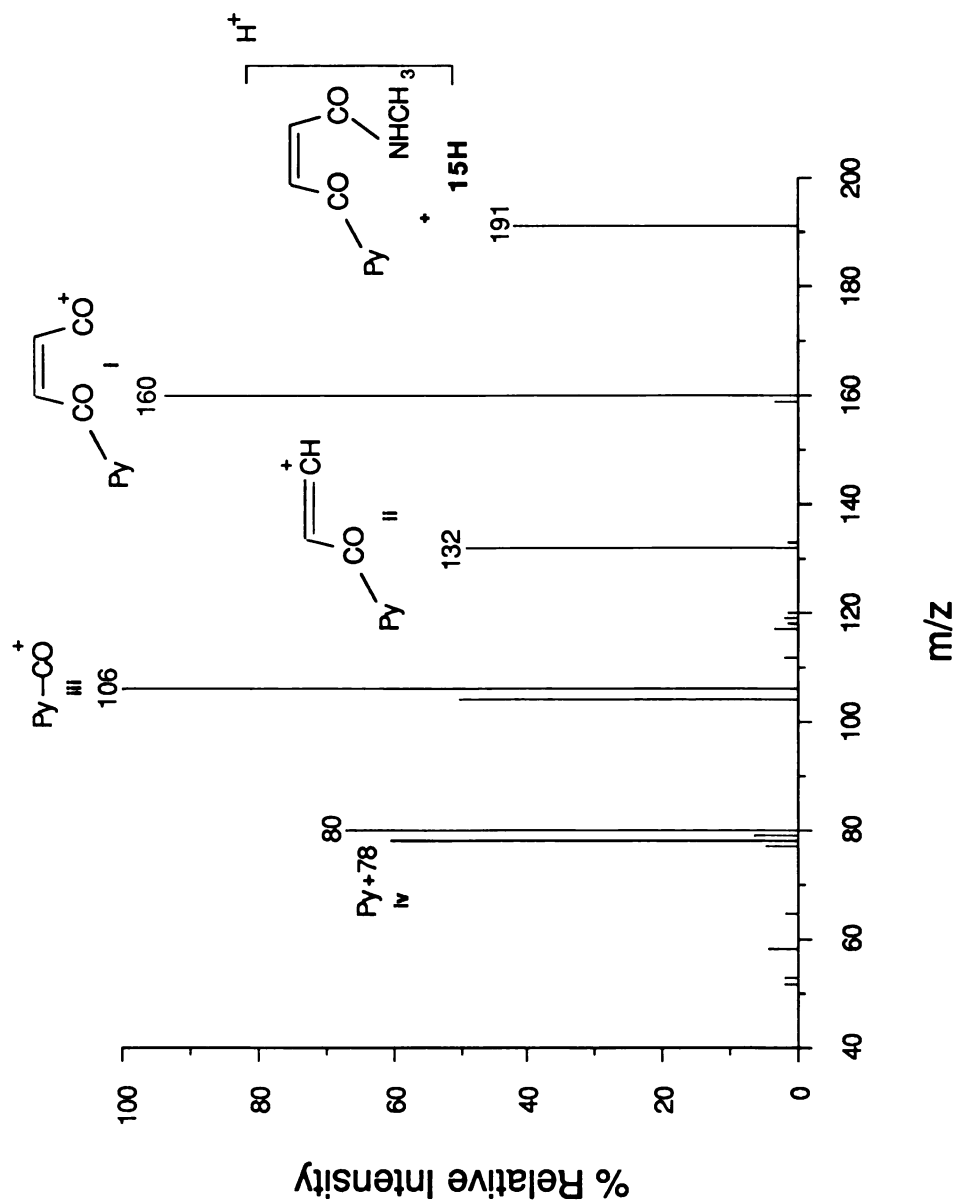
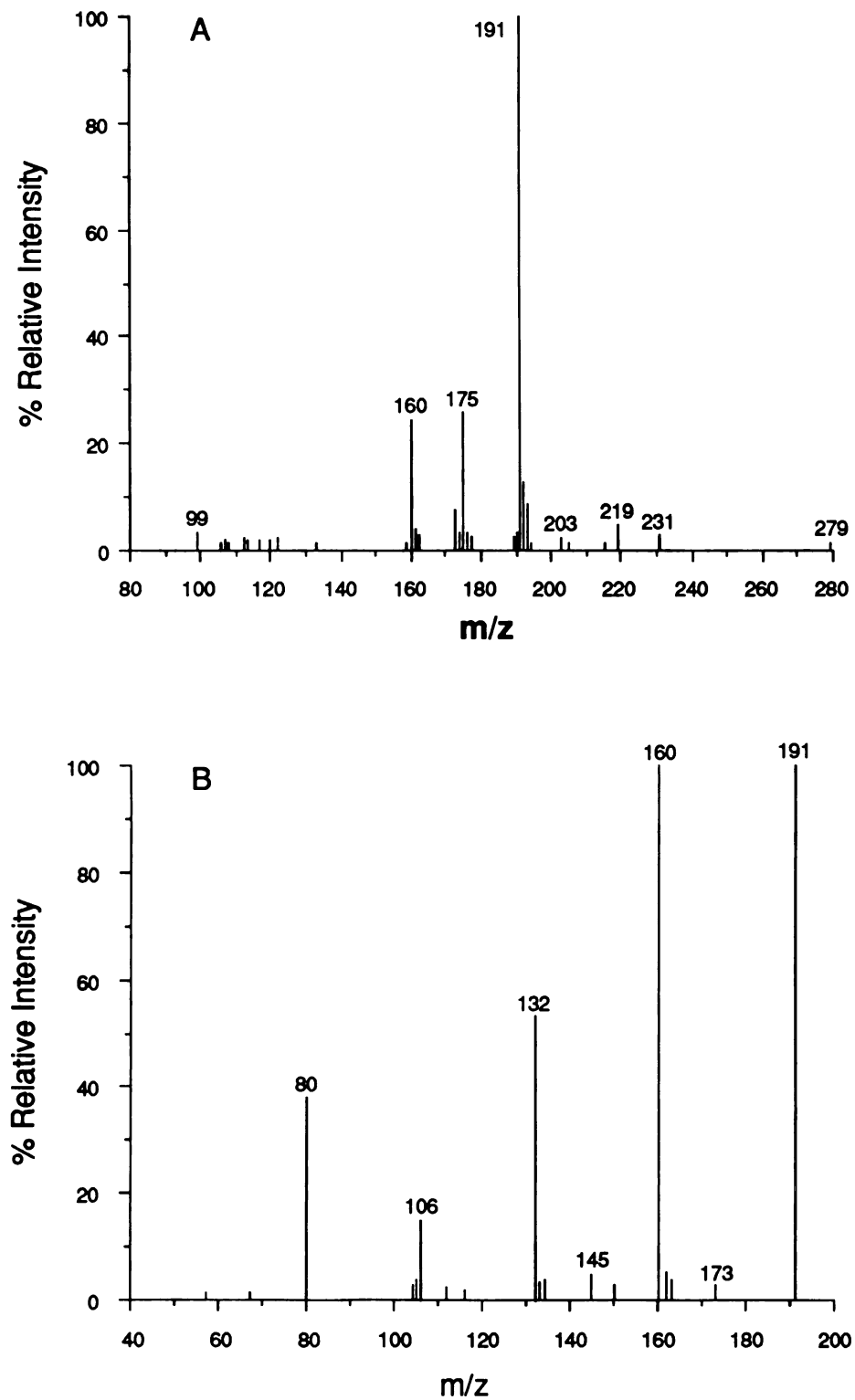


Fig. VI.19 Daughter Ion Spectrum Obtained from the CAD/MS Analysis of the m/z 191 Precursor Ion Derived from "Y".

spectra [ $m/z$  191 (100%) and 175 (70%)] of the two decomposition products "X" and "Y" were similar (Fig.VI.18). Although unknown "X" was too unstable for further analysis, we were able to obtain the product ion mass spectra of the MS/MS of  $m/z$  191 and 175 ions for unknown "Y". The daughter ion spectrum for the  $m/z$  191 species displayed a fragmentation pattern that can be accounted for in terms of the amidoeneone **73** (Fig.VI.19). Loss of  $H_2NCH_3$  from  $MH^+$  ( $73H^+$ ) generates the stable oxonium fragment ion I which subsequently loses CO to form II. Loss of  $HC=CH$  from II generates the stable oxonium fragment ion III which loses CO to form IV.

To facilitate our efforts in identifying the base-catalyzed decomposition product "Y", several nicotine related compounds, with molecular weights ranging from 189-192, were characterized by CI/MS and CAD/MS. The results of these analyses are summarized in Table VI.4. For comparison, the major fragment ions obtained from the CI/MS and CAD/MS of **7** and **8** are also shown. Of the compounds analyzed, the CI/MS characteristics of [1-methyl-5-(3-pyridyl) 5-hydroxy-2-pyrrolinone], 5'-hydroxy  $\Delta^{3',4'}$ -dehydrocotinine (**51**) was found to most closely match that obtained for decomposition product "Y" (Fig.VI.20 A). The daughter ion mass spectrum from the MS/MS of the  $m/z$  191 ion also corresponded to that observed with the breakdown product (Fig.VI.20 B, compare with Fig.VI.19). This compound, which was synthesized as part of another project in this lab, is a compound that would form upon cyclization of **73**.<sup>46</sup> The cyclic structure of **51** had been fully confirmed by IR and  $^1H$  NMR analyses and by comparison with the spectral properties of related compounds. In addition to the similarities between the mass spectral fragmentation profiles obtained from 5'-hydroxy  $\Delta^{3',4'}$ -dehydrocotinine and "Y", the HPLC chromatographic properties and HPLC diode array UV spectrum of **51** and this decomposition product were essentially identical. Based on these data, we assign the structure of this metabolic break-

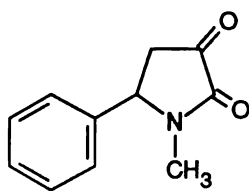


**Fig.VI.20 A and B** (A). CI/MS of Synthetic 5'-hydroxy  $\Delta^{3,4}$ -Dehydrocotinine (51) and (B). CAD/MS of the Precursor Ion Derived from 51

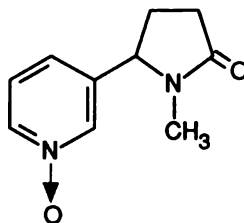
**Table VI.4** Major Fragments Obtained from the CI/MS and CAD/MS Analysis of Various Lactam Derivatives of (S)-Nicotine.

Compound	MW	Major Fragments (Relative Intensity)	
		CI/MS	CAD/MS
57	189	230 (6%), 218 (5%) and <b>190</b> (100%).	<b>190</b> (100%), 172 (12%), 131 (100%), 120 (11%) and 103 (42%).
58	192	217 (3%), 205 (5%), <b>193</b> (11%) and 177 (100%).	<b>193</b> (100%), 176 (13%), 162 (41%), 148 (7%), 134 (12%), 118 (12%), 98 (38%) and 96 (98%).
22	192	233 (4%), 221 (5%) and <b>193</b> (100%).	<b>193</b> (100%), 175 (100%), 157 (8%), 147 (22%), 134 (12%), 118 (96%), 106 (5%), 91 (7%) and 80 (18%).
51	190	231 (3%), 219 (5%), <b>191</b> (100%), 175 (24%) and 160 (23%).	<b>191</b> (100%), 160 (100%), 132 (53%), 106 (16%) and 80 (38%).
3	176	217 (3%), 205 (5%), 193 (22%) and <b>177</b> (100%).	<b>177</b> (100%), 146 (100%), 118 (65%), 98 (16%), 80 (39%) and 58 (34%).
7 and 8	174	215 (3%), 203 (4%), 189 (5%) and <b>175</b> (100%).	<b>175</b> (100%), 160 (6%), 147 (35%), 132 (28%), 117 (44%), 104 (23%) and 78(25%).
<b>Decomp. Product "Y"</b>	190?	231 (4%), 219 (8%), <b>191</b> (100%), 175 (72%) and 160 (12%).	<b>191</b> (43%), 160 (93%), 132 (50%), 106 (100%) and 80 (70%).

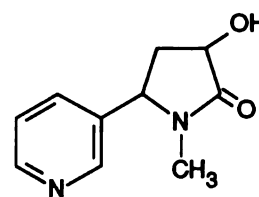
Values in bold face denote the apparent molecular ion detected by CI/MS and the precursor ion analyzed by CAD/MS. The chemical structures for the candidate compounds are shown below.



57



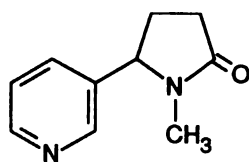
58



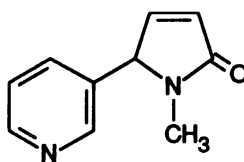
22



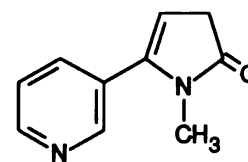
51



3



7

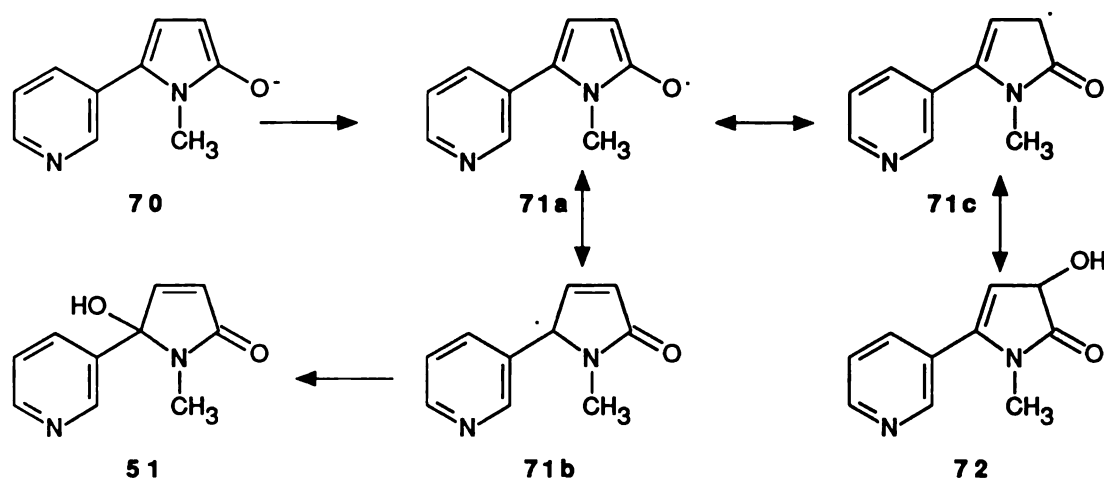


8

down product as **51** and rationalize the fragmentation pattern of the  $m/z$  191 CAD mass spectrum as proceeding via the thermally produced open chain species **73**.

The ion at  $m/z$  175 of the Cl/methane mass spectrum of **51** remains puzzling. The daughter ion mass spectrum of the  $m/z$  175 ion was found to be the same as the corresponding spectrum observed with the  $MH^+$  ion produced in the Cl/methane mass spectrum of pyrrolinone **8**. Since **8** cannot be a contaminant of synthetic **73**, it may be that this pyrrolinone is produced in the mass spectrometer by reduction of **51**. Analogous reductions of electron deficient species such as *o*-quinones<sup>47,48</sup> and nitroarenes<sup>49</sup> have been reported.

The oxidative and base-catalyzed decomposition of **7** to yield the hydroxypyrrolinone **51** may be rationalized as proceeding via the hydroxypyrrole **49** (Scheme VI.3). Loss of an electron to dioxygen would yield the resonance stabilized radical species **71**. Loss of a second electron followed by hydroxide ion attack at C5' (via **71 b**) would generate **51**. Alternatively, hydroxide ion attack at C3' (via **71 c**) would



**Scheme VI.4** Autoxidative Degradation of Pyrrolinones **7** and **8** via anion **70**

lead to the isomeric 3-hydroxypyrrolinone **72**, a candidate structure for the unknown decomposition product "X". The *in vivo* generation of such radical species could lead to the formation of biomacromolecular adducts of toxicological importance. Future studies will examine the bioalkylating potential of  $\beta$ -nicotyrine and the pyrrolinone metabolites derived from it.

## Discussion

We have demonstrated in these studies that  $\beta$ -nicotyrine is a substrate for cytochrome P-450 isozymes present in liver and lung tissues. The structural identification of  $\Delta^{4',5'}$ -dehydrocotinine and  $\Delta^{3',4'}$ -dehydrocotinine, two novel metabolites of  $\beta$ -nicotyrine, have been accomplished by LC-MS coupled with collisional activated dissociation (CAD) mass spectrometry, GC-EIMS, HPLC UV diode array analyses and confirmed by chemical synthesis of the proposed metabolite(s). Initial mass spectral data of the metabolically generated metabolites of  $\beta$ -nicotyrine indicated to us that a single oxygen atom had been inserted into the parent compound. CAD/MS of this metabolite produced fragmentation data which proved useful in assigning the position of oxygen insertion. Our interpretation of the MS/MS studies indicated the insertion of a single oxygen atom at the C-5' position, consistent with 4 of the 5 structures shown in Fig.VI.12, the arene oxide **48**, the hydroxypyrrole **49**, and the dehydrocotinine species **7** and **8**.

The arene oxide **48**, a possible intermediate formed from the initial two electron oxidation of  $\beta$ -nicotyrine, was considered an unlikely candidate for the metabolite because of its highly unstable nature and susceptibility to ring opening reactions. However, the existence of the arene oxide as a transient intermediate is fully consistent with the end products characterized in this study. We predict that the lone pair of electrons on the nitrogen atom of the arene oxide **48**, would delocalize, thereby promoting the opening of the epoxide ring followed by a rearrangement to the

hydroxypyrrole derivative **49**. However, the hydroxypyrrole is a highly electron rich intermediate and would also be expected to undergo further rearrangement. Delocalization of the electrons present on the oxygen atom of **49** would most likely result in its rearrangement to the chemically more stable ring opened products  $\Delta^{3',4'}$ - and/or  $\Delta^{4',5'}$ -dehydrocotinine **7** and **8**. Comparison with a mixture of synthetic **7** and **8**, which exist in equilibrium in aqueous media, established the identity of the metabolically generated product as the pyrrolinone species.

Based on chemical considerations, similar to those described for the initial two electron oxidized intermediate of  $\beta$ -nicotyrine, putative arene oxide intermediates derived from other cyclopentadienoid heterocycles have been equally difficult to isolate for structural characterization. The arene oxide of 4-ipomeanol has been proposed as the reactive and toxic intermediate in 4-ipomeanol induced lung damage, although structural evidence for this highly reactive metabolite is indirect.<sup>24</sup> The cytochrome P-450 dependent oxidation of 4-ipomeanol has been shown to result in an electrophilic intermediate which forms covalent adducts with the soluble nucleophile glutathione. The tentative identification of two glutathionyl adducts suggests an intermediate such as the epoxide may be involved in the toxicity of this compound.<sup>39</sup> Thiophene containing compounds, such as methapyrilene and cephaloridine,<sup>34,15</sup> may exert their toxicities through metabolic activation of the thiophene moiety to reactive intermediates such as that described for 4-ipomeanol. Substituting the thiophene ring with benzene or paramethoxybenzene greatly diminishes the genotoxic effects of these methapyrilene-like compounds<sup>50</sup> A number of other heterocyclic xenobiotics, including aflatoxin<sup>51</sup> and benzo[*a*]pyrene<sup>52</sup> are also thought to exert their genotoxic effects through the formation of highly reactive arene oxide intermediates. On the basis of structural similarities to the compounds mentioned above, and their postulated activation via arene oxide intermediates, enzymatic oxidation of  $\beta$ -nicotyrine to dehydrocotinine via the corresponding epoxide represents a potential bioalkylating pathway for this tobacco



alkaloid. Studies aimed at defining metabolism dependent covalent binding of radiolabeled  $\beta$ -nicotyrine to biomacromolecules would be helpful in elucidating further the potentially reactive nature of its metabolites and the possible role they may serve in the pathogenesis of tobacco related diseases.

The  $\Delta^{3',4'}$ -dehydrocotinine isomer, by virtue of the  $\alpha,\beta$  unsaturated carbonyl system, is an electrophilic species and a potential Michael acceptor. The structurally related compounds maleimides are known to react with sulfhydryl containing compounds, including soluble thiols such as glutathione.<sup>53</sup> The reactivity of thiols toward these compounds has been exploited with compounds such as N-ethylmaleimide (NEM), which is an effective glutathione depleting agent *in vivo*.<sup>54</sup> *Bis* maleimides are used commonly as protein cross linking agents.<sup>55</sup> In addition, the oxidation of the substituted pyrrole, pyrrolnitrin, leads to the formation of a reactive maleimide which reacts with N-acetylcysteine to yield isolable covalent adducts.<sup>38</sup> Characterization of adducts formed between thiol containing compounds and  $\Delta^{3',4'}$ -dehydrocotinine would demonstrate directly, the reactivity of this  $\beta$ -nicotyrine derived metabolite.

Although there is no direct evidence for the metabolism dependent oxidation of pyrroles to the corresponding arene oxide, observations derived from studies on the oxidation of related cyclopentadienoid heterocycles suggest that such a pathway is likely. *In vivo* metabolism of unsubstituted thiophene results in the formation of an isolable mercapturic acid derivative at a position consistent with nucleophilic attack by the sulfhydryl containing compound of an epoxide intermediate, a reaction which results in the opening of the oxiran ring. A reactive intermediate(s) of 4-ipomeanol was demonstrated to form 2 glutathionyl adducts which may reflect attack of a chemically reactive arene oxide intermediate by the nucleophile glutathione.<sup>39</sup> Direct structural confirmation of these adducts have yet to be carried out.

Chemically, 5'-hydroxy  $\Delta^{3',4'}$ -dehydrocotinine may be similar to the maleimides in their reactivity toward nucleophilic compounds, including thiols such as

glutathione and N-acetylcysteine. Demonstration of reactivity toward these thiols would indicate the possibility of covalent adduct formation between this hydroxylated dehydrocotinine species and endogenous nucleophilic functionalities present on biological macromolecules.

## Materials and Methods

### Chemicals

Diisopropylamine, n-butyllithium, phenylselenyl chloride, D<sub>2</sub>O, and (S)-nicotine (1), used in the synthesis of (S)-cotinine (3) and  $\beta$ -nicotyrine tartrate (6a), were purchased from the Aldrich Chemical Co. (Milwaukee, WI). 1-methyl-5-(3-pyridyl)5-hydroxy-2-pyrrolinone [5'-hydroxy  $\Delta^{3',4'}$  dehydrocotinine (51)] was synthesized as detailed previously.<sup>46</sup> EGTA, glucose 6-phosphate and HEPES were purchased from the Sigma Chemical Company (St. Louis, MO). All other chemicals were reagent grade or HPLC grade.

### Animals

Adult male New Zealand White rabbits (3.0 - 3.5 kg) were used to obtain liver and lung microsomes as described in Chapter III. In order to obtain maximum liver microsomal metabolite production required for HPLC/CI mass spectral studies, liver microsomes were prepared from rabbits which had been pretreated with 0.1% phenobarbital (pH 6.9) in their drinking water over a period of 6-10 days. Drinking water and food were provided *ad libitum*. For the study which compared the relative activities of the two tissues, liver and lung microsomes isolated from three rabbits were pooled and prepared as described in the Materials and Methods section of Chapter III.

### Substrate Binding of $\beta$ -Nicotyrine to Microsomal Cytochrome P-450

The binding affinity of  $\beta$ -nicotyrine to liver microsomal cytochrome P-450 was determined by measuring the difference in absorbance at its  $\lambda_{\max}$  and  $\lambda_{\min}$  at different concentrations of substrate. A solution of  $\beta$ -nicotyrine tartrate (30.8 mg in 400  $\mu$ l

H<sub>2</sub>O, 0.25M) was prepared and sonicated to facilitate its solubilization. Solutions of 150, 50, 16.5 and 2.6 mM  $\beta$ -nicotyrine tartrate were prepared from this 0.25 M stock solution. Liver microsomes isolated from phenobarbital pretreated rabbits were added (300  $\mu$ l of a 10 mg/ml stock solution) to two 3 ml cuvettes each containing 2.7 ml of 0.15 M KCl buffer, pH 7.4, to yield a final concentration of 1 mg/ml. Baseline spectra of the sample and reference cuvettes were taken between 370 and 470 nm in an Aminco DW-2 UV/visible spectrophotometer at a setting of 0.2 absorbance units full scale (AUFS). To the sample cuvette 3  $\mu$ l of the appropriate dilution of  $\beta$ -nicotyrine was added, yielding a final concentration of 2.6 -250  $\mu$ M. An equal volume of buffer was added to the reference cuvette and scans were performed immediately. The binding constant,  $K_s$ , was determined by constructing a double reciprocal plot of  $1/\Delta A$  (426-393 nm) vs.  $1/\beta$ -nicotyrine [ $\mu$ M]; the value was estimated by calculating the negative inverse of the intersection between the constructed line and the x-intercept.

#### Incubation conditions

Incubation mixtures (1 ml) containing liver or lung microsomes (1-2 mg/ml),  $\beta$ -nicotyrine tartrate (154  $\mu$ g, 0.5  $\mu$ mol for liver or 30.8  $\mu$ g, 0.1  $\mu$ mol for lung), EGTA (1 mM) in 0.1 M HEPES buffer, pH 7.6, and an NADPH regenerating system (0.5 mM NADP<sup>+</sup>, 8 mM glucose-6-phosphate, 1 unit/ml glucose-6-phosphate dehydrogenase, and 4 mM MgCl<sub>2</sub>) were incubated at 37°C for periods of up to 1 hr in a metabolic shaker. For the experiment described in Fig.VI.4, liver and lung microsomes from untreated rabbits were used. Quantitative measurement of  $\beta$ -nicotyrine metabolism was normalized to microsomal protein content, as determined by the method of Lowry,<sup>56</sup> or cytochrome P-450 content, by the method of Estabrook.<sup>57</sup> (S)-Nicotine (22  $\mu$ g) was added as an internal standard and the resulting mixtures were extracted with CH<sub>2</sub>Cl<sub>2</sub> (1 ml), the extracts vortexed for 1 min, and the phases separated by centrifugation for 3-4 min at 1000 x g. For the kinetic studies, multiple 1 ml samples were prepared and incubated. Each sample was quenched at appropriate time

intervals by placing the corresponding tube containing the incubation mixture in an ice bath followed by the immediate addition of  $\text{CH}_2\text{Cl}_2$ . HPLC/UV analyses were performed directly on the extracts. Attempts to isolate the  $\beta$ -nicotyrine metabolite (Met in Fig.VI.2) by HPLC were unsuccessful since upon storage in the n-propylamine/acetonitrile mobile phase, it underwent autoxidation to decomposition products "X" and "Y". For the characterization of the metabolite and its decomposition products, the  $\text{CH}_2\text{Cl}_2$  layer was transferred to a second vial and was reduced in volume under a gentle stream of  $\text{N}_2$  to about 150  $\mu\text{l}$  for HPLC-Cl/MS analyses.

### Instrumentation

Capillary GC-EI mass spectral analyses were performed in an HP 5970 mass selective detector linked to a 5890A gas chromatograph equipped with a methylphenylsilicone column (12 M x 0.2 mm diameter). The following temperature conditions were used for the GC-EI mass spectral analyses: injection port=225°C, ion source=150°C and mass analyzer=180°C. The GC separations utilized a 70-250°C temperature gradient with a 4.0 min solvent delay and 20°C/min linear ramp. Scans were acquired between 35-250 amu. High resolution (HR) EI and liquid secondary ion (LSI) mass spectra were obtained with a Kratos MS50S using a glycerol matrix. HPLC-Cl/methane mass spectra were recorded in a Finnigan Model 45A triple stage quadrupole mass spectrometer (San Jose, CA) equipped with a chemical ionization source, INCOS model 2300 data system and a Finnigan HPLC-MS moving belt (2.25 cm/sec) interface unit which employed a vaporization temperature of 170°C. A manifold temperature of 133°C was used. The HPLC separations for mass spectral analyses utilized either an Eldex model A-30-S HPLC pump, Eldex Lab (San Carlos, CA), or an Altex model 100A HPLC pump equipped with a 25 cm x 4.6 mm i.d. (for separation of metabolites - retention times:  $\beta$ -nicotyrine, 16.9 min; metabolite, 26.7 min) or a 7.5 cm x 4.6 mm i.d. (for studies of metabolite decomposition products - retention times:  $\beta$ -nicotyrine, 6.3 min; decomposition product "X", 13.0 min; decomposition product "Y", 15 min) 3

$\mu\text{m}$  Chemcosorb silica column, Dychrom (Sunnyvale, CA), and an Alltech direct connect cartridge precolumn packed with 5  $\mu\text{m}$  Absorbosphere silica. The mobile phase consisted of 0.5% n-propylamine in acetonitrile and the flow rate was adjusted to 0.25 ml/min.

Qualitative and quantitative HPLC analyses of metabolic incubation mixtures using (S)-nicotine as an internal standard and employing UV detection (260 nm) were performed with the same mobile phase (flow rate: 1 ml/min; retention times:  $\beta$ -nicotyrine, 1.9 min; metabolite, 2.9 min; (S)-nicotine, 4.1 min) on the 7.5 cm x 4.6 mm i.d. 3  $\mu\text{m}$  silica column which was linked to a Beckman 110-A solvent delivery system and an Hitachi 100-10 spectrophotometer/flow cell combination. Kinetic analyses were performed with individual 1.0 ml incubation mixtures which were processed as described below under "Incubations". Online UV scans (220 nm - 460 nm) were obtained with a Hewlett Packard Model 1040A diode array UV detector.

Proton NMR spectra were recorded with a General Electric 500 MHz instrument linked to a Nicolet 1180 computer or a Varian FT 80. Chemical shifts are reported in parts per million (ppm) relative to tetramethylsilane ( $\text{Me}_4\text{Si}$ ) as an internal standard and spin multiplicities are given as s (singlet), d (doublet), t (triplet), or m (multiplet).

**Syntheses (Performed In Collaboration with Dr. Patricia Caldera-Munoz)**  
**(3RS,5S)-1-Methyl-3-(phenylseleno)-5-(3-pyridyl)-2-pyrrolidinone [(3RS)-Phenylselenyl-(S)-cotinine (50)]**

A solution of diisopropylamine (4.2 ml, 3.03 g, 30 mmol) in 30 ml of dry THF was cooled down to  $-20^\circ\text{C}$  under an atmosphere of  $\text{N}_2$ . Added to this solution was 11.5 ml of 2.6 M n-butyllithium while maintaining the temperature at  $-20^\circ\text{C}$ . After stirring this reaction mixture for an additional 20 min, the solution was cooled to  $-78^\circ\text{C}$ . A solution of (S)-cotinine (2.58 g, 14.6 mmol in 10 ml of THF) was added slowly over the next 10 min. This reaction mixture was stirred for an additional 30 min. A solution

of phenylselenenyl chloride (2.67 g, 14.0 mmol in 10 ml of THF) was added dropwise to the reaction mixture. The reaction mixture was stirred for 30 min at  $-78^{\circ}\text{C}$ , and then allowed to warm to room temperature. The reaction was quenched with 10% HCl. The solution was washed with ether. The aqueous layer was adjusted to basic pH with NaOH and extracted with ether. The ether layer was dried over sodium sulfate. Evaporation of solvent resulted in a slight yellow clear syrup like residue. This crude reaction product was purified by column chromatography on silica gel which gave a non polar selenide by-product with ethyl acetate followed by the desired oily product (3.36 g, 70%) with  $\text{CH}_2\text{Cl}_2:\text{MeOH}$  (9:1):  $^1\text{H}$  NMR ( $\text{CDCl}_3$ )  $\delta$  8.58 [d, 1H, (C6)-H], 8.38 [s, 1H, (C2)-H], 7.73 [m, 2H, (C4,C5)-H], 7.5-7.3 [m, 5H (Ph)-H], 4.06 [dd, 1H  $J_1=3.1$  Hz,  $J_2 = 8.8$  Hz, (C3)-H], 3.98 [t, 1H,  $J = 7.3$  Hz, (C5)-H], 2.62 [m, 1H (C4)-H], 2.4 [m, 1H, (C4)-H], 2.4 [m, 1H, (C4)-H], 2.52 (s, 3H,  $\text{NCH}_3$ ). LSIMS  $m/z$  333 and 331 [(MH) $^+$ , 61%], 176 [(M-SePhH) $^+$ , 100%]. HR-EIMS: Calculated for  $\text{C}_{16}\text{H}_{16}\text{N}_2\text{OSe}$ , 332.0427; found, 332.0422.

**1-Methyl-5-(3-pyridyl)-4,5-pyrrolin-2-one** [ $\Delta^{4',5'}$ -dehydrocotinine (8)]

To a solution of (RS)-3-phenylselenenyl-(S)-cotinine (3.36 g, 10.15 mmol) in 12 ml of MeOH at  $0^{\circ}\text{C}$  was added dropwise 30% HOOH (1.5 ml, 49 mmol) followed by 1.5 ml of  $\text{H}_2\text{O}$ . After stirring for 2 hr at  $0^{\circ}\text{C}$ , the reaction mixture was poured into a 10% solution of  $\text{Na}_2\text{CO}_3$  and extracted with 4 x 100 ml  $\text{CH}_2\text{Cl}_2$ . The combined extracts were washed with water and dried ( $\text{Na}_2\text{SO}_4$ ). Upon standing overnight the slightly yellow solution turned purple in color. Column chromatography on neutral alumina of a 50 ml portion of this colored solution with  $\text{CHCl}_3:\text{MeOH}$  (9:1) gave an early fraction that yielded a few mg of crystalline 1-methyl-5-(3-pyridyl)-4,5-pyrrolin-2-one:  $^1\text{H}$  NMR ( $\text{CDCl}_3$ )  $\delta$  8.6 [m, 2H, (C2,6)-H], 7.65 [dt, 1H, (C4)-H], 7.35 [m, 1H, (C5)-H], 5.35 [t, 1H,  $J = 3$  Hz, (C4)-H], 3.18 (d, 2H,  $J = 3$  Hz, (C3)-H], 3.00 (s, 3H,  $\text{NCH}_3$ ). LSIMS  $m/z$  175 (MH $^+$ ); HPLC-CIMS  $m/z$  175 (MH $^+$ ). Although

moderately stable at pH 7.4, this compound underwent rapid decomposition at pH 10 to the same products ("X" and "Y") observed with the  $\beta$ -nicotyrine derived metabolite which had been isolated by HPLC from microsomal incubation mixtures. All other fractions were oils containing **8** and (as estimated by  $^1\text{H}$  NMR) 10-30% of the corresponding  $\Delta^{3',4'}$  isomer **7** which displayed the following  $^1\text{H}$  NMR spectrum in  $\text{CDCl}_3$ :  $\delta$  8.5 [m, 2H, (C2,6)-H], 7.65 [dt, 1H, (C4)-H], 7.3 [m, 1H, (C5)-H], 7.0 [dd, 1H,  $J_1 = 6$  Hz,  $J_2 < 2$  Hz, (C3)-H], 6.25 [dd, 1H,  $J_1 = 6$  Hz,  $J_2 < 2$  Hz, (C4)-H], 5.0 [unresolved m, 1H, (C5)-H], 2.8 (s, 3H,  $\text{NCH}_3$ ).

#### Deuterium Exchange and Back-Exchange Experiments

Synthetic  $\Delta^{4',5'}$ -dehydrocotinine (approx. 100  $\mu\text{g}$ ) obtained by removal of the  $\text{CDCl}_3$  under a stream of  $\text{N}_2$  from an aliquot of the NMR sample was dissolved in 1 ml  $\text{D}_2\text{O}$  containing 0.05 M deuterated sodium phosphate buffer, pH 7.4. The resulting mixture was incubated for 60 min at  $37^\circ\text{C}$  and then was extracted into an equal volume of toluene:butanol (7:3). This extract then was analyzed by GC-EIMS immediately to estimate deuterium incorporation from the  $\text{D}_2\text{O}$  exchange and after 24 hours to estimate butanol back-exchange.

#### Notes on the Partitioning Properties of **51**

In the studies described earlier, the decomposition of the  $\beta$ -nicotyrine metabolite and the subsequent appearance of the breakdown products "X" and "Y" was shown to be base-catalyzed. However, analysis of methylene chloride extracts of metabolic incubations which had been terminated with base did not reveal detectable quantities of either of these two products. To assess the efficiency of extraction for the polar decomposition product 5'-hydroxy  $\Delta^{3',4'}$ -dehydrocotinine, the partitioning behavior of synthetic **51** was tested. A solution of **51** prepared in methylene chloride was transferred to separate vials and analyzed directly by HPLC with UV detection or added to an equal volume of buffer followed by thorough mixing of the aqueous and organic layers, separation of the phases and analysis of the resulting methylene chloride layer.

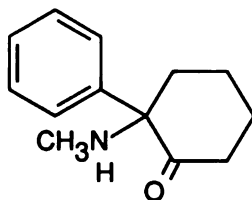
The partition ratio for **51**, defined as the ratio of the peak area units of **51** obtained from analyzing the methylene chloride layer extracted with buffer (pH 7.6) and the nonextracted methylene chloride solution, was approximately 30:1. This result indicates that metabolically generated 5'-hydroxy  $\Delta^{3',4'}$ -dehydrocotinine, if formed, would likely have been undetectable by the analytical methods employed in these studies.. Further studies on the possible metabolic conversion of  $\beta$ -nicotyrine to **51** via the intermediacy of **7** and **8** would require the utilization of a chromatographic technique, such as reversed phase HPLC, which avoids the partitioning problems inherent in the extraction methods used in this study.



## Addendum

Studies described in the previous section of this chapter have shown that  $\beta$ -nicotyrine is oxidized enzymatically by cytochrome P-450. Experiments designed to examine further its high affinity binding to P-450 and its substrate properties are described in this section. The main focus of this section is aimed at understanding better the participation of P-450 isozymes in the oxidation of this compound. In order to perform this assessment, the effects of P-450 inducers on the liver microsomal metabolism of  $\beta$ -nicotyrine were measured. Since the lung is one of the major target organs for tobacco induced toxicities, preliminary studies aimed at characterizing the lung P-450 isozymes which catalyze the oxidation of  $\beta$ -nicotyrine were also pursued.

### Displacement of the Type I Binding Species Ketamine by $\beta$ -Nicotyrine



34

The high affinity binding of  $\beta$ -nicotyrine to cytochrome P-450 shown previously in Fig.VI.1 could result in the competitive displacement of other cytochrome P-450 substrates. Studies described by Stalhandske *et al.*<sup>9</sup> which have shown this compound to be an inhibitor of (S)-nicotine metabolism *in vivo* are consistent with such a proposal. In the present experiment, the competitive binding and displacement of a compound with a relatively high binding affinity to cytochrome P-450 was examined. Ketamine (34) was chosen for this study since its displacement from cytochrome P-450 could be monitored conveniently by measuring the spectral absorption associated with its binding (type I binding) in the absence and presence of

$\beta$ -nicotyrine. Addition of  $\beta$ -nicotyrine (5  $\mu$ M, final concentration) to a microsomal suspension consisting of liver microsomes (1 mg/ml) isolated from phenobarbital pretreated rabbits and 100  $\mu$ M ketamine resulted in an immediate shift from the characteristic type I binding spectrum of ketamine to the type II binding spectrum of  $\beta$ -nicotyrine (Fig.VI.21). The dramatic and rapid shift in the binding spectrum observed upon addition of  $\beta$ -nicotyrine in the presence of a 20-fold excess of a compet-

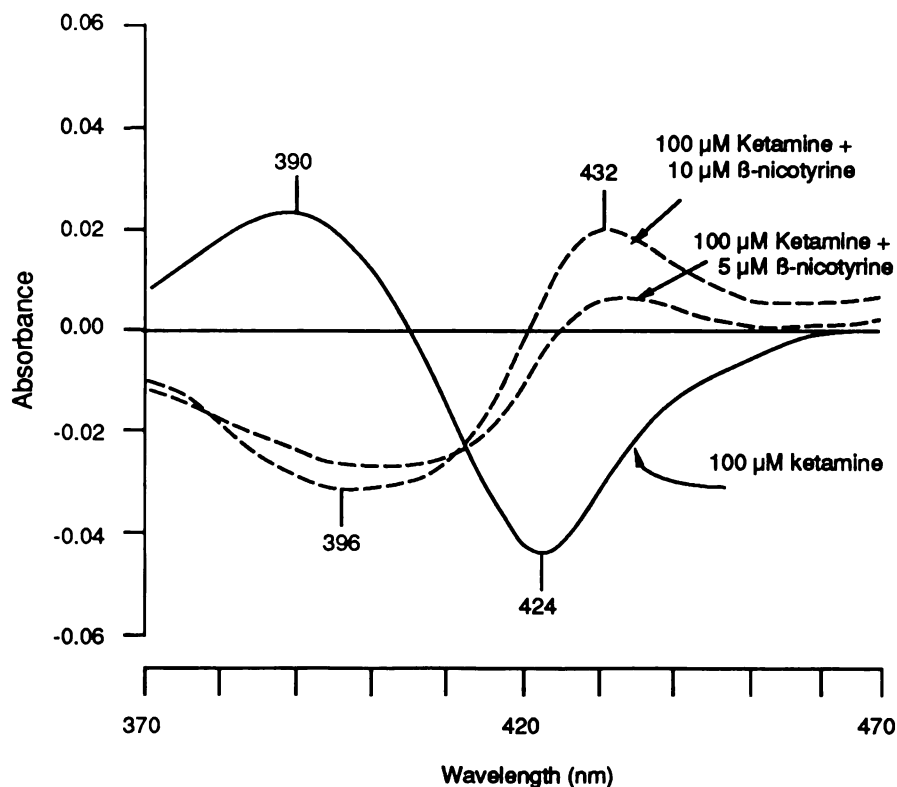


**Fig.VI.21** Displacement of the Type I Substrate Ketamine (100  $\mu$ M) by the Type II Substrate  $\beta$ -Nicotyrine (5 and 10  $\mu$ M) from Unreduced Liver Microsomal Cytochrome P-450.

ing binding substrate is consistent with the high binding affinity illustrated in Fig.VI.1 and provides a plausible explanation for the inhibition of (S)-nicotine metabolism in rodents previously dosed with this compound.<sup>9</sup>

### **Effect of Phenobarbital and 3-Methylcholanthrene Pretreatment of Rabbits on the Liver Microsomal Metabolism of $\beta$ -Nicotyrine**

In order to gain a better understanding of the cytochrome P-450 isozymes which catalyze the oxidation of  $\beta$ -nicotyrine, liver microsomes isolated from rabbits pretreated with the cytochrome P-450 inducing agent phenobarbital and the P-448 inducing agent 3-methylcholanthrene were used in metabolic incubations and compared to the  $\beta$ -nicotyrine oxidase activity of liver microsomes isolated from untreated rabbits. As shown in Fig.VI.22, liver microsomes isolated from phenobarbital pretreated rabbits appear to oxidize  $\beta$ -nicotyrine at a rate comparable to that catalyzed by liver microsomes isolated from untreated rabbits. These observations suggest that the major phenobarbital inducible cytochrome P-450 isozymes present in liver may not contribute significantly to the oxidation of  $\beta$ -nicotyrine as we had previously suggested. Compared to control microsomes, the metabolism of  $\beta$ -nicotyrine was reduced markedly when microsomes isolated from 3-methylcholanthrene were used. Following a 1 hr incubation, liver microsomes isolated from 3-methylcholanthrene pretreated rabbits catalyzed the oxidation of only 13% of  $\beta$ -nicotyrine (1 mM starting substrate concentration). It appears, therefore, that 3-methylcholanthrene inducible isozymes of cytochrome P-450 do not play a significant role in the metabolic oxidation of  $\beta$ -nicotyrine. These results also suggest that 3-methylcholanthrene pretreatment represses the expression of those P-450 isozymes which catalyze its oxidation.

### **Effect of TCDD, Aroclor 1260 and Phenobarbital on the Lung Microsomal Metabolism of $\beta$ -Nicotyrine**

In analogy to the studies with (S)-nicotine as substrate (Chapter IV), the effects of phenobarbital, TCDD and Aroclor 1260 pretreatment on the lung microsomal metabolism of  $\beta$ -nicotyrine were examined. Background information detailing the effects of each of these agents on the lung P-450 isozyme composition are described in Chapter IV.

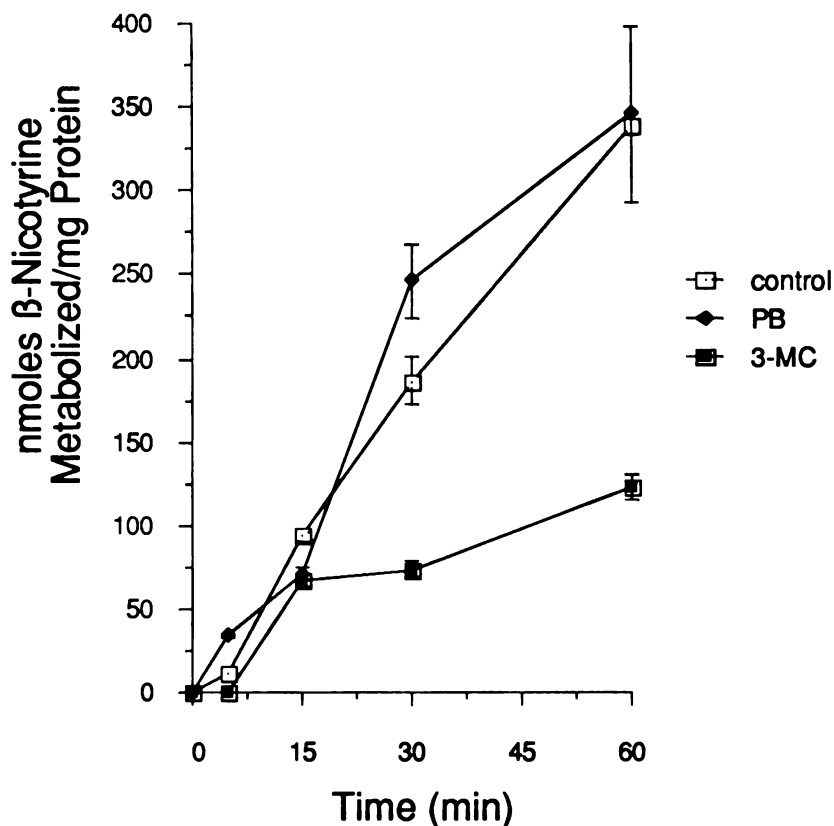


**Fig.VI.22**  $\beta$ -Nicotyrine Metabolism by Liver Microsomes Isolated from Phenobarbital Pretreated, 3-Methylcholanthrene Pretreated and Control (Untreated) Rabbits.  $\beta$ -nicotyrine (1 mM) was incubated with liver microsomes (1 mg/ml) from each source for periods up to 1 hr. The incubation mixtures were processed as described in the Materials and Methods section of Chapter III and analyzed by normal phase HPLC with UV detection at 284 nm as described in the Materials and Methods section. Each point represents the average of four determinations ( $\pm$  S.E.) obtained from two separate experiments.

As shown in Fig.VI.23, lung microsomes isolated from control, TCDD, phenobarbital and Aroclor 1260 pretreated rabbits metabolize  $\beta$ -nicotyrine at approximately the same rate. The apparent lack of induction upon pretreatment of rabbits with TCDD and Aroclor 1260 of the lung microsomal  $\beta$ -nicotyrine oxidase activity would appear to rule out the participation of the P-448 class of P-450 isozymes in this oxidation. This result is consistent with the noninducing effects of 3-methylcholanthrene on the liver microsomal oxidation of  $\beta$ -nicotyrine described in the previous section. However, in contrast to the 3-methylcholanthrene induced repression of liver isozymes which catalyze the oxidation of  $\beta$ -nicotyrine, no loss of

$\beta$ -nicotyrine oxidase activity was observed after pretreatment with either TCDD or Aroclor 1260. The similarity in the  $\beta$ -nicotyrine oxidase activity of lung microsomes isolated from rabbits pretreated with Aroclor 1260, suggests that lung P-450 isozyme-2 does not contribute significantly to the oxidation of this compound since this agent selectively represses this isozyme. These results would appear to suggest that lung P-450 isozyme-5 is largely responsible for catalyzing the oxidation of  $\beta$ -nicotyrine.

### **Effects of Inhibitors of Lung P-450 Isozymes on the Metabolism of $\beta$ -Nicotyrine**

Selective and nonselective inhibitors of lung cytochrome P-450 isozymes were used, in analogy to the studies described in Chapter IV, to assess further the participation of the lung P-450 isozymes in the oxidation of  $\beta$ -nicotyrine. At 1 and 2.5  $\mu$ M of  $\alpha$ -methylbenzylaminobenzotriazole, concentrations which have been shown to inhibit >90% of the isozyme-2 catalyzed 5'-carbon oxidation of (S)-nicotine,  $\beta$ -nicotyrine metabolism was inhibited by only 27.4 and 34.3%, respectively. This result indicates, as suggested above, that the contribution of lung cytochrome P-450 isozymes-2 and -6 towards the oxidation of  $\beta$ -nicotyrine is minor. The effects of norbenzphetamine and N-hydroxyamphetamine on the metabolism of  $\beta$ -nicotyrine was also examined. Norbenzphetamine, a compound which forms metabolic intermediate complexes with lung P-450 isozyme-2 and which effectively inhibits the 5'-carbon oxidation of (S)-nicotine catalyzed by this lung P-450 isozyme, inhibited  $\beta$ -nicotyrine oxidation by only 8.8%. However, N-hydroxyamphetamine, a compound which inhibits lung P-450 isozymes-2 and -5 (but not isozyme-6)\* through the formation of a

\*A control study revealed that compared to control, lung P-450 isozyme-6 catalyzed ethoxyresolufin O-deethylation (EROD) was inhibited by 48% after 10 min in the presence of N-hydroxyamphetamine (0.67 mM). However, beyond this 10 min time point the rate of EROD in the presence or absence of this inhibitor was comparable. This result suggests that the inhibitory properties of N-hydroxyamphetamine on lung P-450 isozyme-6 is through a competitive mechanism and not through the formation of a metabolic intermediate complex.

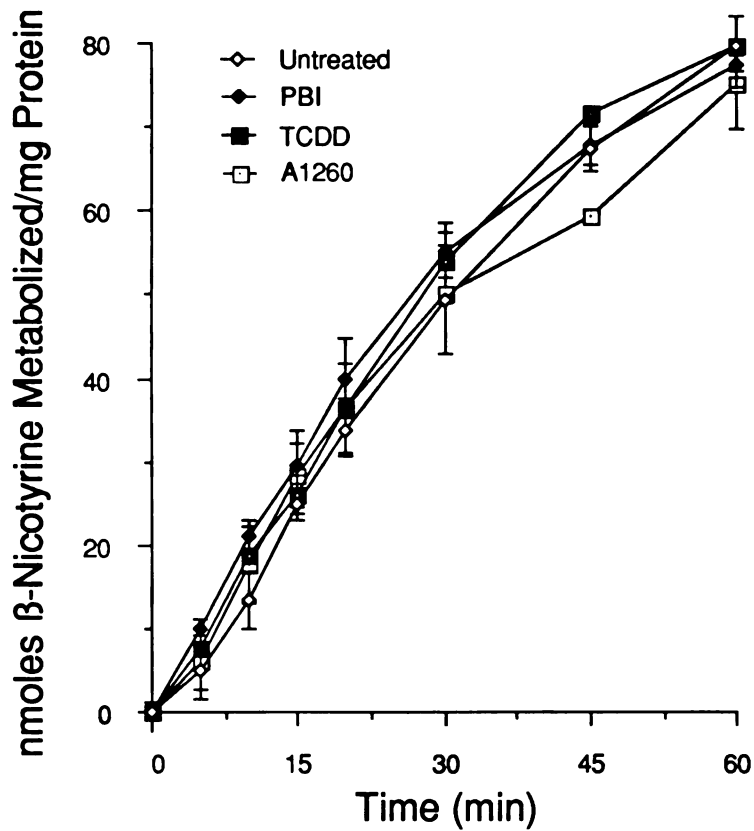


**Fig.VI.23** Effect of Phenobarbital, TCDD and Aroclor 1260 Pretreatment on the Rabbit Lung Microsomal Metabolism of  $\beta$ -Nicotyrine.

similar type of complex, inhibited the oxidation of  $\beta$ -nicotyrine completely. These results support the proposal that lung cytochrome P-450 isozyme-5 contributes, in large part, to the lung microsomal oxidation of  $\beta$ -nicotyrine.

**Discussion-Addendum**

The results of the studies described in this section indicate that the cytochrome P-450 substrate properties of  $\beta$ -nicotyrine are much different from (S)-nicotine.  $\beta$ -Nicotyrine binds with a much higher affinity to cytochrome P-450 than (S)-nicotine and is capable of displacing competing substrates effectively, even at relatively low substrate concentrations. The principal cytochrome P-450 isozyme which catalyzes its oxidation appears to be much different than those which have been shown to catalyze the oxidation of (S)-nicotine. Liver microsomes isolated from phenobarbital pretreated rabbits did not, as we had previously suggested, induce  $\beta$ -nicotyrine oxidase activity. This result suggests that the major phenobarbital inducible P-450, isozyme-2, does not contribute greatly to the oxidation of this compound. Lung microsomes isolated from rabbits pretreated with Aroclor 1260, a mixture which represses lung P-450 isozyme-2 activity, exhibited  $\beta$ -nicotyrine oxidase activity which was essentially identical to the activity in control microsomes. These results support the previous studies which showed little effect of isozyme-2 towards the oxidation of this compound. Selective inhibitors of lung P-450 isozyme-2,  $\alpha$ -methylbenzylaminobenzotriazole and norbenzphetamine also had little effect on the oxidation of  $\beta$ -nicotyrine. It is concluded that the contribution of cytochrome P-450 isozyme-2 towards the lung microsomal oxidation of  $\beta$ -nicotyrine is minor. Although the evidence is indirect, the results of these experiments would appear to suggest that cytochrome P-450 isozyme-5 is an important  $\beta$ -nicotyrine oxidase.

**Materials and Methods-Addendum****Displacement of Ketamine Binding to Cytochrome P-450 by  $\beta$ -Nicotyrine**

Aqueous stock solutions of  $\beta$ -nicotyrine tartrate (5 mM) and ketamine (100 mM) were prepared. Liver microsomes isolated from rabbits pretreated with

phenobarbital were added (300  $\mu$ l of a 10 mg/ml stock solution) to two 3 ml cuvettes each containing 2.7 ml of 0.15 M KCl buffer, pH 7.4, to yield a final concentration of 1 mg/ml. Baseline spectra of the sample and reference cuvettes were taken as described for the estimate of the binding dissociation constant of  $\beta$ -nicotyrine (described in the main Materials and Methods section of this chapter). A volume of 3  $\mu$ l of ketamine (100 mM stock) was added to the 3 ml microsomal suspension to yield a final concentration of 100  $\mu$ M. An equal volume of buffer was added to the reference cuvette and scans were taken immediately. Binding of ketamine to cytochrome P-450 produced an absorbance spectrum typical of a type I binding substrate with a  $\lambda_{\max}$  = 390 nm and a  $\lambda_{\min}$  = 429 nm. At this concentration a difference of 0.066 absorbance units was observed between the absorbance maxima and minima. To assess the competitive binding effects of  $\beta$ -nicotyrine on this absorbance spectrum, 3  $\mu$ l of the 5 mM stock solution of  $\beta$ -nicotyrine was added to the 3 ml microsomal suspension containing ketamine. Immediately upon addition of the competing substrate, scans were resumed. Within seconds, the type I binding spectrum was abolished completely and replaced, within a period of 3-6 min, with the type II binding spectrum characteristic of  $\beta$ -nicotyrine. Addition of a second aliquot of  $\beta$ -nicotyrine, which yielded a final concentration of 10  $\mu$ M, enhanced the overall absorbance due to the type II substrate ( $\lambda_{\max}$  = 432 nm and  $\lambda_{\min}$  = 396 nm) and produced an absolute absorbance difference of 0.05 AU ( $\lambda_{\max}$  -  $\lambda_{\min}$ ).

#### **Phenobarbital and 3-Methylcholanthrene Pretreatment for the Studies of Liver Microsomal Metabolism of $\beta$ -Nicotyrine**

The protocol for pretreating rabbits with phenobarbital is described in the Materials and Methods section of Chapter IV. Rabbits (2.8-3.0 kg; n=3) were pretreated with a solution of 3-methylcholanthrene prepared in corn oil. A single dose of 20 mg/kg was injected intraperitoneally with a 21 gauge needle. The animals were euthanized 4 days later. Metabolic incubations were performed as described in Chapter



III. Incubation mixtures contained  $\beta$ -nicotyrine tartrate (1 mM) and liver microsomes (1 mg/ml) isolated from one of the three sets of animals used in this experiment.

**Pretreatment with Phenobarbital, TCDD and Aroclor 1260 for Studies of the Lung Microsomal Metabolism of  $\beta$ -Nicotyrine**

Pretreatment of rabbits with phenobarbital, TCDD and Aroclor 1260 are described in the Materials and Methods section of Chapter IV. Metabolic incubations were performed in a volume of 0.4 ml and contained 100  $\mu$ M  $\beta$ -nicotyrine tartrate and 1 mg/ml lung microsomes isolated from one of the four groups of animals used in this experiment. The remaining components are described in the Materials and Methods section of Chapter IV. The contents of the incubation mixture were preincubated at 37°C for 5 min prior to the addition of  $\beta$ -nicotyrine tartrate. The metabolic incubations were terminated by transferring the incubation mixtures to an ice bath. The internal standard, (S)-nicotine, was added (40  $\mu$ l of a 1 - 5 mM stock solution) to the quenched incubation mixture and the contents of the metabolic incubation were extracted with 1 ml of CH<sub>2</sub>Cl<sub>2</sub>. Approximately 50  $\mu$ l of the organic extract was analyzed following separation on silica HPLC by UV detection at 286 nm. Details of the HPLC analytical procedure was described previously in Chapter IV.

**Chemical Inhibitors of Lung Cytochrome P-450-2 and -5**

The chemical inhibitor studies used in the experiments described employed the protocol described in Chapter IV.

- 
1. Takeuchi, M., "The metabolic change of nicotine in rabbit liver extract," *Folia Pharmacol Japon* **51**, 62-69 (1955).
  2. Werle, E. and A. Meyer, "Decomposition of tobacco alkaloids by animal tissues," *Biochem. Z.* **321**, 221-235 (1950).
  3. Ivanov, N., "Alkaloids in Bulgarian cigarettes and smoke by means of paper chromatography," *C.R. Acad. Bulg. Sci.* **12**, 317-320 (1959).
  4. Brown, E.V. and I. Ahmad, "Alkaloids of cigarette smoke condensate," *Phytochemistry*, **11**, 3485-3490 (1972).
  5. Woodward, C.F., A. Eisner and P.G. Haines, "Pyrolysis of nicotine to myosmine," *J. Am. Chem. Soc.* **66**, 911-914 (1944).
  6. Wada, E., T. Kasaki and K. Saito, "Autoxidation of nicotine," *Arch. Biochem. Biophys.* **79**, 124-130 (1959).
  7. Clark, M.S.G., M.J. Rand and S. Vanov, "Comparison of pharmacological activity of nicotine and related alkaloids occurring in cigarette smoke," *Arch. Int. Pharmacodyn. Ther.* **156**, 363-379 (1965).
  8. Gassel, M.M., "Inducing skeletal muscle relaxation," U.S. 4,065,561 (Cl. 424-263: A61K31/44), 27 Dec 1977, Appl. 592,124, 30 Jun 1975; 5 pp.
  9. Stalhandske, T. and P. Slanina, "Nicotyrine inhibits *In vivo* metabolism of nicotine without increasing its toxicity," *Tox. Appl. Pharm.* **65**, 366-372 (1982).
  10. Personal communication: James Copland
  11. Schmeltz, I. and D. Hoffman, "Nitrogen-containing compounds in tobacco and tobacco smoke," *Chem. Rev.* **77**, 295-311 (1977).
  12. Beckett, A.H., J.W. Gorrod and P. Jenner, "A possible relation between pKa1 and lipid solubility and the amounts excreted in urine of some tobacco alkaloids given to man," *J. Pharm. Pharmacol.* **23**, 55-61S (1972).
  13. Badgett, W., A. Eisner and H.A. Walens, "Distribution of pyridine alkaloids in the system buffer-t-amyl alcohol," *J. Am. Chem. Soc.* **74**, 4096-4098 (1952).
  14. Jenner, P. and J.W. Gorrod, "Comparative *in vitro* hepatic metabolism of some tertiary N-methyl tobacco alkaloids in various species," *Res. Comm. Chem. Path. Pharm.* **6**, 827-843 (1973).
  15. McMurtry, R.J. and J.R. Mitchell, "Renal and hepatic necrosis after metabolic activation of 2-substituted furans and thiophenes, including furosemide and cephaloridine," *Toxicol. Appl. Pharmacol.* **42**, 285-300 (1977).

- 
16. Boyd, M.R., "Biochemical mechanisms in chemical induced lung injury: Roles of metabolic activation," *CRC Crit. Rev. Toxicol.* **9**, 103-176 (1980).
  17. Bray, H.G., F.M.B. Carpanini and B.D. Waters, "The metabolism of thiophen in the rabbit and the rat," *Xenobiotica* **1**, 157-168 (1971).
  18. Boyd, M.R., T.M. Harris and B.J. Wilson, "Confirmation by chemical synthesis of the structure of 4-ipomeanol, a lung-toxic metabolite of the sweet potato (*ipomea batatas*), *Nature (London) New Biol.* **236**, 158-159 (1972).
  19. Devereux, T.R., G.E.R. Hook, and J. Fouts, "Foreign compound metabolism by isolated cells from rabbit lung," *Drug Metab. Dispos.* **7**, 70-75 (1979).
  20. Doster, A.R., F.E. Mitchell, R.L. Farrell and B.J. Wilson, "Effects of 4-ipomeanol, a product from mold-damaged sweet potatoes, on the bovine lung," *Vet. Pathol.* **15**, 367-375 (1978).
  21. Buckpitt, A.R., C.N. Statham and M.R. Boyd, "*In vivo* studies on the target tissue metabolism, covalent binding, glutathione depletion, and toxicity of 4-ipomeanol in birds, species deficient in pulmonary enzymes for metabolic activation," *Toxicol. Appl. Pharmacol.* **65**, 38-52 (1982).
  22. Dutcher, J.S. and M.R. Boyd, "Species and strain differences in target organ alkylation and toxicity by 4-ipomeanol: Predictive value of covalent binding in studies of target organ toxicities by reactive metabolites," *Biochem. Pharmacol.* **28**, 3367-3372 (1979).
  23. Boyd, M.R. and L.T. Burka, "*In vivo* studies on the relationship between target organ alkylation and the pulmonary toxicity of a chemically reactive metabolite of 4-ipomeanol," *J. Pharmacol. Exp. Ther.* **207**, 687-697 (1978).
  24. Boyd, M.R., L.T. Burka, B.J. Wilson and H.A. Sasame, "*In vitro* studies on the metabolic activation of the pulmonary toxin, 4-ipomeanol, by rat lung and liver microsomes," *J. Pharmacol. Exp. Ther.* **207**, 677-686 (1978).
  25. Mitchell, J.R., W.L. Nelson, W.Z. Potter, H. Sasame and D.J. Jollow, "Metabolic activation of furosemide to a chemically reactive, hepatotoxic metabolite," *J. Pharmacol. Exp. Ther.* **199**, 41-52 (1976).
  26. Walker, R.M. and T.F. McElligott, "Furosemide induced hepatotoxicity," *J. Pathol.* **135**, 301-314 (1981).
  27. Wirth, P.J., C.J. Bettis and W.L. Nelson, "Microsomal metabolism of furosemide. Evidence for the nature of the reactive intermediate involved in covalent binding," *Mol. Pharmacol.* **12**, 759-768 (1976).
  28. Le Fur, J.M. and J.P. Labaune, "Metabolic pathway by cleavage of a furan ring," *Xenobiotica*, **15**, 567-577 (1985).
  29. Schmid, J., A. Prox, A. Reuter, H. Zipp and F.W. Koss, "The metabolism of 8-methoxypsoralen in man," *Eur. J. Drug Metab. Pharm.* **5**, 81-91 (1980).

- 
30. Lijinsky, W., "Chronic toxicity tests of pyrilamine maleate and methapyrilene hydrochloride in F344 rats," *Fd. Chem. Tox.* **22**, 27-30 (1984).
  31. Lijinsky, W., M.D. Reuber, B.N. Blackwell, "Liver tumors induced in rats by oral administration of the antihistaminic methapyrilene hydrochloride," *Science* **209**, 817-819 (1980).
  32. Andrews, A.W., J.A. Fornwald and W. Lijinsky, "Nitrosation and mutagenicity of some amine drugs," *Toxic. Appl. Pharmac.* **52**, 237-244 (1980).
  33. Iype, P.T., R. Ray-Chaudhuri, W. Lijinsky and S.P. Kelley, "Inability of methapyrilene to induce sister chromatid exchanges *in vitro* and *in vivo*," *Cancer Res.* **42**, 4614-4618 (1982).
  34. Lampe, M.A. and R.C. Kammerer, "Cytochrome P-450 dependent binding of methapyrilene to DNA *in vitro*," *Carcinogenesis* **8**, 1525-1529 (1987).
  35. Nelson, S., "Metabolic activation and drug toxicity," *J. Med. Chem.* **25**, 753-765 (1982).
  36. Oker-Blom, C., J. Mäkinen and G. Gothoni, "Toxicological studies on tienilic acid in rats," *Toxicol. Lett.* **6**, 93-99 (1980).
  37. Guengerich, F.P. and M.B. Mitchell, "Metabolic activation of model pyrroles by cytochrome P-450," *Drug. Metab. Dispos.* **8**, 34-38 (1980).
  38. Murphy, P.J. and T.L. Williams, "Biological inactivation of pyrrolnitrin. Identification and synthesis of pyrrolnitrin metabolites," *J. Med. Chem.* **15**, 137-139 (1972).
  39. Buckpitt, A.R. and M.R. Boyd, "The *in vitro* formation of glutathione conjugates with the microsomally activated pulmonary bronchiolar alkylating agent and cytotoxin, 4-ipomeanol," *J. Pharmacol. Exp. Ther.* **215**, 97-103 (1980).
  40. Brueggemeier, R.W. and J.G. Kimball, "Kinetics of inhibition of estrogen 2-hydroxylase by various haloestrogens," *Steroids* **42**, 93-103 (1983).
  41. Schenkman, J.B., H. Remmer and R.W. Estabrook, "Spectral studies of drug interaction with hepatic microsomal cytochrome," *Mol. Pharmacol.* **3**, 113-123 (1967).
  42. Serabjit-Singh, C.J., C.R. Wolfe and R.M. Philpot, "The rabbit pulmonary monooxygenase system: Immunochemical and biochemical characterization of the enzyme components," *J. Biol. Chem.* **254**, 9901-9907 (1979).
  43. Ziegler, D.M., "Flavin-containing monooxygenase: Catalytic mechanism and substrate specificities," *Drug Metab. Rev.* **19**, 1-32 (1988).
  44. Buening, M.K. and M.R. Franklin, "The formation of cytochrome P-450-metabolic intermediate complexes in microsomal fractions from extrahepatic tissues of the rabbit," *Drug Metab. Dispos.* **4**, 556-561 (1976).

- 
45. Chavdarian, C.G., "Optically active nicotine analogs. Synthesis of (S)-(-)-(2,5-dihydro-1-methyl-2-(3-pyridyl)pyrrole((S)-(-)-3',4'dehydronicotine)," *J. Org. Chem.* **48**, 1529-1531 (1983).
  46. Nguyen, T-L., E. Dagne, L. Gruenke, H. Bhargava, and N. Castagnoli, Jr., "The tautomeric structures of 5-hydroxycotinine, a secondary mammalian metabolite of nicotine," *J. Org. Chem.* **46**, 758-760 (1981).
  47. Liberato, D.J., V.S. Byers, R.G. Dennick and N. Castagnoli, Jr., "Regiospecific attack of nitrogen and sulfur nucleophiles on quinones derived from poison oak/ivy catechols (urushiols) and analogues as models for urushiol-protein conjugate formation," *J. Med. Chem.* **24**, 28-33 (1981).
  48. Ukai, S., K. Hirose, A. Tatematsu and T. Goto, "Organic mass spectrometry. IX. The reductive reaction of 1,2-quinones in mass spectrometer," *Tetrahedron Lett.* **49**, 4999-5002 (1967).
  49. Min, B.H. and W.A. Garland, "Determination of clonazepam and its 7-amino metabolite in plasma and blood by gas chromatography-chemical ionization mass spectrometry," *J. Chromatog.* **139**, 121-133 (1977).
  50. Habs, M., P. Shubik and G. Eisenbrand, "Carcinogenicity of methapyrilene hydrochloride, mepyramine hydrochloride, thenyldiamine hydrochloride, and pyribenzamine hydrochloride in Sprague-Dawley rats," *J. Cancer Res. Clin. Oncol.* **111**, 71-74 (1986).
  51. Swenson, D.H., E.C. Miller and J.A. Miller, "Aflatoxin B<sub>1</sub>-2,3-oxide: Evidence for its formation in rat liver *in vivo* and by human liver microsomes *in vitro*," *Biochem. Biophys. Res. Commun.* **60**, 1036-1043 (1974).
  52. Thakker, D.R., H. Yagi, W. Levin, A.W. Wood, A.H. Conney and D.M. Jerina, "Polycyclic aromatic hydrocarbons: metabolic activation to ultimate carcinogens," In: *Bioactivation of foreign compounds*, (M.W. Anders, Ed.), pp. 178-242 Academic Press, Orlando (1985).
  53. Leslie, J., D.L. Williams and G. Gorin, "Determination of mercapto groups in proteins with N-ethylmaleimide," *Anal. Biochem.* **3**, 257-263 (1962).
  54. Gorin, G., P.A. Martic and G. Doughty, "Kinetics of the reaction of N-ethylmaleimide with cysteine and some congeners," *Arch. Biochem. Biophys.* **115**, 593-597 (1986).
  55. Srinivasachar, K. and D.M. Neville Jr., "New protein cross-linking reagents that are cleaved by mild acid," *Biochemistry* **28**, 2501-2509 (1989).
  56. Lowry, O.H., N.J. Rosebrough, A.L. Farr and R.J. Randall, "Protein measurement with the Folin phenol reagent," *J. Biol. Chem.* **193**, 265-275 (1951).
  57. Estabrook, R.W., J. Peterson, J. Baron and A. Hildebrandt: The spectrophotometric measurement of turbid suspension of microsomes associated with drug metabolism. *Methods Pharmacol.* **2**, 303-350 (1972).

**Chapter VII**  
**Summary and Conclusions**

We have shown in this dissertation that the metabolic oxidation of (S)-nicotine results in the formation of one or more chemically reactive metabolites that bind covalently to microsomal macromolecules. The formation of the reactive metabolite(s) appears to be largely dependent on the cytochrome P-450 catalyzed oxidation of (S)-nicotine at its 5'-carbon atom and may involve further metabolic oxidations. The characterization of this process has raised new questions concerning those metabolic routes involved in the bioactivation of this major tobacco alkaloid. The identification and characterization of the metabolic pathway(s) involved in the covalent binding observed in these studies thus constitute the focus of this dissertation. The following section summarizes our findings and provides an integrated overview of (S)-nicotine bioactivation and its possible toxicological significance.

As described in Chapter III, (S)-nicotine is metabolically activated to intermediate(s) which bind covalently to microsomal macromolecules. This process is time, NADPH and cytochrome P-450 dependent. In an effort to identify the chemical nature of the proximate or ultimate reactive species, we attempted to block the covalent binding of reactive (S)-nicotine derived metabolites produced by cytochrome P-450. Sodium cyanide was used to trap the reactive iminium ion intermediates **2** and **14** (See **Scheme III.1**) as the corresponding  $\alpha$ -cyanoamines. However, this approach failed to yield conclusive results since cyanide was also shown to inhibit the metabolism of (S)-nicotine by binding to the cytochrome P-450 isozyme which catalyzes the oxidation of this compound. In a subsequent study which was aimed at identifying the bioalkylating properties of the iminium species **2**, preliminary evidence obtained by a SDS-equilibrium dialysis method showed that the  $\Delta^{1',5'}$ -iminium ion could bind covalently to microsomal macromolecules in a manner reversible by the addition of excess cyanide to the postincubation mixture. The covalent binding measured by this assay was also several fold greater than that measured by the conventional extraction and filtration

methods, a result which probably reflects the less harsh sample workup procedure employed in the former method. Because of the length of time required to process samples by the SDS-equilibrium dialysis technique, however, subsequent measurements of (S)-nicotine covalent binding used the conventional solvent extraction procedure.

The chemical structure of the ultimate reactive species which binds covalently to microsomal macromolecules, as measured by the solvent extraction and filtration techniques, remains obscure. Although the iminium species 2 and 14 have previously been proposed to be responsible for the covalent binding of (S)-nicotine, the known acid labile nature of  $\alpha$ -cyanoamines, in general, provides one argument against these iminium ions being the ultimate reactive species. Thus, the possible instability of this type of covalent adduct makes its detection unlikely by these two methods.

To gain a better understanding about the metabolic pathways of (S)-nicotine that lead to the formation of the ultimate bioalkylating species, bioactivation studies employing lung microsomal and cytosolic enzymes were pursued. The key findings from these studies include the following: 1). Lung microsomal enzymes catalyze the oxidation of (S)-nicotine better than liver microsomes per mole of cytochrome P-450. This result indicates that the lung is enriched in the P-450 isozyme which catalyzes the oxidation of this compound. 2). Lung cytochrome P-450 isozyme-2 is responsible for catalyzing the oxidation of (S)-nicotine at the 5'-carbon atom; the oxidation of (S)-nicotine at the N-methyl carbon atom is catalyzed by a different P-450 isozyme, tentatively identified as lung P-450 isozyme-5. 3). The lung P-450 isozyme-2 catalyzed oxidation of (S)-nicotine at the 5'-carbon position, which results in the formation of the  $\Delta^{1',5'}$ -iminium ion, can account for essentially all of the covalent binding observed since inhibitors or pretreatment of animals with agents which decrease the activity of lung P-450 isozyme-2 inhibit the formation of the  $\Delta^{1',5'}$ -iminium ion species and covalent binding in parallel without appreciably affecting the formation of the other major (S)-nicotine metabolites. This observation argues against the



participation of the nicotine methyleneiminium ion in the covalent binding measured in these studies since the formation of nornicotine, the hydrolysis product of this iminium species, is not affected by inhibitors which block lung P-450 isozyme-2 activity. 4). The lung cytosolic fraction contains a small fraction of the iminium oxidase activity present in the liver cytosolic fraction. Therefore, the probability of the proximate or ultimate bioalkylating species, (S)-nicotine  $\Delta^{1',5'}$ -iminium ion, bioaccumulating is likely to be greater in the lung tissue than in the liver tissue. As a consequence, one might predict that the lung tissue would be more susceptible to (S)-nicotine bioalkylation than the liver tissue. Consistent with this proposal is the finding that the addition of the liver cytosolic fraction blocks the covalent binding of (S)-5-<sup>3</sup>H-nicotine metabolically activated by lung microsomes whereas the lung cytosolic fraction does not. Taken together these results suggest that the lung tissue would be a better target than liver tissue for cytochrome P-450 dependent (S)-nicotine bioalkylation reactions.

Another aspect of (S)-nicotine metabolism which was described in this dissertation was the interaction of (S)-nicotine and its metabolites with the mitochondrial enzyme monoamine oxidase B. Our initial efforts were prompted by epidemiological studies which indicated an inverse correlation between tobacco consumption and Parkinson's disease. The tertiary allylamine MPTP, which has been shown previously to produce symptoms virtually identical to Idiopathic Parkinson's disease, is metabolically activated by monoamine oxidase B to a pyridinium metabolite which is neurotoxic and which irreversibly lesions dopaminergic neurons. We show that the principal metabolite of (S)-nicotine oxidation, (S)-nicotine  $\Delta^{1',5'}$ -iminium ion, inhibits the MAO-B catalyzed oxidation of MPTP. The inhibitory effect of (S)-nicotine  $\Delta^{1',5'}$ -iminium ion on the bioactivation of MPTP provides one possible mechanism for the protective effect of cigarette smoking on Parkinson's Disease. Studies designed to examine the inhibitory effects of (S)-nicotine  $\Delta^{1',5'}$ -iminium ion on MPTP

induced neurotoxicities, *in vivo*, will need to be pursued in order to address the biological relevance of this inhibitory effect.

During the course of the studies described above, the monoamine oxidase B catalyzed oxidation of (S)-nicotine  $\Delta^{1',5'}$ -iminium ion to  $\beta$ -nicotyrine was characterized. This metabolic transformation is interesting both in terms of the possible role it may play in the bioactivation and overall toxicology of (S)-nicotine and the enzymatic mechanisms involved in the formation of  $\beta$ -nicotyrine. The studies described in Chapter VI indicate that  $\beta$ -nicotyrine is oxidized by cytochrome P-450 to the pyrrolinone metabolites **7** and **8** which we propose are formed through the intermediacy of a reactive arene oxide intermediate. If our interpretation of the mechanism of formation of the metabolites **7** and **8** is correct, the metabolic oxidation of  $\beta$ -nicotyrine is likely to represent a bioactivation pathway for this tobacco alkaloid since arene oxide intermediates are, as a general class of compounds, highly reactive bioalkylating species. In order to study the bioactivation of  $\beta$ -nicotyrine, it would be necessary to synthesize a radiolabeled analog of  $\beta$ -nicotyrine and measure the extent of metabolism dependent covalent binding in a manner analogous to the procedure used to examine the bioactivation of (S)-nicotine (described in Chapter III). Use of epoxide hydratase inhibitors in these metabolic incubations might serve as probes for the formation of the proposed reactive arene oxide intermediate **48**. The previously described lung microsomal metabolism studies with (S)-nicotine and  $\beta$ -nicotyrine as substrates demonstrated that different P-450 isozymes participate in the oxidation of these two compounds. (S)-Nicotine is metabolically activated by P-450 isozyme-2, although other enzymes including P-450 isozyme-5 and lung flavin containing monooxygenase also catalyze the oxidation of this compound.  $\beta$ -Nicotyrine appears to be oxidized principally by lung P-450 isozyme-5. The different substrate properties of the two compounds may prove to be useful in designing studies to examine further the metabolic routes involved in the bioactivation of (S)-nicotine. For example, if the

selective inhibition of lung P-450 isozyme-5 blocks the covalent binding of (S)-nicotine, one could speculate that the ultimate reactive species is formed through the intermediacy of  $\beta$ -nicotyrine which requires the catalytic activity of this isozyme for its oxidation.

If  $\beta$ -nicotyrine is metabolically activated to intermediates which bind covalently to microsomal macromolecules, further studies aimed at characterizing the *in vivo* metabolism dependent toxicity of  $\beta$ -nicotyrine should be pursued. Since the cholinergic stimulating properties of  $\beta$ -nicotyrine are minor compared to (S)-nicotine, relatively large doses of this alkaloid could be administered without producing the acute toxicities associated with (S)-nicotine.  $\beta$ -Nicotyrine induced toxicities could be correlated with the extent of covalent binding and the distribution of cytochrome P-450 in the target tissue. If the lungs are identified as a target organ, selective lung P-450 isozyme inhibitors could be used to identify the metabolism dependent nature of the covalent binding and/or toxicities produced by  $\beta$ -nicotyrine. This approach would facilitate our understanding of the toxicological properties of this cyclopentadienoid heterocyclic compound.

A key question which remains to be resolved is the biological relevance of the metabolic pathway linking (S)-nicotine  $\Delta^{1',5'}$ -iminium ion to  $\beta$ -nicotyrine. One area which needs to be studied in further detail is the conversion of the microsome derived  $\Delta^{1',5'}$ -iminium metabolite **2** to  $\beta$ -nicotyrine (**6**), via the catalytic activity of the mitochondrial enzyme MAO-B. The studies described in Chapter V show that the rate of oxidation of (S)-nicotine  $\Delta^{1',5'}$ -iminium ion to  $\beta$ -nicotyrine is slow relative to the aldehyde oxidase catalyzed oxidation of the  $\Delta^{1',5'}$ -iminium ion to (S)-cotinine. Thus it would be important to determine whether mitochondrial MAO-B is involved in the oxidation of (S)-nicotine  $\Delta^{1',5'}$ -iminium ion in an intact cellular system (hepatocytes and lung derived Clara cells are two possible examples) where the potential for

competing metabolic pathways catalyzing the oxidation of this iminium species to another end product are present.

Studies on the NADPH dependent microsomal metabolism of (S)-nicotine  $\Delta^{1',5'}$ -iminium ion deserves further attention. The rationale for pursuing these studies further is encouraged by the findings described in Chapter V which show that monoamine oxidase-B (MAO-B) catalyzes the oxidation of (S)-nicotine  $\Delta^{1',5'}$ -iminium ion to  $\beta$ -nicotyrine. Previous reports documenting the similarities between the catalytic mechanism of the MAO-B and cytochrome P-450 oxidation of substituted cyclopropylamines opens up the possibility that the iminium species could be metabolized further to  $\beta$ -nicotyrine by a P-450 catalyzed reaction.<sup>1</sup> Designing an experiment to determine this route of oxidation may be difficult since  $\beta$ -nicotyrine is metabolized by this same enzyme system to the pyrrolinone metabolites **7** and **8**. Direct quantitation of  $\beta$ -nicotyrine, therefore, would not appear to be feasible. A better experimental approach might involve the quantitative estimation of the pyrrolinone metabolites **7** and **8** derived from the two electron oxidation of  $\beta$ -nicotyrine. Identification of either of these two products from the microsomal oxidation of (S)-nicotine  $\Delta^{1',5'}$ -iminium ion would support further the proposed similarities between the catalytic mechanisms of the two enzyme systems described previously by Tullman and Hanzlik.<sup>1</sup> The demonstration of such activity for cytochrome P-450 would point to a novel metabolic pathway for the oxidation of the enamine species and establish a connection between  $\beta$ -nicotyrine and the bioactivation of (S)-nicotine.

Shown in **Scheme VII.1** is a summary of the metabolic routes for (S)-nicotine which we postulate are involved in its bioactivation. The  $\alpha$ -carbon oxidations of (S)-nicotine at the 5'-carbon and N-methyl carbon atoms, depicted by pathways **A** and **B**, yield the (S)-nicotine  $\Delta^{1',5'}$ -iminium ion (**2**) and (S)-nicotine methyleneiminium ion (**14**) species, respectively. Both compounds are electrophilic metabolites which may bind covalently to microsomal macromolecules. The iminium metabolite **2** via the

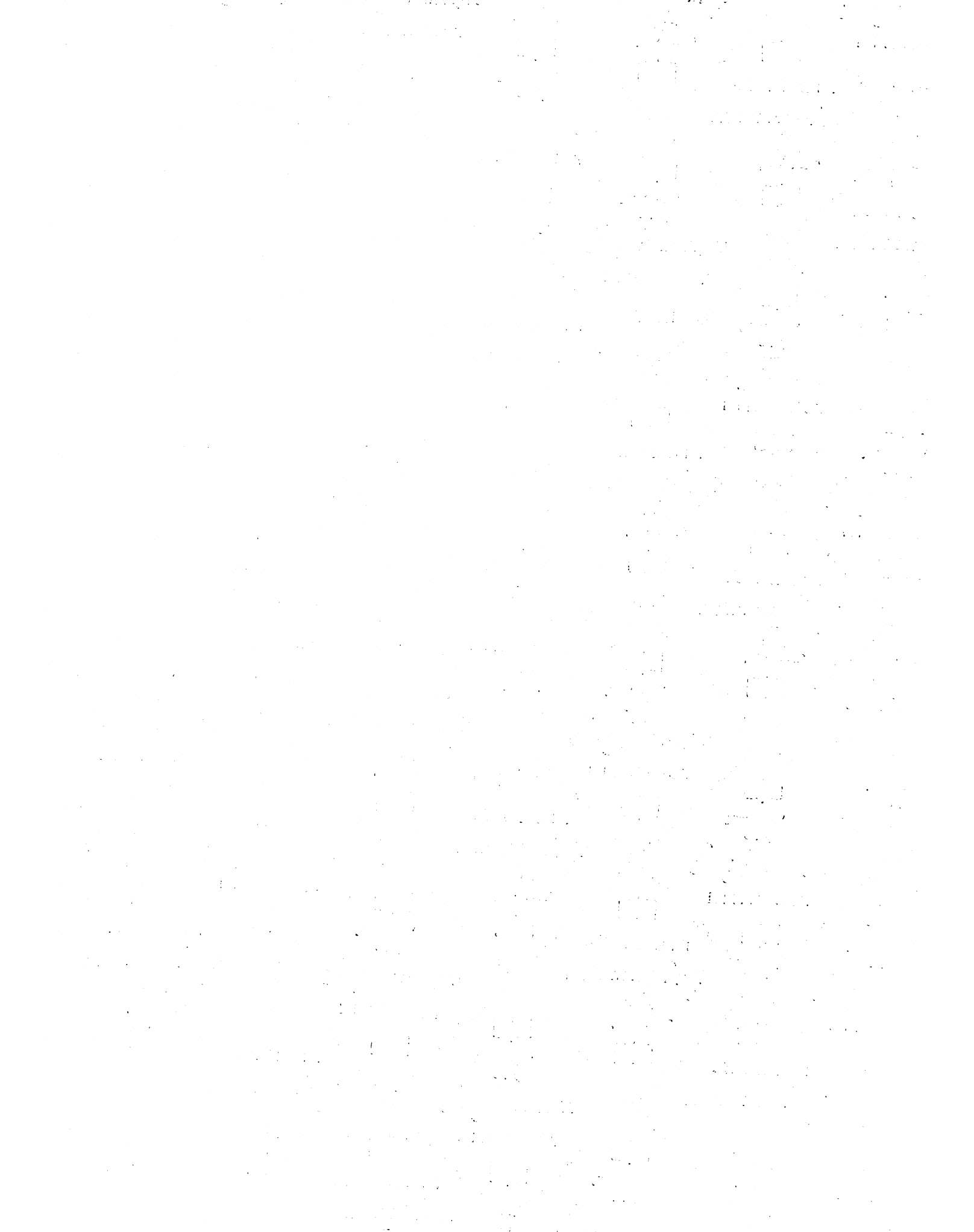


enamine species **19** can suffer a further two electron oxidation. The oxidation of **19** by cytochrome P-450, for example, could in principle yield the reactive arene oxide intermediate **23** which may bind covalently to biomacromolecules (pathway C). The MAO-B catalyzed oxidation of **2** via **19** is another two electron oxidation reaction described in this dissertation. Based on the arguments of MacDonald *et al.* the formation of **6**, described in Chapter V, may also be catalyzed by cytochrome P-450.<sup>2</sup> We propose that the further oxidation of **6** by cytochrome P-450 yields the reactive arene oxide species **48** which may bind directly to nucleophilic constituents on biomacromolecules (pathway D) or rearrange to the dehydrocotinine species **7** and **8** which we propose also exists in equilibrium with the hydroxypyrrole derivative **49**. The formation of the neutral radical species **71 a-c**, via the one electron oxidation of the hydroxypyrrole **49**, represents yet another source of reactive intermediates. The *in vivo* generation of these reactive carbon centered (**71b** and **71c**) and oxyl radical (**71a**) species could lead to the formation of toxicologically important biomacromolecular adducts. Further studies will need to be performed in order to address these possibilities.

---

<sup>1</sup>Tullman, R.H. and R.P. Hanzlik, "Inactivation of cytochrome P-450 and monoamine oxidase by cyclopropylamines," *Drug Metab. Rev.* **15**, 1163-1182 (1984).

<sup>2</sup>MacDonald, T.M., K. Zirvi, L.T. Burka, P. Peyman and F.P. Guengerich, "Mechanism of cytochrome P-450 inhibition by cyclopropylamines," *J. Am. Chem. Soc.* **104**, 2050-2052 (1982).





562368



3 1378 00562 3684

FOR REFERENCE

NOT TO BE TAKEN FROM THE ROOM



CAT. NO. 23 012

